
THE UNIVERSITY
*of* EDINBURGH

# Technique and Muscle Activity of the Water Polo Eggbeater Kick at Different Levels of Fatigue

Nuno Oliveira

Doctor of Philosophy

The University of Edinburgh

2014

**Technique and Muscle Activity of the Water Polo Eggbeater Kick at Different Levels of Fatigue**

The eggbeater kick is a skill used frequently in water polo and synchronized swimming to elevate the upper body for shooting, passing, blocking or compete with the opponent for position in the water. The hips, knees, and ankles are involved in creating favourable orientations of the feet so that propulsive forces in the vertical direction can be created. Literature reporting the technique of the eggbeater kick is scarce and limited to description of kinematics or muscle activity. The relationship of the kinematics to the demands on specific muscles has not been established. The purpose of this study was to analyze the kinematics and muscle activity of the water polo eggbeater kick in fatigued and unfatigued states to provide foundational knowledge on which training programs can be based. Twelve water polo players were tested executing the eggbeater kick in the vertical position while trying to maintain as high a position as possible for the duration of the test. The test was terminated when the player could not keep the top of the sternum marker above water. Anthropometric data were collected using the 'eZone' method. Three dimensional coordinates for the lower limbs and two dimensional coordinates of the above water top of the sternum marker were obtained. Surface electromyography recorded the muscle activity of the *Tibialis Anterior, Rectus Femoris* and *Biceps Femoris* muscles on both legs. Differences between fatigued and unfatigued conditions and between dominant and non-dominant sides were tested using a two factor ANOVA with repeated measures. Differences within subjects were also investigated on a subject by subject basis with regard to muscle activity. Results indicated differences for kinematic and muscle activity variables between fatigue levels. The amplitude of anatomic angles and speed of the feet decreased with fatigue. Significant differences were found between dominant and non-dominant sides for the ankle motion. The non-dominant ankle was more inverted and adducted than the dominant ankle during the knee flexion phase of the cycle. The *Rectus Femoris* muscle had consistent patterns across subjects, while *Tibialis Anterior* and *Biceps Femoris* muscles were more subject specific in their responses. The Rectus Femoris and the Biceps Femoris have an agonist/antagonist relationship during knee flexion and extension. The Tibialis Anterior was active for long periods in the cycle while dorsiflexing and inverting the foot. As a consequence activity in these muscles decreased with fatigue. These findings point towards the necessity for players and coaches to address specific motions and muscles during the training of the eggbeater technique. Future work should focus on developing eggbeater kick training programs that address specific strength and flexibility.

Technique and Muscle Activity of the Water Polo Eggbeater Kick at Different Levels of Fatigue

The University of Edinburgh

Thesis submitted for the degree of Doctor of Philosophy to The University of Edinburgh.

I hereby declare that this thesis is my own work, that it has not been submitted for any other academic award, or part thereof, at this or any other educational institute.

Student: Date:

26/08/2014

# Acknowledgements

I would like to acknowledge the contribution of many people to this project.

First, I would like to thank Prof. Ross Sanders for the guidance and mentoring throughout my thesis. I would like to thank you for encouraging my research and for allowing me to grow as a research scientist.

I would like to express my special appreciation to Dr. Simon Coleman and Dr. Dave Sounders for the advice and insightful comments in the writing of this thesis.

To all the CARE team, namely Marlies Declerck, Jacki Thow, Tomohiro Gonjo, Chuang-Yaun Chiu and Jon Kelly. It was great to be part of the team and I can say I have learned a lot from each one of you.

To all the water polo players that participated in this study, your commitment was truly amazing!

Finally, I would like to thank my parents – Manuel and Margarida – for being always there throughout these years, and Sarah for her personal support and great patience at all times.

# Table of Contents

# List of Figures

# List of Tables

# List of Abbreviations

| | |
|---|---|
| NF | Non-fatigued |
| TP | Time Point |
| F | Fatigued |
| EMG | Electromyography |
| Max | Maximum |
| Min | Minimum |
| TA | Tibialis Anterior |
| RF | Rectus Femoris |
| BF | Biceps Femoris |
| MVC | Muscle Voluntary Contraction |
| MVIC | Muscle Voluntary Isometric Contraction |
| COM | Centre of Mass |
| ROM | Range of Motion |
| BSP | Body Segment Parameters |
| Avg | Average |
| eZone | Elliptical Zone Method |
| APAS | Ariel Performance Analysis System |
| 3D | Three dimensional |
| SD | Standard Deviation |
| N | Number |
| DLT | Direct Linear Transformation |

# Chapter One: Introduction

# 1 Introduction

The eggbeater kick is a skill in water polo used to raise the upper body out of the water in order to execute a wide range of technical skills (shooting, passing, blocking) or to compete with the opponent for position in the water (Bratusa et al., 2003). The hips, knees, and ankles are involved in creating favourable orientations of the feet so that small pitch angles (the water hits the underside of the foot at an acute angle) can be created, thereby generating propulsive forces (Sanders, 1999b).

Compared with most sport skills, little work has been done concerning the eggbeater kick. Current literature reveals a lack of depth about its biomechanics, physiology, and consequently, its training methodology. Most existing studies are based on analysis of the kinematics (Sanders, 1999a, Homma and Homma, 2005) focusing on the movement of the lower limbs. Sanders (1999a) focused on the role of the feet, relating specific variables in the execution of the eggbeater kick (foot velocity, pitch and sweepback angles of the feet, and foot paths) with the height attained. Homma and Homma (2005) compared the motion of the lower limbs between different levels of performance (excellent-poor). Both studies provided important information about the kinematics of the movement. However, to further improve understanding of the relationship between technique and performance, analysis of kinetics and muscles activity needs to be conducted taking into account the height and the mass of the players.

The search of literature did not yield any studies indicating the instantaneous force being produced during the eggbeater kick. This information is critical to investigate three main questions, 1) the link between technique and performance 2) the fatigue induced changes in the eggbeater kick technique and 3) asymmetries that might be present in the movement.

Logically, the measure of performance should be the vertical force produced during the cycle. In accordance with the definition of fatigue as '*failure to maintain the required or expected power output*' (Fitts, 1994), changes in the ability to generate vertical force is a viable external indicator of fatigue. Given that the force produced depends on the technique used, and that force diminishes with fatigue, there is a clear link between technique, performance, and fatigue. Thus it is of interest to investigate how technique affects performance (force produced) and how technique changes with fatigue (decrease in force). This knowledge would establish a foundation from which specific training programs could be designed.

Further, to understand the fatigue process and its influence on technique the activity of the muscles should be quantified. Based on knowledge of the actions used in the eggbeater kick in combination with knowledge of muscle functional anatomy Sanders (2002) suggested which muscles should be trained. However, the level of muscle activity and the durations of activity of each muscle within the eggbeater kick cycle must be quantified to understand fully the demands on the muscles involved. This would inform strength and conditioning programs to improve eggbeater kick performance and

endurance. Two main features of muscle activity are important to understand their roles in the performance of the eggbeater kick:

- The initiation (on-offset times) of muscle activation. This indicates the timing sequence of one or more muscles when performing an action (De Luca, 1997).
- The amplitude of the EMG signal relative to MVC reflects the force contribution of individual muscles or muscle groups (De Luca, 1997). This information can highlight the importance of particular muscles in critical phases of the cycle.

Thus, research that links muscle activity to the 3D kinematics and to the vertical force produced has valuable implications for training.

Current training programs do not appear to be underpinned by a scientific rationale based on knowledge of the eggbeater kick. Anecdotal evidence from water polo coaches indicates that the training of the eggbeater kick is directed under very general guidelines that are not supported with scientific evidence. They include both the strength exercises used and their planning. In addition, some coaches and players believe that dry land strength training for the lower limbs might be counterproductive to performing the eggbeater kick. The lack of evidence makes it hard to dispel that belief. The most common form of training for development of an effective eggbeater kick is squats. However, there is little evidence that squats improve eggbeater kick performance. It is known that squats are effective in developing strength and endurance of the hip and knee extensors (Young et al., 1998, Cormie et al., 2007). While hip and knee extensions occur during the eggbeater kick, many other actions are involved including internal and external rotation of the hip, hip abduction and adduction, hip and knee flexion, ankle

plantar and dorsiflexion, and ankle inversion and eversion (Sanders, 1999a, Homma and Homma, 2005). Thus, squats would not be expected, in isolation, to develop optimal strength and endurance of the muscles involved in the eggbeater kick actions. Thus, linking analysis of muscle function with 3D kinematics and with the production of vertical forces could provide an accurate description of variables associated with performance, and changes associated with fatigue.

Consequently, one of the outcomes of this study is foundational information to develop strength and conditioning programs that address the specific demands of the eggbeater kick. Researchers and coaches can look to improve specific strength and conditioning training programs for the eggbeater kick based on scientific evidence.

## 1.1 Purpose of the Study

The purpose of this study was to analyse the kinematics and muscle activity of the water polo eggbeater kick in fatigued and unfatigued states to provide foundational knowledge on which training programs can be based.

# Chapter Two: Review of the Literature

# 2 Review of the Literature

To address the purposes of this study literature has been reviewed that relates to both performance of the eggbeater kick as well as research that informs the development of appropriate methodological approaches to investigating the skill. However, due to the paucity of literature dedicated to the study of the eggbeater kick our knowledge and understanding of the skill is limited. Therefore, the search for related literature has been extended to include literature that is relevant by virtue of commonality of particular aspects of performance in cyclical tasks performed in aquatic environments. In the first section of the review current knowledge of the eggbeater kick is presented. The second section deals with the issue of side dominance and asymmetry. The third section deals with issues relating to the methods that could be employed to address the purposes of this research.

## 2.1 The Eggbeater Kick

The eggbeater kick is a complex and unusual movement typically executed in water polo and synchronized swimming. It is an essential technique for water polo and synchronized swimming where it is mostly executed with high intensity while performing other essential skills such as shooting, passing, and blocking.

The main objective of the eggbeater kick is to raise the body to assist in the performance of shooting, blocking, and passing and increase the likelihood of successful outcomes in those tasks. The height achievable in the water can be explained as the result of the interaction of variables controlled by the player (Fig. 2.1). Height has been used an

indicator of performance and mentioned as an important factor in the efficiency of other water polo skills (i.e. shooting, passing, goalkeeper actions) (Davis and Blanksby, 1977, Platanou and Thanopoulos, 2002, Smith, 1998).

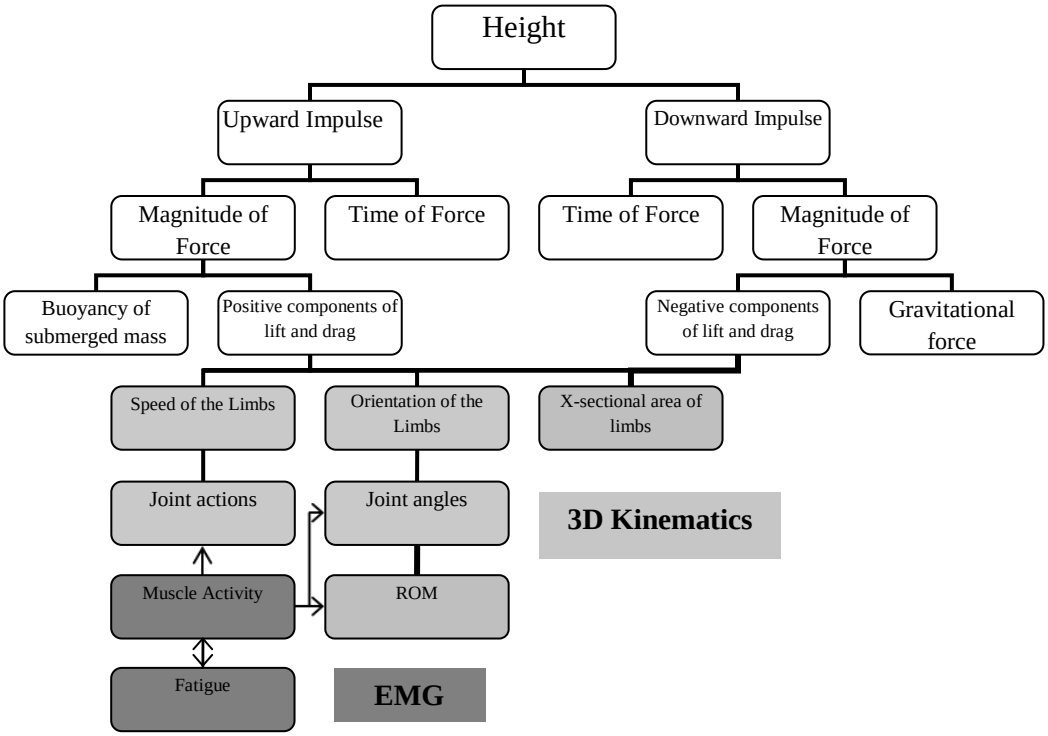


Figure 2.1. Associations between the variables being studied. *Adapted from Sanders (1999a)*

The height attained is the result of the upward/downward impulse produced during the kick. The hips, knees, and ankles are involved in creating favourable orientations of the feet, so that the water hits the underside of the foot at an acute angle, allowing the swimmer to generate vertical forces with their lower limbs (Sanders, 1999a). In addition, foot velocity during the cycle seems to be highly correlated with the height attained (Sanders, 1999a). Thus, muscle activity and fatigue are important variables controlling the two previous factors.

In general, the eggbeater kick consists of a combination of hip flexion and extension, hip adduction and abduction, internal and external rotation, and knee flexion and extension (Sanders, 2002). Motions of the ankle are important (e.g. dorsi-flexion, plantar-flexion, eversion and inversion) to create favourable angles of pitch through as much of the kicking cycle as possible. Effective performers tend to maximize the period of positive pitch by dorsi-flexing the feet during their anterior motion, plantar-flexing the feet during their posterior motion and everting the feet during the period of lateral motion (Sanders, 1999a). Creating small angles between the water surface and the planes of motion of the ankles is also related to skilled performance (Homma and Homma, 2005). Therefore, appropriate orientation of the body segments is fundamental for good performance and seems to require good levels of flexibility and strength in the joints/muscles involved.

There is a paucity of literature relating to the biomechanics and physiology of the eggbeater kick, and consequently, methods of training to optimise performance. Most existing studies focus on the kinematic of the lower limbs (Sanders, 1999a, Homma and Homma, 2005, Klauck et al., 2006) and no studies on fatigue and its implications have been reported. Sanders (1999a) performed a kinematic analysis of the eggbeater kick giving great attention the role of the feet, relating specific variables in the execution of the eggbeater kick including foot velocity, pitch and sweepback angles, with the height attained. However, the angles of the hip, knee and ankle joints that are responsible for the orientation of the feet were not calculated, limiting the information available to describe the technique associated with best performance. On the other hand, Homma and Homma (2005) compared the motion of the lower limbs calculating variables such as

distance profiles for the knees and the heels from the greater trochanter, height of the knees, angle profile between the right and left thigh, foot motion planes or angular velocities of the hip, knee, and ankle, across different levels of performance (excellent-poor) in a sample of synchronized swimmers of international level. Both studies address important questions about the kinematics of the movement but their calculated variables allow a limited representation of the motion of the lower limbs as the totally of degrees of freedom for each joint are not accounted for. Additionally, both studies focused on investigating the technique associated with best performance and do not address the effect of fatigue or assymetries in the movement. Furthermore, performance of the eggbeater kick has been determined by height achieved and does not take into account the stature and mass of the swimmers.

Muscle activity has been scarcely investigated in the eggbeater kick. Oliveira et al. (2010) reported normalized muscle activity values of six muscles for four female water polo players, and Klauck et al. (2006) investigated the muscle coordination of three muscles in one male water polo goalkeeper. Further research is required to investigate the relationship between muscle activity and technique variables, and its association with sustainability of performance and delay of fatigue.

The variation and intermittent nature of water polo make the assessment and interpretation of physiological responses by the players in training and competition technically difficult (Smith, 1998). Water polo players have been described to perform activities at >80 $VO2_{max}$ and >90% $HR_{max}$ involving the eggbeater kick 53% of the time in the water (Smith, 1998, Platanou and Geladas, 2006, Platanou and Thanopoulos, 2002). Additionally, activities that require the execution of the eggbeater kick (contacts,

passing, faking, shooting) showed mean durations below 10s (9.8 ± 0.7 for contacts and 2.6 ± 0.2 for ball skills)(Platanou and Geladas, 2006). However, players have shown for approximately 85% of the time, total velocities of movement in the horizontal plane that reflect a high demand from the anaerobic alactic system, a high demand on the aerobic system for the replenishment of creatine phosphate and a lesser emphasis on anaerobic lactic metabolism for energy provision (Smith, 1998).

The question of neuromuscular fatigue and its effects in the eggbeater kick technique has not been addressed in the literature. However, fatigue has been shown to change IEMG in highly active muscles involved in water sculling movements (Rouard et al., 1997) or change surface EMG parameters in upper body muscles during front crawl (Figueiredo et al., 2013a) and breaststroke (Conceicao et al., 2014) associated with changes in the kinematics. These authors reported changes in aquatic cyclical movements that show some relation to the eggbeater kick, supporting the importance of investigating the effect of fatigue in the muscle activity and kinematics of the eggbeater kick.

There is also a paucity of studies that have yielded information about the strength and conditioning training required for improving performance of the eggbeater kick. Because muscle activity demands and movement patterns are not clear, the role of particular muscles in the movement has been suggested on the basis of the kinematics of the motion, and the anatomical function of the individual muscles. However, to date, no data have been reported regarding the magnitudes and duration of activity of the involved muscles during the eggbeater kick.

To coach towards improved performance of the eggbeater kick it is necessary to learn the specific movement blueprint and, for designing appropriate training programs, the

characteristic muscle activity patterns (Kraemer et al., 1998). As in any sport skill, the eggbeater kick has specific demands on the muscles. Therefore, strength training programs should be designed to meet those demands. The current picture of strength training in water polo indicates a contrast between upper body/core and lower body exercises. Upper body exercises tend to occupy a greater part of strength training programs with the two major goals being to increase strength levels and to reduce the incidence of injury. Little attention has been given to the lower limbs even though the eggbeater kick is a fundamental skill in the game and is used for 45 to 55% of the game (Bratusa et al., 2003, Smith, 1998).

## 2.2 The Issue of Side Dominance and Asymmetries

One of the purposes of this study is to investigate differences between the dominant and non-dominant lower limb during the eggbeater kick. Similar to other bilateral activities where dominant and non-dominant sides have equivalent roles and could have identical spatio-temporal movement patterns (e.g. gait, running, swimming), to maximize performance in the eggbeater kick, players should have the lower limbs on both sides contributing optimally to maximize propulsion. However, even though congruent actions would appear to be ideal, asymmetries can exist. For example, despite breaststroke's symmetrical nature that does not encourage uneven development in terms of the demands of the activity, side dominance causes asymmetries in the kinematics of the leg kick among most breaststroke swimmers (Czabanski, 1975, Czabanski and Koszcyc, 1979, Sanders et al., 2012b, Sanders et al., 2012a). Asymmetries between dominant and

non-dominant sides have been reported for many other bilateral activities such as gait (Sadeghi et al., 2000, Herzog et al., 1989, Leroy et al., 2000), running (Zifchock et al., 2006) or backstroke swimming (Seifert et al., 2005, Formosa et al., 2014).

The lateralization of motor skills is a developmental process influenced throughout childhood and lifespan by several factors: genetic and early environmental (Palmer and Strobeck, 1986, Parson, 1990), developmental (Auerback and Ruff, 2006, Ducher et al., 2005), disease (Chung et al., 2008), injuries (Schiltz et al., 2009, Swaine, 1997, Hunt et al., 2004) or technique demands of a specific activity (Kobayashi et al., 2010, Downwar and Sauers, 2005, Seifert et al., 2008, Sanders, 2013, Sanders et al., 2012c).

When considering what variables might affect the height attained in the eggbeater kick, reference to the model illustrated in Figure 2.1 is useful. Asymmetries can affect both downward impulse and propulsion (i.e. upward impulse) which, together with physiological capacity of the player, are the key determinants of performance. The pattern of force production of the right and left sides might differ due to differences in in limb and foot orientation, range of motion, and speed of motion. These factors must be considered for each of the cycles (dominant and non-dominant) in conjunction with the vertical force patterns.

## 2.3 Methodological Issues

### 2.3.1 Anatomical Descriptors

Given the importance of being able to describe clearly and unambiguously the eggbeater kick motion and its relationship to the player's body, a brief review of the conventions for describing body orientations and motions is useful.

A segmental position or joint movement is typically expressed relative to a designated starting position. This reference position is called the anatomical position. In this position, the body is in an erect stance with the head facing forward, arms at the side of the trunk with palms facing forward, and the legs together with the feet pointing forward (Fig. 2.2) (Tortora and Derrickson, 2008, Hamill and Knutzen, 2003).

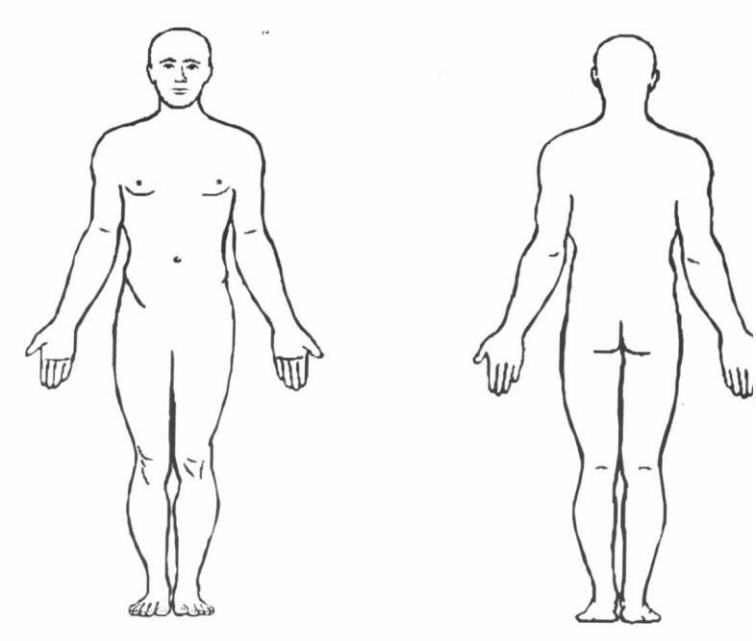

Figure 2.2. Illustration of the anatomical position.

The human body can be divided in three different planes (Gray, 2010). Considering the anatomical position as reference, the coronal or frontal plane divides the body lengthwise, anterior from posterior (front to back); the sagittal plane passes from ventral (front) to dorsal (rear) dividing the body into right and left halves; and, the transverse plane divides the body into superior and inferior (above and below) parts. It is perpendicular to the coronal and sagittal planes.

The term ‘medial’ refers to a position relatively close to the midline of the body or a movement that moves toward the midline. The opposite of medial is ‘lateral’, which is, a position relatively far from the midline or a movement way from the midline. ‘Proximal’ and ‘distal’ are used to describe the relative position with respect to a designated reference point, where proximal represents a position closer to the reference point and distal the position farther from the reference point. The reference point is generally a primary axis of the body passing through its mass centre. The term ipsilateral describes activity or location of a segment or landmark positioned on the same side as a particular reference point. Actions, positions, and landmark locations on the opposite side can be designated as contralateral. When actions take place on both sides of the body they are named bilateral (Hall, 1995).

### 2.3.2 Movement Description

To discuss joint position, we must define the ‘relative angle’ between two segments. A ‘relative angle’ is the included angle between two segments (Robertson et al., 2004). Movement of body segments are classified by the direction in which the affected

structures are moved. For all positions and movements it is assumed that the body is in its anatomical position. The anatomical motions used are (Hamill and Knutzen, 2003):

- Flexion (bending movement that *decreases* the angle between two segments).
- Extension (straightening movement that *increases* the angle between body segments).
- Abduction (motion that pulls a segment *away from* the midline of the body).
- Adduction (motion that pulls a segment *toward* the midline of the body).
- Internal or medial rotation
- External or lateral rotation
- Elevation (movement in a superior direction)
- Depression (movement in an inferior direction)
- Pronation (rotation of the forearm that moves the palm from an anterior-facing position to a posterior-facing position, or palm facing down. Different from medial rotation as this must be performed when the arm is half flexed.)
- Supination (opposite of pronation)
- Dorsiflexion (flexion of the entire foot superiorly)
- Plantarflexion (extension of the entire foot inferiorly)
- Eversion (movement of the sole of the foot away from the median plane)
- Inversion (movement of the sole towards the median plane)

These terms are specific for comparisons made in the anatomical position, or with reference to the anatomical planes. Thus, allowing the identification and comparison of different motions and stages in the eggbeater kick cycle.

### 2.3.3 Joint Angles

Given the involvement of several joints (i.e. hip, knee and ankle) in the eggbeater kick technique, the movement can be described in terms of joint angles. Determining the angles in the different joints throughout the movement is critical to understand the movement, and differences between fatigue levels or dominance that might occur.

To perform accurate observations of motion a reference system is necessary (Hay, 1985, Hall, 1995). The use of joint movements relative to the fundamental or anatomical starting positions can be used as a reference system. A reference frame is arbitrary and can be within or outside of the body. It is placed at a designated spot and is established by axes that intersect at 90° angles at a common point named 'origin'. To describe angular motion, an 'absolute' or a 'relative' frame of reference can be used. When the axes intersect in the centre of the joint and movement of a segment is described with respect to that joint we are referring to the 'absolute' reference frame. A 'relative reference frame' is one in which the movement of a segment is described relative to the adjacent segment. Absolute angles follow the right-hand-rule, which specifies that positive rotations are counter clockwise and negative rotations are clockwise. Curving the fingers of the right hand in the direction of the angle or rotation and then comparing the direction of the thumb to the reference axes determine the sign of an angle or rotation about a particular axis. If the thumb points in the direction of a positive axis, then the angle or rotation is positive.

Segment angles can be quantified using two conventions. The first measures angles ranging from 0 to 360°, the second allows a range from +180 to -180°. For both conventions a problem arises when a segment crosses the 0/360° line or the ±180° line. To solve this problem it is assumed that no angle changes more than 180° from one frame to the other (Robertson et al., 2004, Hamill and Knutzen, 2003).

### 2.3.4 Kinematics

Given the biomechanical nature of this study and its goals, an analysis of kinematics needs to be conducted.

#### 2.3.4.1 Three-Dimensional Kinematics

Kinematics is the study of the motion of bodies or systems of bodies disregarding the causes of motion. It is used to describe and quantify the linear and angular position of bodies and their time derivatives (Robertson et al., 2004). Three-dimensional (3D) kinematics is its application in 3D space. Collection of 3D position data of body landmarks is the first stage of the process and it involves the setup of a multi-camera motion analysis system. In this system each camera provides a set of two-dimensional (2D) coordinates that can be transformed into three-dimensional (3D) spatial coordinates. In this study, the technique by which the two-dimensional coordinates are transformed into 3D coordinates is the direct linear transformation (Abdel-Aziz and Karara, 1971).

#### 2.3.4.1.1 Direct Linear Transformation

The direct linear transformation (DLT) method proposed by Abdel-Aziz and Karara (1971) is a widely used method to transform 2D coordinates into 3D coordinates by the use of a multi-camera setup and a calibrated space within which the motion takes place. On comparing with the other methods, the DLT technique has the advantages of being relatively simple and accurate, and it permits great flexibility in camera setup (Chen et al., 1994, Hatze, 1988, Marzan and Karara, 1975, Miller et al., 1980, Shapiro, 1978). The linear relationship between the 2D coordinates of each body mark and its representation in 3D space is then established. This technique requires a set of control points (points with known coordinates in real units in 3D space) that define a fixed coordinate system. From the 2D coordinates of the *n* control points a set of two equations (1) (2), solved for 11 DLT coefficients is developed for each camera. The DLT parameters establish the relationship between 3D space and the 2D camera view (Allard et al., 1995, Robertson et al., 2004, Chen et al., 1994).

(1) $x_i + L_1X_i + L_2Y_i + L_3Z_i + L_4 + L_9x_iX_i + L_{10}x_iY_i + L_{11}x_iZ_i = 0$

(2) $y_i + L_5x_i + L_6Y_i + L_7Z_i + L_8 + L_9y_iX_i + L_{10}y_iY_i + L_{11}y_iZ_i = 0$

$i$ = number of control points

$x_i$ and $y_i$ = digitized 2D coordinates for the $i^{th}$ control point

$X_i$, $Y_i$ and $Z_i$ = space coordinates of the $i^{th}$ control point

$L_1$ to $L_{11}$ = DLT coefficients

As long as there are at least six control points, the least-squares method can be used to determine the standard 11 DLT parameters. If there are less than six control points, the 11 DLT parameters will be undetermined (Miller et al., 1980).

#### 2.3.4.1.2 Nonlinear Systematic Errors

In the practical context the theoretical image coordinates cannot be determined because of the presence of systematic errors caused by lens distortion, non-orthogonality of video/image axes and other sources of linear, and non-linear and asymmetrical lens distortion. Points across the field of view do not have the same amplification factor, meaning that the actual transformation between the three-dimensional space and the two-dimensional image plane is a nonlinear transformation (Chen et al., 1994, Hatze, 1988). In attempting to correct these sources of error some authors (Hatze, 1980, Chen et al., 1994) have proposed a modified DLT (MDLT) algorithm to satisfy certain orthogonality conditions in the form of a non-linear constraint.

#### 2.3.4.1.3 Advantages of 3D Analysis

Although 2D analysis is simpler and cheaper (as fewer cameras and other equipment are needed, less digitising time is required and fewer methodological problems are present), movements have to be executed in a pre-selected movement plane and measurements of movements out of the plane perpendicular to the camera are not accurate (Bartlett, 1997). Yeadon and Challis (1990) stated that this limitation can be important even for

movements that seem to be mainly two dimensional, such as the long jump. As mentioned previously, the use of 3D analysis minimises the errors that occur in the calculation of variables and, therefore, increases the accuracy and reliability of a study (Keskinen and Keskinen, 1997). Bartlett (1997) suggested further advantages of 3D analysis:

- It can show the body's true spatial motions and is closer to the reality of the movements studied.
- It allows inter-segment angles to be calculated accurately, without viewing distortions. It also allows the calculation of other angles which cannot be easily obtained from a single camera view in many cases.
- It enables the reconstruction of simulated views of the performance other than those seen by the cameras, an extremely useful aid to movement analysis and evaluation.

In conclusion, 3D methodologies should be used by researchers whenever possible in conducting a biomechanical study, particularly when the objective is the accurate and detailed investigation of movements that occur in several planes such as the eggbeater kick.

#### 2.3.4.2 Local Coordinate System

To analyse the movement and anatomical movements of the lower limb segments involved in the eggbeater kick (i.e. trunk, thighs, leg and foot) it is necessary to establish coordinate systems in those segments.

To measure the motion of skeletal structures three non-collinear markers must be used to define the plane of each segment of interest. Four main configurations of markers are frequently used (Robertson et al., 2004, Hamill and Knutzen, 2003):

- Markers mounted on bone pins
- Skin-mounted markers on specific anatomical landmarks
- Arrays of markers on a rigid surface that is attached to the body
- Combination of markers on anatomical landmarks and arrays of markers

The most accurate marker system is where markers are mounted on bone pins (Fuller et al., 1997, Reinschmidt et al., 1997), the least accurate marker system uses markers placed directly on the skin (Fuller et al., 1997, Karlsson and Tranberg, 1999, Reinschmidt et al., 1997). No matter what system is used, it is essential that movement artefacts from the weight of the marker or the movement of the marker attachment device relative to the bones are minimized (Karlsson and Tranberg, 1999).

The marker configuration applied to a body or segment allows creating a local coordinate system. Coordinate systems are systems used to determine the positions or orientation of a point or other geometric element. In spatial or 3D motion analyses there are numerous conventions for reporting the position of a body in space. The most common methods to calculate this are Cartesian coordinates and unit vectors. In the Cartesian coordinate system a position vector has three mutually orthogonal coordinates that uniquely distinguish the point in space. Unit vectors are defined as vectors of unit length along each of the axes of the coordinate system. A vector can be changed to a unit vector by dividing each component by the length of the vector.

#### 2.3.4.3 Transformations between Reference Systems

The orientation of a body or segment moving in three-dimensional space can be transformed into different reference systems. The process by which the coordinates in one reference frame are converted to another coordinate system is called 'transformation'. This process can be linear or rotational (Robertson et al., 2004). Linear transformation consists of describing the relative positions of origin of two coordinate systems by a vector $\vec{V}$, the components of $\vec{V}$ are $V_x$, $V_y$, and $V_z$ (1).

$$(1)\ \vec{V} = \begin{bmatrix} V_x \\ V_y \\ V_z \end{bmatrix}$$

When there is no rotation in the transformation between two local coordinate systems, converting the coordinates of a point $P$ in the initial coordinate system to point $P'$ in the final coordinate system can be accomplished by (2)

$$(2)\ P' = \vec{V} + P$$

When rotation is present between three-dimensional reference systems the coordinates can be converted by calculating the rotation transformation matrix. If the vector components of one coordinate system, $T_P$ are represented by the unit vector matrix (3)

$$(3)\ [T_P] = \begin{bmatrix} \vec{\imath'}_x & \vec{\imath'}_y & \vec{\imath'}_z \\ \vec{\jmath'}_x & \vec{\jmath'}_y & \vec{\jmath'}_z \\ \vec{k'}_x & \vec{k'}_y & \vec{k'}_z \end{bmatrix}$$

And those for another coordinate system $T_D$ (4)

$$(4)\ [T_D] = \begin{bmatrix} \vec{\imath''}_x & \vec{\imath''}_y & \vec{\imath''}_z \\ \vec{\jmath''}_x & \vec{\jmath''}_y & \vec{\jmath''}_z \\ \vec{k''}_x & \vec{k''}_y & \vec{k''}_z \end{bmatrix}$$

The rotation transformation matrix $[T_R]$ (5) is calculated by taking the dot product of a unit vector matrix from one coordinate system and the unit vector matrix of another coordinate system.

$$(5)\ [T_P] = \begin{bmatrix} \vec{\imath''} \cdot \vec{\imath'} & \vec{\imath''} \cdot \vec{\jmath'} & \vec{\imath''} \cdot \vec{k'} \\ \vec{\jmath''} \cdot \vec{\imath'} & \vec{\jmath''} \cdot \vec{\jmath'} & \vec{\jmath''} \cdot \vec{k'} \\ \vec{k''} \cdot \vec{\imath'} & \vec{k''} \cdot \vec{\jmath'} & \vec{k''} \cdot \vec{k'} \end{bmatrix}$$

#### 2.3.4.4 Joint Angles

Different methods can be used to determine the relative orientation of two coordinate systems (Chao, 1980, Grood and Suntay, 1983, Spoor and Veldpaus, 1980, Woltring, 1991). The most used methods are the Cardan/Euler Angles (Apkarian et al., 1989,

Kabada et al., 1990, Davis et al., 1991, Engsberg et al., 1988), joint coordinate system (Grood and Suntay, 1983, Soutas-Little et al., 1987) and helical angles (Woltring, 1991). The principle behind Cardan/Euler angles and joint coordinate system techniques is the same and neither of them appears to have any obvious advantages or disadvantages over each other (Robertson et al., 2004).

#### 2.3.4.4.1 Cardan/Euler Angles

Cardan/Euler angles are calculated by the projections of the vectors of one coordinate system on the orthogonal planes of another coordinate system. The orientation of a coordinate system in space is determined using three independent projection angles that correspond to three rotational degrees of freedom. Since these rotations must be performed in a specific order because they are not commutative, several rotation sequences can be used. However, sequences usually take the same order, the first rotation is about an axis in one coordinate system, the second is about a floating axis, and the third about an axis fixed in the final coordinate system. A common Cardan rotation sequence used in biomechanics is a Xyz sequence (An and Chao, 1991, Cole et al., 1993, Apkarian et al., 1989, Kabada et al., 1990). This sequence involves, first (α), rotation about the medially directed axis (X); second (β), rotation about the anteriorly directed axis (y); and third (γ), about the vertical axis (z) (Fig. 2.3).

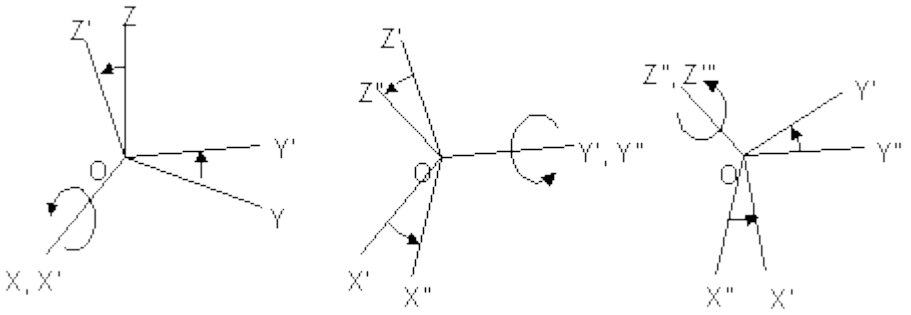


Figure 2.3. Xyz rotation sequence

Cardan/Euler angles are widely used in biomechanics and provide a well understood anatomical representation of the joint movement. On the other hand, the sequence dependence or gimbal lock (when the second rotation results in mathematical singularity) problems might be seen as a disadvantage.

#### 2.3.4.4.2 Joint Coordinate Systems

The joint coordinate system technique gives all three rotations between body segments a functional anatomical meaning. It can be defined as a *Joint Coordinate System* described by two segment-fixed axes and a mutually orthogonal floating axis. It was proposed by Grood and Suntay (1983) to eliminate the temporal sequence dependency of Euler angle techniques and to encourage the use of clinically relevant models. The joint coordinate system is defined by two independent body-fixed axes and the common perpendicular. Angular rotation of the bodies is about one or more of these spatial axes**.** The major drawback to the joint coordinate system technique is that an orthogonal coordinate system is not guaranteed (Robertson et al., 2004, Hamill and Knutzen, 2003).

#### 2.3.4.4.3 Helical Angles

The Helical angles approach consists of defining a position vector and an orientation vector. Thus, any finite movement from a reference position can be described in terms of a rotation about and translation along a single axis (helical axis) in space. This axis may not coincide with any of the defined axes of the local coordinate system, giving the instantaneous position and orientation of one local coordinate system with respect to the other (Spoor and Veldpaus, 1980).

### 2.3.4.5 Reference Systems in the Eggbeater Kick

To investigate the eggbeater kick technique it is required the use of references systems. Sanders (1999a) and Homma and Homma (2005) reported several hip, knee, and ankle joint motions (e.g. flexion-extension, abduction-adduction, internal-external rotation, inversion-eversion) involved in the eggbeater kick movement. These motions can be described using reference systems that can indicate the position and orientation of each lower limb segment (i.e. thigh, shank, foot). That allows determining the relative orientation between the reference systems of two lower limb segments, and providing an accurate description of the specific motions involved in the eggbeater kick and their anatomical meaning.

### 2.3.5 Kinetics

Kinetics, particularly methods to calculate the centre of mass (COM) of a body, are essential in this study to determine the position of the lower limbs system's COM (thighs, legs, feet) during the eggbeater kick. An accurate calculation of the COM allows calculation of the vertical force produced during the eggbeater kick cycle to establish a performance indicator that can be associated with other variables.

#### 2.3.5.1 Methods of Calculating COM

Body segment parameter data including segment masses, and segment mass centre locations relative to the segment endpoints, are required to calculate the centre of mass. The techniques available to obtain estimates of these parameters include studies of cadavers, mathematical models, and data from radiation and MRI techniques.

##### 2.3.5.1.1 Data from Cadavers

Dissection techniques have been used to advance the understanding of human physiological and biomechanical functions. Details of the planes of dissection recorded by Dempster (1955), resulted in a degree of standardisation of methodologies for subsequent research. By studying eight Caucasian male cadavers (52-83yrs; mass: 49.43-72.11 kg), Dempster quantified both segmental centres of gravity with a balance plate and volumes using immersion methods. The mass moments of inertia of each

segment were calculated around the transverse (through the centre of mass) and parallel axes (through the centre of the proximal joint) by a free swinging pendulum system.

Using similar techniques, Clauser et al. (1969) dissected thirteen Caucasian male cadavers (49.31 ± 13.69yrs; 172.72 ± 5.94 cm; 66.52 ± 8.7 kg) and calculated the segmental mass, volume and centre of mass. This author calculated a series of regression equations that could estimate segmental parameters, based on his anthropometric measurements. These included the length, circumference and breadth/ depth of each body segment. Additionally, one hundred and sixteen anthropometric measurements and segmental properties using methods similar to Clauser et al. (1969) were calculated from both the entire cadaver and individual segments. Some of the results from this study were compared to data collected by Santschi et al. (1963) on living subjects and it was concluded that a satisfactory level of agreement exists between the two datasets. Chandler et al. (1975) considered their data should be interpreted with caution and not be assumed to reflect population parameters due to the limited subject sample. However, others authors still consider their data the most valid estimates of the segment moments of inertia available that can be used as a criterion for comparing other estimates (Miller and Nelson, 1973, Jensen and Nassas, 1988).

#### 2.3.5.1.1.1 Limitations with Cadaver Data

Many concerns have been identifies with respect to the interpretation and implementation of data from cadaver studies. Differences between the density of tissues in cadavers and living subjects (Katch and Gold, 1976, Zatsiorsky, 2002) have been

highlighted in the literature. This would raise questions about using cadaver data in living subjects. Additionally, the limited sample size and diversity with respect to race, age, height or weight may not be representative of the average adult population.

Therefore, when impossible to obtain direct data from subjects, cadaver data can be used cautiously to estimate the segmental properties (Katch and Gold, 1976, Plagenhoef et al., 1983).

#### 2.3.5.1.2 Additional Techniques and Computations to Calculate Body Segment Parameters

Regression equations have been formulated to try to overcome the difficulty of ascertaining segmental characteristics from living subjects. Based on certain anthropometric measurements, these equations calculate the appropriate segmental information with minimal subject intrusion. Initially a fixed relationship determined from cadaver data between the segment and that of the total body was assumed. This approach is very fast and easy to use (Sprigings et al., 1987) since it does not need any prior anthropometric measurements on the subject being analysed. Using the cadaver data of Dempster (1955), Barter (1957) presented regression equations that predicted the segment mass as a function of total body weight. With the use of direct proportions or regression equations, obtaining information on body segment parameters was simplified. However, the limited number of Caucasian adult male cadavers (with the exception of Zatsiorsky and Seluyanov (1983) used in most studies is a reason to interpret data with caution.

Radiation techniques based on the principle that photon transmission is dependent on the mass and composition of the body have been used to estimate segment mass. Zatsiorsky

and Seluyanov (1983) developed the gamma-mass scanning technique to quantify the segment mass and its distribution directly. The radiation was measured before and after it passed through the body, providing an indication of the segment density. de Leva (1996) highlighted the limitations of Zatsiorsky and Seluyanov (1983) results, noting that this kind of data is rarely preferred to cadaver data, due to the use of bony landmarks as reference points for locating the segmental centre of mass and defining segment lengths. Computed Tomography (CT) is an alternate radioactive technique used to measure in vivo segmental inertial parameters. Studies have shown that there is generally good agreement between the CT-derived bone, muscle and fat density values in comparison to traditional methods as described previously (Ackland et al., 1988, Huang and Wu, 1976). Ackland et al. (1988) found that there was a 1.9% difference between the CT-derived density values and the hydrostatic weighing values for a cadaver leg when comparing it to CT scans. Similarly, Rodrigue and Gagnon (1983) calculated density and volume within the range of 0.1-4.8% and 5.4-35.9% respectively, of the values obtained by direct measurement.

Using magnetic resonance imaging (MRI) Mungiole and Martin (1990) examined the lower leg inertial properties for 12 adult male athletes (age: 28.59 ± 3.41yrs; mass: 66.24 ± 3.72 kg; height: 177.69 ± 4.54 cm). Their estimates, especially the centre of mass data, closely agreed with other methods.

Based on mathematical modelling techniques Ackland et al. (1988) showed that the assumption of segment uniform density was invalid based on the 10% variation in density along the segment length. However, it only produced minor errors when estimating inertial parameters of leg segments. Mungiole and Martin (1990) supported

this argument when observed less variation in segment density (2.3%) along the longitudinal axes of the leg.

#### 2.3.5.1.3 Human Body Models

The first human body model was developed by Hanavan (1964) to calculate the segmental and total body principal moments of inertia and centre of mass location. It consisted of a 15-segment computerised model (Fig. 2.4) and incorporated Barter (1957) regression equations, based on 12 cadavers, to estimate the segment masses. Twenty-five anthropometric measurements, including body weight, height, segment lengths and girths were required to be inputted to personalise the model for each subject.

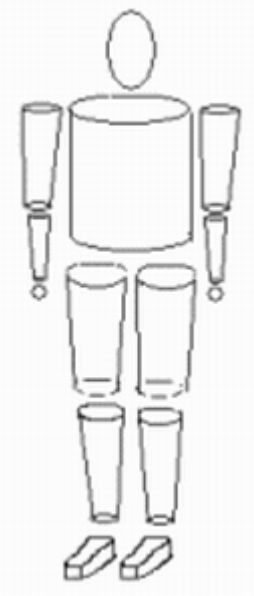

Figure 2.4. Illustration of Hanavan's segment model.

The oversimplified geometrical shapes and uniform density assumption constitute the main limitations for this model (Bartlett, 1999, Jensen, 1978).

A later model developed by Hatze (1980) was made subject-specific by inputting 242 anthropometric measurements for each subject. It allowed for sex differences by use of different density functions and mass distributions and the use of more complex segment structures that were neither simple nor symmetrical (Bartlett, 1999) (Fig. 2.5).

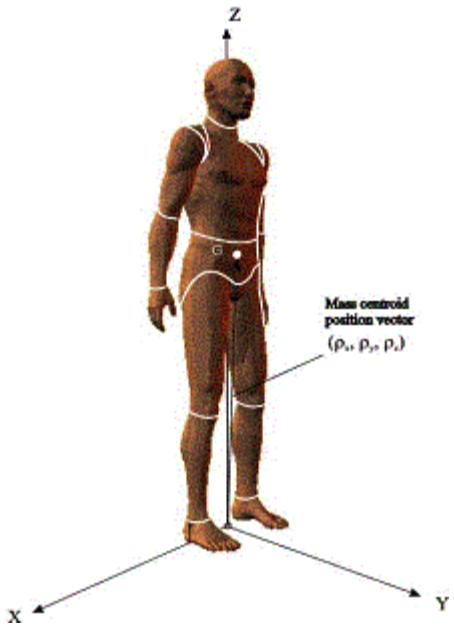


Figure 2.5. Illustration of Hatze's segment model.

Overall accuracy of the model was approximately 3%, and subject to a maximum error of about 5% for each of the 17 segments, average error results between the measured and computed total body mass which was reported as 0.06%. Accuracy and fast

computation time were recognised as the main advantages of this method (Hatze, 1980, Sprigings et al., 1987). The major drawback of this method is the time required (approx. 80mins/subject) to gather the 242 subject-specific anthropometric measurements (Hatze, 1980, Sprigings et al., 1987, Bartlett, 1999).

More recently Yeadon (1990) developed a model that divided the body into 11-segments and subdivided the body into 39 stadium solids, and 1 semi-ellipsoid for the cranium (Fig.2.6), and included 95 anthropometric measurements (34 lengths, 41 perimeters, 17 widths and 3 depths). This model is recognized as having an acceptable level of accuracy without being constrained by the time consuming subject specific measurements from Hatze (1980).

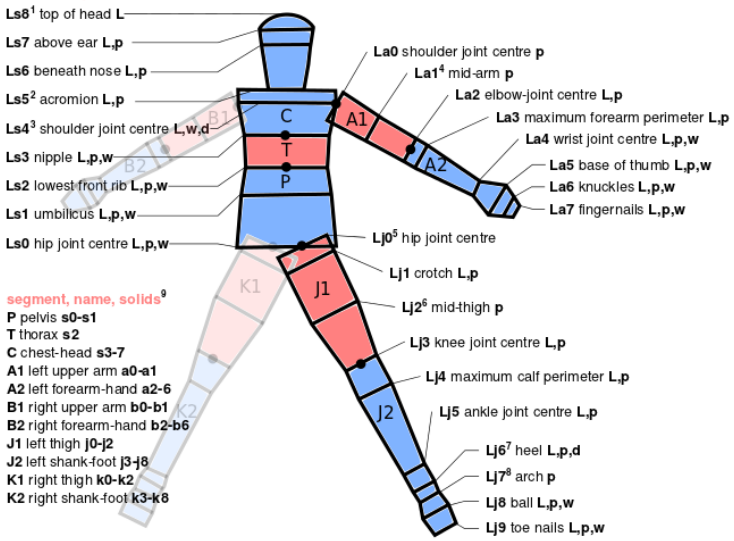


Figure 2.6. Yeadon's segments and subsegments (adapted from Dembia (2011)).

#### 2.3.5.1.3.1 Jensen's Elliptical Zone Method

The Matlab programme (Deffeyes and Sanders, 2005) used to calculate the body segment parameters in this study is based on the Jensen's 'elliptical zone' method. For this reason, the description of Jensen (1978) initial and modified models is done separately.

Jensen (1978) developed a 16-segment model where segments were composed of elliptical zones 2cm wide (Fig. 2.7). This allowed a more precise recognition of the segment's shape. Segment densities were assumed and used with the calculated segment volumes to give the segment masses. Two photographs were taken of the subject lying in a prone anatomical reference position, one from the frontal view and the other from the lateral view. Next, the segments were sectioned into 2cm ellipses and radii is calculated from both the front and lateral views. Using the formulas developed by Jensen (1978) the volume, mass, centre of mass location and moments of inertia of each elliptical cylinder were calculated. Segment mass is obtained by summing the masses of the elliptical zones within each segment and the location of the segments centre of mass is calculated by summing the moments of the elliptical zones using the positions of the centroid of the cylinders with respect to the proximal endpoint as the moment arm (Deffeyes and Sanders, 2005). Finally, the moment of inertia of the segments for the anteroposterior, mediolateral and proximal-distal axes of the segment are calculated by summing the local and remote moment of inertia terms in accordance with the parallel axis theorem (Deffeyes and Sanders, 2005).

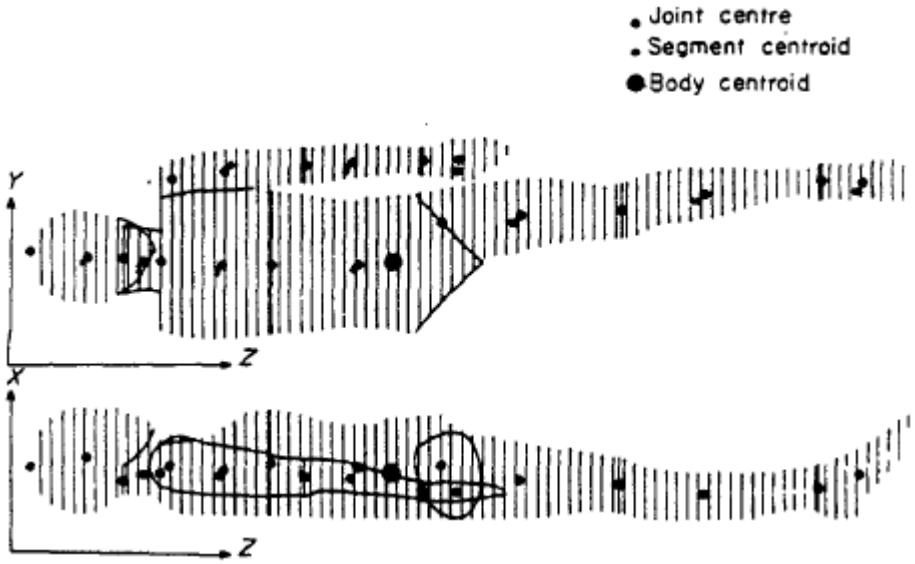


Figure 2.7. Illustration of Jensen's elliptical model (from Jensen (1978)).

Sanders et al. (1991) applied the elliptical zone method to measure whole body mass of two male and two female subjects and found that the estimates were within ± 3%, which is within the similar range of error previously reported by Jensen (1978) of 1.16, 1.17, and 1.82 %, and are within the standard deviations reported by Jensen and Nassas (1988) of 2.63 % for the males. Wicke and Lopers (2003) validity study of Jensen's elliptical zone method volume functions tested 20 subjects: 10 males (24.3 ± 1.4yrs; 178.8 ± 6.6 cm; 75.4 ± 9.5 kg) and 10 females (23.8 ± 1.4yrs; 161.4 ± 6.1 cm; 62.7 ± 10.9 kg) and concluded that the volumes of several segments, as well as the whole body provide valid volume estimates.

Using the same technique established by Jensen (1978) with the exception of the subject's body position (upper limb body segments are not aligned vertically), Deffeyes

and Sanders (2005) developed a Matlab software (eZone) that combines the functions of digitising digital photographs to obtain the diameters of the ellipses, with the ability to calculate the body segment parameters data. Subsequent studies evaluating this software reported the whole body mass within 5% of its actual value (Deffeyes and Sanders, 2005) and mean differences between calculated and real values for the whole body mass as -0.2 ± 0.9 kg or -3 ± 1.3% (expressed as a percentage of the real body mass values) (Psycharakis, 2006).

The abovementioned studies indicate that the eZone software offers an accurate method of obtaining anthropometric data. Combined with precise digitising it can calculate the centre of mass position of the whole body or particular body segments and derive the respective velocity and acceleration. In this study, the vertical force produced during the eggbeater kick, was calculated using the acceleration of the lower limb system which is determined using the calculated position of its centre of mass.

### 2.3.6 Electromyography

One of the purposes of this study is to investigate the muscle activity of lower limb muscles during the eggbeater kick. This knowledge allows improving the performance and training of the eggbeater kick. Electromyography is the tool that can detect and record the muscle activity. Consequently, it is necessary to understand the EMG signal, particularities of its application in the water and its relationship with force and fatigue.

#### 2.3.6.1 The EMG Signal

Muscles constitute approximately 45% of body weight (Huxley, 1965, Brooks et al., 1996). Skeletal muscle is an important tissue for bioenergetics homeostasis during rest and exercise, it is not only the major site of energy transduction, but it is also a major site of energy storage (McArdle et al., 2001). Skeletal muscle is the fundamental basis of human biodynamics. Human movement through the action of muscles requires conversion of the chemical energy in adenosine triphosphate (ATP) to mechanical energy. The muscle action begins at the neuromuscular junction when a motor unit pool is recruited with an electrical impulse by the motor neuron. The action potential (Fig. 2.8) causes the depolarization of the T-tubule system and $Ca^{2+}$ is released from the lateral sacs of the sarcoplasmic reticulum, triggering the excitation-contraction coupling mechanism (Langley and Telford, 1980, McArdle et al., 2001). Since multiple muscle fibres are innervated by a single motor neuron, the firing of a motor neuron results in the near-simultaneous discharge of many muscle fibres. The summed activity of all this muscle fibres results in the generation of a motor unit action potential. The amplitude of the motor unit action potential is determined by the individual muscle fibre action potentials, summed both temporally and spatially. The action potentials responsible for recruiting the motor units and the respective contraction in the skeletal muscle are the signals recorded by electromyography.

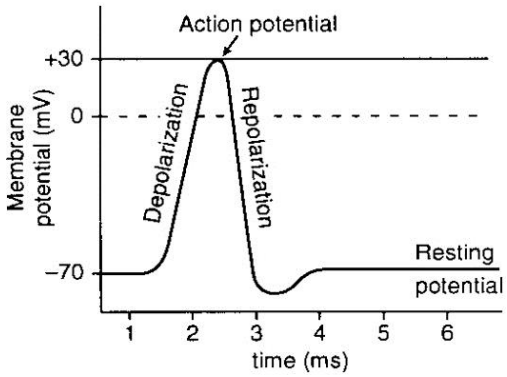


Figure 2.8. Illustration of the action potential mechanism.

The EMG signal is the electrical manifestation of the neuromuscular activation associated with a contracting muscle (Basmajian, 1978). At any point in time, the EMG signal is a composite electrical sum of all of the active motor units. A large peak in the EMG signal might be the result of the activation of two or more motor units separated by a short interval. As the signal has both positive and negative components, when the signal crosses the baseline, a positive phase of one motor unit action potential is likely balanced by the negative phase of another (Yao et al., 2000).

#### 2.3.6.2 Factors Affecting the EMG Signal

Many factors directly affect the EMG signal (De Luca, 1997). These include physiological, anatomical of biochemical factors such as the number of active motor units (affects the amplitude of the signal) (Yao et al., 2000) fibre type (Kupa et al., 1995), blood flow (Larsson et al., 1995), depth and location of the active fibres with respect to the electrode detection surfaces or the amount of tissue between the surface of

the muscle and the electrode (De la Barrera and Milner, 1994, Lindstrom and Petersen, 1983). Some of these factors are also related with the muscle fiber conduction velocity. The muscle fibre conduction velocity has been shown to strongly influence the EMG signal (Arendt-Nielsen and Zwarts, 1989, Zwarts and Arendt-Nielsen, 1988, Arendt-Nielsen and Mills, 1985). Muscle fibre conduction velocity has been shown to depend upon a number of muscle fibre characteristics such as the intramuscular milieu (Juel, 1988), temperature (Stalberg, 1966), muscle fibre diameter and muscle morphology (Stalberg, 1966, Gantchev et al., 1992, Li and Sakamoto, 1996), muscle length (Arendt-Nielsen et al., 1992, Kossev et al., 1992), fibre type (Hopf et al., 1974, Sadoyama et al., 1988) or muscle fatigue (Sadoyama et al., 1985, Zwarts and Arendt-Nielsen, 1988).

Extrinsic factors that can affect the EMG signal are controlled by the investigator and are associated with the electrode structure, its placement on the surface of the skin above the muscle, electrode configuration such as the area and shape of the electrode detection surfaces (Zipp, 1978) or the distance between the electrodes detection surfaces (Fuglevand et al., 1992). Additionally the location of the electrode on the muscle surface (Mesin et al., 2009, Rainoldi et al., 2004, Campanini et al., 2007) and the orientation of the detection surface with respect to the muscle fibres have been shown to affect the value of the measured conduction velocity of the action potentials and, consequently the amplitude of the signal (Zedka et al., 1997, Weir et al., 1999).

In the process of recording an EMG signal, the source of the generated signal can come additionally from any electrical fields or artifacts that occur around an electrode and lead cables (electronics components, ambient noise from sources of electromagnetic

radiation, motion artifacts or movement of the cable connecting the electrode to the amplifier) (Huigen et al., 2002).

#### 2.3.6.3 Issues with EMG Recording in the Eggbeater Kick

To record quality EMG signal during the eggbeater kick two critical particularities of the present study need to be addressed: 1) the eggbeater kick is an intense, dynamic movement that involves several joints and motions, and 2) the signal was detected underwater.

To record the muscle activity of the particular muscles of interest it is important to reduce the amount of 'crosstalk' (i.e. muscle activity from muscles nearby) detected by the electrodes. In the eggbeater kick where several muscles in the lower limb are active at the same time during the cycle this issue is critical for good quality of the EMG signal of particular muscles. The use of double-differential electrodes was specifically designed to reduce the presence of EMG crosstalk emanating from muscles underneath and adjacent to the muscle of interest. It works on the principle that a signal originating from a source further away (some other muscle) will arrive at adjacent detection surfaces with less relative latency than a signal which originates from the muscle beneath the electrode. By performing two subtractions, the signals with short relative latency (those originating from distant sources) cancel out. This causes the output amplitude of the signal to be approximately 1.5 times larger than the single differential electrode (De Luca et al., 2012, De Luca and Merletti, 1988). Additionally, because the EMG system used in this study is wireless, possible artifact around the cables were eliminated.

In general, recording an EMG signal in a water environment is no different from the common methodology of surface EMG, but there are certain specifics in that case. The EMG signal is an electrical impulse very sensitive to changes in conductivity that can be affected by the contact of water with the EMG sensors and electrodes, making it essential to isolate it from the water. Great attention has been paid in the literature to the issue of the different effect of water and dry environments on the nature of the EMG recording itself (Kelly et al., 2000, Masumoto et al., 2004, Masumoto et al., 2005, Rainoldi et al., 2004, Veneziano et al., 2006), with several works reporting decrease in the EMG signal in the underwater environment (Clarys et al., 1985, Fujisawa et al., 1998, Kelly et al., 2000, Poyhonen et al., 1999, Poyhonen et al., 2001) and others (Rainoldi et al., 2004, Veneziano et al., 2006) showing no decrease in the signal amplitude as long as the electrodes were protected by water-resistant taping. In their work, Rainoldi et al. (2004) demonstrated (1) that water leakages can cause a huge decrement in the sEMG signals; (2) that electrodes have to be properly protected in order to provide reliable results. This leads to complex experimental set ups to minimize the exposure of the equipment to the water and restricted waterproofing techniques that significantly limit the duration of test protocols (lifespan of the waterproofing). These two issues have been the main difficulties to perform underwater EMG measurements and implement appropriate standards.

Most underwater EMG studies have focused on: isometric contractions and the differences between the dry and underwater signal (Rainoldi et al., 2004, Pinto et al., 2010, Carvalho et al., 2010), dynamic knee extension-flexion (Poyhonen et al., 1999, Poyhonen et al., 2001, Tovin et al., 1994, Coulange et al., 2006), in water walking

(Masumoto et al., 2004, Masumoto et al., 2005, Miyoshi et al., 2004, Chevutschi et al., 2007, Jung et al., 2010) and running (Kaneda et al., 2008, Silvers and Dolny, 2011). In sports, underwater EMG recordings have been used to study freestyle swimming (Caty et al., 2007, Clarys et al., 1983, Rouard and Clarys, 1995, Yoshizawa et al., 1983), sculling motions (Rouard et al., 1997), flip turn (Araujo et al., 2010) and backstroke start (Hohmann et al., 2008, De Jesus et al., 2011). The most frequently used waterproofing technique to isolate the EMG electrodes has been described as covering the electrodes with only water-resistant taping and transparent adhesive film (Chevutschi et al., 2007, Hohmann et al., 2008, De Jesus et al., 2011, Kaneda et al., 2008, Silvers and Dolny, 2011, Poyhonen et al., 2001) or with additional foam pads (Masumoto et al., 2004) to prevent water from contacting the skin-electrode interface and to prevent electrical leakage during the tests. Even though most of the abovementioned studies consist of stationary activities (i.e. isometric contraction studies), very limited (e.g. knee or elbow extension) or moderate velocity movements that are hard to compare with the maximum intensity eggbeater kick performed in this study, the swimming studies at higher intensities and more aggressive to the electrode isolation indicate that successful water proofing techniques are available.

#### 2.3.6.4 EMG/Force Relationship

The EMG signal recorded during the eggbeater kick can provide useful information about the role of the studied muscles in the cycle. The amplitude of the signal can indicate when a particular muscle is more active and producing more force. However,

the observation that the EMG signal amplitude generally increases as the force and/or contraction velocity of the muscle increases only provides a qualitative indication of a relationship between the variables (De Luca, 1997). This relationship is hard to establish due to a complex interaction of anatomical, physiological, detection, and calculation factors. Cross talk and the stationarity (maintaining signal characteristics in time) of the signal are the main issues when establishing this relationship. Signal stationarity is greatly affected by two factors: (a) stability of the electrode position with respect to active muscle fibers (movement would affect the amplitude of the motor unit action potentials and possibly bring the electrode to the territory of an active motor unit not previously detected), and (b) stability of the motor unit activation pattern (De Luca et al., 1996). In its turn, surface EMG crosstalk is the EMG signal detected over a non-active muscle and generated by a nearby muscle, it is present in most contractions and efforts can be made to eliminate or minimize it (e.g. double differential electrodes).

In isometric contractions the EMG/Force relationship becomes monotonic but still remains problematic to establish a linear one. First, because the detection volume of the electrode is smaller than the volume of the muscle, the number of motor unit action potentials detected by the electrode is less than the number active in the muscle. For fixed-size electrodes, this problem is more pronounced in larger muscles. Secondly, as the muscle force output increases beyond the level of a newly recruited motor unit, the firing rate of the recruited motor unit increases but the force contribution of the motor unit does not increase. As each motor unit action potential continues to provide energy to the EMG signal, the force contribution saturates to a near constant value. This

nonlinear relationship causes the amplitude of the EMG signal to increase more than the force output (De Luca et al., 1996).

The reports on the relationship between EMG magnitude and muscular force are controversial. This relationship has been described as linear by some authors (Lippold, 1952, Knowlton et al., 1956, Moritani and deVries, 1978, Kawazoe et al., 1981, Milner-Brown and Stein, 1975, Bouisset and Maton, 1972, Jacobs and van Ingen Schenau, 1992, Milner-Brown et al., 1975), but other studies have reported non-linear relationships between force and EMG amplitude (Lawrence and De Luca, 1983, Alkner et al., 2000, Metral and Cassar, 1981, Stokes et al., 1987, Maton and Bouisset, 1977, Thorstensson et al., 1976, Woods and Biglandritchie, 1983).

In an anisometric contraction, the relationship between signal amplitude and muscle force is affected by various mechanical, physiological, anatomical, and electrical modifications that occur throughout the contraction. Several factors limit the force/EMG signal relationship: a) in most joints, the length of the moment arm changes with muscle length b) as the length of the muscle fibers changes so does the force generated by the fiber c) the inertia components of the net torque (De Luca, 1997) and d) the force-length relationship of the muscle fibers varies nonlinearly, and the shapes of the motor units action potentials that construct the EMG signal are altered because the relative position of the electrode fixed on the skin surface changes with respect to the contracting muscle fibers (De Luca and Forrest, 1973).

The force-EMG relationship in dynamic contractions has been studied by several investigators. Using the elbow extensors, Aoki et al. (1986) reported a linear relationship between kinematic variables such as peak velocity and acceleration, and EMG

amplitude. Similar relationships have been obtained for the elbow flexors (Barnes, 1980, Bouisset and Maton, 1972, Komi, 1973) and plantarflexors (Bigland and Lippold, 1954). Other studies have reported a nonlinear force-EMG relationship during rapid contractions in the first dorsal interosseous (Bronks and Brown, 1987) or no relationship between amplitude and angular velocity in knee extensor muscles (Gerdle et al., 1988). As the muscle shortens, the EMG-force relationship becomes nonlinear (Currier, 1972, Edwards and Lippold, 1956) meaning that more linear relationships are observed at longer muscle lengths. This can explain the variation of the EMG-force relationship slope with joint angle (Bouisset, 1973).

The evidence indicates that for dynamic activities such as the eggbeater kick the EMG signal amplitude should be interpreted with caution. Quantitative comparisons between muscles or between subjects are not possible and any assumption of the force being produced can be misleading. Additionally, because the eggbeater kick in this study is executed at maximum intensity all the time, it would be expected that fatigue levels result in a decrease of force that is not accompanied by an equal decrease of EMG amplitude.

#### 2.3.6.5 EMG and Fatigue

One of the main purposes of this study is to compare the muscle activity of six muscles at different fatigue levels. That requires an understanding of the relationship between muscle fatigue and the EMG signal, and the different methods available for signal processing and analysis for that purpose.

Surface electromyography signals are usually processed by using some data reduction techniques to obtain quantities describing their amplitude and dominating frequency (Farina and Merletti, 2000). When force produced by a muscle (or moment of force produced at a joint) is kept unchanged with time, fatigue results in a downward shift of the frequency spectrum of the signal and increase in the signal amplitude (Ferdjallah et al., 2000, Tarata, 2003). The most common procedure is to monitor the relative changes in the mean and median power frequencies and to relate these measures to the initial value or non-fatigue state mean and median power frequencies. The shift towards lower frequencies of the EMG signal frequency spectrum has been used as an estimator of muscle fatigue (Kaljumae et al., 1994, Gerdle et al., 1989, So et al., 2002, Lindstrom et al., 1974, Tesch et al., 1983). This definition of fatigue is always correct when an isometric muscle contraction protocol at a given performance is used. It was noted that the relationship between EMG power frequency and fatigue development, as observed in isometric protocols, cannot be simply applied in dynamic exercise (Jansen et al., 1997).

One limitation of spectral analysis of the EMG signal to investigate fatigue is the underlying assumption that the signal is stationary. This is because the spectral analysis requires recording of the EMG signal over a substantial time period meaning the temporal aspect of the signal changes (Karlson et al., 1999). When the muscle contracts in dynamic conditions, the myoelectric signal generated by the muscle may no longer be considered as a stationary process. If the signal is not stationary, classical spectral estimation techniques should not be used because the classical signal analysis techniques cannot cater for the movement component of the signal, and noise (Karlsson and Gerdle,

2001). Stability of the electrode position with respect to the active muscle fibers and the decrease of muscle fiber conduction velocity with greater muscle length are the main reasons (De Luca, 1997, Morimoto, 1986, Kamen and Caldwell, 1996).

Fatigue also has a relationship with the amplitude of the EMG signal. The changes in EMG amplitude during fatiguing isometric contractions are well documented. During a maximal isometric contraction, EMG amplitude declines (Bigland-Ritchie, 1979, Gerdle and Fugl-Meyer, 1992, Moritani et al., 1986, Stephens and Taylor, 1972). This decline is due to decreases in motor unit firing rate (Bigland-Ritchie et al., 1983), neuromuscular propagation failure (Bellemare and Garzaniti, 1988) and the slowing of conduction velocity produced by the added $K^+$ ions and the depletion of the $Na^+$ inside the muscle fiber.

During sustained submaximal contractions, EMG amplitude is initially stable but then increases (Krogh-Lund and Jorgensen, 1991). This is due to the need for increased motor unit recruitment to maintain the required force (Fuglevand et al., 1993, Krogh-Lund, 1993, Maton and Gamet, 1989).

Similar to the spectral characteristics, the interpretation of EMG signals from dynamic contractions is much more difficult because movement introduces additional factors that affect their characteristics. Muscle force capacity is highly dependent on fiber length and is also inversely related to shortening (concentric) velocity (Hill, 1938, Wilkie, 1950) and directly related to lengthening (eccentric) velocity (Joyce et al., 1969, Komi, 1973). Generally, EMG amplitude has been observed to increase during repetitive, dynamic submaximal efforts (Arendt-Nielsen and Sinkjaer, 1991, Bouissou et al., 1989, Tesch et al., 1990) and decrease during maximal efforts (Gerdle et al., 1987, Komi and Tesch,

1979). Given the maximal and dynamic nature of the eggbeater kick movement performed during the test it is expected that a decrease of the amplitude of the EMG signal should be related with increasing fatigue and this should be evident across the fatigue levels.

## 2.4 Summary of Literature Review

While there are some indications of what characteristics in the eggbeater kick technique are associated with performance, the relationship between them and their relative impact in the production of vertical force during the cycle remain unclear. Additionally, there are no reports in the extant literature about fatigue induced changes in the eggbeater kick technique, differences between the dominant and non-dominant lower limbs during the movement, or the particular role of the muscles involved in the cycle. Having this information would allow improvement in the technique and conditioning of the eggbeater kick through bespoke training programs.

To investigate these issues it is necessary to quantify the vertical force produced during the cycle, and surface EMG to assess the role of particular muscles in the eggbeater kick cycle.

# Chapter Three: Methods

# 3 Methods

This chapter describes the methodological approaches used to address the previously stated purposes of this study. It covers the subject preparation, set up, data collection procedures, data analysis and statistical analysis of the kinematic, kinetic and EMG data.

## 3.1 Participants

Twelve national level male water polo players (aged: 22.41 ± 1.50 years; body mass: 81.25 ± 6.08 kg; height: 184.75 ± 5.11 cm) from two Scottish water polo clubs were tested. Participants were required to be in full training and competition, and free of injury or any limiting medical condition.

Before all testing sessions participants were provided with a volunteer information sheet (Appendix A), which contained a brief purpose of the study, the requirements of the participants, and the testing protocols. The possible risks the subject might experience and the benefits for their participation were also outlined. Subsequent to reading the volunteer information document, and the investigator addressing any concerns expressed by the participants, each player signed the supplied informed consent form (Appendix B).

All testing procedures were approved by the University of Edinburgh Ethics Committee. To protect the players' identities, individual data was anonymized. Thus, a number given to each player is used throughout this thesis.

## 3.2 Participant Preparation

### 3.2.1 Skin Markers

All participants wore brief water polo trunks so that all joints were clearly visible and easy to identify. Subjects' height and body mass measurements were recorded using a stadiometer and weighing scales (Seca 780-2317008).

Participants were marked before the testing protocols for two purposes: i) to track the movement of the player's lower limbs for 3D kinematics calculations and ii) to enable the calculation of the inertial properties of the limbs using the elliptical zone method (Ezone) (Jensen, 1976, Deffeyes and Sanders, 2005).

To increase accuracy and reliability of digitizing and subsequent calculations, participants were marked with skin markers (black) consisting of wax based cream (Grimas Crème Make up) applied by a 45mm diameter sponge. For better visibility during the digitizing process for the foot ($1^{st}$ interphalangeal and $5^{th}$ metatarsophalangeal joints) and ankle (lateral malleolus - fibula and medial malleolus - tibia) joints, red and black plastic spherical markers (2cm diameter ) were attached using adhesive tape (Leukotape-P) and hot glue. Although this kind of marker can produce more drag during the movement, it was determined during pilot work that given the speed of the feet, for clear visibility of foot markers it was necessary to use ball markers. Table 3.1 describes the markers used for the 3D kinematics.

Table 3.1 Location of the body markers for digitizing

| Marker | Location | Type of marker | Number of markers |
|---|---|---|---|
| Pelvis | Iliac crest | Wax based cream | 1 |
| Hip | Great trochanter | Wax based cream | 1 |
| Thigh | Half way in the line from hip marker to lateral knee marker | Black Ball | 1 |
| Knee (Medial marker/ Lateral marker) | Medial side of the knee | Wax based cream | 2 |
| | Lateral side of the knee | Wax based cream | |
| Shank | Half way in the line from lateral knee marker to lateral ankle marker | Black Ball | 1 |
| Heel | Calcaneus bone | Wax based cream | 1 |
| Ankle (Medial marker / Lateral marker) | Medial malleolus - tibia | Red Ball | 2 |
| | Lateral malleolus - fibula | Red Ball | |
| Foot (Medial marker/ Lateral marker) | 1st Interphalangeal | Black Ball | 1 |
| | 5th Metatarsophalangeal | Black Ball | 1 |

For the Ezone method calculations, markers additional to those applied as black wax based crème described above were necessary to define specific the upper body segments. Since these markers were not used for the testing trials, black tape was used. These additional markers were placed at the following locations: mandible angle, 2nd cervical

vertebra, 7th cervical vertebra, axes of the head of each humerus, acromioclavicular joint, hip and the line of the xiphoid process, olecranon process of ulna, wrist axis, 3rd distal phalanx, greater tubercle of the humerus and vertex. Table 3.2 shows the additional markers used for the Ezone protocol.

Table 3.2. Location of the additional body markers for the Ezone.

| Marker | Location |
|---|---|
| Vertex | Vertex |
| Mandible | Mandible angle |
| Chin | 2nd Cervical Vertebra |
| Neck | 7th Cervical Vertebra |
| Trunk | Xiphoid Process Line |
| Shoulder | Humeral Axis |
| Shoulder | Acromioclavicular Joint |
| Shoulder | Greater Tubercle of the Humerus |
| Elbow | Olecranon Process of Ulna |
| Wrist | Wrist Axis |
| Hand | 3rd Distal Phalanx |

For the calculations of the height achieved and the weight + buoyancy a black tape on a white tape background was placed in the superior part of the sternum (manubrium). Overlaying the two tapes assured maximum contrast between both tapes and improved the durability of the tapes on the skin.

### 3.2.2 Surface Electromyography

For the surface electromyography (sEMG) collection, before the testing session, participants' skin was shaved and cleaned with alcohol swabs at the intended location of the sEMG sensors. After the skin was prepared electrodes were placed over each muscle following SENIAM (1999) and Hermens et al. (2000) recommendations (see Appendix B). Finally, each electrode was covered using Opsite Flexifix film to waterproof the area and taped with adhesive tape (Leukotape-P) for durability and resistance to movement (Figueiredo et al., 2013b, Figueiredo et al., 2013a) (Fig. 3.1). The muscles analysed using this method were: Right *Tibialis Anterior*, Right *Rectus Femoris*, Right *Biceps Femoris*, Left *Tibialis Anterior*, Left *Rectus Femoris*, Left *Biceps Femoris*. Figure 3.2 shows the final stage of participant preparation.

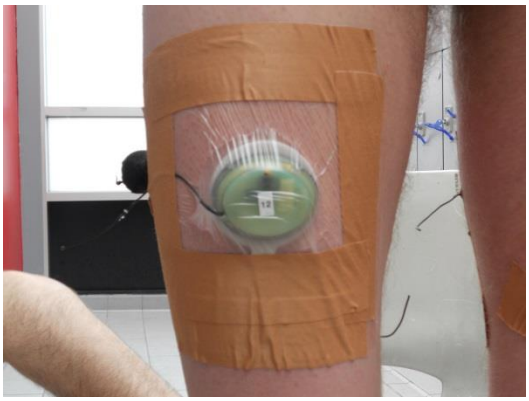

Figure 3.1. Individual muscle surface EMG waterproofing final stage.

Figure 3.2. Final result of participant preparation. Markers and EMG waterproofing.

## 3.3 Experimental Design

### 3.3.1 Swimming Pool Details

Data were collected in a 25m x 13.25m x 2m indoor swimming pool at 27C water temperature. Evenly diffused and distributed lighting at 1000 Lux was provided by large lights and reflectors.

### 3.3.2 Camera Settings

Five (4 cameras below and 1 above the water surface) portable ELMO PTC-450C cameras (PAL 470,000 pixels, 470 TV lines (H) x 420 TV lines (V) resolution, internal

sync. System, 1lx min. lumination), recorded the movement. These cameras were inside a waterproof box that could be attached in any place on the swimming pool wall thereby enabling optimal positioning to capture all markers by at least two cameras throughout the kick cycle. Camera sampling frequency was set at 25 frames per second, with an electronic shutter speed of 1/250 seconds, to reduce the blurring of the image that occurs when recording fast underwater movements. A frequency of 25Hz was considered adequate because most human movements have been reported to occur at less than 6Hz (fastest eggbeater kick cycle took approximately 0.45s (2.2Hz))(Bartlett, 1997), hence following the Nyquist Theorem. Additionally, being a movement totally executed underwater it is not subject to the typical high-frequency motions/vibrations resultant from impacts/shocks in dry land activities. In four sessions a 'gen-locked' JVC KY32 CCD camera (PAL 440,000pixels, 580 TV lines resolution, internal sync. system, 7.5lx min. lumination), with the same setup, was used to replace one of the portable cameras, this was due to water leaking into the portable camera box which diminished the picture quality. This type of camera is permanently fixed in the water in built boxes in the pool walls. Transparent perspex protective screens which normally shield that camera were removed for video data collection to reduce errors due to distortion and refraction (Kwon, 1999, Kwon and Casebolt, 2006). Each camera had an individual time code generator and was connected to a recorder. All time code generators were synchronized. The video recorded from the five cameras was synchronized to the same time using time codes imprinted on the video frames.

### 3.3.3 Calibration Frame

The 3D calibration frame (Psycharakis et al., 2005) was adapted from the one used by Psycharakis and Sanders (2009) and McCabe (2008). In this study only one third (1.5m length, 1.5m height and 1m width) of the original frame (4.5m length, 1.5m height and 1m width) was used because there was minimal movement in the X direction. Thus the frame dimensions for this study were (1.5m length, 1.5m height and 1m width). Using a smaller version made it easier to transport and set up. Also, the cameras were zoomed to this reduced space to achieve even greater accuracy and reliability of 3D coordinate calculation than that established by Psycharakis et al. (2005).

The legs supporting the calibration frame were shortened, resulting in the calibration frame being lower in the water. These changes were appropriate because when executing the eggbeater kick subjects adopt a vertical position with their lower limbs deeper than when swimming.

## 3.4 Testing Set Up

The cameras were placed in the pool as shown in Figure 3.3. Underwater cameras were placed at different heights to avoid errors with respect to the camera axes being in the same plane as the axes of the calibration frame plane and while ensuring that all control points were clearly visible (Fig. 3.4). The above water camera was placed at an elevated position (1m) to the water level (Fig. 3.5). All cameras were set up with a field of view enclosing the whole calibration frame plus some extra space (approx. 0.5m), to allow for the participant moving slightly from his initial position during the test.

After the camera set up the calibration frame was recorded for a period of 10s for calibration purposes. The calibration frame was then taken out of the water. During the test trial the players occupied the 3D calibrated space. To achieve that position, players were instructed to be aligned with the above water camera and four cones on the poolside aligned with the outer planes of the calibration frame.

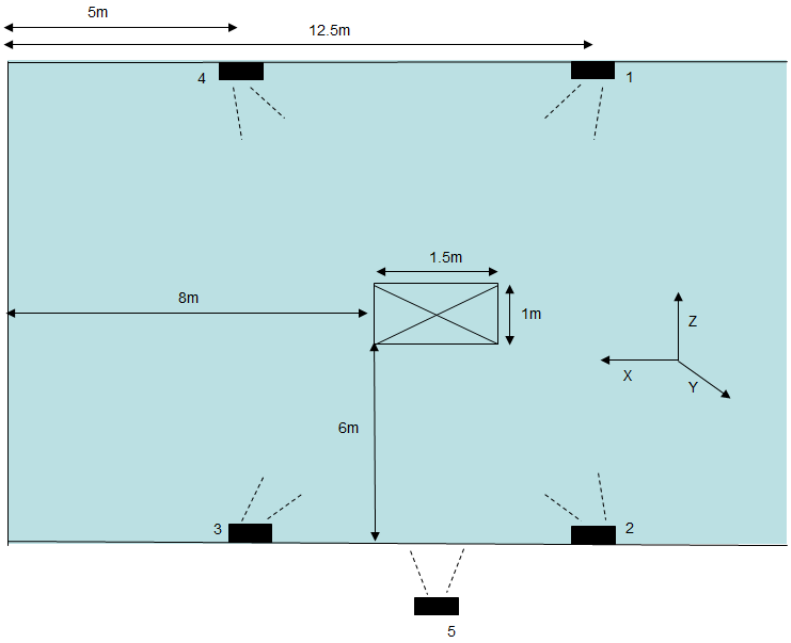


Figure 3.3. Position of the underwater (1-4) and above water cameras (5).


Figure 3.4. An underwater view of calibration frame from camera 1 perspective.

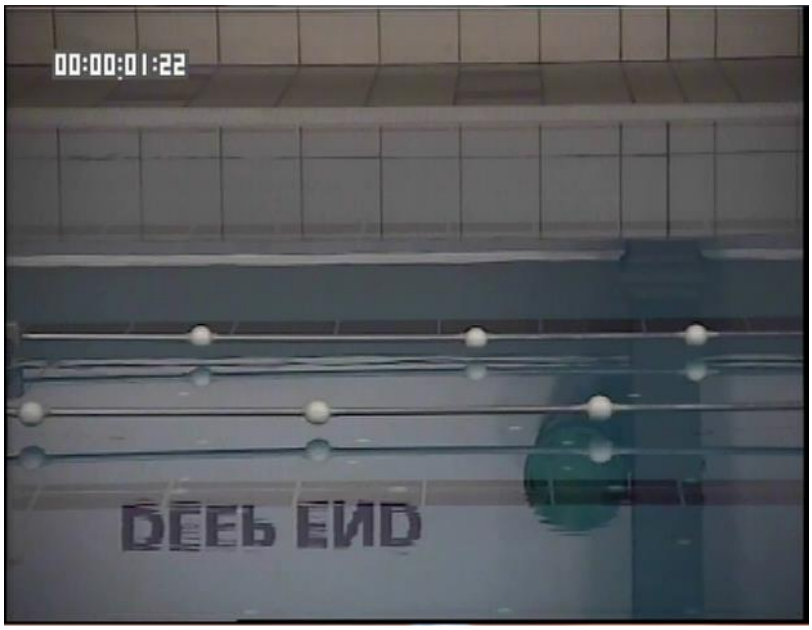


Figure 3.5. Above view of calibration frame from camera 5 perspective.

### 3.5 Testing Procedure

The data collection for each participant required one session (morning 9am-1pm). Participants had limited time (approx. 2min) to warm up before the eggbeater test trial. This was due to the short lifespan of the sEMG waterproofing and the necessity to keep the electrodes dry. After the warm up each player performed the eggbeater kick trial. Players were asked to hold their position at maximum height with the arms vertically extended out of the water until told to stop (Fig. 3.6), *'raise and hold your body as high as possible out of the water in the vertical position with your arms up'*. The test would be completed (player was told to stop) when the player could not keep the black tape (top of the sternum) above the water surface (participants were not aware of this). During the trial players were reminded to keep their arms still and received verbal encouragement to hold the position as high as possible.


Figure 3.6. Above view of the player during the eggbeater kick trial.

## 3.6 Data Collection Methods

### 3.6.1 Surface Electromyography

Surface electromyography (sEMG) was used to record the activity of three muscles on each leg (Tibialis Anterior, Biceps Femoris, Rectus Femoris). These muscles were chosen based on two factors: i) their anatomical function and perceived role in the execution of the eggbeater kick (Sanders, 2002) and ii) their anatomical location, since the use of surface electromyography requires muscles to be superficial. The sEMG signal was recorded using a wireless double-differential 16-channel sEMG system (KinePro) with a sampling rate of 1600Hz and with bandpass frequencies of 20Hz and 500Hz. Synchronization with the video was achieved using a synchronization device created at The University of Edinburgh (Figure 3.7). This device has two main parts: 1) a small box with an on/off button and an attachment for one of the sEMG sensors, and 2) a small box with a Light-Emitting Diode (LED) (Figure 3.6). When turning on (pressing the on/off button) the device, an electrical impulse was sent to the sEMG sensor (Figure 3.8) at the same time the LED went on. A camera placed in front of the LED box recorded the exact frame and respective time code of the event. This synchronized the video and EMG signal with an accuracy of ½ frame (± 0.02s).

Figure 3.7. Synchronization device.

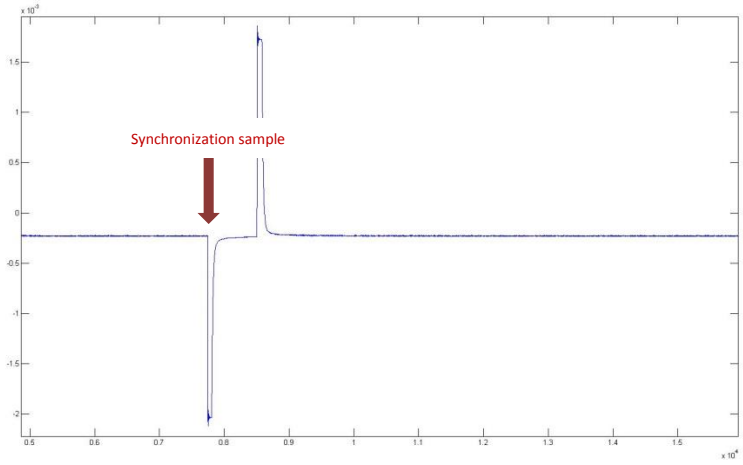


Figure 3.8. Representation of the electric impulse from the synchronization device. The red arrow shows the time when the electric impulse was created.

### 3.6.2 Maximum Voluntary Isometric Contractions

After the swimming pool test the sEMG signal for the Maximum Voluntary Isometric Contraction (MVIC) of each muscle was recorded using a Biodex dynamometer. This method provided an easier way to establish standard body position for the participant,

better control of the joint angle during the contraction and the recording of the force produced. Angles and duration of the contractions are described in table 3.3.

Table 3.3. MVIC test protocol.

| Muscle | Number of contractions | Duration (s) | Rest between contractions (s) | Movement | Angle of contraction (degrees) |
|---|---|---|---|---|---|
| Rectus Femoris | 2 | 5 | 15 | Extension of the knee | 90 |
| Biceps Femoris | 2 | 5 | 15 | Flexion of the knee | 90 |
| Tibialis Anterior | 2 | 5 | 15 | Dorsiflexion of the foot | 15 |

### 3.6.3 Anthropometric Data

Anthropometric data were calculated using the MATLAB software developed by Deffeyes and Sanders (2005). This software uses the elliptical zone method of Jensen (1976) which has been validated previously (Jensen, 1978, Yokoi et al., 1985, Jensen, 1986, Jensen and Nassas, 1988, Sanders et al., 1991, Wicke and Lopers, 2003) to calculate anthropometric data and the COM.

The anthropometric data collection method used in this study was very similar to the one used by McCabe (2008). This updated version requires three photographs taken simultaneously (frontal view and both side views) instead of two.

The two types of cameras used in this study were the Sony TX10 (16.2 megapixel) and the Panasonic HC-V100 (2.1 megapixel). With the exception of using one camera on both sides of the participant, set up and collection were identical to those used by McCabe (2008).

### 3.6.4 Weight + Buoyancy Measurement

In order to calculate the vertical force being produced during the eggbeater kick the weight + buoyancy had to be calculated. To calculate the weight + buoyancy participants were suspended in the vertical position using a swimming pool hoist and a harness (Figure 3.9). The harness was attached to the hoist through a load cell (transducer: 10.0v, maximum drop in each supply lead 0.25v; analogue to digital conversion: 5qV per digit to 135 qV in three ranges sensitivity, ±0.05% of full scale linearity, reading rate of 3 per second) that indicated the weight (KgF). A video camera was placed in front of the participant so that the black tape on the top of the sternum, the water surface and the load cell display were in view. Each participant was lowered very slowly until the black tape was no longer visible. This produced a video file where the height (distance from the black tape to water surface) and the corresponding weight + buoyancy (displayed in the load cell display x 9.8m/s$^2$) could be determined in each frame.

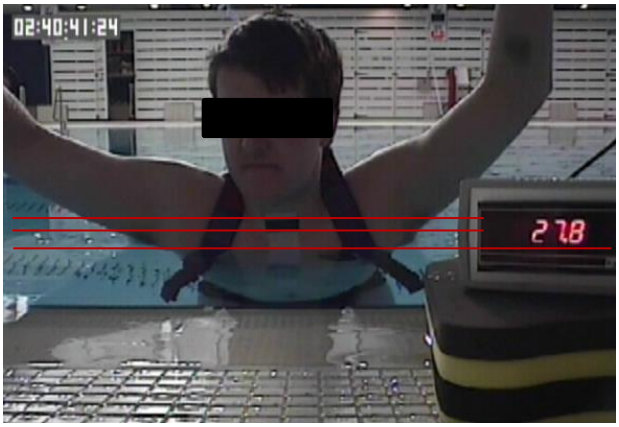


Figure 3.9. Camera view and digitising screen for weight + buoyancy assessment

### 3.6.5 3D Kinematics Dynamic Validation

A T shape wand with two markers at 48cm from each other was used to perform a dynamic validity test in the calibration space. Applying the same camera set up used to test each subject the wand was passed through the whole calibration space. The two markers were digitised in 131 frames across the calibration space.

## 3.7 Data Processing

### 3.7.1 Eggbeater Kick Trial Digitising

The use of four underwater cameras maximized the accuracy and visibility of the submerged markers, meaning that each marker was clearly visible by at least two cameras. The Ariel Performance Analysis System (APAS) version 13.3.0.3 from Ariel Dynamics Inc. was used to digitize the body markers of each frame and of each camera view and to calculate the 3D coordinates using the Direct Linear Transformation (DLT) (Abdel-Aziz and Karara, 1971) equations generated from the known coordinates of the

calibration frame. The first step of this process was to select (trim) the parts of the trial of interest. In this study the first nine cycles of the trial (first nine cycles after the indication to start the test is given and the participant stabilizes his position) correspond to the non-fatigued condition, the last nine cycles of the trial (last nine cycles before the black tape is no longer visible) correspond to the fatigued condition, and the nine cycles in the middle of that interval of time (first nine – last nine) correspond to the 50% time point condition. The beginning of a cycle was determined as the frame with largest extension of the knee. In order to prevent possible inaccuracies selecting this instant and to avoid inaccuracies at the ends of the data set due to signal processing and filtering procedures five extra frames at the beginning and at the end of the nine cycle selection were added.

The specified body markers were digitised in the following order: right $1^{st}$ interphalangeal, right $5^{th}$ metatarsophalangeal, right calcaneus bone, right medial malleolus – tibia, right lateral malleolus – fibula, right shank, right knee, right thigh, right great trochanter, right iliac crest, left $1^{st}$ interphalangeal, left $5^{th}$ metatarsophalangeal, left calcaneus bone, left medial malleolus – tibia, left lateral malleolus – fibula, left shank, left knee, left thigh, left great trochanter, left iliac crest, sternum. When the digitising process was completed, the x, y and z coordinates for each body marker at every frame were output by APAS.

### 3.7.2 Height Assessment

To determine the height attained during the selected nine cycles the video from the above camera (camera 5) was used. Using a MATLAB program three points were digitised for each frame: the top edge of the black tape, the bottom edge of the black tape and the water surface (Fig. 3.10). The width of the black tape was known (1.9cm) and the height (cm) was calculated to account for possible movement in the frontal and lateral planes during the eggbeater kick trial:

$$height = \frac{d1 \times 1.9}{d2}$$

where:

$$d1 = top\ tape - water\ surface$$

$$d2 = top\ tape - bottom\ tape$$

Figure 3.10. Camera view and digitising screen for height assessment

### 3.7.3 Weight + Buoyancy Assessment

To calculate the weight + buoyancy force during the selected nine cycles a MATLAB program was used. In that program four input values were inserted for every frame during the lowering of the participant: 1) value displayed from the load cell 2) top of black tape 3) bottom of black tape 4) water surface. When the digitising was completed a 2$^{nd}$ degree regression equation (height/weight+buoyancy) for best fit, was calculated for each participant using the polyfit function (Figure 3.11). This allowed determining the weight + buoyancy supported by each participant during the eggbeater kick trail.

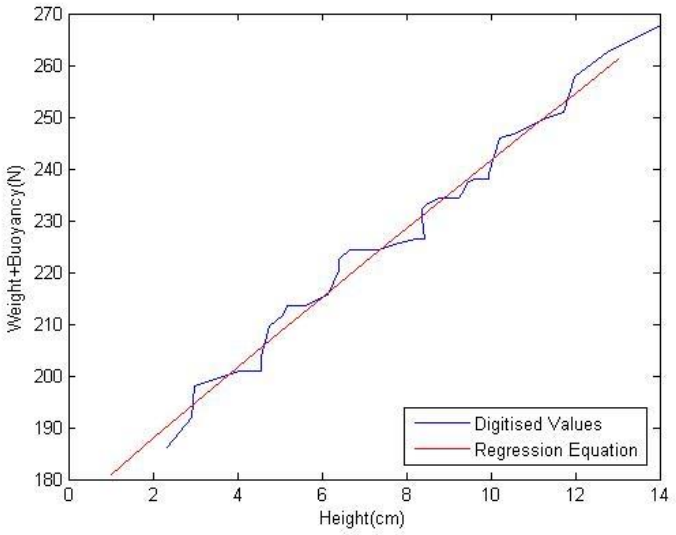


Figure 3.11. Second degree regression equation calculated for the weight + buoyancy.

## 3.8 Calculations of Variables

All raw video data were processed in MATLAB. To remove noise a 4$^{th}$-order Butterworth digital filter with a cut off frequency of 6Hz was used (Bartlett, 1997, Antonsson and Mann, 1985, McCabe, 2008). Given the differences in sampling

frequency between the sEMG (1600Hz) and the video data (25Hz), the latter was interpolated using a cubic spline, continuous at the 2nd derivative, function in MATLAB. This method was appropriate since the plots of the filtered data were compared with the interpolated data and proven identical.

After dividing the data into individual cycles, each cycle was normalized to a 101 points percentile using a Fourier transform retaining 20 harmonics. These points represented the eggbeater kick cycle as a percentage (0 to 100 percent) allowing comparison between and within subjects of movement and EMG patterns.

### 3.8.1 Joint Angles

To calculate the anatomic angles (flexion/extension, abduction/adduction, external/internal rotation) during the eggbeater kick, coordinate frames were established in the lower limb segments.

#### 3.8.1.1 Coordinate Frames Transformations

Four coordinate frames were created in four different segments of the lower limb: pelvis, thigh, shank and foot (Fig. 3.12). The moving coordinate frame at the pelvis was formed by the hip (left-right) vector (x1), the iliac crest-hip vector (z1), and the cross-product vector of x1 and z1 (y1).

The moving coordinate frame for the thigh was formed by the hip-knee vector (z2), cross-product vector of middle femur-hip and middle femur-knee vectors (y2), and the cross-product vector of z2 and y2 (x2).

The moving coordinate frame for the shank was formed by the knee-ankle vector (z3), the cross-product vector of middle shank-knee and middle shank-ankle vectors (y3), and the cross-product vector of z3 and y3 (x3). The moving coordinate frame for the foot was formed by the 1st interphalangeal-heel vector (y4); the cross-product vector of the 1st interphalangeal-heel vector and the 5th metatarsophalangeal-heel vector (z4); the cross-product vector of y4 and z4 (x4).

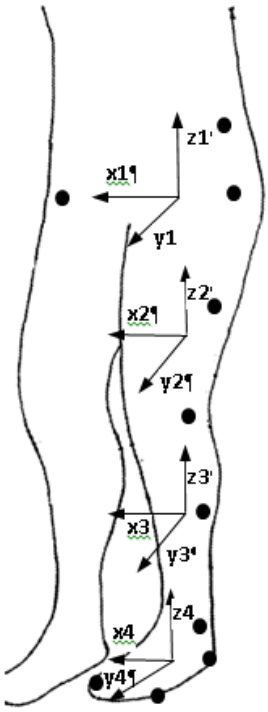


Figure 3.12. Representation of the body markers and the lower limb coordinate frames.

The sequence of rotation for the hip was flexion/extension (T1) followed by abduction/adduction (T2) then internal/external rotation (T3). The ankle followed the

same sequence but different terminology was adopted: plantarflexion/dorsiflexion (T1), inversion/evertion (T2) and adduction/abduction (T3). Following this sequence the resulting transformation matrix (T) was calculated:

$$T = T3 \times T2 \times T1$$

$$T = \begin{bmatrix} cos2 \times cos3 & cos3 \times sin1 \times sin2 - cos1 \times sin3 & sin1 \times sin3 + cos1 \times cos3 \times sin2 \\ cos2 \times sin3 & sin1 \times sin2 \times sin3 + cos1 \times cos3 & cos1 \times sin2 \times sin3 - cos3 \times sin1 \\ -sin2 & cos2 \times sin1 & cos1 \times cos2 \end{bmatrix}$$

From this rotation matrix a solution θ1 (flex/ext), θ2 (abd/add) and θ3 (int/ext rot) for the hip joint, θ1 (flex/ext) for the knee joint, and θ1 (plantarflex/dorsiflex), θ2 (inversion/eversion) and θ3 (adduction/abduction) for the ankle joint was calculated:

$$\theta 2 = -sin^{-1}(T(3,1))$$

$$\theta 1 = cos^{-1}(T(3,3)/\cos(\theta 2))$$

$$\theta 3 = sin^{-1}(T(2,1)/\cos(\theta 2))$$

The output variables for the mean concerning the movement of both sides were calculated using the following formula:

$$mean\ angle = \frac{mean\ angle\ cycle_{dominant} + mean\ angle\ cycle_{non-dominant}}{2}$$

The output variables for the maximum value concerning the movement of both sides were calculated using the following formula:

$$mean\ maximum\ angle = \frac{max\ angle\ cycle_{domiant} + max\ angle\ cycle_{non-dominant}}{2}$$

#### 3.8.1.2 Angular Velocities

Angular velocities were calculated using the coordinate frames of each body segment. Angular velocity vector ω = ($\omega_x$, $\omega_y$, $\omega_z$) was extracted from the skew-symmetric matrix S = S($\omega$):

$$S_{(\omega)} = \begin{bmatrix} 0 & -\omega_z & \omega_y \\ \omega_z & 0 & -\omega_x \\ -\omega_y & \omega_x & 0 \end{bmatrix}$$

Where $\omega$ is the angular velocity of the rotating frame with respect to the fixed frame $S_{(\omega)}$ is the differential of the rotation matrix as follows:

$$S_{(\omega)} = \frac{dR_t}{dt} R_{(t)}^{-1}$$

Where *R* is the rotation matrix and *t* is the time interval between frames.

### 3.8.2 Foot Speed

To calculate the speed of the foot, the centre of the foot was determined as the mean of the three foot markers used (1st interphalangeal joint, 5th metatarsophalangeal joint and heel). X, Y, and Z component velocities were obtained by differentiation with respect to

time of the respective foot center coordinates. With the player upright and the mediolateral axis aligned with the X axis of the calibrated space, the Z velocity vectors described anteroposterior motions, the Y velocity vectors described vertical motions, and the X velocity vectors represent medio-lateral motions. The score for foot speed was calculated by summing, across the whole eggbeater kick cycle, the instantaneous foot speeds (Sanders, 1999a). The score for foot speed over an *n* samples cycle was:

$$\text{Foot speed score} = \left(\sum_{i=1}^{n} |R_i|^2\right)/n$$

Where $R_i$ is the resultant foot velocity for the $n^{th}$ sample.

As calculated by Sanders (1999a), the percentage of velocity components was the sum, across the cycle, of the squared instantaneous velocity components expressed as a percentage of the sum of the squares of the foot speed. Being:

$$|R|^2 = |x|^2 + |y|^2 + |z|^2$$

The contributions of the motions in the X, Y, and Z directions were:

$$\text{x contribution} = \left(\sum_{i=1}^{n} |x_i|^2\right)/n$$

$$\text{y contribution} = \left(\sum_{i=1}^{n} |y_i|^2\right)/n$$

$$\text{z contribution} = \left(\sum_{i=1}^{n} |z_i|^2\right)/n$$

Then, the percentage contributions were:

$$x\ percentage\ contribution = \frac{x\ contribution \times 100}{foot\ speed\ score}$$

$$y\ percentage\ contribution = \frac{y\ contribution \times 100}{foot\ speed\ score}$$

$$z\ percentage\ contribution = \frac{z\ contribution \times 100}{foot\ speed\ score}$$

### 3.8.3 Pitch Angles

The definition of pitch and sweepback angles followed the technique described by Schleihauf (1979) for the hand in swimming, and later applied to the eggbeater kick by Sanders (1999a). Thus, pitch ($\theta$), expressed in degrees, was defined by the angle between the plane of the foot and the direction of water flow (i.e. along the line of the foot velocity vector ($v$)):

$$\theta = \left(\frac{\pi}{2} - \cos^{-1}\left[N \cdot \frac{v}{|N||v|}\right]\right) \cdot \frac{360}{2\pi}$$

$N$ was the vector normal to the plane of the foot determined as the cross-product of the vectors joining the heel marker to each of the phalangeal joint markers. Pitch angle (ranging from -90º to 90º) was positive when water flow hit the plantar surface of the foot and negative when the water flow hit the dorsal surface of the foot (Fig. 3.13).

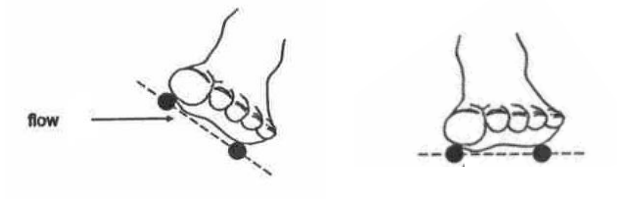


Figure 3.13. Foot pitch angles at 30° and 0°.

### 3.8.4 Sweepback Angles

Sweepback angle ($\varphi$), expressed in degrees, defines the angle from which water flow is coming. To calculate the sweepback angle an internal reference frame for the foot was defined. The x axis was defined as the line from the heel marker to the midpoint of the two phalangeal markers, and y was determined as the cross product of the x vector and *N* (the normal to the foot plane). Sweepback angle was then the angle between the y axis vector of the foot plane and the projection of the foot velocity vector onto that plane (Sanders, 1999b, Sanders, 1999a)(Fig. 3.14):

$$\varphi = \left(\cos^{-1}\left[\frac{y\left(v_x + v_y\right)}{|y|\left|v_x + v_y\right|}\right]\right) \cdot \frac{360}{2\pi}$$

where: $v_x = v \cdot \frac{x}{|x|}$ and $v_y = v \cdot \frac{y}{|y|}$

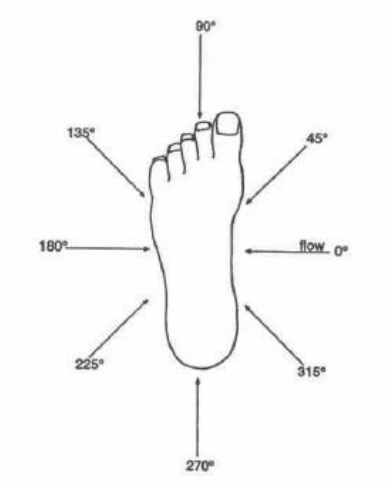


Figure 3.14. Illustration of sweepback angles. Black arrows indicates different sweepback angles.

### 3.8.5 Vertical Component of the Force

In this study the vertical force produced during the eggbeater kick was calculated as performance indicator. Although the height attained was assessed, such methods are limited to the position of one anatomic marker (i.e. vertex, trochanter) and do not account for the subject's mass or buoyancy factors. Additionally, by calculating the instantaneous net force during the eggbeater kick anthropometrics of individual subjects

are taken into account and it offers a detailed continuous indication of net force that can be linked to the body actions and orientations.

The vertical force produced during the eggbeater kick was calculated using the following formula:

$$V\ Force_i = ((Weight + buoyancy)_i \times 9.8) + (y\ddot{FST}com_\iota \times FSTmass) + (y\ddot{HAT}_i \times HATmass)$$

$i$ = sample number

The weight + buoyancy was calculated by determining the height (3.7.2) at each sample and inserting it in the 2nd degree regression equation previously calculated on 3.7.3 for each specific player.

The FST system corresponds to the foot, shank and thigh system. The mass of the whole system was calculated by adding the segment masses obtained from Ezone. Each coordinate of the system's COM was determined by summing the segmental mass-moments and dividing by the mass of the whole system:

$$Xcom_{fst} = \frac{Xrthigh + Xrshank + Xrfoot + Xlthigh + Xlshank + Xlfoot}{FST\ mass}$$

$$X\ segment = (x1 + ((x2 - x1) \times cmfd)) \times segment\ mass$$

Where x1 is the x coordinate of the proximal marker of the segment, x2 is the distal marker of the segment and *cmfd* is the centre of mass fractional distance calculated with the Ezone method.

The same process was conducted to calculate $Ycom_{fst}$ and $Zcom_{fst}$ for the n samples of each eggbeater kick cyle. Having calculated the coordinates of the FST COM the vertical acceleration of the system was calculated using the central difference method:

$$y\ddot{FST}com_{\imath} = (Ycom_{i+1} - 2(Ycom_i) + Ycom_{i-1}) \times sf^2$$

*i* = sample number

*sf* = sample frequency

The head, arms and trunk (HAT) was considered as a one body complex since players were instructed to keep their arms and head completely still, resulting in very limited segmental motion. It was represented by the point digitised at the top of the black tape (point mass). Thus, the vertical HAT acceleration can be calculated using the height calculated previously:

$$y\ddot{HAT}_{\imath} = (yHAT_{i+1} - 2(yHAT_i) + yHAT_{i-1}) \times sf^2$$

*i* = sample number

*sf* = sample frequency

### 3.8.6 Surface Electromyography

#### 3.8.6.1 Amplitude of the EMG Signal

To determine its amplitude the EMG signal was analysed using a MATLAB program. An offset component was removed by subtracting the mean. The signal was full-wave rectified and a linear envelope of the raw data was created using a $4^{th}$-order Butterworth low-pass filter with a 20Hz cut-off frequency.

#### 3.8.6.2 Activation Timing

The activation timing of each muscle was determined in the mean cycle which was calculated by averaging the 9 cycles for every percentile point.

The activation timing of each individual muscle was calculated in MATLAB using a double threshold method. An initial cut off value for signal amplitude was determined as 20% of the maximum value in the cycle. When the EMG signal exceeded this level for at least 10% of the cycle the start and finish of that continuous period above the 20% threshold was considered the onset and offset respectively of the muscle activity.

#### 3.8.6.3 Normalized Signal

To compare the muscle activity within and between subjects the EMG signal was normalized to the MVIC.

#### 3.8.6.3.1 Normalized to Maximum Voluntary Isometric Contraction

The maximum value from the recorded MVIC signal of each muscle was used as reference value to calculate the normalized to MVIC EMG:

$$Normalized\ to\ MVIC\ EMG\ (\%) = \frac{EMG\ signal}{MVIC\ signal}$$

#### 3.8.6.3.2 Normalized to Maximum Value in the Cycle

The maximum EMG signal value from the linear envelope in each cycle ($Cycle_{max}$)was used as reference value for the respective cycle.

$$Normalized\ to\ Maximum\ Value\ in\ the\ Cycle\ (\%) = \frac{EMG\ signal}{Cycle_{max}}$$

## 3.9 Reliability

To assess the reliability of the digitising process responsible for the kinematic variables, one single eggbeater kick cycle at two different moments in the trial (non-fatigued, fatigued) was digitised nine times for all four underwater camera views. For each of the kinematic and kinetic variables, the standard deviation and 95% error limits ($SD \times Tscore$) of the nine repeat digitisations were used as an indication of the reliability.

### 3.10 Statistical Analysis

The processed data were analysed using the Statistical Package for Social Sciences (SPSS) version 20.0. Descriptive statistics including the mean, and standard deviations were calculated for all the data in Microsoft Office Excel 2010 software.

A two factor repeated measures ANOVA with fatigued level (non-fatigued, 50% time point, fatigued) and dominance (dominant, non-dominant) as factors was performed. The differences between fatigued levels and dominance as well as the interactions between these, were tested with the alpha level of 0.05. Post hoc analysis was also performed and a Bonferroni adjustment made for multiple comparisons.

In statistical analysis using a repeated measures ANOVA the criterion of sphericity, that is, homogeneity of variance and homogeneity of covariance must be met. Homogeneity of covariance means that the relationships, or correlations, on the dependent variable among all of the three repeated measures are equal. However, when only two repeated measures are employed, this assumption is not applicable, because there are too few points to establish a correlation coefficient.

To complement the above, a 95% Confidence Interval (*CI*) of the true mean was quantified for each variable. The upper and lower CI boundaries were presented on the graphs instead of the standard error bars to indicate the range in which the true value of the variable fell 95% of the time. All CI calculations were quantified using Microsoft Office Excel 2010 software, using the formula:

$$CI = \bar{X} \pm (T \times SE)$$

Whereby $\bar{X}$ is the mean, *T* is the T-score for the particular confidence level of interest and *SE* is the standard error. The SE is calculated as:

$$SE = SD / \sqrt{n}$$

Where SD is the standard deviation and *n* is the number of cycles/subjects.

The effect size (*d*) for each variable was also calculated to measure the magnitude of change between fatigue levels and to assess the magnitude of the differences between dominance. The general effect size formula is given as:

$$\text{Effect Size} = (\text{Mean1} - \text{Mean2}) / \text{Standard Deviation}$$

To calculate the effect size of the differences in means between fatigue levels the SD of the pre-test was used (Hopkins, 2000). To calculate the effect size of the differences in means between dominant and non-dominant side a 'pooled' standard deviation, which is the average of the standard deviations of both datasets, was used (Coe, 2002). The criteria for interpreting the absolute effect size, was based on Cohen (1992) suggestion that effect sizes of 0.2 are small, 0.5 are moderate and 0.8 are large. Hopkins (2002) has extended this scale to a new one where 0.2 are small, 0.6 are moderate, 1.2 are large, 2.0 are very large and 4.0 are nearly perfect.

The Pearson product-moment correlation coefficient (*r*) was calculated using SPSS to measure the linear correlation (dependence) between kinematic, muscle activity and performance (vertical force normalized to body weight) variables.

# Chapter Four: Results

# 4 Results

In this section, the results of the kinetic, kinematic and muscle activity variables from different levels of fatigue during the eggbeater kick trial (non-fatigued, 50% time point and fatigued) are presented. Tables and graphs are used to illustrate the results and to highlight the differences between the different levels of fatigue and performance.

## 4.1 3D Kinematics Dynamic Validity

The results from the dynamic validity test showed a root mean squared error of 6.56mm which corresponds to an average 1.31% of error between the true value (480mm) and the distance calculated from the digitized data.

## 4.2 Reliability of Calculated Variables

Table 4.1 presents the results from the reliability calculations, based on the same eggbeater kick cycle at NF and F state digitised nine times. The 95% confidence intervals show the range in which 95% of samples of that particular variable would fall and the percentage error the standard deviation as percentage of the mean. Standard deviation values were considered small relative to the magnitude of the variable being measured.

Table 4.1. Reliability results for nine cycles at NF and F conditions.

| hgfhVariable | Non Fatigued | | | | | Fatigued | | | | |
|---|---|---|---|---|---|---|---|---|---|---|
| | Mean | Standard Deviation | 95% Confidence Interval | | Percentage Error | Mean | Standard Deviation | 95% Confidence Interval | | Percentage Error |
| | | | Lower | Upper | | | | Lower | Upper | |
| Avg Vertical Force (N) | 278.0 | 0.37 | 277.1 | 278.8 | 0.1 | 202.8 | 0.15 | 202.4 | 203.1 | 0.1 |
| Max Vertical Force (N) | 469.7 | 7.25 | 453.0 | 486.4 | 1.5 | 283.6 | 3.91 | 274.6 | 292.6 | 1.4 |
| Avg RHip Abduction (°) | 17.1 | 0.39 | 16.2 | 18.1 | 2.3 | 8.45 | 0.38 | 7.57 | 9.33 | 4.5 |
| Avg LHip Abduction (°) | 12.1 | 0.57 | 10.8 | 13.4 | 4.7 | 7.94 | 0.44 | 6.91 | 8.96 | 5.5 |
| Avg RHip Flexion (°) | 54.2 | 0.17 | 53.8 | 54.6 | 0.3 | 48.6 | 0.35 | 47.8 | 49.4 | 0.7 |
| Avg LHip Flexion (°) | 49.5 | 1.19 | 46.7 | 52.2 | 2.4 | 45.2 | 0.96 | 43.0 | 47.5 | 2.1 |
| Avg RHip Internal Rot (°) | 4.8 | 1.27 | 1.9 | 7.8 | 26.5 | 8.47 | 0.87 | 6.46 | 10.4 | 10.3 |
| Avg LHip Internal Rot (°) | 28.0 | 1.34 | 25.0 | 31.1 | 4.8 | 44.9 | 1.42 | 41.6 | 48.2 | 3.2 |
| Avg RKnee Flexion (°) | 94.2 | 0.14 | 93.3 | 94.6 | 0.1 | 92.4 | 0.09 | 92.2 | 92.6 | 0.1 |
| Avg LKnee Flexion (°) | 91.7 | 0.45 | 90.7 | 92.8 | 0.5 | 93.4 | 0.31 | 92.7 | 94.1 | 0.3 |
| Avg RAnkle Plantarflexion (°) | 20.3 | 0.28 | 19.7 | 21.0 | 1.4 | 21.8 | 0.33 | 21.0 | 22.6 | 1.5 |
| Avg LAnkle Plantarflexion (°) | 17.4 | 0.54 | 16.1 | 18.6 | 3.1 | 16.0 | 0.28 | 15.3 | 16.6 | 1.8 |
| Avg RAnkle Inversion (°) | -3.2 | 0.30 | -3.9 | -2.5 | 9.4 | 2.11 | 0.35 | 1.28 | 2.93 | 16.6 |
| Avg LAnkle Inversion (°) | 4.2 | 0.35 | 3.4 | 5.0 | 8.3 | 13.7 | 0.28 | 13.0 | 14.3 | 2.0 |
| Avg RAnkle Adduction (°) | 22.3 | 1.01 | 20.0 | 24.7 | 4.5 | 18.7 | 0.61 | 17.2 | 20.1 | 3.3 |

| | | | | | | | | | | |
|---|---|---|---|---|---|---|---|---|---|---|
| Avg LAnkle Adduction (°) | 30.0 | 0.55 | 28.7 | 31.2 | 1.8 | 28.1 | 0.69 | 26.5 | 29.7 | 2.5 |
| Max RHip Abduction (°) | 24.4 | 0.49 | 23.3 | 25.6 | 2.0 | 12.9 | 0.61 | 11.5 | 14.3 | 4.7 |
| Max LHip Abduction (°) | 19.3 | 1.15 | 16.6 | 22.0 | 6.0 | 14.0 | 0.55 | 12.7 | 15.3 | 3.9 |
| Max RHip Flexion (°) | 77.9 | 0.54 | 76.7 | 79.2 | 0.7 | 71.9 | 0.80 | 70.1 | 73.8 | 1.1 |
| Max LHip Flexion (°) | 71.5 | 1.23 | 68.7 | 74.4 | 1.7 | 71.9 | 2.16 | 67.0 | 76.9 | 3.0 |
| Max RHip Internal Rot (°) | 27.1 | 1.37 | 23.2 | 30.3 | 5.1 | 37.3 | 1.63 | 33.5 | 41.1 | 4.4 |
| Max LHip Internal Rot (°) | 53.0 | 1.64 | 49.2 | 56.8 | 3.1 | 72.7 | 2.16 | 67.7 | 77.7 | 3.0 |
| Max RKnee Flexion (°) | 131.7 | 0.23 | 131.2 | 132.2 | 0.2 | 125.5 | 0.34 | 124.7 | 126.3 | 0.3 |
| Max LKnee Flexion (°) | 136.6 | 1.52 | 133.1 | 140.1 | 1.1 | 137.5 | 2.47 | 131.8 | 143.2 | 1.8 |
| Max RAnkle Plaflx (°) | 43.5 | 1.10 | 40.9 | 46.0 | 2.5 | 42.8 | 0.63 | 41.3 | 44.3 | 1.5 |
| Max LAnkle Plaflx (°) | 40.6 | 0.70 | 39.0 | 42.2 | 1.7 | 37.1 | 1.13 | 34.5 | 39.8 | 3.0 |
| Max RAnkle Inversion (°) | 18.8 | 1.14 | 16.2 | 21.4 | 6.1 | 21.4 | 0.88 | 19.4 | 23.5 | 4.1 |
| Max LAnkle Inversion (°) | 37.9 | 0.62 | 36.4 | 39.3 | 1.6 | 36.4 | 0.44 | 35.4 | 37.5 | 1.2 |
| Max RAnkle Adduction (°) | 51.2 | 1.61 | 47.4 | 54.9 | 3.1 | 42.2 | 1.51 | 38.7 | 45.7 | 3.6 |
| Max LAnkle Adduction (°) | 68.2 | 0.72 | 66.5 | 69.9 | 1.1 | 60.9 | 0.87 | 58.9 | 63.0 | 1.4 |
| Min RHip Abduction (°) | 11.4 | 1.03 | 9.03 | 13.8 | 9.0 | 4.76 | 0.82 | 2.87 | 6.66 | 17.2 |
| Min LHip Abduction (°) | 3.30 | 0.87 | 1.27 | 5.32 | 26.4 | -1.88 | 0.58 | -3.23 | -0.53 | 30.9 |
| Min RHip Flexion (°) | 34.7 | 0.44 | 33.7 | 35.8 | 1.3 | 28.6 | 0.66 | 27.0 | 30.1 | 2.3 |
| Min LHip Flexion (°) | 29.7 | 1.01 | 27.4 | 32.1 | 3.4 | 26.4 | 0.53 | 25.1 | 27.6 | 2.0 |
| Min RHip Internal Rot (°) | -29.8 | 2.33 | -35.2 | -24.4 | 7.8 | -35.1 | 1.25 | -35.0 | -32.2 | 3.6 |

| | | | | | | | | | | |
|---|---|---|---|---|---|---|---|---|---|---|
| Min LHip Internal Rot (°) | -13.8 | 1.83 | -18.0 | -9.60 | 13.3 | -6.08 | 2.15 | -11.0 | -1.12 | 35.4 |
| Min RKnee Flexion (°) | 52.4 | 0.36 | 51.5 | 53.2 | 0.7 | 53.1 | 0.26 | 52.5 | 53.8 | 0.5 |
| Min LKnee Flexion (°) | 42.6 | 1.26 | 39.7 | 45.6 | 3.0 | 47.8 | 0.53 | 46.6 | 49.1 | 1.1 |
| Min RAnkle Plaflx (°) | -4.90 | 1.16 | -7.59 | -2.21 | 23.7 | -0.63 | 0.76 | -2.40 | 1.13 | 120.6 |
| Min LAnkle Plaflx (°) | -14.6 | 0.94 | -16.8 | -12.4 | 6.4 | -13.5 | 0.37 | -14.3 | -12.6 | 2.7 |
| Min RAnkle Inversion (°) | -26.5 | 0.60 | -27.9 | -25.1 | 2.3 | -17.8 | 0.47 | -18.9 | -16.7 | 2.6 |
| Min LAnkle Inversion (°) | -17.6 | 1.05 | -20.1 | -15.2 | 6.0 | -4.1 | 0.63 | -5.59 | -2.65 | 15.4 |
| Min RAnkle Adduction (°) | -2.68 | 1.59 | -6.35 | 0.99 | 59.3 | -3.20 | 1.48 | -6.62 | 0.20 | 46.3 |
| Min LAnkle Adduction (°) | 10.3 | 1.12 | 7.79 | 12.9 | 10.9 | 17.6 | 1.14 | 15.0 | 20.3 | 6.5 |
| RHip Abduction Range (°) | 13.0 | 1.04 | 10.6 | 15.4 | 8.0 | 8.19 | 0.80 | 6.34 | 10.0 | 9.8 |
| LHip Abduction Range (°) | 16.0 | 0.88 | 14.0 | 18.0 | 5.5 | 15.9 | 0.85 | 13.9 | 17.8 | 5.3 |
| RHip Flexion Range (°) | 43.1 | 0.74 | 41.4 | 44.8 | 1.7 | 43.3 | 0.99 | 41.0 | 45.6 | 2.3 |
| LHip Flexion Range (°) | 41.8 | 1.34 | 38.7 | 44.9 | 3.2 | 45.5 | 1.99 | 40.9 | 50.1 | 4.4 |
| RHip Internal Rot Range (°) | 57.0 | 2.39 | 51.5 | 62.5 | 4.2 | 72.5 | 1.85 | 68.2 | 76.8 | 2.6 |
| LHip Internal Rot Range (°) | 66.9 | 2.83 | 60.3 | 73.4 | 4.2 | 78.8 | 2.79 | 72.3 | 85.2 | 3.5 |
| RKnee Flexion Range (°) | 79.3 | 0.45 | 78.2 | 80.3 | 0.6 | 72.3 | 0.47 | 71.2 | 73.2 | 0.7 |
| LKnee Flexion Range (°) | 93.9 | 1.21 | 91.1 | 96.7 | 1.3 | 89.6 | 2.75 | 83.3 | 96.0 | 3.1 |
| RAnkle Plaflx Range (°) | 48.4 | 2.08 | 43.6 | 53.2 | 4.3 | 43.4 | 1.14 | 40.8 | 46.1 | 2.6 |
| LAnkle Plaflx Range (°) | 55.6 | 1.49 | 52.1 | 59.0 | 2.7 | 50.7 | 1.32 | 47.6 | 53.7 | 2.6 |
| RAnkle Inversion Range (°) | 45.4 | 2.08 | 43.6 | 53.2 | 4.6 | 39.3 | 1.06 | 36.8 | 41.7 | 2.7 |

| | | | | | | | | | | |
|---|---|---|---|---|---|---|---|---|---|---|
| LAnkle Inversion Range (°) | 55.2 | 0.92 | 53.1 | 57.4 | 1.7 | 40.6 | 0.93 | 38.4 | 42.7 | 2.3 |
| RAnkle Adduction Range (°) | 48.5 | 2.29 | 43.2 | 53.8 | 4.7 | 39.0 | 1.72 | 35.0 | 43.0 | 4.4 |
| LAnkle Adduction Range (°) | 78.6 | 1.30 | 75.6 | 81.6 | 1.7 | 78.6 | 1.51 | 75.1 | 82.1 | 1.9 |
| Avg RFoot Pitch Angle (°) | -11.1 | 0.29 | -11.8 | -10.4 | 2.6 | -7.59 | 0.14 | -7.93 | -7.25 | -1.8 |
| Avg LFoot Pitch Angle (°) | 7.72 | 0.23 | 7.18 | 8.27 | 3.0 | 6.65 | 0.10 | 6.41 | 6.90 | 1.5 |
| Max RFoot Pitch Angle (°) | 23.1 | 0.36 | 22.2 | 23.9 | 1.6 | 31.6 | 0.32 | 30.8 | 32.3 | 1.0 |
| Max LFoot Pitch Angle (°) | 41.4 | 0.34 | 40.6 | 42.2 | 0.8 | 43.8 | 0.33 | 43.0 | 44.6 | 0.8 |
| Min RFoot Pitch Angle (°) | -52.0 | 0.84 | -54.0 | -50.1 | 1.6 | -54.8 | 0.59 | -56.2 | -53.4 | -1.1 |
| Min RFoot Pitch Angle (°) | -37.6 | 0.19 | -38.0 | -37.1 | 0.5 | -48.7 | 0.26 | -49.3 | -48.0 | -0.5 |
| Time of Pos Pitch Rfoot (%) | 39.0 | 0.86 | 37.0 | 40.9 | 2.2 | 43.5 | 0.52 | 42.3 | 44.7 | 1.2 |
| Time of Pos Pitch Lfoot (%) | 56.2 | 0.97 | 53.9 | 58.4 | 1.7 | 59.8 | 0.33 | 59.1 | 60.6 | 0.6 |
| RF Medio-Lateral Motion (%) | 35.1 | 0.17 | 34.7 | 35.5 | 0.5 | 46.7 | 0.17 | 46.3 | 47.1 | 0.4 |
| LF Medio-Lateral Motion (%) | 25.4 | 0.13 | 25.1 | 25.7 | 0.5 | 36.1 | 0.22 | 35.6 | 36.7 | 0.6 |
| RFoot Vertical Motion (%) | 34.5 | 0.10 | 34.3 | 34.8 | 0.3 | 28.5 | 0.08 | 28.3 | 28.6 | 0.3 |
| LFoot Vertical Motion (%) | 37.8 | 0.09 | 37.6 | 38.1 | 0.2 | 31.2 | 0.11 | 31.0 | 31.5 | 0.4 |
| RF Ant-Pos Motion (%) | 30.2 | 0.15 | 29.8 | 30.5 | 0.5 | 24.7 | 0.20 | 24.2 | 25.1 | 0.8 |
| LF Ant-Pos Motion (%) | 34.6 | 0.10 | 34.4 | 34.9 | 0.3 | 34.9 | 0.11 | 34.7 | 35.2 | 0.3 |
| Average Rfoot Speed (m/s) | 2.80 | 0.003 | 2.79 | 2.80 | 0.1 | 2.05 | 0.003 | 2.04 | 2.06 | 0.1 |
| Average Lfoot Speed (m/s) | 2.78 | 0.002 | 2.77 | 2.78 | 0.1 | 2.09 | 0.002 | 2.08 | 2.10 | 0.1 |
| Avg RH Abd Ang Vel ($rad \cdot s^{-1}$) | 2.8 | 0.06 | 2.7 | 2.9 | 2.1 | 1.7 | 0.07 | 1.6 | 1.8 | 4.1 |

| | | | | | | | | | | |
|---|---|---|---|---|---|---|---|---|---|---|
| Avg LH Abd Ang Vel (rad·s$^{-1}$) | 4.5 | 0.09 | 4.4 | 4.6 | 2.0 | 2.61 | 0.1 | 2.51 | 2.71 | 3.8 |
| Avg RH Flx Ang Vel (rad·s$^{-1}$) | 4.4 | 0.1 | 4.3 | 4.5 | 2.3 | 3.3 | 0.05 | 3.2 | 3.4 | 1.5 |
| Avg LH Flx Ang Vel (rad·s$^{-1}$) | 4.4 | 0.1 | 4.3 | 4.5 | 2.3 | 3.3 | 0.1 | 3.2 | 3.4 | 3.0 |
| Avg RH Rot Ang Vel (rad·s$^{-1}$) | 3.9 | 0.1 | 3.8 | 4.0 | 2.6 | 3.9 | 0.1 | 3.8 | 4.0 | 2.6 |
| Avg LH Rot Ang Vel (rad·s$^{-1}$) | 7.9 | 0.07 | 7.8 | 8.0 | 0.9 | 5.7 | 0.06 | 5.6 | 5.8 | 1.1 |
| Avg RK Flx Ang Vel (rad·s$^{-1}$) | 4.9 | 0.05 | 4.8 | 5.0 | 1.0 | 3.7 | 0.03 | 3.7 | 3.7 | 0.8 |
| Avg LK Flx Ang Vel (rad·s$^{-1}$) | 8.9 | 0.1 | 8.8 | 9.0 | 1.1 | 6.1 | 0.09 | 6.0 | 6.2 | 1.5 |
| Avg RAnk Inv Ang Vel (rad·s$^{-1}$) | 3.2 | 0.08 | 3.1 | 3.3 | 2.5 | 2.4 | 0.04 | 2.4 | 2.4 | 1.7 |
| Avg LAnk Inv Ang Vel (rad·s$^{-1}$) | 5.1 | 0.1 | 5.0 | 5.2 | 2.0 | 4.0 | 0.03 | 4.0 | 4.0 | 0.8 |
| Avg RAnk Plaflx Ang Vel (rad·s$^{-1}$) | 5.4 | 0.1 | 5.3 | 5.5 | 1.9 | 4.0 | 0.05 | 3.9 | 4.1 | 1.3 |
| Avg LAnk Plaflx Ang Vel (rad·s$^{-1}$) | 6.1 | 0.1 | 6.0 | 6.2 | 1.6 | 4.1 | 0.07 | 4.0 | 4.2 | 1.7 |
| Avg RAnkle Add Ang Vel (rad·s$^{-1}$) | 7.9 | 0.08 | 7.8 | 8.0 | 1.0 | 5.5 | 0.04 | 5.5 | 5.5 | 0.7 |
| Avg LAnkle Add Ang Vel (rad·s$^{-1}$) | 4.8 | 0.04 | 4.8 | 4.8 | 0.8 | 3.9 | 0.04 | 3.9 | 3.9 | 1.0 |

## 4.3 Comparisons between Fatigue Level and Dominance

Section 4.3 presents the results for each fatigue state and for both sides. The value for each state represents the mean for the 12 subjects. Each subject score is the mean of the average, maximum or minimum value for each particular variable during the cycle for nine cycles. Error bars represent the standard deviation of the group.

The time to fatigue (i.e. from non-fatigued condition to fatigued condition) across all subjects was 30.66 ± 4.09s.

### 4.3.1 Average Vertical Force

Table 4.2 shows the mean of the twelve participants' average vertical force during the cycle.

Table 4.2. Mean (N) and standard deviation of average vertical force for non-fatigued (NF), 50% time point (50% TP) and fatigued (F) conditions. * indicates statistical differences.

| | NF | 50% TP | F |
|---|---|---|---|
| Average Vertical Force (N) | 212.2 ± 27.6** | 184.5 ± 21.6** | 164.3 ± 22.2** |

There was a statistical difference between fatigue conditions as determined by one-way repeated measures ANOVA ($F_{1.351,14.85}$ = 48.952, $p < 0.001$, $\eta^2 = 0.817$). A Bonferroni post-hoc test revealed that the vertical force produced was statistically significantly lower in the F condition ($p < 0.001$, $d = 1.90$) and at the 50% TP ($p < 0.001$, $d = 1.11$) compared to the NF condition. 50% TP was statistically significantly higher than F condition ($p = 0.001$, $d = 0.92$) (Fig. 4.1).

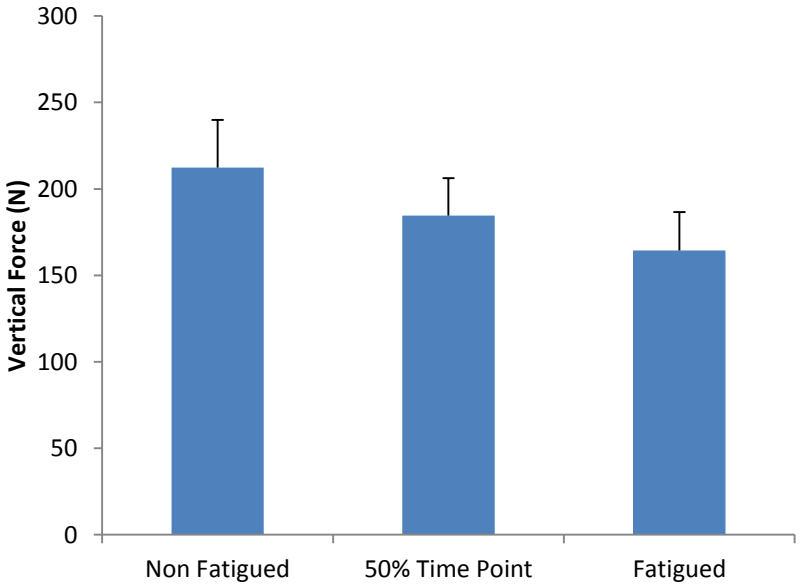


Figure 4.1. Average Vertical Force produced for the three fatigue conditions studied. Error bars represent the group's standard deviation.

### 4.3.2 Mean Maximum Vertical Force

Table 4.3 shows the mean of the twelve participants' maximum vertical force during the cycle.

Table 4.3. Mean (N) and standard deviation of maximum vertical force for non-fatigued (NF), 50% time point (50% TP) and fatigued (F) conditions. * indicates statistical differences.

| | NF | 50% TP | F |
|---|---|---|---|
| Maximum Vertical Force (N) | 353.0 ± 58.7** | 297.1 ± 56.6* | 259.1 ± 30.2* |

There was a statistical difference between fatigue conditions as determined by one-way repeated measures ANOVA ($F_{2,22} = 39.649$, $p < 0.001$, $\eta^2 = 0.783$). A Bonferroni post-

hoc test revealed that the maximum vertical force produced was statistically significantly lower in the F condition ($p < 0.001$, $d = 2.01$) and at the 50% TP ($p = 0.01$, $d = 0.96$) compared to the NF condition. There was no statistically significant difference between the 50% TP and F condition ($p = 0.015$, $d = 0.83$) (Fig. 4.2).

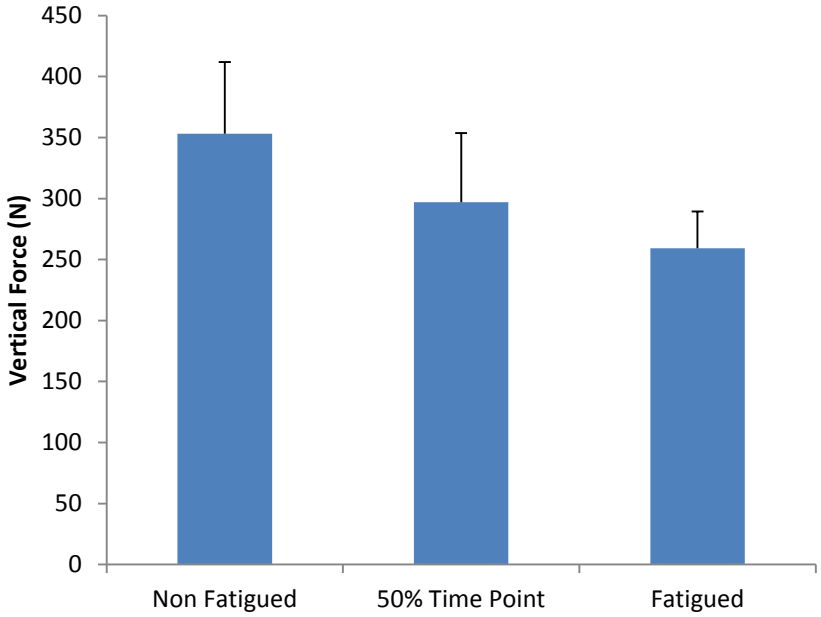


Figure 4.2. Maximum vertical force produced for the three conditions studied. Error bars represent the group's standard deviation.

### 4.3.3 Hip Joint

#### 4.3.3.1 Average Angles

Table 4.4 shows the mean of the twelve participants' average angle for hip abduction, flexion and internal rotation during the cycle.

Table 4.4. Mean (°) and standard deviation of average hip abduction, flexion and internal rotation for, non-fatigued (NF), 50% time point (50% TP) and fatigued (F) conditions and both sides. † indicates statistical differences between fatigue conditions.

| | Abduction | | | Flexion | | | Internal Rotation | | |
|---|---|---|---|---|---|---|---|---|---|
| | NF | 50% TP | F | NF | 50% TP | F | NF | 50% TP | F |
| Dominant side (°) | 34.0 ± 7.6† | 32.3 ± 7.1† | 31.0 ± 5.7†† | 46.7 ± 9.7† | 45.0 ± 8.6 | 43.2 ± 7.5† | 20.6 ± 11.8† | 23.0 ± 11.5 | 23.3 ± 11.9† |
| Non-dominant side (°) | 34.0 ± 7.8† | 32.7 ± 6.6† | 31.2 ± 6.6†† | 44.4 ± 11.4† | 40.8 ± 10.0 | 40.5 ± 9.3† | 20.0 ± 8.3† | 22.9 ± 10.4 | 24.4 ± 10.3† |

There was no statistically significant interaction between fatigue conditions and dominance for hip abduction ($F_{2,22}$ = 0.197, $p$ = 0.823, $\eta^2$ = 0.018). Significant differences were found between fatigue conditions ($F_{2,22}$ = 10.120, $p$ = 0.001, $\eta^2$ = 0.479) but not between sides ($F_{1,11}$ = 0.013, $p$ = 0.910, $\eta^2$ = 0.001). Post hoc Bonferroni test revealed that NF was statistically significantly higher than F ($p$ = 0.012, $d$ = 0.43) and 50% TP was statistically significantly higher than F ($p$ = 0.037, $d$ = 0.22).

There was no statistically significant interaction between fatigue conditions and dominance for hip flexion ($F_{2,22}$ = 2.313, $p$ = 0.123, $\eta^2$ = 0.174). There were statistically significant differences between conditions ($F_{2,22}$ = 7.758, $p$ = 0.003, $\eta^2$ = 0.414) but not between sides ($F_{1,11}$ = 3.792, $p$ = 0.077, $\eta^2$ = 0.256). A post hoc Bonferroni test revealed NF was statistically significantly higher than F condition ($p$ = 0.027, $d$ = 0.38).

There was no statistically significant interaction between hip internal rotation fatigue conditions and dominance ($F_{2,22}$ = 0.509, $p$ = 0.608, $\eta^2$ = 0.044). There was statistically significant differences between conditions ($F_{2,22}$ = 7.601, $p$ = 0.003, $\eta^2$ = 0.409) but not

between sides ($F_{1,11}$ = 0.002, $p$ = 0.969, $\eta^2$ < 0.001). A post hoc Bonferroni test revealed NF was statistically significantly higher than F condition ($p$ = 0.009, $d$ = 0.33).

#### 4.3.3.2 Maximum Angles

Table 4.5 shows the mean of the twelve participants' maximum angle for hip abduction, flexion and internal rotation during the cycle.

Table 4.5. Mean (°) and standard deviation of maximum hip abduction, flexion and internal rotation for non-fatigued (NF), 50% time point (50% TP) and fatigued (F) conditions and both sides. * indicates statistical differences between sides. † indicates statistical differences between fatigue conditions.

| | Abduction | | | Flexion | | | Internal Rotation | | |
|---|---|---|---|---|---|---|---|---|---|
| | NF | 50% TP | F | NF | 50% TP | F | NF | 50% TP | F |
| Dominant side (°) | 40.0 ± 7.9† | 38.3 ± 8.9 | 36.9 ± 6.8† | 64.5 ± 13.4† | 63.1 ± 12.6 | 60.7 ± 11.5† | 41.3 ± 10.5*† | 45.2 ± 10.6* | 45.4 ± 10.5*† |
| Non-dominant side (°) | 41.5 ± 9.1† | 40.3 ± 8.3 | 38.9 ± 8.0† | 63.8 ± 15.2† | 58.0 ± 12.0 | 57.2 ± 10.6† | 52.3 ± 9.91*† | 55.6 ± 10.4* | 56.6 ± 10.7*† |

There was no statistically significant interaction between fatigue conditions and dominance for maximum hip abduction ($F_{2,22}$ = 0.094, $p$ = 0.911, $\eta^2$ = 0.008). There were differences between conditions ($F_{2,22}$ = 9.048, $p$ = 0.001, $\eta^2$ = 0.451) but not between sides ($F_{1,11}$ = 0.949, $p$ = 0.351, $\eta^2$ = 0.079). A post hoc Bonferroni test revealed NF was statistically significantly higher than F condition ($p$ = 0.005, $d$ = 0.36).

There was no statistically significant interaction between fatigue conditions and dominance for maximum hip flexion ($F_{1.236,13.596}$ = 3.030, $p$ = 0.099, $\eta^2$ = 0.216). There

were differences between conditions ($F_{2,22}$ = 7.525, $p$ = 0.003, $\eta^2$ = 0.406) but not between sides ($F_{1,11}$ = 3.376, $p$ = 0.093, $\eta^2$ = 0.235). A post hoc Bonferroni test revealed NF was statistically significantly higher than F conditions ($p$ = 0.02, $d$ = 0.41).

There was no statistically significant interaction between fatigue conditions and dominance for the maximum hip internal rotation ($F_{1.338,14.716}$ = 0.058, $p$ = 0.877, $\eta^2$ = 0.005). There were differences between conditions ($F_{2,22}$ = 7.015, $p$ = 0.004, $\eta^2$ = 0.389) and between sides ($F_{1,11}$ = 9.615, $p$ = 0.010, $\eta^2$ = 0.466). A post hoc Bonferroni test revealed NF was statistically significantly higher than F conditions ($p$ = 0.04, $d$ = 0.35).

#### 4.3.3.3 Minimum Angles

Table 4.6 shows the mean of the twelve participants' minimum angle for hip abduction, flexion and internal rotation during the cycle.

Table 4.6. Mean (°) and standard deviation of minimum hip abduction, flexion and internal rotation for non-fatigued (NF), 50% time point (50% TP) and fatigued (F) conditions and both sides. † indicates statistical differences between fatigue conditions.

| | Abduction | | | Flexion | | | Internal Rotation | | |
|---|---|---|---|---|---|---|---|---|---|
| | NF | 50% TP | F | NF | 50% TP | F | NF | 50% TP | F |
| Dominant side (°) | 8.59 ± 7.9† | 7.06 ± 6.9 | 5.77 ± 5.7† | 33.3 ± 7.4†† | 30.7 ± 6.1† | 29.2 ± 5.0† | -5.62 ± 20.9 | -5.68 ± 19.3 | -3.50 ± 19.4 |
| Non-dominant side (°) | 6.09 ± 7.9† | 4.56 ± 7.0 | 2.98 ± 5.5† | 29.2 ± 8.4†† | 26.6 ± 7.0† | 26.3 ± 6.8† | -18.6 ± 7.7 | -16.7 ± 11.7 | -13.0 ± 10.0 |

There was no statistically significant interaction between fatigue conditions and dominance for minimum hip abduction ($F_{2,22}$ = 0.088, $p$ = 0.916, $\eta^2$ = 0.008). There

were differences between conditions ($F_{2,22}$ = 7.466, $p$ = 0.003, $\eta^2$ = 0.404) but not between sides ($F_{1,11}$ = 2.034, $p$ = 0.182, $\eta^2$ = 0.156). A post hoc Bonferroni test revealed NF was statistically significantly higher than F condition ($p$ = 0.031, $d$ = 0.43).

There was no statistically significant interaction between fatigue conditions and dominance for minimum hip flexion ($F_{1.963,21.598}$ = 1.979, $p$ = 0.163, $\eta^2$ = 0.152). There were differences between conditions ($F_{1.412,15.537}$ = 11.586, $p$ = 0.002, $\eta^2$ = 0.513) and between sides ($F_{1,11}$ = 8.238, $p$ = 0.015, $\eta^2$ = 0.428). A post hoc Bonferroni test revealed NF was statistically significantly higher than F ($p$ = 0.014, $d$ = 0.49) and 50% TP ($p$ = 0.009, $d$ = 0.35) conditions.

There was no statistically significant interaction between fatigue condition and dominance for the minimum hip internal rotation ($F_{1.746,19.207}$ = 0.742, $p$ = 0.472, $\eta^2$ = 0.063). There were no differences between conditions ($F_{1.350,14.852}$ = 3.149, $p$ = 0.087, $\eta^2$ = 0.223) nor between sides ($F_{1,11}$ = 3.438, $p$ = 0.091, $\eta^2$ = 0.238).

#### 4.3.3.4 Hip Range of Motion

Table 4.7 shows the mean of the twelve participants' range of motion for hip abduction, flexion and internal rotation during the cycle.

Table 4.7. Mean (°) and standard deviation of range of motion hip abduction, flexion and internal rotation for non-fatigued (NF), 50% time point (50% TP) and fatigued (F) conditions and both sides. * indicates statistical differences between sides.

| | Abduction | | | Flexion | | | Internal Rotation | | |
|---|---|---|---|---|---|---|---|---|---|
| | NF | 50% TP | F | NF | 50% TP | F | NF | 50% TP | F |
| Dominant side (°) | 31.4 ± 3.5* | 31.2 ± 5.0* | 31.1 ± 3.8* | 31.1 ± 9.5 | 32.3 ± 9.6 | 31.5 ± 9.5 | 46.9 ± 17.5* | 50.9 ± 13.9* | 48.9 ± 14.3* |
| Non-dominant side (°) | 35.4 ± 4.8* | 35.8 ± 4.4* | 35.9 ± 5.1* | 34.6 ± 9.5 | 31.4 ± 6.1 | 30.9 ± 5.5 | 71.0 ± 11.4* | 72.4 ± 13.7* | 69.7 ± 13.8* |

There was no statistically significant interaction between fatigue conditions and dominance for hip abduction range of motion ($F_{2,22} = 0.201$, $p = 0.819$, $\eta^2 = 0.018$). The were no differences between conditions ($F_{2,22} = 0.009$, $p = 0.991$, $\eta^2 = 0.001$) but there were between sides ($F_{1,11} = 10.482$, $p = 0.008$, $\eta^2 = 0.488$).

There was no statistically significant interaction between fatigue conditions and dominance for hip flexion range of motion ($F_{2,22} = 3.074$, $p = 0.066$, $\eta^2 = 0.218$). There were no differences between conditions ($F_{2,22} = 1.374$, $p = 0.274$, $\eta^2 = 0.111$) nor between sides ($F_{1,11} = 0.264$, $p = 0.618$, $\eta^2 = 0.023$).

There was no statistically significant interaction between fatigue conditions and dominance for the hip internal rotation range of motion ($F_{2,22} = 0.522$, $p = 0.601$, $\eta^2 = 0.045$). There were no differences between conditions ($F_{2,22} = 1.062$, $p = 0.363$, $\eta^2 = 0.088$) but there were differences between sides ($F_{1,11} = 21.570$, $p = 0.001$, $\eta^2 = 0.662$).

### 4.3.4 Knee Joint

#### 4.3.4.1 Average Angles

Table 4.8 shows the mean of the twelve participants' average knee flexion during the cycle.

Table 4.8. Mean (°) and standard deviation of average knee flexion for non-fatigued (NF), 50% time point (50% TP) and fatigued (F) conditions and both sides.

| | NF | 50% TP | F |
|---|---|---|---|
| Dominant side (°) | 91.0 ± 4.6 | 89.9 ± 4.4 | 89.0 ± 4.4 |
| Non-dominant side (°) | 90.9 ± 5.6 | 89.3 ± 6.3 | 89.0 ± 4.5 |

There was no significant interaction between fatigue conditions and dominance for average knee flexion ($F_{2,22} = 0.321$, $p = 0.729$, $\eta^2 = 0.028$). There was a significant main effect on the fatigue conditions ($F_{2,22} = 4.800$, $p = 0.019$, $\eta^2 = 0.304$). A post hoc Bonferroni test revealed no significant differences between levels. There was no significant main effect on dominance ($F_{1,11} = 0.045$, $p = 0.836$, $\eta^2 = 0.004$).

#### 4.3.4.2 Maximum Angles

Table 4.9 shows the mean of the twelve participants' average knee flexion during the cycle.

Table 4.9. Mean (°) and standard deviation of maximum knee flexion for non-fatigued (NF), 50% time point (50% TP) and fatigued (F) conditions and both sides. * indicates statistical differences between sides.

| | NF | 50% TP | F |
|---|---|---|---|
| Dominant side (°) | 139.5 ± 6.2* | 137.5 ± 7.1 | 135.2 ± 6.5* |
| Non-dominant side (°) | 145.2 ± 8.0* | 144.0 ± 8.1 | 142.0 ± 7.7* |

There was no significant interaction between fatigue conditions and dominance ($F_{2,22}$ = 0.634, $p$ = 0.540, $\eta^2$ = 0.054). There were differences between conditions ($F_{2,22}$ = 8.595, $p$ = 0.002, $\eta^2$ = 0.439), but not between sides ($F_{1,11}$ = 5.230, $p$ = 0.043, $\eta^2$ = 0.322). A post hoc Bonferroni test revealed NF was statistically significantly higher than F condition ($p$ = 0.011, $d$ = 0.48).

#### 4.3.4.3 Minimum Angles

Table 4.10 shows the mean of the twelve participants' minimum knee flexion during the cycle.

Table 4.10. Mean (°) and standard deviation of minimum knee flexion for non-fatigued (NF), 50% time point (50% TP) and fatigued (F) conditions and both sides.

| | NF | 50% TP | F |
|---|---|---|---|
| Dominant side (°) | 37.0 ± 9.3 | 35.6 ± 8.5 | 36.4 ± 9.0 |
| Non-dominant side (°) | 38.7 ± 10.9 | 35.8 ± 11.4 | 36.9 ± 9.6 |

A two way repeated measures ANOVA showed no significant interaction between fatigue conditions and dominance for average knee flexion ($F_{2,22}$ = 0.752, $p$ = 0.483, $\eta^2$ = 0.064). There was no significant main effect on the fatigue conditions ($F_{2,22}$ = 2.600, $p$ = 0.097, $\eta^2$ = 0.191) nor significant main effect on dominance ($F_{1,11}$ = 0.076, $p$ = 0.788, $\eta^2$ = 0.007).

#### 4.3.4.4 Knee Range of Motion

Table 4.11 shows the mean of the twelve participants' range of motion for knee flexion during the cycle.

Table 4.11. Mean (°) and standard deviation of knee flexion range of motion for non-fatigued (NF), 50% time point (50% TP) and fatigued (F) conditions and both sides. † indicates statistical differences between fatigue conditions.

| | NF | 50% TP | F |
|---|---|---|---|
| Dominant side (°) | 102.5 ± 11.8† | 101.9 ± 12.6 | 98.7 ± 12.9† |
| Non-dominant side (°) | 106.4 ± 16.2† | 108.1 ± 15.9 | 105.0 ± 15.6† |

There was no statistically significant interaction between fatigue conditions and dominance for knee flexion range of motion ($F_{2,22}$ = 1.811, $p$ = 0.187, $\eta^2$ = 0.141). There was a significant difference between fatigue conditions ($F_{2,22}$ = 3.943, $p$ = 0.034, $\eta^2$ = 0.264) but not between sides ($F_{1,11}$ = 1.059, $p$ = 0.326, $\eta^2$ = 0.088). A post hoc Bonferroni test revealed NF was statistically significantly higher than F condition ($p$ = 0.045, $d$ = 0.17).

### 4.3.5 Ankle Joint

The complex morphology of the ankle joint results in a complex axis of rotation of the ankle. The coexistence of the 'true ankle joint' (consisting of the tibia, fibula, and talus) and the subtalar joint, creates longitudinal and oblique axes of rotation that make motions of the ankle concurrent (i.e. inversion and evertion motions are naturally accompanied with abduction and adduction of the ankle). This should be kept in mind when interpreting ankle results.

#### 4.3.5.1 Average Angles

Table 4.12 shows the mean of the twelve participants' average angle for ankle abduction, flexion and external rotation during the cycle.

Table 4.12. Mean (°) and standard deviation of average ankle inversion, plantarflexion and adduction for, non-fatigued (NF), 50% time point (50% TP) and fatigued (F) conditions and both sides. * indicates statistical differences between sides. † indicates statistical differences between fatigue conditions.

| | Inversion | | | Plantarflexion | | | Adduction | | |
|---|---|---|---|---|---|---|---|---|---|
| | NF | 50% TP | F | NF | 50% TP | F | NF | 50% TP | F |
| Dominant side (°) | -0.77 ± 4.2*†† | 2.93 ± 4.0*† | 3.43 ± 3.8*† | 22.1 ± 7.2* | 22.8 ± 7.0* | 22.7 ± 6.5* | 16.5 ± 11.3* | 17.4 ± 10.8* | 16.3 ± 10.3* |
| Non-dominant side (°) | 5.26 ± 4.9*†† | 7.78 ± 5.1*† | 9.00 ± 4.7*† | 19.3 ± 2.6* | 18.7 ± 2.9* | 19.9 ± 2.9* | 26.7 ± 10.8* | 24.5 ± 10.8* | 25.9 ± 10.1* |

There was no statistically significant interaction between ankle inversion fatigue conditions and dominance ($F_{2,22}$ = 2.425, $p$ = 0.112, $\eta^2$ = 0.181). There were differences between fatigue conditions ($F_{2,22}$ = 28.760, $p$ < 0.001, $\eta^2$ = 0.723) and between sides ($F_{1,11}$ = 9.263, $p$ = 0.011, $\eta^2$ = 0.457). A Bonferroni post hoc test revealed NF was statistically significantly higher than F ($p$ < 0.001, $d$ = 0.75) and 50% TP ($p$ < 0.001, $d$ = 0.58) conditions.

There was no statistically significant interaction between ankle plantarflexion fatigue conditions and dominance ($F_{2,22}$ = 1.738, $p$ = 0.199, $\eta^2$ = 0.136). There were no differences between conditions ($F_{2,22}$ = 0.011, $p$ = 0.989, $\eta^2$ = 0.001), but there were differences between sides ($F_{1,11}$ = 5.195, $p$ = 0.044, $\eta^2$ = 0.321).

There was a statistically significant interaction between ankle adduction fatigue conditions and dominance ($F_{2,22}$ = 6.189, $p$ = 0.007, $\eta^2$ = 0.360). There were no differences between fatigue conditions ($F_{2,22}$ = 0.643, $p$ = 0.535, $\eta^2$ = 0.055), but there were differences between sides ($F_{1,11}$ = 5.718, $p$ = 0.036, $\eta^2$ = 0.342).

#### 4.3.5.2 Maximum Angles

Table 4.13 shows the mean of the twelve participants' maximum angle for ankle abduction, flexion and external rotation during the cycle.

Table 4.13. Mean (°) and standard deviation of maximum ankle inversion, plantarflexion and adduction for, non-fatigued (NF), 50% time point (50% TP) and fatigued (F) conditions and both sides. * indicates statistical differences between sides.

| | Inversion | | | Plantarflexion | | | Adduction | | |
|---|---|---|---|---|---|---|---|---|---|
| | NF | 50% TP | F | NF | 50% TP | F | NF | 50% TP | F |
| Dominant side (°) | 16.5 ± 9.2* | 20.2 ± 8.2* | 18.5 ± 6.7* | 45.8 ± 7.1 | 45.7 ± 7.1 | 44.3 ± 6.1 | 33.4 ± 15.5* | 35.3 ± 13.3* | 33.1± 12.8* |
| Non-dominant side (°) | 34.1 ± 7.7* | 33.7 ± 7.1* | 33.8 ± 6.9* | 43.2 ± 5.0 | 42.0 ± 5.4 | 42.0 ± 5.1 | 54.9 ± 11.8* | 51.7 ± 13.5* | 53.5 ± 9.7* |

There was no statistically significant interaction between maximum ankle inversion fatigue conditions and dominance ($F_{2,22}$ = 3.441, $p$ = 0.050, $\eta^2$ = 0.238). There were no differences between fatigue conditions ($F_{2,22}$ = 2.293, $p$ = 0.125, $\eta^2$ = 0.172), but there were differences between sides ($F_{1,11}$ = 28.372, $p < 0.001$, $\eta^2$ = 0.721).

There was no statistically significant interaction between maximum ankle plantarflexion fatigue conditions and dominance ($F_{2,22}$ = 0.928, $p$ = 0.410, $\eta^2$ = 0.078). There were no

differences between conditions ($F_{2,22}$ = 2.979, $p$ = 0.072, $\eta^2$ = 0.213) nor between sides ($F_{1,11}$ = 1.244, $p$ = 0.288, $\eta^2$ = 0.102).

There was a statistically significant interaction between maximum ankle adduction fatigue conditions and dominance ($F_{2,22}$ = 4.218, $p$ = 0.028, $\eta^2$ = 0.277). There were no significant differences between conditions ($F_{2,22}$ = 0.433, $p$ = 0.654, $\eta^2$ = 0.038), but there were differences between sides ($F_{1,11}$ = 18.623, $p$ = 0.001, $\eta^2$ = 0.629).

#### 4.3.5.3 Minimum Angles

Table 4.14 shows the mean of the twelve participants' minimum angle for ankle abduction, flexion and external rotation during the cycle.

Table 4.14. Mean (°) and standard deviation of minimum ankle inversion, plantarflexion and adduction for, non-fatigued (NF), 50% time point (50% TP) and fatigued (F) conditions and both sides. * indicates statistical differences between sides. † indicates statistical differences between fatigue conditions.

| | Inversion | | | Plantarflexion | | | Adduction | | |
|---|---|---|---|---|---|---|---|---|---|
| | NF | 50% TP | F | NF | 50% TP | F | NF | 50% TP | F |
| Dominant side (°) | -5.61 ± 8.6* | -4.42 ± 8.1* | -4.83 ± 8.1* | -17.9 ± 6.8†† | -14.5 ± 6.3†† | -12.4 ± 5.2†† | -2.32 ± 12.3 | -1.56 ± 11.5 | -0.41± 10.5 |
| Non-dominant side (°) | -12.5 ± 5.8* | -13.3 ± 5.6* | -13.1 ± 4.9* | -18.5 ± 6.5†† | -14.4 ± 6.5†† | -13.3 ± 5.9†† | -5.67 ± 12.6 | -7.62 ± 12.3 | -7.71 ± 11.2 |

There was no statistically significant interaction between minimum ankle inversion fatigue conditions and dominance ($F_{1.302,14.323}$ = 3.739, $p$ = 0.065, $\eta^2$ = 0.254). There

were no differences between fatigue conditions ($F_{1.332,14.652}$ = 0.086, $p$ = 0.841, $\eta^2$ = 0.008) but there were differences between sides ($F_{1,11}$ = 19.254, $p$ = 0.001, $\eta^2$ = 0.636).

There was no statistically significant interaction between minimum ankle plantarflexion fatigue conditions and dominance ($F_{2,22}$ = 0.693, $p$ = 0.511, $\eta^2$ = 0.059). There were differences between conditions ($F_{2,22}$ = 42.609, $p$ < 0.001, $\eta^2$ = 0.795) but not between sides ($F_{1,11}$ = 0.032, $p$ = 0.861, $\eta^2$ = 0.003). A post hoc Bonferroni test revealed NF was statistically significantly higher than F conditions ($p$ < 0.001, $d$ = 0.89) and 50% TP ($p$ < 0.001, $d$ = 0.58) conditions, 50% TP was statistically significantly higher than F ($p$ = 0.048, $d$ = 0.27).

There was a statistically significant interaction between minimum ankle adduction fatigue conditions and dominance ($F_{1.454,15.992}$ = 3.580, $p$ = 0.064, $\eta^2$ = 0.246). There was no differences between fatigue conditions ($F_{1.400,15.395}$ = 0.203, $p$ = 0.740, $\eta^2$ = 0.018) nor between sides ($F_{2,22}$ = 2.607, $p$ = 0.135, $\eta^2$ = 0.192).

#### 4.3.5.4 Ankle Range of Motion

Table 4.15 shows the mean of the twelve participants' range of motion angle for ankle inversion, plantarflexion and adduction during the cycle.

Table 4.15. Mean (°) and standard deviation of the ankle's inversion, planatrflexion and adduction range of motion for non-fatigued (NF), 50% time point (50% TP) and fatigued (F) conditions and both sides. * indicates statistical differences between sides. † indicates statistical differences between fatigue conditions.

| | Inversion | | | Plantarflexion | | | Adduction | | |
|---|---|---|---|---|---|---|---|---|---|
| | NF | 50% TP | F | NF | 50% TP | F | NF | 50% TP | F |
| Dominant side (°) | 22.2 ± 6.2* | 24.7 ± 5.1* | 23.4 ± 3.6* | 63.8 ± 12.1†† | 60.3 ± 12.1† | 56.7 ± 10.4† | 35.7 ± 17.3* | 36.8 ± 16.0* | 33.6 ± 14.6* |
| Non-dominant side (°) | 46.7 ± 7.0* | 47.1 ± 8.1* | 46.9 ± 7.1* | 61.8 ± 9.6†† | 56.5 ± 10.3† | 55.3 ± 9.0† | 60.6 ± 15.9* | 59.3 ± 18.5* | 61.2 ± 16.0* |

There was no statistically significant interaction between fatigue conditions and dominance for ankle inversion range of motion ($F_{2,22}$ = 0.597, $p$ = 0.559, $\eta^2$ = 0.051). There were no differences between conditions ($F_{2,22}$ = 1.598, $p$ = 0.225, $\eta^2$ = 0.127) but there were between sides ($F_{1,11}$ = 98.353, $p < 0.001$, $\eta^2$ = 0.999).

There was no statistically significant interaction between fatigue conditions and dominance for ankle plantarflexion range of motion ($F_{2,22}$ = 1.130, $p$ = 0.341, $\eta^2$ = 0.093). There were differences between conditions ($F_{2,22}$ = 28.750, $p < 0.001$, $\eta^2$ = 0.723) but not between sides ($F_{1,11}$ = 0.298, $p$ = 0.596, $\eta^2$ = 0.026). A post hoc Bonferroni test revealed NF was statistically significantly higher than F ($p < 0.001$, $d$ = 0.66) and 50% TP ($p$ = 0.01, $d$ = 0.40) conditions.

There was no statistically significant interaction between fatigue conditions and dominance for ankle adduction range of motion ($F_{2,22}$ = 2.192, $p$ = 0.135, $\eta^2$ = 0.166). There were no differences between fatigue conditions ($F_{2,22}$ = 0.409, $p$ = 0.669, $\eta^2$ = 0.036) but there were between sides ($F_{1,11}$ = 16.681, $p$ = 0.002, $\eta^2$ = 0.603).

### 4.3.6 Joint Angular Velocity

#### 4.3.6.1 Hip Motions

Table 4.16 shows the mean of the twelve participants' angular velocity for the hip abduction-adduction, flexion-extension, and rotation during the cycle.

Table 4.16. Mean ($rad \cdot s^{-1}$) and standard deviation of angular velocity for the hip abduction-adduction, flexion-extension, and rotation for, non-fatigued (NF), 50% time point (50% TP) and fatigued (F) conditions and both sides. * indicates statistical differences between sides. † indicates statistical differences between fatigue conditions.

| | Hip Abduction | | | Hip Flexion | | | Hip Rotation | | |
|---|---|---|---|---|---|---|---|---|---|
| | NF | 50% TP | F | NF | 50% TP | F | NF | 50% TP | F |
| Dominant side ($rad \cdot s^{-1}$) | 4.8 ± 1.0*†† | 1.8 ± 0.5*† | 1.86 ± 0.4*† | 3.4 ± 0.8*†† | 3.3 ± 0.5*† | 3.0 ± 0.4*† | 2.2 ± 1.0*† | 2.1 ± 0.9*† | 2.0 ± 1.1*†† |
| Non-dominant side ($rad \cdot s^{-1}$) | 3.8 ± 0.8*†† | 3.3 ± 0.7*† | 3.2 ± 0.6*† | 3.9 ± 0.5*†† | 3.6 ± 0.4*† | 3.4 ± 0.4*† | 5.8 ± 0.8*† | 5.2 ± 0.7*† | 4.6 ± 0.6*†† |

There was a statistically significant interaction between hip abduction-adduction angular velocity fatigue conditions and dominance ($F_{1.151,12.662} = 43.415$, $p < 0.001$, $\eta^2 = 0.798$). There were differences between fatigue conditions ($F_{1.375,15.124} = 82.640$, $p < 0.001$, $\eta^2 = 0.883$) and between sides ($F_{1,11} = 21.273$, $p = 0.001$, $\eta^2 = 0.659$). A post hoc Bonferroni tests revealed NF was statistically significantly higher than F ($p < 0.001$, $d = 1.87$) and between 50% TP ($p < 0.001$, $d = 1.68$) conditions.

There was no statistically significant interaction between hip flexion-extension angular velocity fatigue conditions and dominance ($F_{2,22} = 1.242$, $p = 0.308$, $\eta^2 = 0.101$). There were differences between conditions ($F_{2,22} = 10.399$, $p = 0.001$, $\eta^2 = 0.486$) and between sides ($F_{1,11} = 5.620$, $p = 0.037$, $\eta^2 = 0.338$). A post hoc Bonferroni tests revealed NF was

statistically significantly higher than F ($p$ = 0.013, $d$ = 0.78) and 50% TP ($p$ = 0.015, $d$ = 0.28) conditions.

There was a significant interaction between hip rotation angular velocity fatigue conditions and dominance ($F_{1.888,20.769}$ = 28.205, $p$ < 0.001, $\eta^2$ = 0.719). There were differences between conditions ($F_{1.501,16.601}$ = 30.799, $p$ < 0.001, $\eta^2$ = 0.737) and between sides ($F_{1,11}$ = 141.824, $p$ < 0.001, $\eta^2$ = 0.928). A post hoc Bonferroni test revealed NF was statistically significantly higher than F ($p$ < 0.001, $d$ = 0.41) and 50% TP ($p$ = 0.013, $d$ = 0.19) conditions. F was statistically significantly lower than 50% TP ($p$ < 0.001, $d$ = 0.23).

#### 4.3.6.2 Knee Motion

Table 4.17 shows the mean of the twelve participants' angular velocity for the knee flexion-extension during the cycle.

Table 4.17. Mean ($rad \cdot s^{-1}$) and standard deviation knee flexion-extension angular velocity for non-fatigued (NF), 50% time point (50% TP) and fatigued (F) conditions and both sides. * indicates statistical differences between sides. † indicates statistical differences between fatigue conditions.

| | NF | 50% TP | F |
|---|---|---|---|
| Dominant side ($rad \cdot s^{-1}$) | 4.7 ± 0.4*†† | 4.2 ± 0.4*†† | 3.9 ± 0.4*†† |
| Non-dominant side ($rad \cdot s^{-1}$) | 6.2 ± 1.0*†† | 5.5 ± 0.7*†† | 5.2 ± 0.7*†† |

There was no statistically significant interaction between knee flexion angular velocity fatigue conditions and dominance ($F_{2,22}$ = 2.960, $p$ = 0.073, $\eta^2$ = 0.212). There were differences between conditions ($F_{2,22}$ = 32.703, $p$ < 0.001, $\eta^2$ = 0.748), and differences

between sides ($F_{1,11}$ = 44.512, $p$ < 0.001, $\eta^2$ = 0.802). A post hoc Bonferroni test revealed NF was statistically significantly higher than F ($p$ < 0.001, $d$ = 0.96) and 50% TP ($p$ = 0.006, $d$ = 0.40) conditions. F was statistically significantly lower than 50% TP ($p$ = 0.002, $d$ = 0.60).

#### 4.3.6.3 Ankle Motions

Table 4.18 shows the mean of the twelve participants' angular velocity for the ankle inversion-eversion, plantarflexion-dorsiflexion, and abduction-adduction during the cycle.

Table 4.18. Mean (rad·s$^{-1}$) and standard deviation of angular velocity for the ankle inversion-eversion, plantarflexion-dorsiflexion, and abduction-adduction for, non-fatigued (NF), 50% time point (50% TP) and fatigued (F) conditions and both sides. * indicates statistical differences between sides. † indicates statistical differences between fatigue conditions.

| | Ankle Inv-Eve | | | Ankle Pla-Dor | | | Ankle Abd-Add | | |
|---|---|---|---|---|---|---|---|---|---|
| | NF | 50% TP | F | NF | 50% TP | F | NF | 50% TP | F |
| Dominant side (rad·s$^{-1}$) | 3.1 ± 0.4*†† | 2.8 ± 0.5*†† | 2.4 ± 0.3*†† | 4.9 ± 1.0*†† | 4.5 ± 0.9*†† | 4.1 ± 0.6*†† | 5.8 ± 1.0*†† | 5.3 ± 0.7*†† | 5.0 ± 0.6*†† |
| Non-dominant side (rad·s$^{-1}$) | 4.8 ± 0.5*†† | 4.4 ± 0.6*†† | 3.9 ± 0.4*†† | 4.3 ± 0.6*†† | 3.7 ± 0.6*†† | 3.4 ± 0.5*†† | 4.8 ± 1.0*†† | 4.6 ± 1.0*†† | 4.3 ± 0.8*†† |

There was no statistically significant interaction between ankle inversion-eversion angular velocity conditions and dominance ($F_{2,22}$ = 2.374, $p$ = 0.117, $\eta^2$ = 0.178). There were differences between fatigue conditions ($F_{2,22}$ = 47.177, $p$ < 0.001, $\eta^2$ = 0.811) and between sides ($F_{1,11}$ = 74.515, $p$ < 0.001, $\eta^2$ = 0.871). A post hoc Bonferroni test revealed differences between NF and F conditions ($p$ < 0.001, $d$ = 0.84), between NF

and the 50% TP ($p < 0.001$, $d = 0.38$), and between F and the 50% TP ($p < 0.001$, $d = 0.43$).

There was statistically significant interaction between ankle plantarflexion-dorsiflexion angular velocity fatigue conditions and dominance ($F_{2,22} = 0.382$, $p = 0.687$, $\eta^2 = 0.034$). There were differences between conditions ($F_{2,22} = 26.265$, $p < 0.001$, $\eta^2 = 0.705$) and between sides ($F_{1,11} = 17.146$, $p = 0.002$, $\eta^2 = 0.609$). A post hoc Bonferroni test revealed differences between NF and F conditions ($p < 0.001$, $d = 1.06$), between NF and the 50% TP ($p = 0.005$, $d = 0.54$), and between F and the 50% TP ($p = 0.014$, $d = 0.47$).

There was a statistically significant interaction between ankle abduction-adduction angular velocity fatigue conditions and dominance ($F_{2,22} = 3.844$, $p = 0.037$, $\eta^2 = 0.259$). There were differences between fatigue conditions ($F_{2,22} = 17.681$, $p < 0.001$, $\eta^2 = 0.616$) and differences between sides ($F_{1,11} = 16.133$, $p = 0.002$, $\eta^2 = 0.595$). A post hoc Bonferroni tests revealed differences between NF and F conditions ($p = 0.002$, $d = 0.68$), between NF and the 50% TP ($p = 0.023$, $d = 0.33$), and between F and the 50% TP ($p = 0.010$, $d = 0.36$).

### 4.3.7 Feet Pitch Angles

#### 4.3.7.1 Average, Maximum and Minimum

Table 4.19 shows the mean of the twelve participants' average, maximum and minimum foot pitch angles during the cycle.

Table 4.19. Mean (°) and standard deviation of average, maximum and minimum foot pitch angles for, non-fatigued (NF), 50% time point (50% TP) and fatigued (F) conditions and both sides. * indicates statistical differences between sides.

| | Average | | | Maximum | | | Minimum | | |
|---|---|---|---|---|---|---|---|---|---|
| | NF | 50% TP | F | NF | 50% TP | F | NF | 50% TP | F |
| Dominant side (°) | 11.5 ± 3.7* | 11.1 ± 3.7* | 9.8 ± 3.4* | 53.8 ± 11.0* | 51.6 ± 10.3* | 50.0 ± 8.5* | -30.0 ± 5.6* | -31.9 ± 7.1* | -33.4 ± 7.0* |
| Non-dominant side (°) | 9.1 ± 4.6* | 9.6 ± 3.7* | 7.7 ± 5.1* | 60.7 ± 9.2* | 61.0 ± 8.5* | 60.1 ± 9.7* | -41.44 ± 10.9* | -38.6 ± 8.7* | -43.7 ± 14.2* |

There was no statistically significant interaction between average feet pitch angles fatigue conditions and dominance ($F_{2,22} = 0.205$, $p = 0.816$, $\eta^2 = 0.018$). There were no differences between conditions ($F_{2,22} = 3.401$, $p = 0.052$, $\eta^2 = 0.236$), but there were between sides ($F_{1,11} = 6.133$, $p = 0.031$, $\eta^2 = 0.358$).

There was no statistically significant interaction between maximum feet pitch angles fatigue conditions and dominance ($F_{2,22} = 1.226$, $p = 0.313$, $\eta^2 = 0.100$). There were no differences between conditions ($F_{1.191,13.098} = 1.516$, $p = 0.246$, $\eta^2 = 0.121$) but there were between sides ($F_{1,11} = 11.185$, $p = 0.007$, $\eta^2 = 0.504$).

There was no statistically significant interaction between minimum feet pitch angles fatigue conditions and dominance ($F_{2,22} = 1.493$, $p = 0.247$, $\eta^2 = 0.120$). There were no differences between conditions ($F_{1.244,13.687} = 1.921$, $p = 0.189$, $\eta^2 = 0.149$), but there were between sides ($F_{1,11} = 19.721$, $p = 0.001$, $\eta^2 = 0.642$).

#### 4.3.7.2 Positive Pitch Angle Time

Table 4.20 shows the mean of the twelve participants' percentage of positive feet pitch angles during the cycle.

Table 4.20. Mean (%) and standard deviation of percentage of positive feet pitch angles for non-fatigued (NF), 50% time point (50% TP) and fatigued (F) conditions and both sides. * indicates statistical differences between sides.

| | NF | 50% TP | F |
|---|---|---|---|
| Dominant side (%) | 64.9 ± 3.9* | 65.3 ± 4.8* | 64.4 ± 4.9* |
| Non-dominant side (%) | 62.4 ± 6.1* | 62.2 ± 4.2* | 60.6 ± 3.3* |

There was no significant interaction between the percentage of positive feet pitch angles fatigue conditions and dominance ($F_{2,22} = 0.289$, $p = 0.752$, $\eta^2 = 0.026$). There were no differences between conditions ($F_{2,22} = 2.347$, $p = 0.119$, $\eta^2 = 0.176$), but there were differences between sides ($F_{1,11} = 6.538$, $p = 0.027$, $\eta^2 = 0.373$).

### 4.3.8 Average Foot Sweepback Angles

Table 4.21 shows the mean of the twelve participants' average sweepback angles of the feet during the cycle.

Table 4.21. Mean (°) and standard deviation of average sweepback angles of the feet for non-fatigued (NF), 50% time point (50% TP) and fatigued (F) conditions and both sides. † indicates statistical differences between fatigue conditions.

| | NF | 50% TP | F |
|---|---|---|---|
| Dominant side (°) | 185.4 ± 4.9† | 188.3 ± 5.2† | 190.3 ± 5.7†† |
| Non-dominant side (°) | 188.6 ± 11.7† | 190.1 ± 10.1† | 193.9 ± 10.5†† |

There was no significant interaction between average sweepback angles of the feet fatigue conditions and dominance ($F_{2,22}$ = 0.917, $p$ = 0.415, $\eta^2$ = 0.077). There were significant differences between conditions ($F_{2,22}$ = 11.501, $p$ < 0.001, $\eta^2$ = 0.511), but there were no differences between sides ($F_{1,11}$ = 1.207, $p$ = 0.295, $\eta^2$ = 0.099). A post hoc Bonferroni test revealed NF was statistically significantly higher than F condition ($p$ = 0.006, $d$ = 0.58), and 50% TP was statistically significantly higher than F ($p$ = 0.023, $d$ = 0.34).

### 4.3.9 Average Foot Speed

Table 4.22 shows the mean of the twelve participants' average foot speed during the cycle.

Table 4.22. Mean (m/s) and standard deviation of average foot speed for non-fatigued (NF), 50% time point (50% TP) and fatigued (F) conditions and both sides. † indicates statistical differences between fatigue conditions.

| | NF | 50% TP | F |
|---|---|---|---|
| Dominant side (m/s) | 2.80 ± 0.1†† | 2.55 ± 0.1†† | 2.34 ± 0.1†† |
| Non-dominant side (m/s) | 2.77 ± 0.1†† | 2.54 ± 0.1†† | 2.32 ± 0.1†† |

There was no significant interaction between average foot speed fatigue conditions and dominance ($F_{2,22}$ = 0.470, $p$ = 0.631, $\eta^2$ = 0.041). There were significant differences between conditions ($F_{1.064,11.709}$ = 78.458, $p$ < 0.001, $\eta^2$ = 0.877), but there were no differences between sides ($F_{1,11}$ = 1.038, $p$ = 0.330, $\eta^2$ = 0.086). A post hoc Bonferroni test revealed NF was statistically significantly higher than F ($p$ < 0.01, $d$ = 2.99) and

50% TP ($p < 0.01$, $d = 1.64$). 50% TP was statistically significantly higher than F ($p < 0.01$, $d = 1.46$).

### 4.3.10 Feet Motion

Table 4.23 shows the mean of the twelve participants' average anterior-posterior, vertical and medio-lateral motion components of the feet during the cycle.

Table 4.23. Mean (%) and standard deviation of average anterior-posterior, vertical and medio-lateral motion components of the feet for, non-fatigued (NF), 50% time point (50% TP) and fatigued (F) conditions and both sides.

| | Anterior-Posterior Motion | | | Vertical Motion | | | Medio-Lateral Motion | | |
|---|---|---|---|---|---|---|---|---|---|
| | NF | 50% TP | F | NF | 50% TP | F | NF | 50% TP | F |
| Dominant side (%) | 32.8 ± 5.2 | 35.2 ± 6.0 | 35.7 ± 4.9 | 37.9 ± 5.6 | 35.9 ± 5.9 | 35.7 ± 4.8 | 29.1 ± 5.8 | 28.8 ± 3.7 | 28.5 ± 4.7 |
| Non-dominant side (%) | 33.3 ± 7.6 | 35.5 ± 6.1 | 36.2 ± 8.2 | 38.0 ± 7.6 | 36.2 ± 7.7 | 35.3 ± 7.5 | 26.8 ± 5.9 | 27.3 ± 5.8 | 27.8 ± 6.5 |

There was no statistically significant interaction between the anterior-posterior motion component fatigue conditions and dominance ($F_{1.355,14.903} = 0.010$, $p = 0.064$, $\eta^2 = 0.001$). There were no differences between conditions ($F_{2,22} = 2.196$, $p = 0.135$, $\eta^2 = 0.166$) nor between sides ($F_{1,11} = 0.042$, $p = 0.841$, $\eta^2 = 0.004$).

There was no statistically significant interaction between the vertical motion component fatigue conditions and dominance ($F_{2,22} = 0.237$, $p = 0.791$, $\eta^2 = 0.021$). There were no differences between conditions ($F_{2,22} = 1.161$, $p = 0.332$, $\eta^2 = 0.095$) nor between sides ($F_{1,11} = 0.001$, $p = 0.982$, $\eta^2 < 0.001$).

There was no statistically significant interaction between the medio-lateral motion component fatigue conditions and dominance ($F_{1.308,14.387}$ = 0.746, $p$ = 0.437, $\eta^2$ = 0.064). There were no differences between conditions ($F_{2,22}$ = 0.026, $p$ = 0.974, $\eta^2$ = 0.002) nor sides ($F_{1,11}$ = 0.652, $p$ = 0.437, $\eta^2$ = 0.056).

### 4.3.11 Summary Table

Table 4.24 shows the main effect on fatigue, main effect on dominance and interaction between fatigue and dominance values for all kinematic variables.

Table 4.24. Main effect (ME) fatigue, main effect dominance and interaction between fatigue and dominance. Statistical differences (p<0.05) are indicated in bold.

| Variable | ME Fatigue | ME Dominance | Interaction |
|---|---|---|---|
| Average Hip Abduction | **$p$ = 0.001, $\eta^2$ = 0.479** | $p$ = 0.910, $\eta^2$ = 0.001 | $p$ = 0.823, $\eta^2$ = 0.018 |
| Average Hip Flexion | **$p$ = 0.003, $\eta^2$ = 0.414** | $p$ = 0.077, $\eta^2$ = 0.256 | $p$ = 0.123, $\eta^2$ = 0.174 |
| Avg Hip Internal Rotation | **$p$ = 0.003, $\eta^2$ = 0.409** | $p$ = 0.969, $\eta^2$ < 0.001 | $p$ = 0.608, $\eta^2$ = 0.044 |
| Average Knee Flexion | **$p$ = 0.019, $\eta^2$ = 0.304** | $p$ = 0.836, $\eta^2$ = 0.004 | $p$ = 0.729, $\eta^2$ = 0.028 |
| Avg Ankle Plantarflexion | $p$ = 0.989, $\eta^2$ = 0.001 | **$p$ = 0.044, $\eta^2$ = 0.321** | $p$ = 0.199, $\eta^2$ = 0.136 |
| Average Ankle Inversion | **$p$ < 0.001, $\eta^2$ = 0.723** | **$p$ = 0.011, $\eta^2$ = 0.457** | $p$ = 0.112, $\eta^2$ = 0.181 |
| Average Ankle Adduction | $p$ = 0.535, $\eta^2$ = 0.055 | **$p$ = 0.036, $\eta^2$ = 0.342** | **$p$ = 0.007, $\eta^2$ = 0.360** |
| Max Hip Abduction | **$p$ = 0.001, $\eta^2$ = 0.451** | $p$ = 0.351, $\eta^2$ = 0.079 | $p$ = 0.911, $\eta^2$ = 0.008 |
| Max Hip Flexion | **$p$ = 0.003, $\eta^2$ = 0.406** | $p$ = 0.093, $\eta^2$ = 0.235 | $p$ = 0.099, $\eta^2$ = 0.216 |
| Max Hip Internal Rotation | **$p$ = 0.004, $\eta^2$ = 0.389** | **$p$ = 0.010, $\eta^2$ = 0.466** | $p$ = 0.877, $\eta^2$ = 0.005 |
| Max Knee Flexion | **$p$ = 0.002, $\eta^2$ = 0.439** | **$p$ = 0.043, $\eta^2$ = 0.322** | $p$ = 0.540, $\eta^2$ = 0.054 |
| Max Ankle Plantarflexion | $p$ = 0.072, $\eta^2$ = 0.213 | $p$ = 0.288, $\eta^2$ = 0.102 | $p$ = 0.410, $\eta^2$ = 0.078 |
| Max Ankle Inversion | $p$ = 0.125, $\eta^2$ = 0.172 | **$p$ < 0.001, $\eta^2$ = 0.721** | $p$ = 0.050, $\eta^2$ = 0.238 |
| Max Ankle Adduction | $p$ = 0.654, $\eta^2$ = 0.038 | **$p$ = 0.001, $\eta^2$ = 0.629** | **$p$ = 0.028, $\eta^2$ = 0.277** |
| Min Hip Abduction | **$p$ = 0.003, $\eta^2$ = 0.404** | $p$ = 0.182, $\eta^2$ = 0.156 | $p$ = 0.916, $\eta^2$ = 0.008 |
| Min Hip Flexion | **$p$ = 0.002, $\eta^2$ = 0.513** | **$p$ = 0.015, $\eta^2$ = 0.428** | $p$ = 0.163, $\eta^2$ = 0.152 |
| Min Hip Internal Rotation | $p$ = 0.087, $\eta^2$ = 0.223 | $p$ = 0.091, $\eta^2$ = 0.238 | $p$ = 0.472, $\eta^2$ = 0.063 |

| | | | |
|---|---|---|---|
| Min Knee Flexion | $p = 0.097$, $\eta^2 = 0.191$ | $p = 0.788$, $\eta^2 = 0.007$ | $p = 0.483$, $\eta^2 = 0.064$ |
| Min Ankle Plantarflexion | **$p < 0.001$, $\eta^2 = 0.795$** | $p = 0.861$, $\eta^2 = 0.003$ | $p = 0.511$, $\eta^2 = 0.059$ |
| Min Ankle Inversion | $p = 0.841$, $\eta^2 = 0.008$ | **$p = 0.001$, $\eta^2 = 0.636$** | $p = 0.065$, $\eta^2 = 0.254$ |
| Min Ankle Adduction | $p = 0.740$, $\eta^2 = 0.018$ | $p = 0.135$, $\eta^2 = 0.192$ | $p = 0.064$, $\eta^2 = 0.246$ |
| Hip Abduction Range | $p = 0.991$, $\eta^2 = 0.001$ | **$p = 0.008$, $\eta^2 = 0.488$** | $p = 0.819$, $\eta^2 = 0.018$ |
| Hip Flexion Range | $p = 0.274$, $\eta^2 = 0.111$ | $p = 0.618$, $\eta^2 = 0.023$ | $p = 0.066$, $\eta^2 = 0.218$ |
| Hip Internal Rot Range | $p = 0.363$, $\eta^2 = 0.088$ | **$p = 0.001$, $\eta^2 = 0.662$** | $p = 0.601$, $\eta^2 = 0.045$ |
| Knee Flexion Range | **$p = 0.034$, $\eta^2 = 0.264$** | $p = 0.326$, $\eta^2 = 0.088$ | $p = 0.187$, $\eta^2 = 0.141$ |
| Ankle Plaflexion Range | **$p < 0.001$, $\eta^2 = 0.723$** | $p = 0.596$, $\eta^2 = 0.026$ | $p = 0.341$, $\eta^2 = 0.093$ |
| Ankle Inversion Range | $p = 0.225$, $\eta^2 = 0.127$ | **$p < 0.001$, $\eta^2 = 0.999$** | $p = 0.559$, $\eta^2 = 0.051$ |
| Ankle Adduction Range | $p = 0.669$, $\eta^2 = 0.036$ | **$p = 0.002$, $\eta^2 = 0.603$** | $p = 0.135$, $\eta^2 = 0.166$ |
| Average Foot Pitch Angle | $p = 0.052$, $\eta^2 = 0.236$ | $p = 0.031$, $\eta^2 = 0.358$ | $p = 0.816$, $\eta^2 = 0.018$ |
| Maximum Foot Pitch Angle | $p = 0.246$, $\eta^2 = 0.121$ | **$p = 0.007$, $\eta^2 = 0.504$** | $p = 0.313$, $\eta^2 = 0.100$ |
| Minimum Foot Pitch Angle | $p = 0.189$, $\eta^2 = 0.149$ | **$p = 0.001$, $\eta^2 = 0.642$** | $p = 0.247$, $\eta^2 = 0.120$ |
| Time of Positive Pitch Foot | $p = 0.119$, $\eta^2 = 0.176$ | **$p = 0.027$, $\eta^2 = 0.373$** | $p = 0.752$, $\eta^2 = 0.026$ |
| Avg Foot Sweepback Ang | **$p < 0.001$, $\eta^2 = 0.511$** | $p = 0.295$, $\eta^2 = 0.099$ | $p = 0.415$, $\eta^2 = 0.077$ |
| Foot Medio-Lateral Motion | $p = 0.974$, $\eta^2 = 0.002$ | $p = 0.437$, $\eta^2 = 0.056$ | $p = 0.437$, $\eta^2 = 0.064$ |
| Foot Vertical Motion | $p = 0.332$, $\eta^2 = 0.095$ | $p = 0.982$, $\eta^2 < 0.001$ | $p = 0.791$, $\eta^2 = 0.021$ |
| Foot Ant-Pos Motion | $p = 0.135$, $\eta^2 = 0.166$ | $p = 0.841$, $\eta^2 = 0.004$ | $p = 0.064$, $\eta^2 = 0.001$ |
| Average foot Speed | **$p < 0.001$, $\eta^2 = 0.877$** | $p = 0.330$, $\eta^2 = 0.086$ | $p = 0.631$, $\eta^2 = 0.041$ |
| Avg Hip Abduction Ang Vel | **$p < 0.001$, $\eta^2 = 0.883$** | **$p = 0.001$, $\eta^2 = 0.659$** | **$p < 0.001$, $\eta^2 = 0.798$** |
| Avg Hip Flexion Ang Vel | **$p = 0.001$, $\eta^2 = 0.486$** | **$p = 0.037$, $\eta^2 = 0.338$** | $p = 0.308$, $\eta^2 = 0.101$ |
| Avg Hip Rotation Ang Vel | **$p < 0.001$, $\eta^2 = 0.737$** | **$p < 0.001$, $\eta^2 = 0.928$** | **$p < 0.001$, $\eta^2 = 0.719$** |
| Avg Knee Flexion Ang Vel | **$p < 0.001$, $\eta^2 = 0.748$** | **$p < 0.001$, $\eta^2 = 0.802$** | $p = 0.073$, $\eta^2 = 0.212$ |
| Avg Ankle Inversion Ang Vel | **$p < 0.001$, $\eta^2 = 0.811$** | **$p < 0.001$, $\eta^2 = 0.871$** | $p = 0.117$, $\eta^2 = 0.178$ |
| Avg Ank Plaflexion Ang Vel | **$p < 0.001$, $\eta^2 = 0.705$** | **$p = 0.002$, $\eta^2 = 0.609$** | $p = 0.687$, $\eta^2 = 0.034$ |
| Avg Ankle Add Ang Vel | **$p < 0.001$, $\eta^2 = 0.616$** | **$p = 0.002$, $\eta^2 = 0.595$** | **$p = 0.037$, $\eta^2 = 0.259$** |

## 4.4 Muscle Activity

Section 4.4 presents the results for each fatigue level for each individual muscle tested. The value for each state represents the mean for the 12 subjects. Each subject score is the mean of the average for each particular variable during the cycle for nine cycles. Error bars represent 95% confidence interval of the true mean.

Repeated measures ANOVA tests were used for the average muscle activity that was not compared between sides. Repeated measures two-way ANOVA tests were used for the average normalized muscle activity.

### 4.4.1 Tibialis Anterior

#### 4.4.1.1 Average Activity

A repeated measures ANOVA for the average Right Tibialis Anterior activity showed significant differences between fatigue conditions ($F_{1.286,12.862} = 13.337$, $p = 0.002$, $\eta^2 = 0.572$). A post hoc Bonferroni test revealed NF was statistically significantly higher than F conditions ($p = 0.007$, $d = 0.80$) and 50% TP ($p = 0.047$, $d = 0.50$). 50% TP was statistically significantly higher than F ($p = 0.011$, $d = 0.40$) (Fig. 4.3).

There was a significant main effect between average Left Tibialis Anterior activity between fatigue conditions ($F_{1.282,12.818} = 18.989$, $p < 0.001$, $\eta^2 = 0.655$). A post hoc Bonferroni test revealed NF was statistically significantly higher than F ($p = 0.001$, $d = 0.98$) and the 50% TP ($p = 0.013$, $d = 0.68$) conditions. 50% TP was statistically significantly higher than F ($p = 0.027$, $d = 0.41$) (Fig. 4.3).

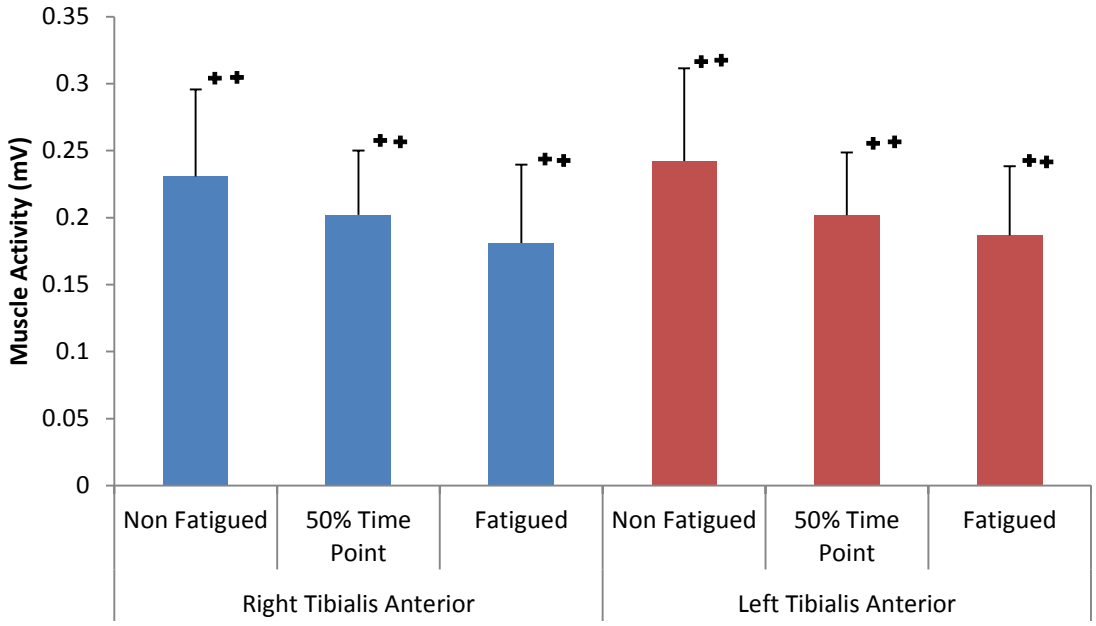


Figure 4.3. Average Right Tibialis Anterior activity for the three fatigue conditions. Error bars represent the group's standard deviation. ✚ indicates statistical differences between fatigue conditions.

#### 4.4.1.2 Normalized to MVC

There was no statistically significant interaction between the Tibialis Anterior activity normalized to MVC fatigue conditions and dominance ($F_{2,20}$ = 1.021, $p$ = 0.383, $\eta^2$ = 0.113). There were differences between fatigue conditions ($F_{2,20}$ = 20.636, $p < 0.001$, $\eta^2$ = 0.721), but not between sides ($F_{1,10}$ = 0.697, $p$ = 0.428, $\eta^2$ = 0.080). Post hoc Bonferroni tests revealed NF was statistically significantly higher than F ($p$ = 0.003, $d$ = 0.89) and 50% TP ($p$ = 0.011, $d$ = 0.59) conditions. F was statistically significantly lower than 50% TP ($p$ = 0.015, $d$ = 0.37) (Fig. 4.4).

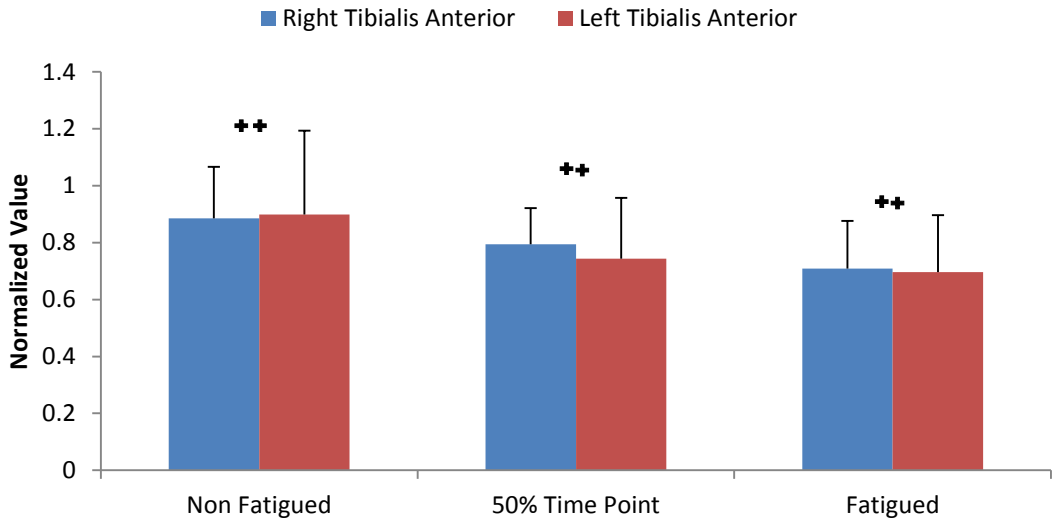


Figure 4.4. Average Left Tibialis Anterior activity normalized to MVC for the three fatigue conditions. Error bars represent the group's standard deviation. ✚indicates statistical differences between fatigue conditions.

#### 4.4.1.3 Normalized to Peak of the Cycle

There was no statistically significant interaction between the Tibialis Anterior activity normalized to peak of the cycle fatigue conditions and dominance ($F_{2,20}$ = 0.105, $p$ = 0.901, $\eta^2$ = 0.011). There were differences between fatigue conditions ($F_{2,20}$ = 28.715, $p$ < 0.001, $\eta^2$ = 0.761), but not between sides ($F_{1,10}$ = 0.333, $p$ = 0.578, $\eta^2$ = 0.036). Post hoc Bonferroni tests revealed NF was statistically significantly higher than F ($p$ < 0.001, $d$ = 0.82) and 50% TP ($p$ = 0.005, $d$ = 0.47) conditions (Fig. 4.5).

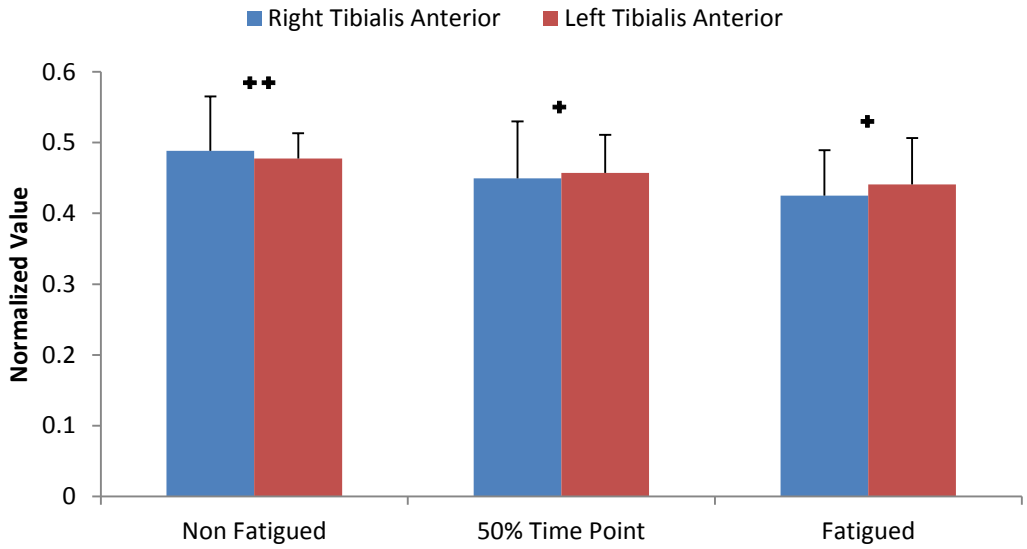


Figure 4.5. Average Left Tibialis Anterior normalized to peak of the cycle for the three fatigue conditions. Error bars represent the group's standard deviation. ✚indicates statistical differences between fatigue conditions.

#### 4.4.1.4 Pattern of Muscle Activity

The group's level of muscle activity is constant during the cycle (Fig. 4.6), with no significant peak or low periods of activity. Looking at individual data (appendix C), subjects 1, 2, 3, 4, 7 and 8 show lower activity from 55 to 70% of the cycle. This is supported by the individual activations timings (Fig. 4.7). Other subjects (6, 9, 10, 11 and 12) do not follow this trend and seem to have more individualized patterns of muscle activity for the Right Tibialis Anterior. Larger 95% confidence interval from 80 to 90% in the fatigued condition results from some subjects (1, 2, 3, 4, 6, 9 and 12) showing a peak of activity during that period. There is a general trend of decrease in amplitude as the subjects become fatigued. Figure 4.6 shows no significant differences

between the patterns of muscle activity between fatigue conditions (NF and F). Figure 4.7 shows the individual activation timings for the Right Tibialis Anterior muscle for the NF condition.

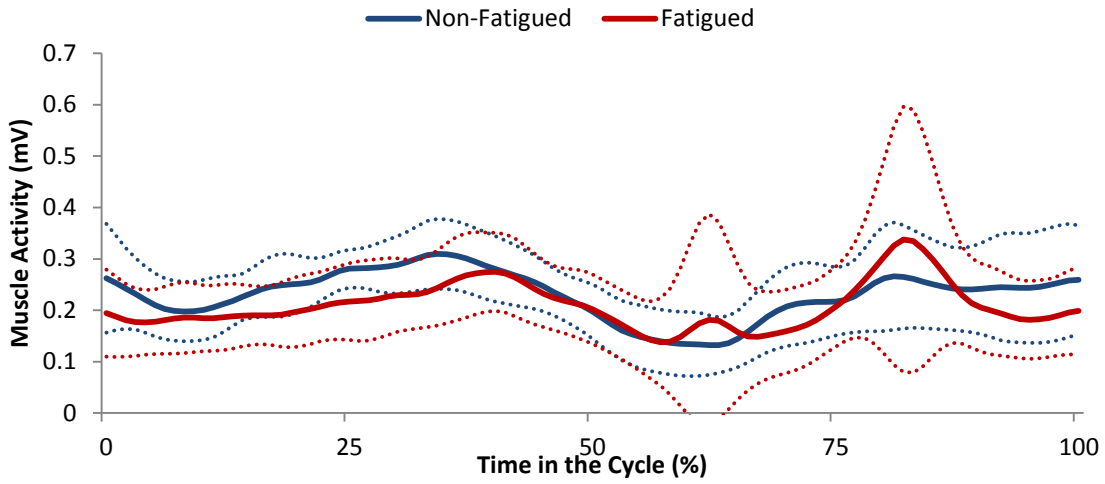


Figure 4.6. Right Tibialis Anterior activity pattern for non-fatigued and fatigued conditions. Solid line represents the mean, dotted line the 95% confidence interval of the true mean.

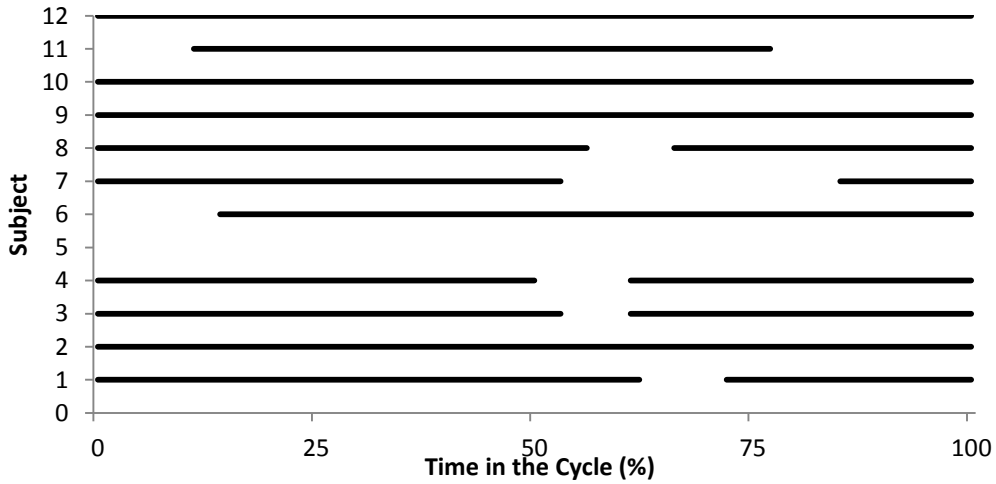


Figure 4.7. Individual activation times of the Right Tibialis Anterior for the non-fatigue condition following the double-threshold method.

The Left Tibialis Anterior group's level of muscle activity seems to have two moments of higher activity, 20 – 40% and 80 – 95%. Subjects 1, 10, 11 and 12 support the group's trend. However, other subjects seem to adopt individualized patterns of muscle activity. Figure 4.8 shows no significant differences between the patterns of muscle activity between NF and F conditions. At the same time, when comparing conditions, all subjects seem to maintain the same pattern for F condition with a decrease in amplitude. Figure 4.9 shows the individual activation timings for the Left Tibialis Anterior muscle for NF condition.

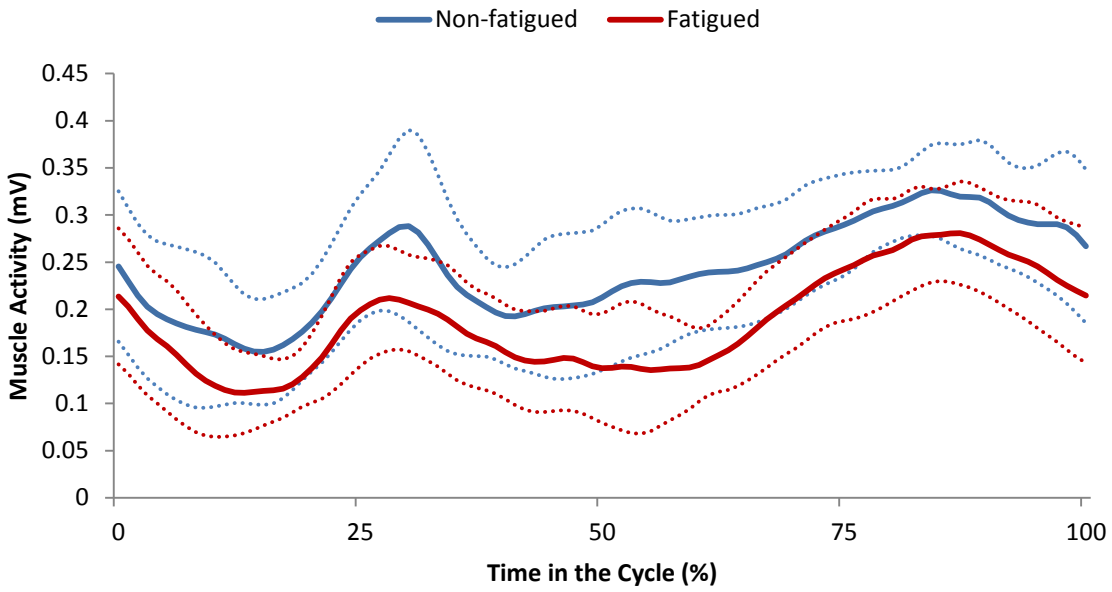


Figure 4.8 Left Tibialis Anterior activity pattern for non-fatigued and fatigued conditions. Solid line represents the mean, dotted line the 95% confidence interval of the true mean.

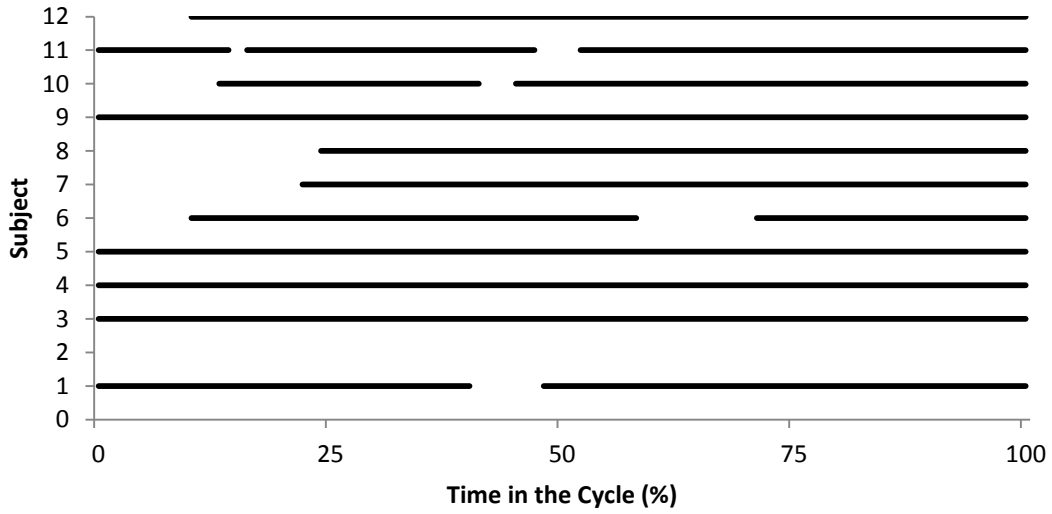


Figure 4.9 Individual activation times of the Left Tibialis Anterior for the non-fatigue condition following the double-threshold method.

### 4.4.2 Rectus Femoris

#### 4.4.2.1 Average Activity

A repeated measures ANOVA for average Right Rectus Femoris activity showed no significant differences between fatigue conditions ($F_{1.288,14.163} = 2.534$, $p = 0.128$, $\eta^2 = 0.187$) (Fig. 4.10) .

There was a significant main effect between average Left Rectus Femoris activity between fatigue conditions ($F_{2,22} = 3.756$, $p = 0.039$, $\eta^2 = 0.255$). A post hoc Bonferroni test revealed no statistically significant differences between fatigue conditions (Fig. 4.10).

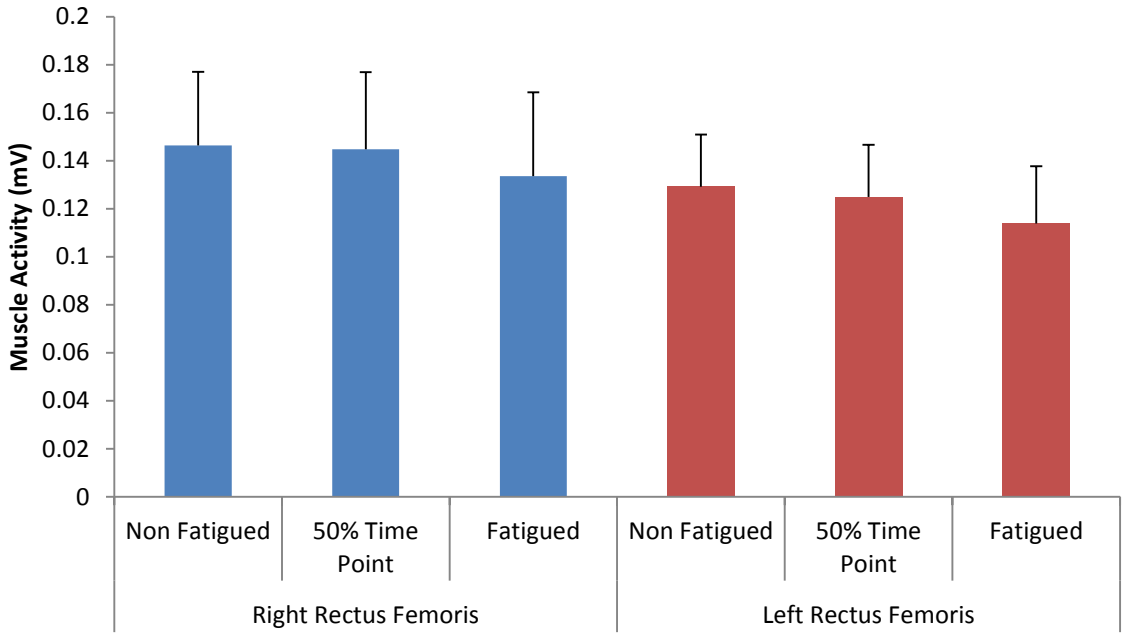


Figure 4.10. Average Right Rectus Femoris and Left Rectus Femoris activity for the three fatigue conditions. Error bars represent the group's standard deviation.

#### 4.4.2.2 Normalize to MVC

There was no statistically significant interaction between the Rectus Femoris activity normalized to MVC fatigue conditions and dominance ($F_{2,22}$ = 0.270, $p$ = 0.766, $\eta^2$ = 0.024). There were no differences between fatigue conditions ($F_{2,22}$ = 2.316, $p$ = 0.122, $\eta^2$ = 0.174) nor between sides ($F_{1,11}$ = 0.069, $p$ = 0.797, $\eta^2$ = 0.006) (Fig. 4.11).

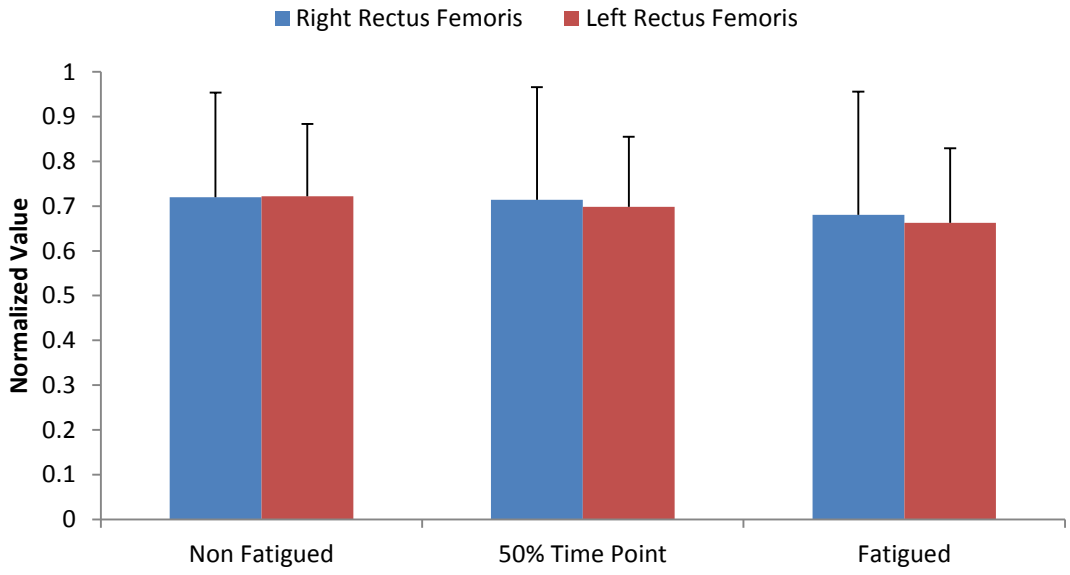


Figure 4.11. Average Left Rectus Femoris activity normalized to MVC for the three fatigue conditions. Error bars represent the group's standard deviation.

#### 4.4.2.3 Normalized to Peak of the Cycle

There was no statistically significant interaction between the Rectus Femoris activity normalized to peak of the cycle fatigue conditions and dominance ($F_{2,22}$ = 0.343, $p$ = 0.713, $\eta^2$ = 0.030). There were differences between fatigue conditions ($F_{2,22}$ = 13.624, $p$ < 0.001, $\eta^2$ = 0.553), but not between sides ($F_{1,11}$ = 0.226, $p$ = 0.644, $\eta^2$ = 0.020). A post hoc Bonferroni test revealed NF was statistically significantly higher than F ($p$ = 0.005, $d$ = 1.38) and 50% TP ($p$ = 0.038, $d$ = 0.87) conditions. F was statistically significantly lower than 50% TP ($p$ = 0.004, $d$ = 0.49) (Fig. 4.12).

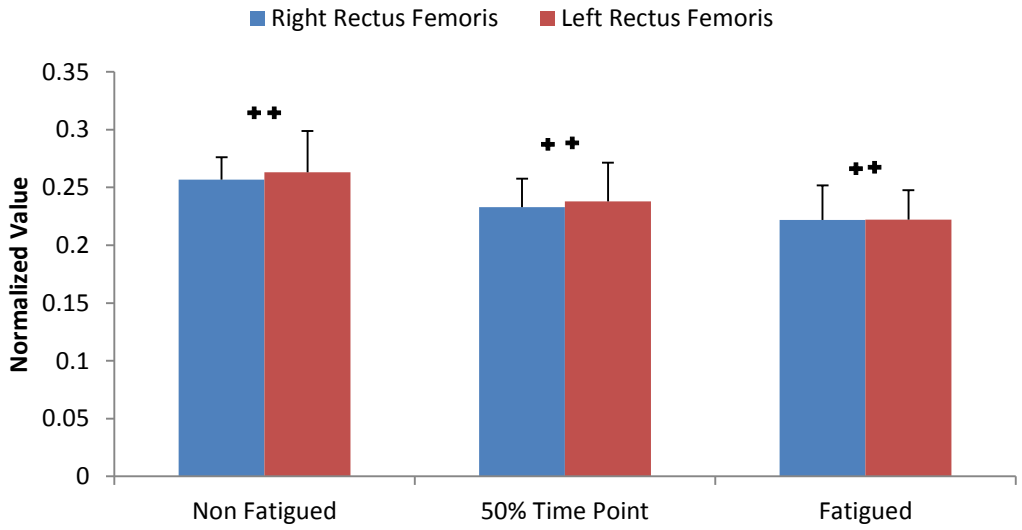


Figure 4.12. Average Left Rectus Femoris normalized to peak of the cycle for the three fatigue conditions. Error bars represent the group's standard deviation. ✚ indicates statistical differences between fatigue conditions.

#### 4.4.2.4 Pattern of Muscle Activity

The group's level of muscle activity of the Right Rectus Femoris seems to have two distinct phases, one period corresponding to the initial (0 – 30%) and final (70 – 100%) parts of the cycle, and one period where the muscle activity increase from 30 to 70% of the cycle (Fig. 4.13). This is supported by the individual activations timing (Fig. 4.14). Figure 4.13 shows significant differences between the patterns of muscle activity between NF and F conditions. There seems to be a delay for the fatigued condition during the activation phase (30 – 45%). This is supported when looking at the individual data (appendix C). All subjects with the exception of subject 11 show this trend. Figure

4.14 shows the individual activation timings for the Right Rectus Femoris muscle for the F condition.

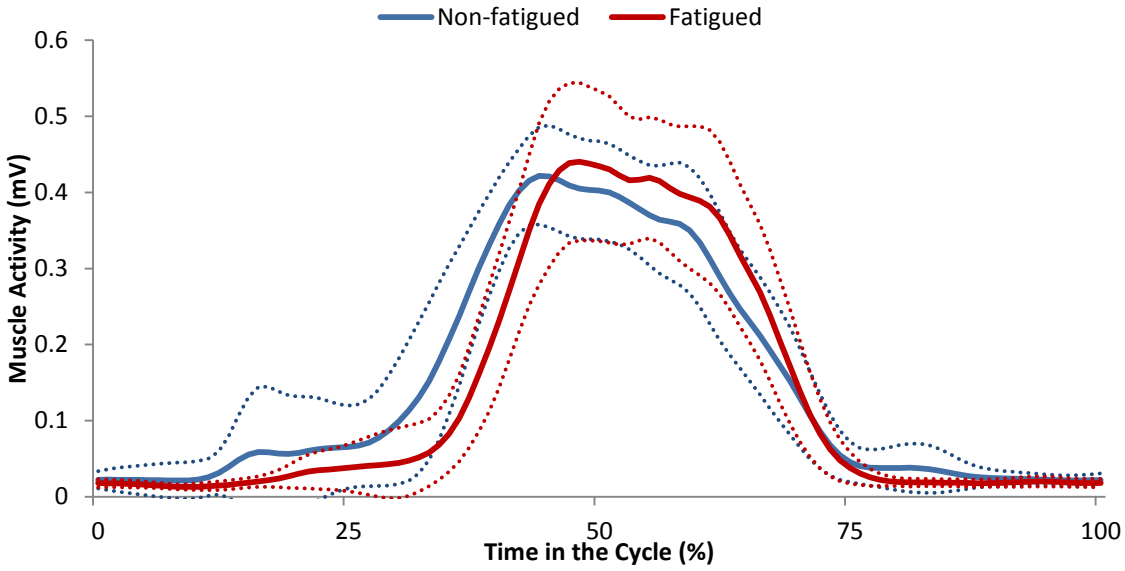


Figure 4.13. Right Rectus Femoris activity pattern for non-fatigued and fatigued conditions. Solid line represents the mean, dotted line the 95% confidence interval.

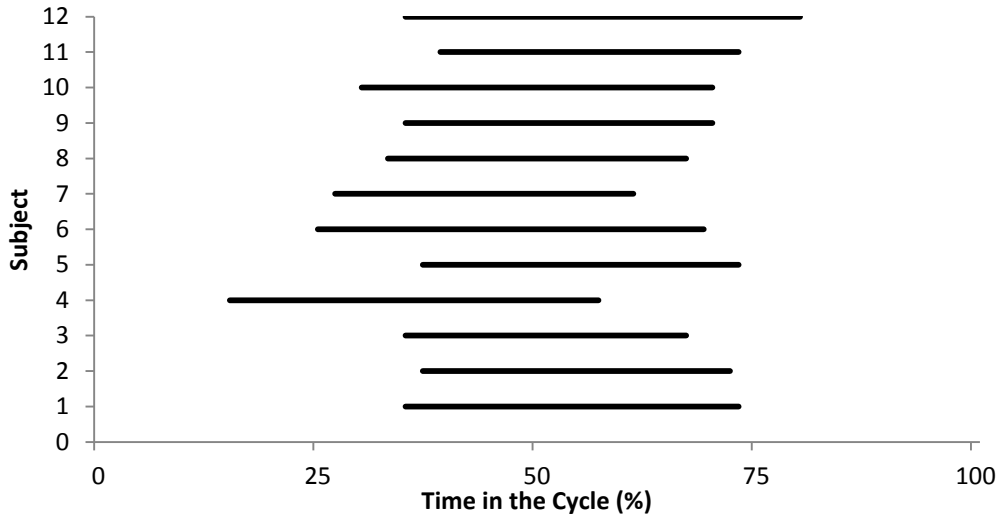


Figure 4.14. Individual activation times of the Right Rectus Femoris for the non-fatigue condition following the double-threshold method.

The group's level of muscle activity of the Left Rectus Femoris seems to have two distinct phases, one period corresponding to the initial (0 – 25%) and final (75 – 100%) parts of the cycle where the activity is high, and one period, from 30 to 70% of the time in the cycle, where the muscle activity decreases (Fig. 4.15). Individual data (appendix C) shows that all shows that all subjects follow the same pattern. Figure 4.15 shows no significant differences between the patterns of muscle activity between NF and F conditions. When looking at individual data, however, subjects 1, 2, 3, 5, 6, 7, 8 and 12 show the same fatigued trend observed for the Right Rectus Femoris (activation delay). Figure 4.16 shows the individual activation timings for the Left Rectus Femoris muscle for the NF condition.

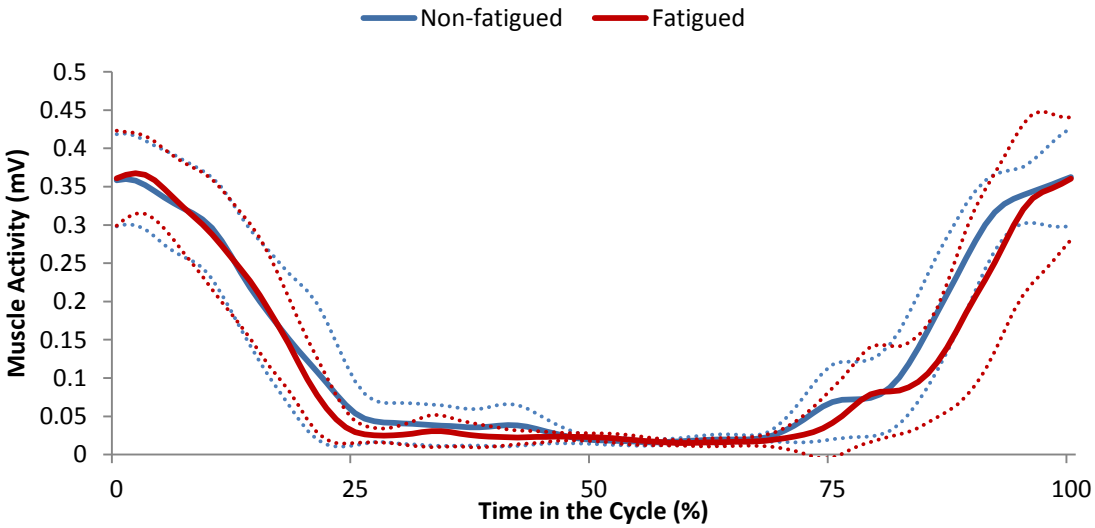


Figure 4.15. Left Rectus Femoris activity pattern for non-fatigued and fatigued conditions. Solid line represents the mean, dotted line the 95% confidence interval.

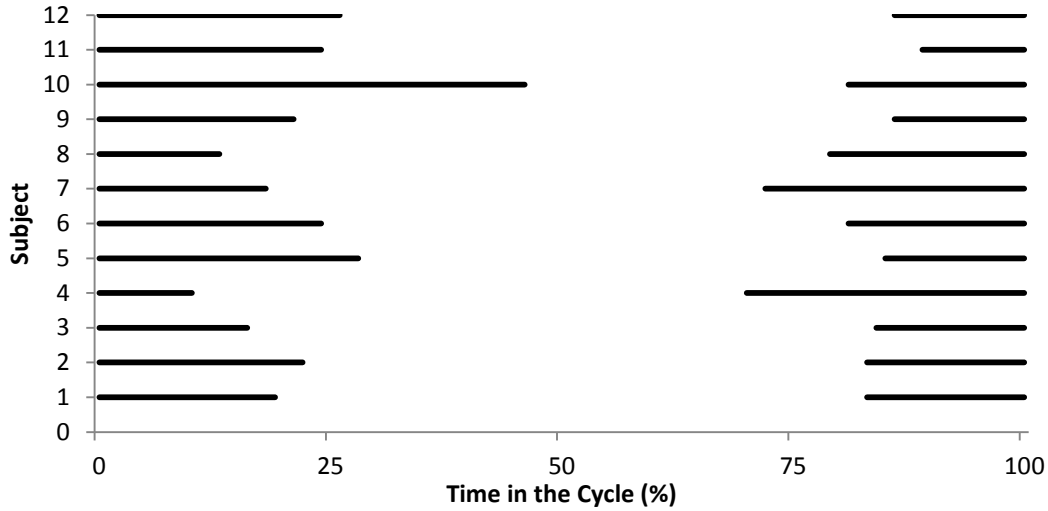


Figure 4.16. Individual activation times of the Left Rectus Femoris for the non-fatigue condition following the double-threshold method.

### 4.4.3 Biceps Femoris

#### 4.4.3.1 Average Activity

A repeated measures ANOVA for average Right Biceps Femoris activity showed no significant differences between fatigue conditions ($F_{1.108,9.970} = 2.894$, $p = 0.118$, $\eta^2 = 0.243$) (Fig. 4.17).

There was a significant main effect between average Left Biceps Femoris activity between fatigue conditions ($F_{2,18} = 3.863$, $p = 0.043$, $\eta^2 = 0.326$). Post hoc Bonferroni tests revealed no statistically significant differences between fatigue conditions (Fig. 4.17).

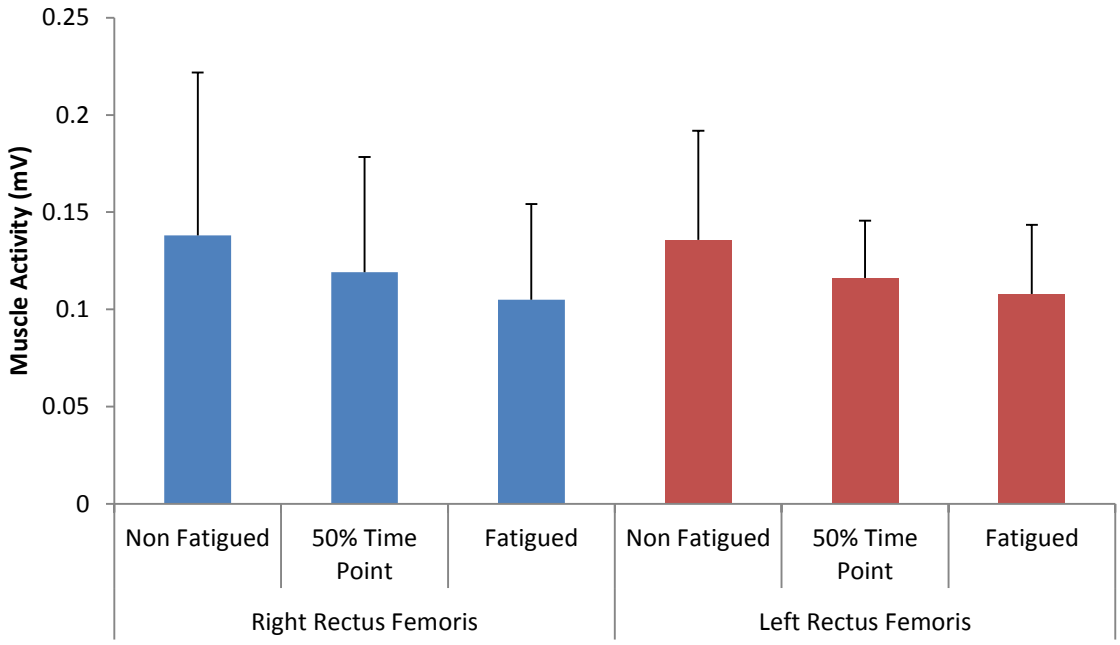


Figure 4.17. Average Left Biceps Femoris activity for the three fatigue conditions. Error bars represent the group's standard deviation.

#### 4.4.3.2 Normalize to MVC

There was no statistically significant interaction between the Biceps Femoris activity normalized to MVC fatigue conditions and dominance ($F_{2,14}$ = 0.513, $p$ = 0.610, $\eta^2$ = 0.068). There were differences between fatigue conditions ($F_{2,14}$ = 7.595, $p$ = 0.006, $\eta^2$ = 0.520), but not between sides ($F_{1,7}$ = 1.565, $p$ = 0.251, $\eta^2$ = 0.183). Post hoc Bonferroni tests did not reveal any significant differences between conditions (Fig. 4.18).

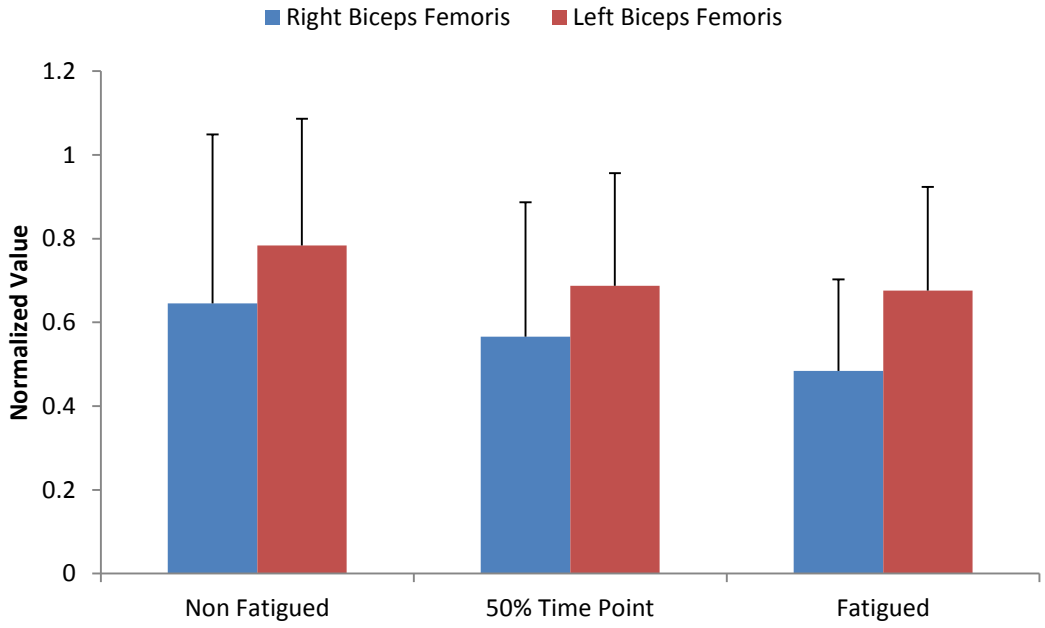


Figure 4.18. Average Left Biceps Femoris activity normalized to MVC for the three fatigue conditions. Error bars represent the group's standard deviation.

#### 4.4.3.3 Normalized to Peak of the Cycle

There was no statistically significant interaction between the Biceps Femoris activity normalized to peak of the cycle fatigue conditions and dominance ($F_{2,14}$ = 0.205, $p$ = 0.817, $\eta^2$ = 0.028). There were differences between fatigue conditions ($F_{2,14}$ = 9.989, $p$ < 0.002, $\eta^2$ = 0.588), but not between sides ($F_{1,7}$ = 1.685, $p$ = 0.235, $\eta^2$ = 0.194). Post hoc Bonferroni tests revealed NF was statistically significantly higher than F ($p$ = 0.007, $d$ = 0.54) and 50% TP ($p$ = 0.014, $d$ = 0.49) conditions (Fig. 4.19).

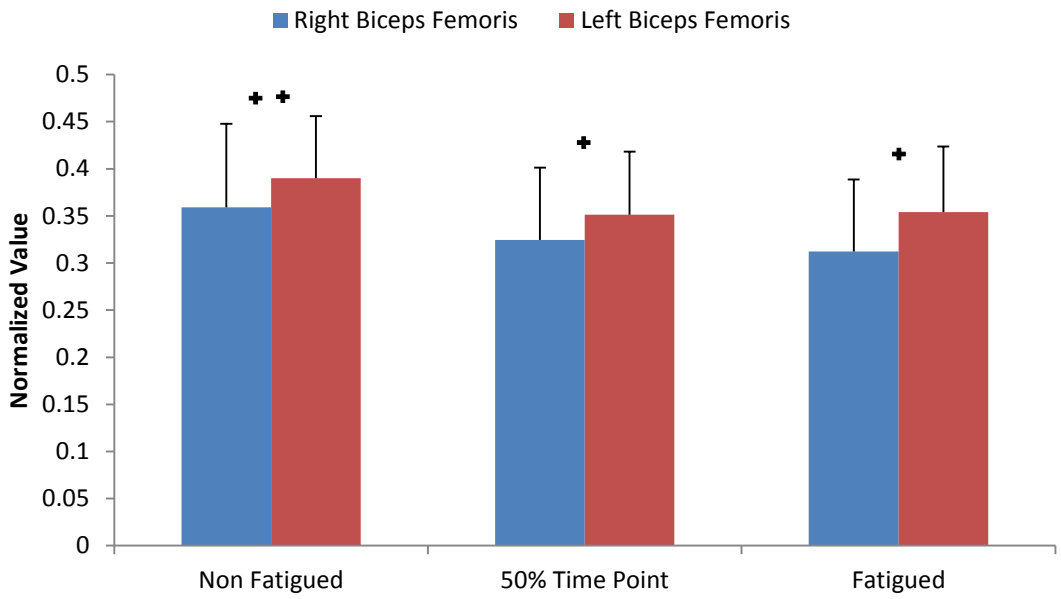


Figure 4.19. Average Left Biceps Femoris activity normalized to peak of the cycle for the three fatigue conditions. Error bars represent the group's standard deviation. ✚ indicates statistical differences between fatigue conditions.

#### 4.4.3.4 Pattern of Muscle Activity

The group's level of muscle activity seems to have three periods of high activity and two periods of low activity (Fig. 4.20). The general pattern consists of higher activity during the initial (0 – 25%) and final (80 – 100%) phases of the cycle with low peaks of activity around 25 – 30% and 70 – 80%. Looking at individual data (appendix C) this is supported by subjects 1, 2, 3, 5, 8, 9 and 10. Subject 4 and 11 showed higher activity in the middle of the cycle (30 – 70%). Figure 4.21 shows no significant differences between the patterns of muscle activity between fatigue conditions (NF and F). Figure 4.40 shows the individual activation timings for the Right Biceps Femoris muscle for the NF condition.

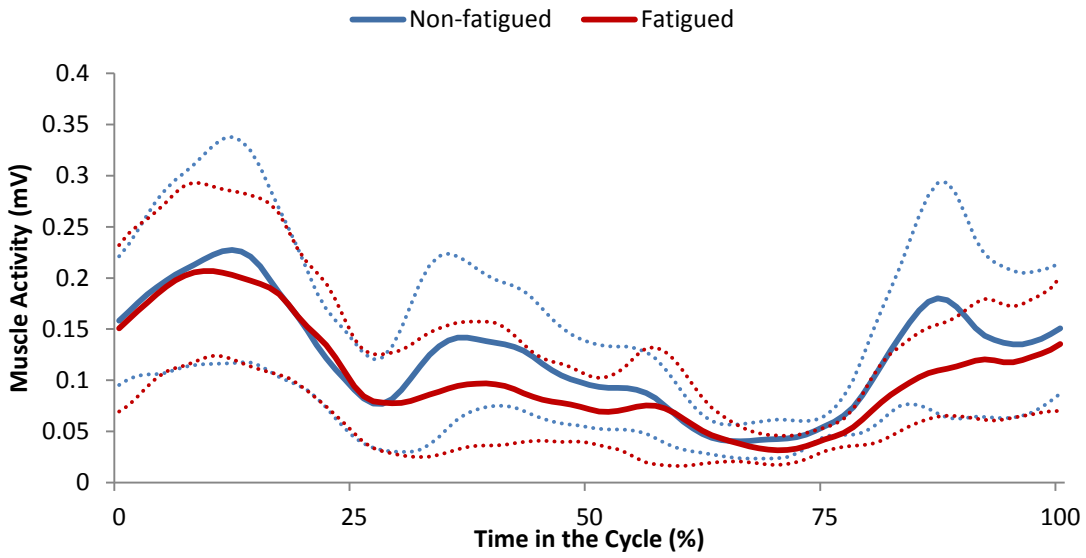


Figure 4.20. Right Biceps Femoris activity pattern for non-fatigued and fatigued conditions. Solid line represents the mean, dotted line the 95% confidence interval.

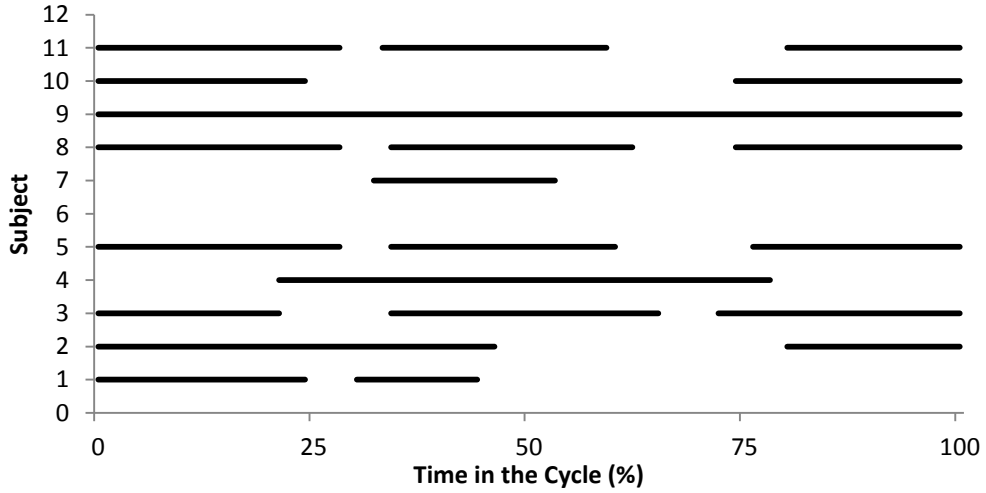


Figure 4.21. Individual activation times of the Right Biceps Femoris for the non-fatigue condition following the double-threshold method.

The group's level of muscle activity seems to have a phase of higher activity corresponding to the period from 25 to 70% of the time in the cycle (Fig. 4.22). Looking at individual data (appendix C) this is patent in subjects 2, 8, 9 and 12. Other subjects showed more individualized patterns of muscle activity. Figure 4.22 shows no significant differences between the patterns of muscle activity between fatigue conditions (NF and F). Figure 4.23 shows the individual activation timings for the Left Biceps Femoris muscle for the NF condition.

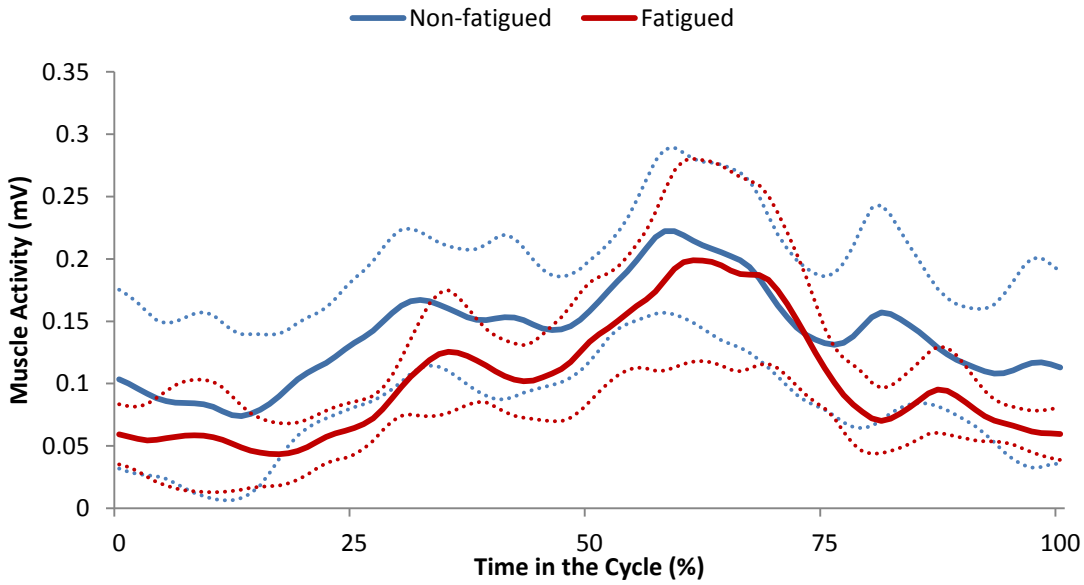


Figure 4.22. Left Biceps Femoris activity pattern for non-fatigued and fatigued conditions. Solid line represents the mean, dotted line the 95% confidence interval.

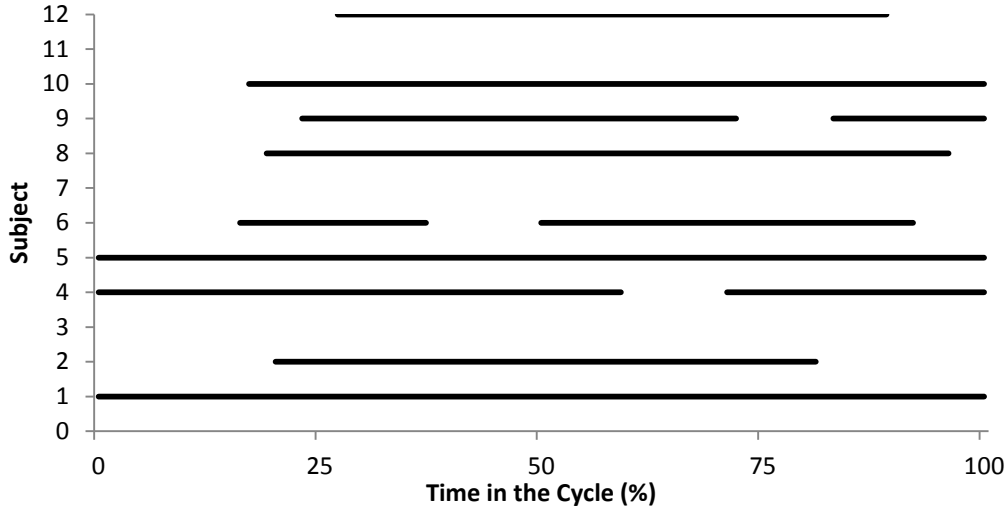


Figure 4.23. Individual activation times of the Left Biceps Femoris for the non-fatigue condition following the double-threshold method.

### 4.4.4 Summary Table

Table 4.25 shows the main effect on fatigue, main effect on dominance and interaction between fatigue and dominance values for the normalized muscle activity variables. Non normalized activity shows the main effect on fatigue for each side.

Table 4.25. Main effect (ME) fatigue, main effect dominance and interaction between fatigue and dominance. Crossed out cells indicate no statistical test. Statistical differences ($p<0.05$) are indicated in bold.

| Variable | ME Fatigue | ME Dominance | Interaction |
|---|---|---|---|
| Avg Right TA Activity | **$p = 0.002$, $\eta^2 = 0.572$** | | |
| Avg Left TA Activity | **$p < 0.001$, $\eta^2 = 0.655$** | | |
| Avg MVC TA Activity | **$p < 0.001$, $\eta^2 = 0.721$** | $p = 0.428$, $\eta^2 = 0.080$ | $p = 0.383$, $\eta^2 = 0.113$ |
| Avg Peak Cycle TA Activity | **$p < 0.001$, $\eta^2 = 0.761$** | $p = 0.578$, $\eta^2 = 0.036$ | $p = 0.901$, $\eta^2 = 0.011$ |
| Avg Right RF Activity | $p = 0.128$, $\eta^2 = 0.187$ | | |
| Avg Left RF Activity | $p = 0.039$, $\eta^2 = 0.255$ | | |
| Avg MVC RF Activity | $p = 0.122$, $\eta^2 = 0.174$ | $p = 0.797$, $\eta^2 = 0.006$ | $p = 0.766$, $\eta^2 = 0.024$ |
| Avg Peak Cycle RF Activity | **$p < 0.001$, $\eta^2 = 0.553$** | $p = 0.644$, $\eta^2 = 0.020$ | $p = 0.713$, $\eta^2 = 0.030$ |
| Avg Right BF Activity | $p = 0.118$, $\eta^2 = 0.243$ | | |
| Avg Left BF Activity | **$p = 0.043$, $\eta^2 = 0.326$** | | |
| Avg MVC BF Activity | **$p = 0.006$, $\eta^2 = 0.520$** | $p = 0.251$, $\eta^2 = 0.183$ | $p = 0.610$, $\eta^2 = 0.068$ |
| Avg Peak Cycle BF Activity | **$p < 0.002$, $\eta^2 = 0.588$** | $p = 0.235$, $\eta^2 = 0.194$ | $p = 0.817$, $\eta^2 = 0.028$ |

## 4.5 Correlations between Vertical Force and Studied Variables

Table 4.26 shows the correlation values between vertical force normalized to body weight and the variables calculated in this study for the three fatigue levels.

Table 4.26. Correlation (r) between calculated variables and vertical force normalized to body weight for the three fatigue levels. *indicates $p < 0.01$ significance level.

| Variable | Non-fatigued | 50% Time Point | Fatigued |
|---|---|---|---|
| Average RHip Abduction (°) | 0.593, $p = 0.042$ | 0.150, $p = 0.642$ | -0.247, $p = 0.440$ |
| Average LHip Abduction (°) | 0.461, $p = 0.135$ | 0.256, $p = 0.422$ | -0.060, $p = 0.854$ |
| Average RHip Flexion (°) | 0.682, $p = 0.015$ | 0.551, $p = 0.063$ | 0.106, $p = 0.743$ |
| Average LHip Flexion (°) | 0.669, $p = 0.017$ | 0.382, $p = 0.221$ | 0.110, $p = 0.733$ |
| Average RHip Internal Rotation (°) | 0.346, $p = 0.270$ | 0.416, $p = 0.178$ | 0.110, $p = 0.734$ |
| Average LHip Internal Rotation (°) | 0.151, $p = 0.640$ | 0.122, $p = 0.705$ | -0.107, $p = 0.740$ |
| Average RKnee Flexion (°) | 0.662, $p = 0.042$ | 0.446, $p = 0.146$ | 0.004, $p = 0.990$ |
| Average LKnee Flexion (°) | 0.695, $p = 0.012$ | 0.422, $p = 0.172$ | 0.193, $p = 0.547$ |
| Average RAnkle Plantarflexion (°) | 0.048, $p = 0.882$ | -0.173, $p = 0.592$ | -0.580, $p = 0.048$ |
| Average LAnkle Plantarflexion (°) | -0.137, $p = 0.670$ | -0.283, $p = 0.373$ | -0.631, $p = 0.028$ |
| Average RAnkle Inversion (°) | 0.133, $p = 0.681$ | -0.265, $p = 0.406$ | 0.105, $p = 0.746$ |
| Average LAnkle Inversion (°) | -0.126, $p = 0.695$ | -0.161, $p = 0.617$ | 0.113, $p = 0.726$ |
| Average RAnkle Adduction (°) | 0.289, $p = 0.362$ | 0.147, $p = 0.648$ | 0.158, $p = 0.624$ |
| Average LAnkle Adduction (°) | 0.126, $p = 0.695$ | 0.147, $p = 0.649$ | 0.339, $p = 0.280$ |
| Max RHip Abduction (°) | **0.736*, $p = 0.006$** | 0.183, $p = 0.569$ | -0.089, $p = 0.784$ |
| Max LHip Abduction (°) | 0.513, $p = 0.088$ | 0.372, $p = 0.233$ | -0.008, $p = 0.979$ |
| Max RHip Flexion (°) | **0.739*, $p = 0.006$** | 0.576, $p = 0.050$ | 0.221, $p = 0.491$ |
| Max LHip Flexion (°) | **0.813*, $p = 0.001$** | 0.453, $p = 0.140$ | -0.004, $p = 0.990$ |
| Max RHip Internal Rotation (°) | 0.362, $p = 0.248$ | 0.312, $p = 0.323$ | -0.084, $p = 0.795$ |
| Max LHip Internal Rotation (°) | 0.112, $p = 0.729$ | 0.072, $p = 0.823$ | -0.395, $p = 0.204$ |
| Max RKnee Flexion (°) | 0.328, $p = 0.165$ | 0.01, $p = 0.988$ | 0.273, $p = 0.391$ |
| Max LKnee Flexion (°) | 0.215, $p = 0.503$ | 0.046, $p = 0.888$ | 0.032, $p = 0.922$ |
| Max RAnkle Plantarflexion (°) | 0.106, $p = 0.744$ | 0.068, $p = 0.833$ | -0.677, $p = 0.016$ |
| Max LAnkle Plantarflexion (°) | 0.027, $p = 0.933$ | 0.080, $p = 0.804$ | -0.258, $p = 0.418$ |
| Max RAnkle Inversion (°) | 0.294, $p = 0.353$ | 0.237, $p = 0.458$ | -0.083, $p = 0.798$ |
| Max LAnkle Inversion (°) | -0.227, $p = 0.477$ | 0.029, $p = 0.929$ | 0.015, $p = 0.964$ |
| Max RAnkle Adduction (°) | 0.310, $p = 0.327$ | 0.316, $p = 0.317$ | 0.204, $p = 0.526$ |
| Max LAnkle Adduction (°) | 0.240, $p = 0.253$ | 0.592, $p = 0.042$ | 0.646, $p = 0.023$ |
| Min RHip Abduction (°) | 0.483, $p = 0.112$ | 0.118, $p = 0.714$ | -0.372, $p = 0.234$ |
| Min LHip Abduction (°) | 0.355, $p = 0.258$ | 0.152, $p = 0.637$ | -0.252, $p = 0.429$ |
| Min RHip Flexion (°) | 0.556, $p = 0.061$ | 0.358, $p = 0.254$ | -0.005, $p = 0.988$ |
| Min LHip Flexion (°) | 0.614, $p = 0.034$ | 0.249, $p = 0.434$ | -0.140, $p = 0.665$ |
| Min RHip Internal Rotation (°) | 0.317, $p = 0.315$ | 0.437, $p = 0.155$ | -0.079, $p = 0.807$ |

| | | | |
|---|---|---|---|
| Min LHip Internal Rotation (°) | 0.089, $p = 0.783$ | 0.394, $p = 0.205$ | -0.472, $p = 0.121$ |
| Min RKnee Flexion (°) | 0.485, $p = 0.110$ | 0.510, $p = 0.090$ | -0.002, $p = 0.994$ |
| Min LKnee Flexion (°) | 0.639, $p = 0.025$ | 0.503, $p = 0.096$ | 0.289, $p = 0.362$ |
| Min RAnkle Plantarflexion (°) | -0.503, $p = 0.095$ | -0.360, $p = 0.251$ | 0.210, $p = 0.511$ |
| Min LAnkle Plantarflexion (°) | -0.067, $p = 0.836$ | -0.192, $p = 0.549$ | -0.061, $p = 0.850$ |
| Min RAnkle Inversion (°) | 0.071, $p = 0.827$ | 0.017, $p = 0.958$ | -0.189, $p = 0.556$ |
| Min LAnkle Inversion (°) | -0.070, $p = 0.828$ | -0.367, $p = 0.241$ | -0.438, $p = 0.642$ |
| Min RAnkle Adduction (°) | 0.042, $p = 0.897$ | -0.009, $p = 0.978$ | 0.311, $p = 0.325$ |
| Min LAnkle Adduction (°) | 0.131, $p = 0.684$ | -0.013, $p = 0.968$ | 0.095, $p = 0.769$ |
| RHip Abduction Range (°) | 0.569, $p = 0.054$ | 0.162, $p = 0.615$ | 0.391, $p = 0.209$ |
| LHip Abduction Range (°) | 0.379, $p = 0.224$ | 0.458, $p = 0.134$ | 0.262, $p = 0.410$ |
| RHip Flexion Range (°) | 0.606, $p = 0.037$ | 0.531, $p = 0.076$ | 0.271, $p = 0.395$ |
| LHip Flexion Range (°) | **0.759*, $p = 0.004$** | 0.607, $p = 0.036$ | 0.165, $p = 0.608$ |
| RHip Internal Rotation Range (°) | 0.162, $p = 0.615$ | 0.366, $p = 0.241$ | 0.169, $p = 0.600$ |
| LHip Internal Rotation Range (°) | -0.157, $p = 0.626$ | 0.392, $p = 0.207$ | 0.650, $p = 0.022$ |
| RKnee Flexion Range (°) | -0.158, $p = 0.042$ | -0.345, $p = 0.272$ | 0.139, $p = 0.667$ |
| LKnee Flexion Range (°) | -0.535, $p = 0.073$ | -0.385, $p = 0.216$ | -0.163, $p = 0.613$ |
| RAnkle Plantarflexion Range (°) | 0.344, $p = 0.273$ | 0.148, $p = 0.646$ | -0.425, $p = 0.169$ |
| LAnkle Plantarflexion Range (°) | 0.060, $p = 0.853$ | 0.165, $p = 0.608$ | -0.062, $p = 0.642$ |
| RAnkle Inversion Range (°) | 0.336, $p = 0.286$ | 0.411, $p = 0.184$ | 0.268, $p = 0.400$ |
| LAnkle Inversion Range (°) | -0.189, $p = 0.556$ | 0.278, $p = 0.382$ | 0.319, $p = 0.313$ |
| RAnkle Adduction Range (°) | 0.248, $p = 0.437$ | 0.270, $p = 0.396$ | -0.037, $p = 0.909$ |
| LAnkle Adduction Range (°) | 0.074, $p = 0.819$ | 0.441, $p = 0.151$ | 0.328, $p = 0.297$ |
| RFoot Average Pitch Angles (°) | 0.465, $p = 0.128$ | 0.166, $p = 0.606$ | -0.374, $p = 0.231$ |
| LFoot Average Pitch Angles (°) | 0.046, $p = 0.887$ | -0.457, $p = 0.072$ | -0.414, $p = 0.181$ |
| RFoot Maximum Pitch Angles (°) | 0.464, $p = 0.129$ | 0.222, $p = 0.488$ | -0.310, $p = 0.327$ |
| LFoot Maximum Pitch Angles (°) | 0.299, $p = 0.345$ | 0.086, $p = 0.790$ | 0.154, $p = 0.633$ |
| RFoot Minimum Pitch Angles (°) | -0.63, $p = 0.846$ | -0.004, $p = 0.989$ | -0.401, $p = 0.196$ |
| LFoot Minimum Pitch Angles (°) | -0.312, $p = 0.323$ | -0.459, $p = 0.133$ | -0.332, $p = 0.292$ |
| Time of Positive Pitch Rfoot (%) | 0.395, $p = 0.203$ | 0.297, $p = 0.348$ | -0.041, $p = 0.901$ |
| Time of Positive Pitch Lfoot (%) | 0.009, $p = 0.977$ | 0.231, $p = 0.470$ | -0.296, $p = 0.350$ |
| RFoot Average Sweepback Angle (°) | 0.162, $p = 0.616$ | -0.048, $p = 0.882$ | -0.175, $p = 0.585$ |
| LFoot Average Sweepback Angle (°) | 0.056, $p = 0.863$ | -0.181, $p = 0.572$ | -0.143, $p = 0.658$ |
| RFoot Medio-Lateral Motion (%) | 0.118, $p = 0.716$ | 0.386, $p = 0.216$ | 0.361, $p = 0.248$ |
| LFoot Medio-Lateral Motion (%) | 0.055, $p = 0.865$ | 0.240, $p = 0.452$ | 0.284, $p = 0.371$ |
| RFoot Vertical Motion (%) | -0.472, $p = 0.121$ | -0.480, $p = 0.114$ | -0.100, $p = 0.758$ |

| | | | |
|---|---|---|---|
| LFoot Vertical Motion (%) | -0.654, $p = 0.021$ | **-0.748*, $p = 0.005$** | -0.335, $p = 0.288$ |
| RFoot Anterior-Posterior Motion (%) | 0.118, $p = 0.716$ | 0.139, $p = 0.668$ | -0.273, $p = 0.391$ |
| LFoot Anterior-Posterior Motion (%) | 0.390, $p = 0.210$ | 0.515, $p = 0.087$ | 0.207, $p = 0.519$ |
| Average Rfoot Speed (m/s) | 0.433, $p = 0.160$ | 0.121, $p = 0.708$ | 0.556, $p = 0.061$ |
| Average Lfoot Speed (m/s) | 0.364, $p = 0.245$ | 0.060, $p = 0.853$ | 0.462, $p = 0.130$ |
| Avg RHip Abduction Ang Vel (°/s) | 0.155, $p = 0.631$ | 0.051, $p = 0.874$ | 0.190, $p = 0.554$ |
| Avg LHip Abduction Ang Vel (°/s) | 0.085, $p = 0.793$ | 0.370, $p = 0.236$ | 0.031, $p = 0.924$ |
| Avg RHip Flexion Ang Vel (°/s) | 0.378, $p = 0.226$ | 0.650, $p = 0.022$ | 0.329, $p = 0.297$ |
| Avg LHip Flexion Ang Vel (°/s) | 0.587, $p = 0.045$ | 0.439, $p = 0.154$ | 0.009, $p = 0.977$ |
| Avg RHip Rotation Ang Vel (°/s) | 0.430, $p = 0.163$ | 0.509, $p = 0.091$ | 0.321, $p = 0.309$ |
| Avg LHip Rotation Ang Vel (°/s) | 0.203, $p = 0.526$ | 0.017, $p = 0.959$ | -0.097, $p = 0.763$ |
| Avg RKnee Flexion Ang Vel (°/s) | 0.613, $p = 0.058$ | 0.448, $p = 0.144$ | 0.126, $p = 0.696$ |
| Avg LKnee Flexion Ang Vel (°/s) | **0.746*,$p = 0.005$** | **0.718*, $p = 0.009$** | 0.460, $p = 0.132$ |
| Avg RAnkle Inversion Ang Vel (°/s) | 0.362, $p = 0.247$ | 0.577, $p = 0.049$ | 0.490, $p = 0.106$ |
| Avg LAnkle Inversion Ang Vel (°/s) | -0.026, $p = 0.935$ | 0.190, $p = 0.554$ | -0.053, $p = 0.870$ |
| Avg RAnk Plantarflexion Ang Vel (°/s) | 0.301, $p = 0.342$ | 0.430, $p = 0.163$ | 0.030, $p = 0.926$ |
| Avg LAnk Plantarflexion Ang Vel (°/s) | 0.603, $p = 0.038$ | 0.446, $p = 0.147$ | 0.169, $p = 0.599$ |
| Avg RAnkle Adduction Ang Vel (°/s) | 0.253, $p = 0.005$ | 0.133, $p = 0.680$ | 0.072, $p = 0.824$ |
| Avg LAnkle Adduction Ang Vel (°/s) | 0.155, $p = 0.631$ | 0.394, $p = 0.206$ | 0.007, $p = 0.982$ |
| **EMG** | | | |
| RTA normalized to MVC | -0.135, $p = 0.709$ | -0.386, $p = 0.271$ | -0.155, $p = 0.668$ |
| RRF normalized to MVC | -0.163, $p = 0.612$ | -0.447, $p = 0.145$ | -0.011, $p = 0.973$ |
| RBF normalized to MVC | -0.312, $p = 0.380$ | -0.236, $p = 0.512$ | -0.030, $p = 0.935$ |
| LTA normalized to MVC | -0.586, $p = 0.058$ | -0.568, $p = 0.068$ | -0.139, $p = 0.683$ |
| LRF normalized to MVC | -0.201, $p = 0.531$ | -0.249, $p = 0.435$ | -0.147, $p = 0.649$ |
| LBF normalized to MVC | -0.642, $p = 0.045$ | -0.484, $p = 0.157$ | -0.464, $p = 0.177$ |
| RTA normalized to peak cycle | -0.017, $p = 0.961$ | -0.149, $p = 0.663$ | -0.179, $p = 0.599$ |
| RRF normalized to peak cycle | 0.446, $p = 0.147$ | 0.392, $p = 0.207$ | 0.486, $p = 0.110$ |
| RBF normalized to peak cycle | 0.094, $p = 0.795$ | -0.142, $p = 0.696$ | -0.266, $p = 0.458$ |
| LTA normalized to peak cycle | -0.047, $p = 0.892$ | -0.040, $p = 0.907$ | -0.091, $p = 0.791$ |
| LRF normalized to peak cycle | 0.295, $p = 0.352$ | 0.147, $p = 0.648$ | 0.579, $p = 0.049$ |
| LBF normalized to peak cycle | -0.325, $p = 0.352$ | -0.328, $p = 0.354$ | -0.209, $p = 0.563$ |

# Chapter Five: Discussion

# 5 Discussion

The purpose of this study was to analyze the kinematics and muscle activity of the water polo eggbeater kick in fatigued and unfatigued states to provide foundational knowledge on which training programs can be based. In the previous chapter, the results of this study were presented in relation to fatigue conditions, dominance, and the interaction between fatigue conditions and dominance.

In this chapter the variables studied across different fatigue levels and dominance are discussed relative to the implications they have for development of eggbeater kick technique and training. In addition, the relationship between specific variables and eggbeater kick performance will be discussed.

## 5.1 Factors Influencing Performance when not Fatigued

The average vertical force normalized to body weight was the performance indicator in this study.

The results revealed some important implications with respect to which aspects of the eggbeater kick motion are associated with high level performance and distinguish between players in terms of ability. However, given the large number of correlations investigated and the small sample size in this study, correlations should be interpreted with caution as a value representing the degree of linear association between a particular variable and performance level, and a measure of explained variance. Based on the correlations it is apparent that better players were characterized by keeping the hips

more abducted (average angle: dominant, $r$=0.593 and non-dominant, $r$=0.461; max angle: dominant, $r$=0.736 and non-dominant, $r$=0.513), flexed (average angle: dominant, $r$=0.682 and non-dominant, $r$=0.669; max angle: dominant, $r$=0.739 and non-dominant, $r$=0.813); having larger hip flexion range of motion (dominant, $r$=0.606; non-dominant, $r$=0.759) throughout the cycle; and having foot paths with less vertical motion than players with lower levels of performance (dominant, $r$=-0.472; non-dominant, $r$=-0.654). Average knee flexion was also significantly correlated with performance (dominant, $r$=0.662; non-dominant, $r$=0.695) giving an advantage to players that keep their knees more flexed during the cycle. However, larger average knee flexion positively correlated with performance seems to come from lower maximum knee extension (dominant, $r$=0.485; non-dominant, $r$=0.639) and not from larger maximum knee flexion values ($r$=0.328, $r$=0.215). This result agrees with Sanders (1999a) who noted that excessive extension would be a disadvantage because of the difficulty of recovering the foot without having substantial magnitude and duration of negative pitch. Despite the large maximum abduction, flexion and internal rotation angles of the hip, ranges of motion were small. In contrast, ranges of knee angular motion were large. Additionally, average abduction and flexion of the hip were negatively correlated (not statistically significant or the dominant side) with vertical motion of the feet, $r$=-0.351 (dominant) and $r$=-0.523 (non-dominant) for abduction, and $r$=-0.392 (dominant) and $r$=-0.617 (non-dominant) for flexion. Therefore, considering all of the above, it is reasonable to interpret that the main function of the hip is to keep the thighs oriented in positions that enable effective motion of the feet. In its turn, the knees due to their large range of motion are important

to move the feet (Fig. 5.1). Consequently, it is apparent that the role of the hips is to promote horizontal - and more effective - motion of the feet.

During the cycle, vertical force corresponded temporally with knee angular velocity. Small values of knee angular velocity corresponded to the minimum values of vertical force and large values of knee angular velocity corresponded closely to the peaks of vertical force (Fig. 5.2). Positive correlations, across the different levels of fatigue, between normalized vertical force and knee flexion angular velocity supported this finding (dominant side, r=0.613; non-dominant side r=0.746, p=0.005).

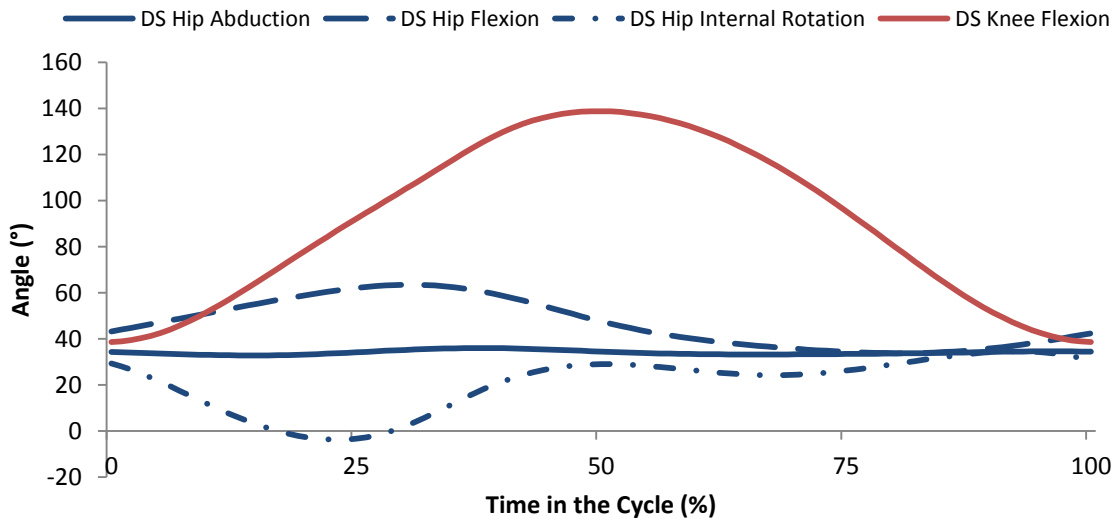


Figure 5.1. Dominant side hip abduction, flexion, internal rotation, and knee flexion during the non-fatigued cycle across all subjects.

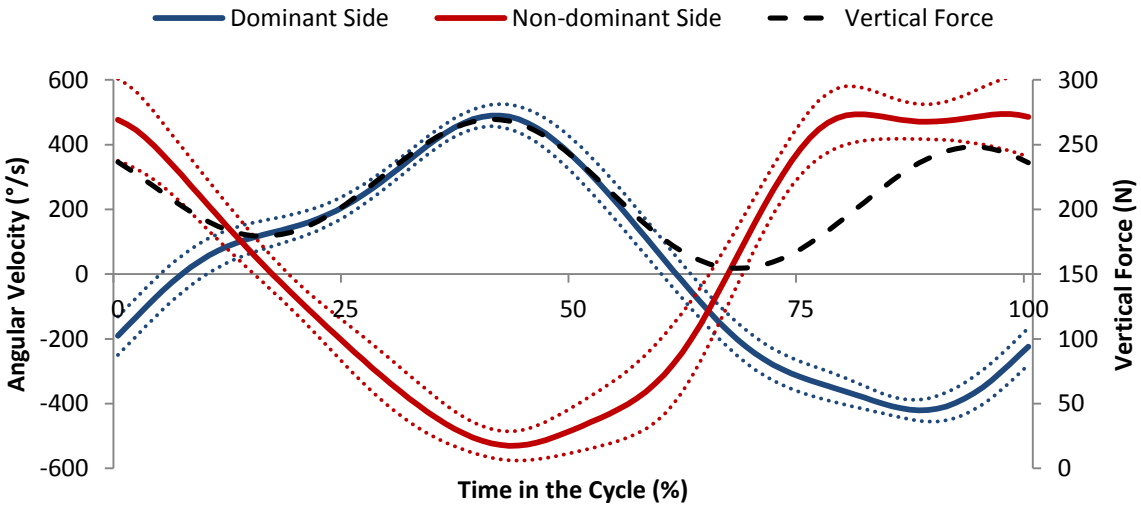


Figure 5.2. Knee flexion-extension angular velocity (AV) across all subjects during the non-fatigued cycle (solid lines). Vertical Force during the cycle (dashed line). Dotted lines indicate the 95% confidence interval of the true mean.

Given that foot motion depends strongly on knee angular velocity, and that the force acting on an object moving in water is related to its speed in accordance with the relationship (French, 1970, Clarys, 1979, Toussaint et al., 1988):

$$F = \frac{1}{2}\rho v^2 C_{D/L} A$$

where

$\rho$ is the density of water

$v$ is the velocity of the fluid

$C_{D/L}$ is the drag/lift coefficient

$A$ is the cross-sectional area

It is expected that knee angular velocity would be related to vertical force (Fig. 5.3). However, only small positive correlations were found for vertical force and foot speed (dominant side, r=0.433; non-dominant side r=0.364). Sanders (1999a) reported a strong linear relationship between the squared foot speeds and the height maintained in the 'hold' ($r = 0.82$, $p < 0.01$). However, given that height maintained and vertical force are not the same performance variable, the findings of the two studies are difficult to compare and an attempt to do so could be misleading. In particular, the relationship between force generated by an object moving in water and its speed is not linear. Furthermore, all players, not merely the ones with higher normalized vertical force, had considerable foot speeds compared with Sanders (1999a), thereby restricting the variation among predictor and outcome variables. In the present study, average foot velocities ranged from 2.56m/s to 2.92m/s in the non-fatigued condition. Additionally, the anthropometric characteristics of the players, particularly the length of the lower limb body segments, can be a factor influencing the eggbeater kick performance. Longer shanks and thighs can be favorable to create longer foot trajectories, and the size of the feet can influence its cross sectional area and be beneficial to the production of lift/drag forces.

Because of the sculling nature of the eggbeater kick, in which the swimmer tries to utilize lift forces rather than drag (Sanders, 1998), high foot speeds combined with small positive pitch angles to create favorable lift forces would be expected. This was found to be the case in this study in which positive pitch angles were dominant throughout the cycle (65%). The period of positive pitch started when the knee was near maximum flexion and the foot was being moved laterally, posteriorly and upwards. Because the

ankle was plantarflexed while still inverted and abducted from the previous phase, the ability to create positive pitch angles at this stage depended largely on the ability to quickly dorsiflex and evert the ankle. As this motion continued with the ankle becoming increasingly dorsiflexed, larger positive pitch angles were attained.

This motion was interrupted by the maximum flexion of the knee. As the knee started extending, while the foot maintains its previous orientation, pitch angles started to decrease until close to zero. At this point, negative pitch angles were avoided (pitch angles start increasing again) by a change of motion of the foot. The foot started moving medially instead of laterally and downwards instead of upwards. At the same time, the ankle became more everted and less adducted, resulting in increasingly larger positive pitch angles as the knee was being extended.

During the last part of the medial/downwards motion, when the foot started moving posteriorly instead of anteriorly, the ankle was inverted and plantarflexed to adapt to the change in the anterior-posterior motion and prolong the period of positive pitch. Pitch angles became negative when the knee was flexing with the ankle still inverted and plantarflexed (Fig. 5.4).

The period of negative pitch observed by Sanders (1999a), was also identified during the phase of knee flexion (inwards phase). The inability of players to create positive pitch angles during the whole cycle was due to physical limitations on the inversion-eversion and adduction-abduction ranges of motion of the ankle. These limited the ankle to orientate the foot in effective ways that create positive pitch angles during the period of the cycle when the knee was flexing.

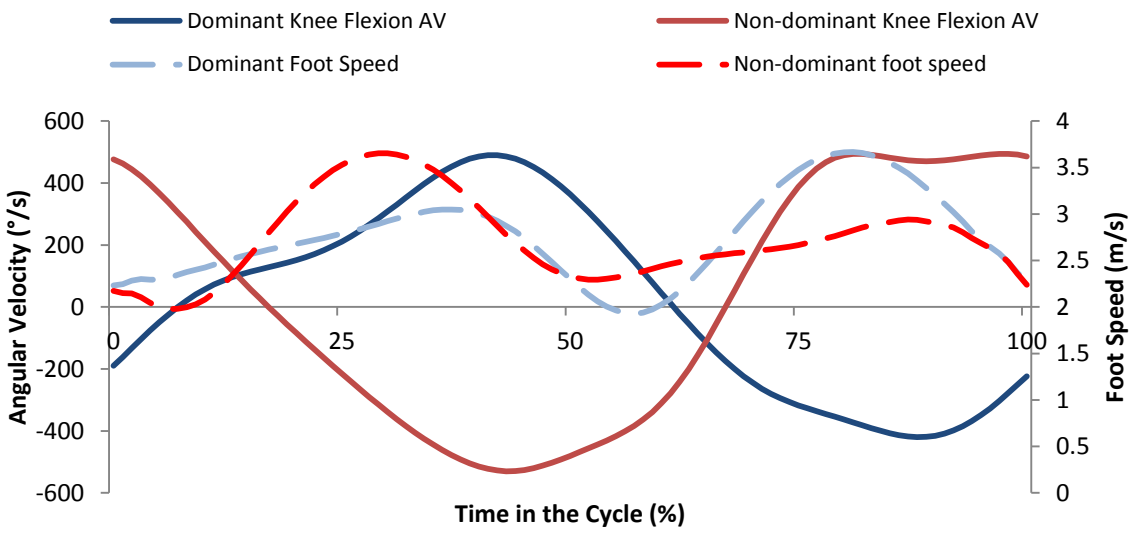


Figure 5.3. Knee flexion-extension angular velocity (solid lines) and foot speed (dashed lines) for the non-fatigued cycle across all subjects.

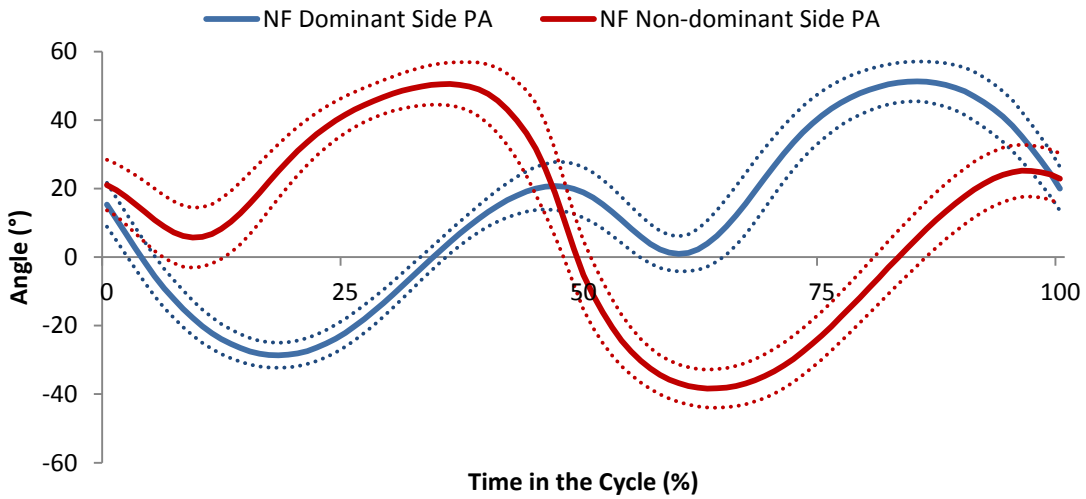


Figure 5.4. Feet pitch angles for dominant and non-dominant side during the non-fatigued cycle across all subjects. Dotted lines indicate the 95% confidence interval.

Because the periods of positive pitch corresponded to times in the cycle of medial water flow in the feet it is apparent that the foot is able to create positive pitch angles in the

cycle more easily when the flow is moving from the medial to lateral side of the foot. This corresponds to the time in the cycle where the knee is being extended and foot speeds are high.

During the non-fatigued cycle players keep the sweepback angle on the medial side (between 0°/90° and 270°/360°) of the foot for about 55% of the time in the cycle (Fig. 5.5). Sanders (1999a) reported that his subjects kept the flow mostly on the medial side of the foot for about 66% of the time of the cycle.

Assuming that the eggbeater kick is mainly a sculling movement where the production of lift forces should be advantaged, the vertical force, angular velocities, and pitch angle data indicate that the phase in the cycle during which the knee was being extended (until maximum extension) was the most propulsive phase in the cycle.

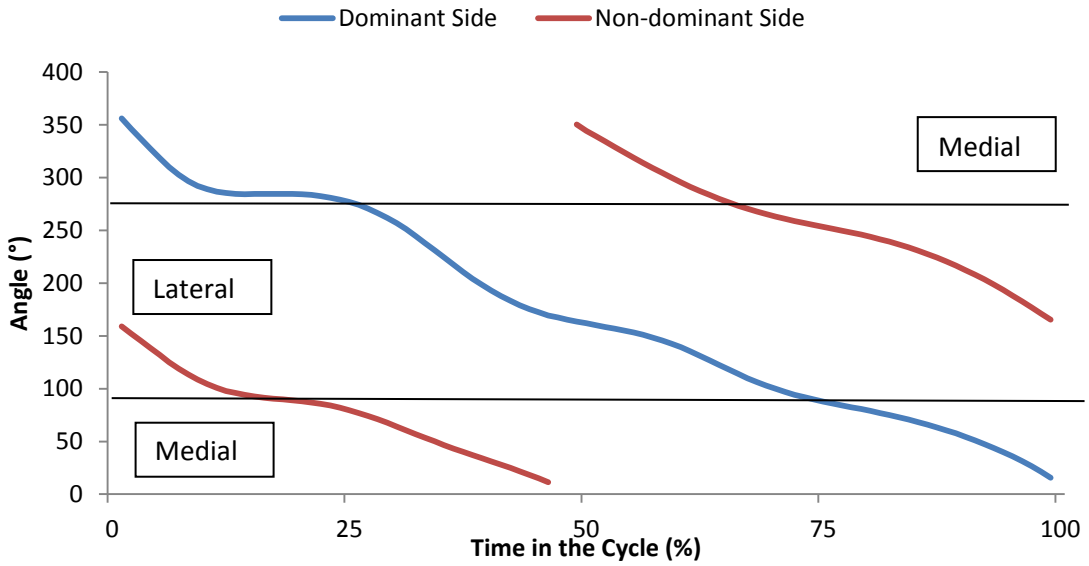


Figure 5.5. Feet sweepback angles for dominant and non-dominant side during the non-fatigued cycle for a typical subject. Black lines show when the flow changes from medial to lateral and vice-versa.

The above highlights the importance of technique and foot speed to performance. Players that performed better kept their hips abducted and flexed to reduce the vertical motion of the feet. In its turn, reducing vertical motion of the feet was essential to maximize the percentage of time in the cycle of positive pitch angles. This was supported by the significant negative correlation between vertical motion and the percentage of time of positive pitch angles in the cycle (dominant side, r=-0.704; non-dominant side r=-0.630). Minimizing vertical motion would increase the use of anterior-posterior and medio-lateral motions and increase the time during which the ankle can enable positive pitch angles of the feet. This is important because some negative pitch angle during the phase of knee flexion (phase with most vertical motion) is unavoidable, since the ankle is unable to dorsiflex enough. Additionally, high speed of the feet, created mainly by the extension of the knee is essential to produce larger propulsive forces.

### 5.1. Fatigue Induced Changes in the Eggbeater Kick Cycle

The vertical force produced during the eggbeater kick cycle decreases with fatigue (Fig. 5.6). Reduced vertical force with fatigue was observed throughout the whole cycle, and particularly during the time near the positive force peaks for which the difference between fatigue conditions was consistently significant statistically. This corresponded to the part in the cycle during which the knee was being extended. This change in performance can be explained by some of the changes that occur in the movement with fatigue.

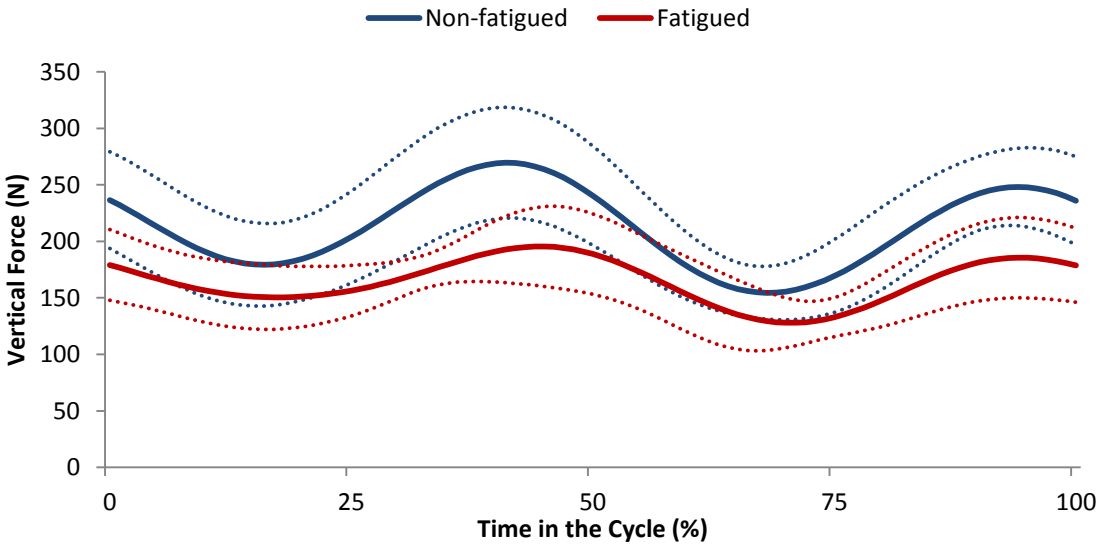


Figure 5.6. Vertical force produced during the cycle for non-fatigued and fatigued conditions across all subjects. Dotted lines indicate the 95% confidence interval of the true mean.

One of the main indicators of fatigue was the decrease of cycle rate. With fatigue, players tended to increase the duration of the cycle – 0.51s (*SD* = 0.03) for non-fatigued, 0.56s (*SD* = 0.03) for the mid time point, and 0.59s (*SD* = 0.03) for the fatigued condition – while maintaining the range of motion for most motions with the exception of knee flexion-extension. Increasing the cycle time differs from other cyclical aquatic sports such as swimming (Arellano et al., 1994, Chatard et al., 2001a, Chatard et al., 2001b, Chatard et al., 2001c, Chatard et al., 2001d, Pelayo et al., 1996) where cycle time decreases. This difference in fatigue adaptations of the movement between swimming strokes and the water polo eggbeater kick might be explained by two factors:

- The above water recovery in swimming strokes affords the opportunity to increase stroke rate with only small increases in resistance to the motion.

This means that reducing recovery time is an efficient way to increase stroke frequency.

- The pull phase of the swimming stroke can be shortened by decreasing the range of motion or by changing the orientation of the hand to reduce the resistive force so that stroke rate can be maintained despite fatigue.

In contrast, the range of joint motion and resistance to motion cannot be changed readily in the egg-beater kick without further adverse effects on performance. The hip needs to rotate internally and adduct to create favorable pitch angles and that happens when the knee is flexed. At the same time, the knee needs a large range of motion to create high foot speed and take advantage of the favorable pitch angles arranged when the knee is flexed.

Although the range of motion was maintained, amplitude of anatomical angles tended to decrease with increasing fatigue. Average angles reduced when fatigued for all movements with the exceptions of ankle plantar flexion and adduction. However, this did not result in a decrease of range of motion of the hip. Instead, players conserved their range of motion by having smaller minimum and maximum angles. Despite the fact that reducing both maximum and minimum ankle angle while conserving range of motion has been identified as a strategy present in running (Christina et al., 2001), fatigue has been mainly related to declines in range of motion of the lower limbs for activities such as squats (Hooper et al., 2013), posture during lifting exercises (Sparto et al., 1997), and jump and side-step skills (Cortes et al., 2012).

Figure 5.7 shows that the hip maintained range of motion for abduction, flexion and internal rotation across fatigue levels. With fatigue, maximum hip abduction and flexion moves towards the neutral anatomic position (0°) as this reduces demand on the muscles. By contrast internal rotation of the hip increases with fatigue, that is, away from 0°. Increasing internal rotation might be an adaptation of the hip joint to compensate for the inability to abduct and flex with fatigue, meaning that internally rotating the hip, while not as effective in the technique, might be less demanding in terms of muscle activity than abducting and flexing the hips.

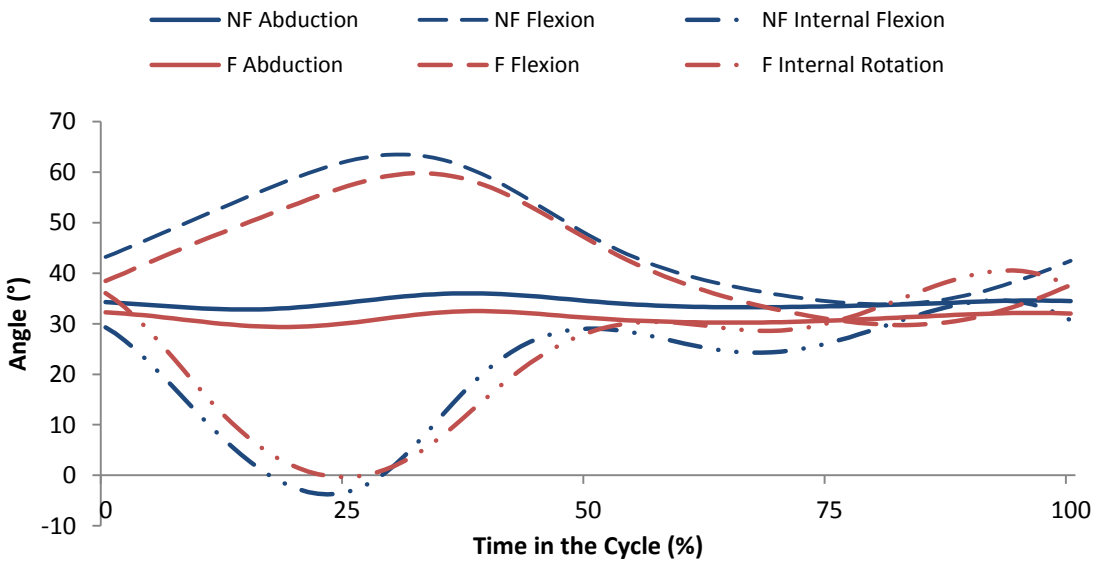


Figure 5.7. Dominant side hip abduction, flexion, and internal rotation for the non-fatigued (NF) and fatigued (F) cycle across all subjects.

The knee reduced its range of motion with fatigue by decreasing its maximum flexion while maintaining its maximum extension, suggesting that the phase of the cycle where

the knee was flexed might have been more demanding than the phase when the knee was extended.

Range of ankle motion was reduced with fatigue by decreasing maximum dorsiflexion. This difficulty in dorsiflexing the foot when fatigued might explain the strong negative correlations (dominant, $r$=-0.580; non-dominant, $r$=-0.631) for fatigued condition between normalized vertical force and average ankle plantar flexion angle.

Despite the differences between fatigue levels in the eggbeater kick technique, particularly in terms of amplitude of the movement and sweepback angles, the resultant feet pitch angles remained unchanged across fatigued states. Although average sweepback angles tended to increase with fatigue, relative durations of medial and lateral flow remained unchanged. The fact that changes induced by fatigue in the anatomical angles of the lower limbs did not result in changes in pitch angles is surprising. It would be expected that changes in the orientation of the thighs, legs and feet due to fatigue would result in a significant change of feet pitch angles. Instead, players seem to adapt to the effects of fatigue on the hip and knee joint angles to conserve the same pitch angles throughout the cycle. Thus, the decrease in performance was not related to a decrease in ability to maintain appropriate pitch angles.

## 5.2 Dominant vs Non-Dominant Side

Figure 5.8 shows the vertical force produced throughout the non-fatigued eggbeater kick cycle (the same two peak pattern is maintained for other fatigue levels) across all subjects. Although no significant differences were observed ($p$ = 0.054), there was a

difference in the magnitude of the vertical force produced between the two halves of the cycle. Larger maximum and minima of vertical force during the first half (0 – 50% of the time in the cycle) suggest an asymmetry in the contributions of the dominant and non-dominant sides to the vertical force produced. Similar movement asymmetries in other cyclical activities such running (Karamanidis et al., 2003), cycling (Smak et al., 1999, Carpes et al., 2007) or swimming (Barden et al., 2011, dos Santos et al., 2013, Seifert et al., 2008, Sanders, 2013) have been reported. In the eggbeater kick the maximum periods of force were generated when one knee was fully extended (40% and 94% in the time) and the opposite knee was being flexed. The two minimum values (16% and 68% in the time) occurred when one knee was at the beginning of flexion and the opposite knee was starting its extension. In the first part of the cycle (0 – 50%), when the dominant knee was being flexed and the non-dominant knee was extending, the vertical force produced was larger than during the second half (50 – 100%), when the dominant knee was extending and the non-dominant knee was being flexed. Because both sides moved at the same time in opposite phases, these differences could be due to either increased propulsion during knee extension of the non-dominant side or increased propulsion during the recovery phase of knee flexion of the dominant side.

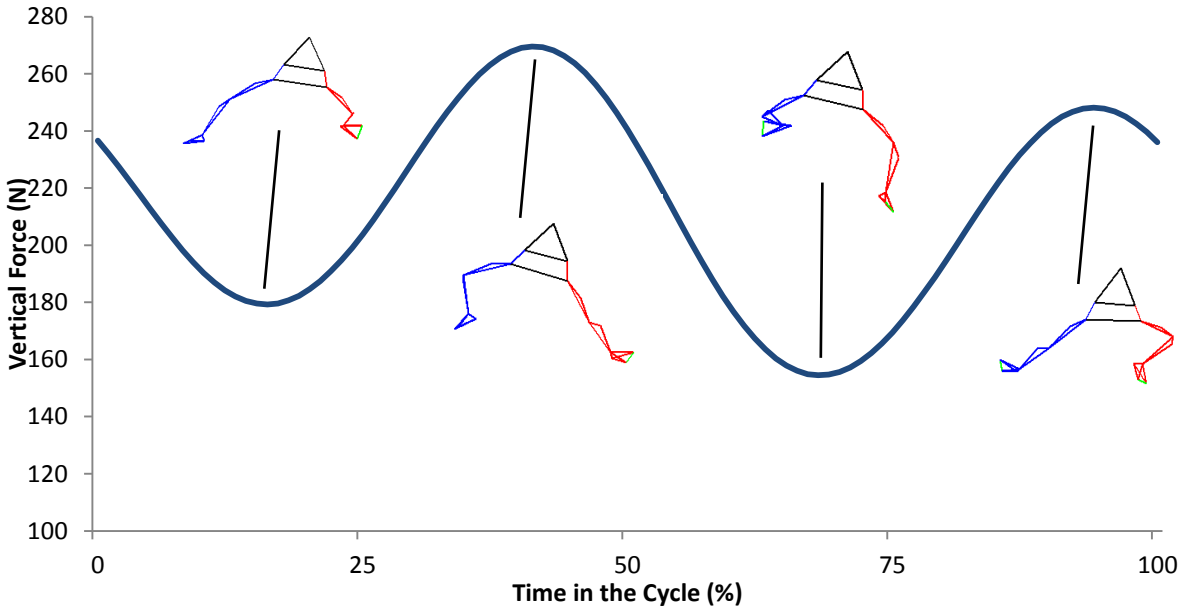


Figure 5.8. Mean vertical force produced during the non-fatigued eggbeater kick cycle across all subjects. Stick figures show position of the lower limbs at 16%, 40%, 68% and 94% of the time in the cycle.

Significant differences in technique between dominant and non-dominant side were evident mainly in the hip and ankle motions. In the case of the hip, although both sides had identical average angles, the non-dominant side had a larger rotation range of motion with increased maximum and decreased minimum (more negative) (Fig. 5.9). It is likely that these differences in kinematics contributed to the differences in patterns of force production during the first and second halves of the eggbeater kick cycle.

The different movement patterns between sides can be explained by differences in the motion of the dominant and non-dominant ankle during the knee flexion phase of the cycle (Fig. 5.9).

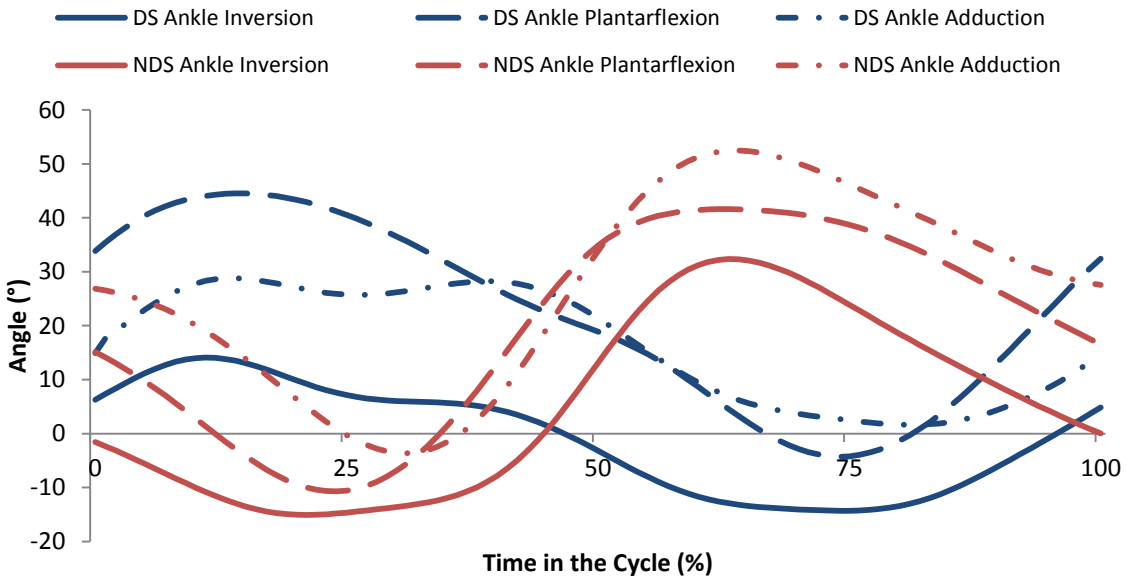


Figure 5.9 Mean ankle angles for dominant (DS) and non-dominant (NDS) side during the non-fatigued cycle across all subjects.

By the end of knee extension, when the foot was moving medially and starting to move upwards, some adduction and inversion of the foot was required to create positive pitch angles. However, while the dominant ankle was able to keep the foot adducted and inverted just enough to create positive pitch angles, the non-dominant ankle adducted and inverted the foot totally. This created larger positive pitch angles for the non-dominant side than the dominant side (Fig. 5.4). While this would not create any disadvantage during that phase, the large adduction and inversion would have been a disadvantage during the next phase, that is, the part of the cycle where the knee was flexed with the foot was starting to move outwards. This is because the ankle must be abducted and everted to produce positive angles of pitch during the outward movement of the foot. Because the dominant ankle was less adducted and inverted than the non-

dominant foot at the equivalent time in its cycle it was able to make the transition to abduction and eversion more quickly than the non-dominant foot. This meant that the non-dominant foot had larger negative pitch angles and for a longer duration than the dominant foot during the equivalent phases immediately following the transition between the medial and lateral movement of the foot. The more rapid transition of the dominant ankle facilitated its abduction and eversion when moving the foot laterally and downwards during knee extension, thereby creating positive pitch angles earlier in that period than the non-dominant ankle.

Another consequence of the differences between ankle motions is the different range of rotation of the hip between the dominant and non-dominant side (Fig. 5.10). When the knee was flexed, the medial-lateral motion of the foot was controlled by the rotation of the hip (i.e. internally rotating the hip with the knee flexed would move the foot outwards and vice-versa). Because the non-dominant ankle was more adducted and inverted than the dominant ankle during knee flexion, it required more time to abduct and evert for the beginning of the knee extension phase. The time to execute this action was controlled by the rotation of the hip. At the beginning of knee flexion the ankle was adducted and inverted, and, because the hip was externally rotated, the foot was located medially at this time of the cycle. By the time the ankle was abducted and everted with the knee flexed, the hip was internally rotated and the foot located on the laterally. Because the non-dominant ankle was initially more adducted and inverted than the dominant ankle, the non-dominant hip rotated more internally and externally to increase the medial-lateral path of the non-dominant foot and allow more time for it to abduct and evert for the phase of knee flexion. The knee flexion phase is a critical period in the

cycle during which the ankle needs to be abducted and everted as much as possible to ensure positive pitch angles that, in combination with high foot speeds as the foot moves laterally, result in the most propulsive phase in the cycle. The dominant ankle, on the other hand, because it was less adducted and inverted than the non-dominant one required less time to abduct and evert resulting in less hip rotation range of motion for the dominant hip.

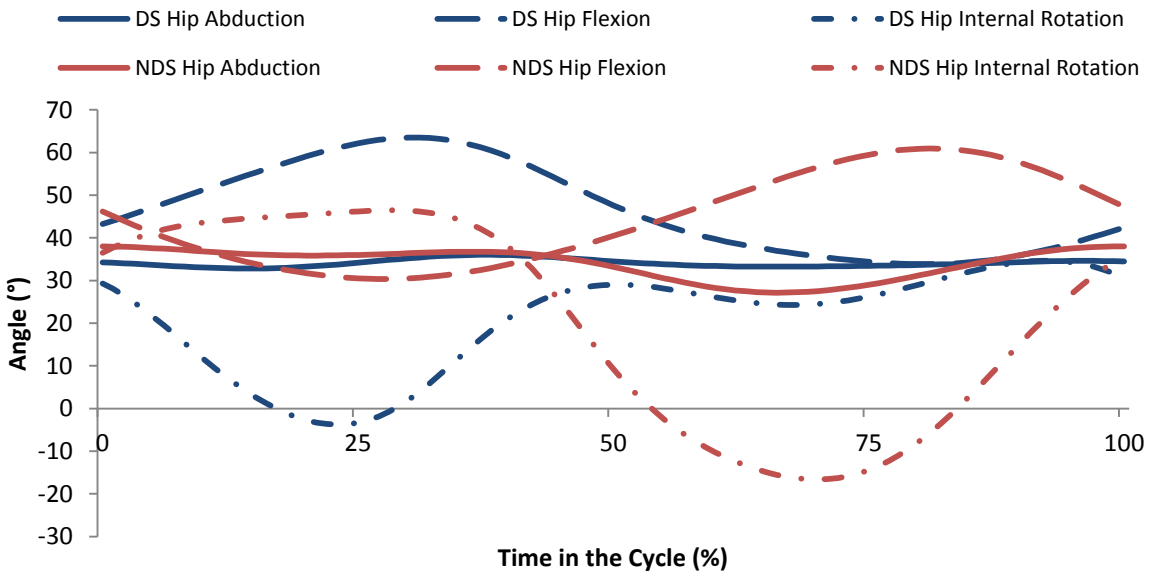


Figure 5.10 Hip angles for dominant (DS) and non-dominant (NDS) side during the non-fatigued cycle across all subjects.

The difference between the motions each side executes to bring the ankle everted and abducted in preparation for the knee extension is an interesting finding from the motor control prespective. While the non-dominant side 'preferred' to execute one quick 'all or nothing' abduction-adduction and inversion-eversion motion of the ankle, the dominant

side showed smoother, more refined motions, and controlled them more independently to its advantage. Adopting different motor strategies for the dominant and non-dominant side has been reported particularly for the upper limb extremity (hand) (Annett et al., 1979, Steenhuis and Bryden, 1989, Triggs et al., 2000) and arm (Sainburg and Kalakanis, 2000, Bagesteiro and Sainburg, 2002, Sainburg, 2002).

The abovementioned supports the idea that the vertical force asymmetries observed in Figure 5.8 are related with the knee flexion phase when the foot is moving outwards. Despite the differences in the orientations of the hip and ankle across the cycle both sides manage to have the ankle identically abducted and everted for the propulsive knee extension phase, however, the longer adduction and inversion of the non-dominant foot results in larger negative pitch angles during the knee flexion phase.

## 5.3 Implications for Training to Improve Performance

### 5.3.1 Role of the Muscles in the Cycle

In order to interpret the movement and recognize the most demanding periods of the cycle, it is essential to understand the role of the tested muscles during the cycle. This will allow designing training programs and exercises that can focus not only on important muscles for the eggbeater kick cycle but also maximize their role in the cycle when their action is important to create propulsive forces.

The Tibialis Anterior actions are dorsiflexion and inversion of the ankle (Basmajian, 1978). In the eggbeater kick cycle it is mostly active when the knee is being flexed and

the foot is inverted, plantarflexed and adducted (Fig. 5.11a), and when the ankle is everted, dorsiflexed and abducted at the beginning of knee extension (Fig. 5.11b).

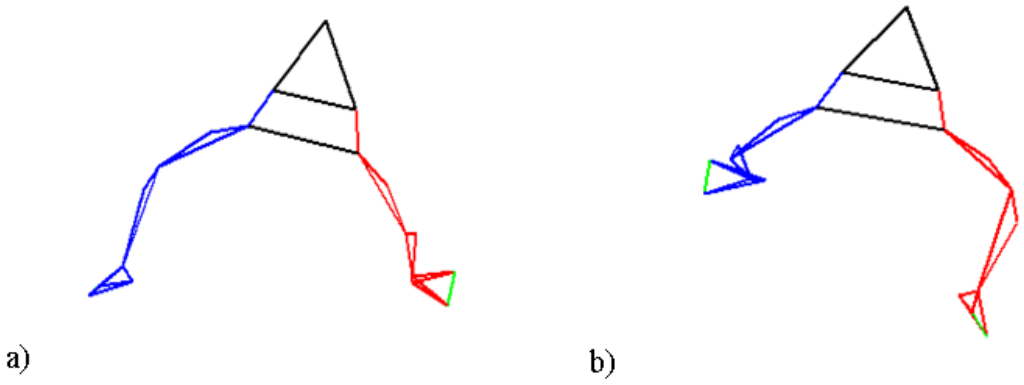


Figure 5.11 Illustration of moments in the cycle where the Right Tibialis Anterior is most active. Blue represents the right side and red the left. Green indicates the anterior part of the foot.

The first period of activity might be explained by its role in inverting the ankle when the ankle is plantar flexed during the part of the cycle where the knee is extended and moving medially. The second period of activity corresponds to the period during which the ankle is dorsiflexed when the knee is extending and moving outwards (Fig. 5.11a-5.11b). Tibialis Anterior was close to maximum MVC for long periods in the cycle. This supports the suggestion of Sanders (2002) that this muscle would play an important role when the foot is moved upward, backward and outward towards the end of the period of knee flexion. Average muscle activity of the Tibialis Anterior decreased with fatigue. This is a further indication of the demand on this muscle and the necessity to maintain high levels of activation during the whole cycle to optimise performance. Thus, the evidence suggests that because this muscle was involved in the cycle with constant

levels of high activity it also fatigued more than muscles characterized by bursts of activity. Normalized activity decreased significantly with fatigue (an average normalized to MVC activity of 88% when not fatigued, and an average normalized to MVC activity of 70% when fatigued). The major consequence of this decline in activity was a decrease in the minimum plantar flexion angles of the ankle. In other words, the ankle lost the capacity to dorsi flex during the part of the cycle when the knee was extending and the foot was moving outwards (Fig. 5.11b). Because dorsiflexion of the ankle during this phase of the cycle is advantageous to create positive pitch angles, it is apparent that the fatigue of the Tibialis Anterior was one of the causes of the decline of performance with fatigue.

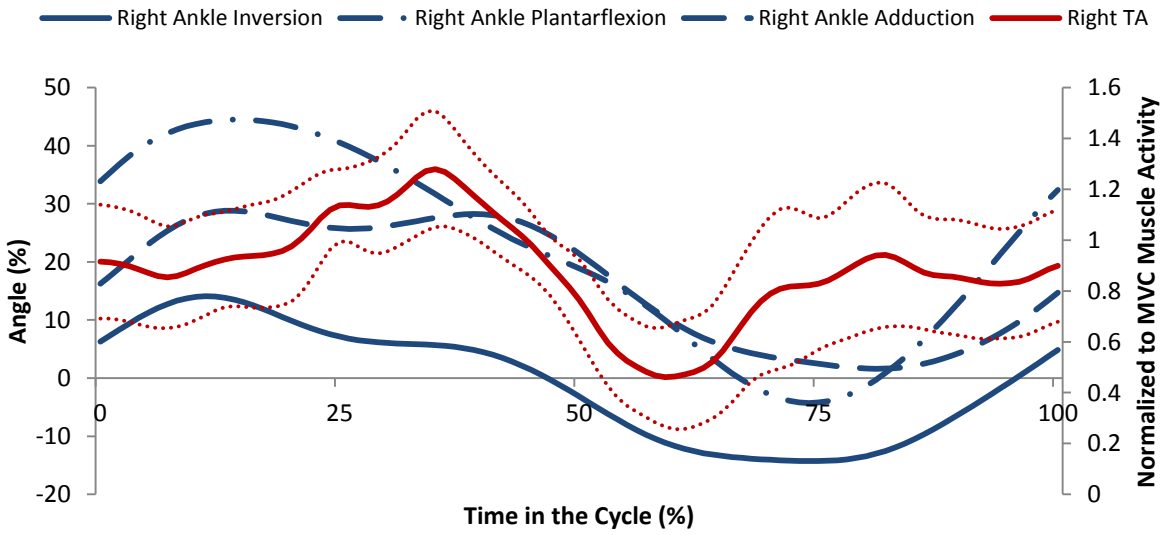


Figure 5.12 Right ankle inversion, plantar flexion and adduction with Right Tibialis Anterior normalized activity during the cycle for non-fatigued condition. Mean TA activity is represented by the solid line and dotted lines indicate the 95% confidence interval.

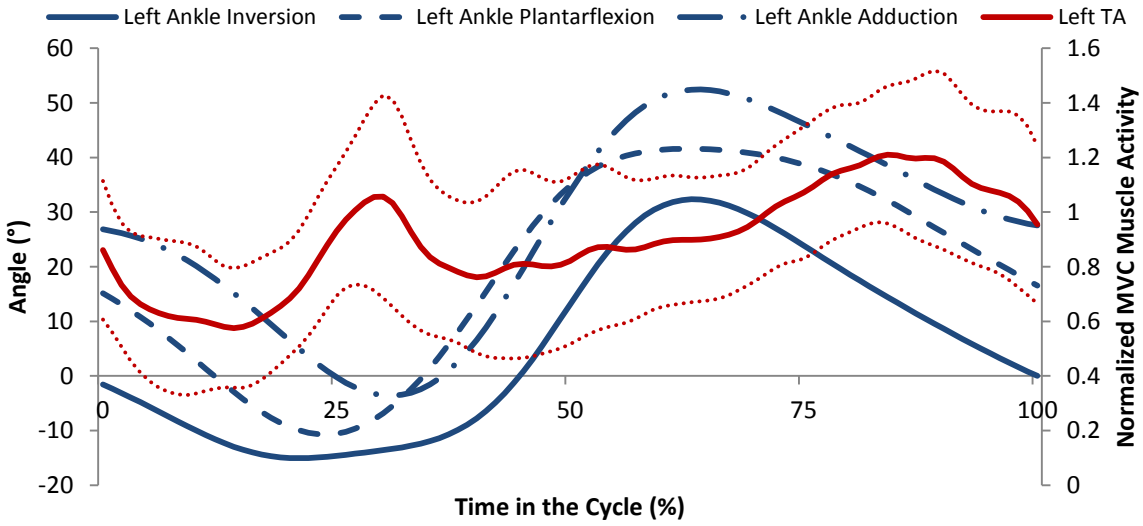


Figure 5.13 Left ankle inversion, plantarflexion and adduction and Left Tibialis Anterior activity during the cycle for non-fatigued condition. Mean TA activity is represented by the solid lines and dotted lines indicate the 95% confidence interval.

The Rectus Femoris' actions are knee extension and hip flexion (Basmajian, 1978). It was active during the part in the cycle when the knee was near the end of its flexion and moving into the extension phase (Fig. 5.14).

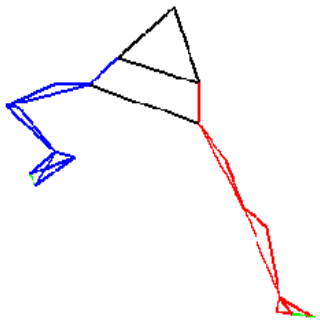

Figure 5.14 Illustration of time in the cycle where the Right Rectus Femoris was most active. Blue represents the right side and red the left. Green indicates the anterior part of the foot.

The peak Rectus Femoris activity coincided closely with peak knee flexion angular velocity. The high angular velocities involved in flexing the knee activate the Rectus Femoris to initially decelerate the flexion of the knee and initiate the extension. The evidence suggests that this muscle played a coactivation agonist/antagonist role (Hallett and Marsden, 1979, Lesticnne, 1979, Marsden et al., 1983, Aagaard et al., 1995, Hallett et al., 1975) in the cycle by working together with the Biceps Femoris. Figure 5.15 shows that the highest muscle activity was recorded when the knee flexion angular velocity decreased and knee extension angular velocity increased. Additionally, when comparing with the fatigued condition, the delay of Rectus Femoris activation observed with fatigue might have been a consequence of the reduced knee flexion angular velocity for the same condition. Activation delay of the antagonist muscle due to longer duration of the movement (reduced angular velocity of the movement) has been reported for the flexion/extension of the elbow when studying the Biceps Brachii's and the Triceps Brachii's agonist/antagonist relationship (Barnett and Harding, 1955, Brown and Cooke, 1981, Marsden et al., 1983, Bouisset and Lestienne, 1974) and isokinetic knee extensions (Quad/Hamstrings) (Weir et al., 1998). Furthermore, the timing of the antagonist muscle as a function of the agonist (Biceps Femoris) burst (Marsden et al., 1983) and torque output (Wierzbicka et al., 1986) has also been established in the elbow. Because the Rectus Femoris has an agonist/antagonist relationship with the Biceps Femoris, the reduced torque produced by the Biceps Femoris with fatigue resulted in reduced flexion angular velocity and consequently a delay in the activation of the

antagonist (Rectus Femoris). Moreover, the significant decrease in average muscle activity with fatigue found for the Biceps Femoris but not for the Rectus Femoris supported this idea. Additionally, since the antagonist is the major responsible for the time (stop motion) of the movement (Wierzbicka et al., 1986), the intense burst of activity by the Rectus Femoris indicates that during the cycle the performer tried to minimize the flexed position of the knee, further indicating that this position was not a favorable one to create propulsive forces. This evidence supports the idea of a critical knee flexion phase during the cycle that should be addressed in terms of muscle activation and response with the purpose of minimizing the time the percentage of time of this phase during the cycle, minimize the negative pitch angles created at this stage and maximize the duration of positive ones.

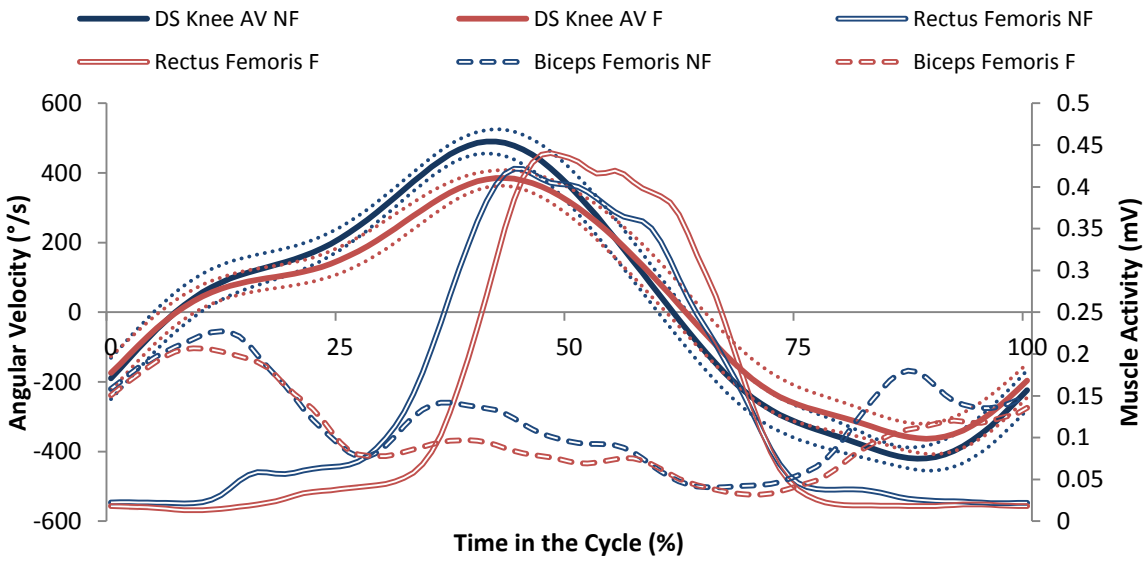


Figure 5.15 Dominant (DS) knee flexion angular velocity (AV), Rectus Femoris and Biceps Femoris activity during the cycle for non-fatigued (NF) and fatigued (F) condition. Dotted lines indicate the 95% confidence interval of the true mean.

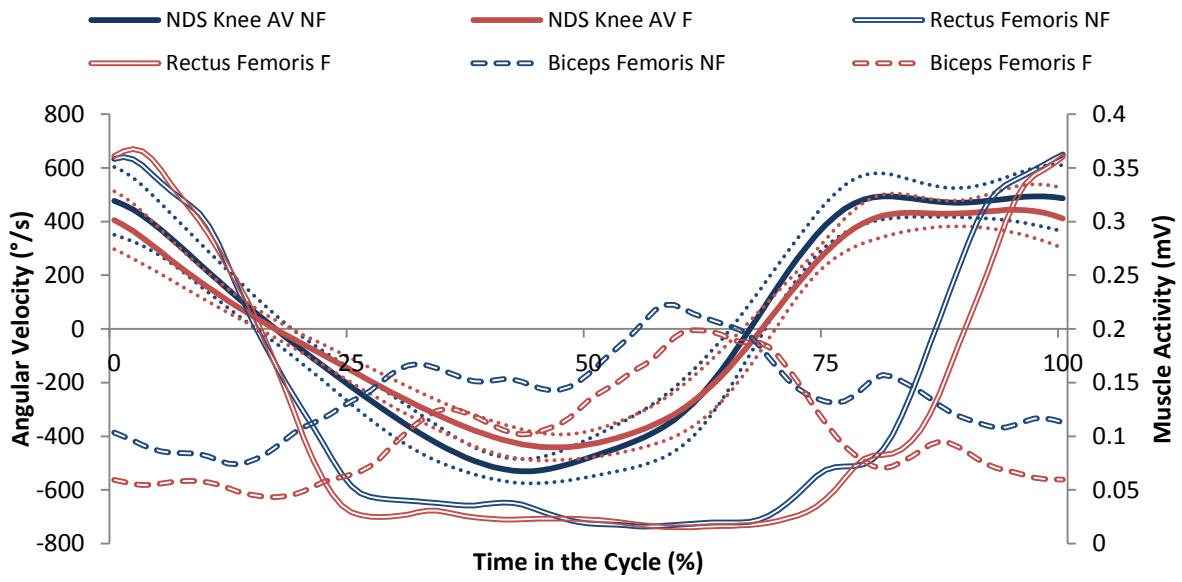


Figure 5.16 Non-dominant (NDS) knee flexion angular velocity (AV), Rectus Femoris and Biceps Femoris activity during the cycle for non-fatigued (NF) and fatigued (F) condition. Dotted lines indicate the 95% confidence interval of the true mean.

High levels of activity for the Rectus Femoris when the knee is flexed at more than 90° have been reported for other activities (Escamilla et al., 2001, Wretenberg et al., 1993, McCaw and Melrose, 1999, Escamilla et al., 1998, Isear et al., 1997). Highest activity normalized to MVIC goes beyond the MVIC recorded (100%). While this was not expected, it can be explained due to three factors:

1. The dynamic nature of the contraction and its similar features to a ballistic movement (e.g. throwing, kicking…). In this type of movement, muscle activity normalized to MVIC values have been frequently over 100% (Brophy et al., 2007, Dorge et al., 1999, DiGiovine et al., 1992, Shaffer et al., 1993, Smith et al., 2004, Kellis and Katis, 2007).

2. The fact that the MVIC tests had to be performed after the eggbeater kick test in order to preserve the quality of the waterproofing procedure, might have resulted in reduced MVCs due to fatigue at the time of the MVIC tests.
3. The extreme flexion of the knee (140°) might add some artifact activity by stretching the waterproof covering the sensor.

The Biceps Femoris actions are knee flexion and hip extension, but it also laterally rotates the leg when the knee is flexed (Basmajian, 1978).

The Biceps Femoris was most active near the time of maximum knee extension (Fig. 5.17). The evidence suggests that the Biceps Femoris, through an agonist/antagonist relationship, was involved with the Rectus Femoris in the flexion/extension of the knee during the eggbeater kick. Similar to the Rectus Femoris, the Biceps Femoris was most active when it was acting as an antagonist-agonist. It acted as an antagonist at the end of the knee extension to decelerate the motion and acted as an agonist immediately after when initiating the knee flexion motion. Additionally, greater antagonist hamstring co-activation towards full knee extension (10-30°) than in midrange of joint movement (40-70°) has been reported (Aagaard et al., 2000). This agrees with the findings of the present study and suggests that the Biceps Femoris is more important in stabilizing and controlling the extension/flexion of the knee in the cycle when it is extended than when it is at midrange and flexed.

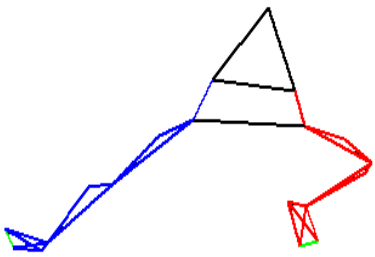

Figure 5.17 Illustration of moments in the cycle where the Right Biceps Femoris is most active. Blue represents the right side. Green indicates the anterior part of the foot.

Normalized activity of the Biceps Femoris was close to MVC level when the knee was ending extension and starting to be flexed (Fig. 5.17). Muscle activity across fatigue levels revealed a similar behavior to the Rectus Femoris whereby declines in muscle activity due to fatigue occurred when the Biceps Femoris was acting as an antagonist (Fig. 5.18).

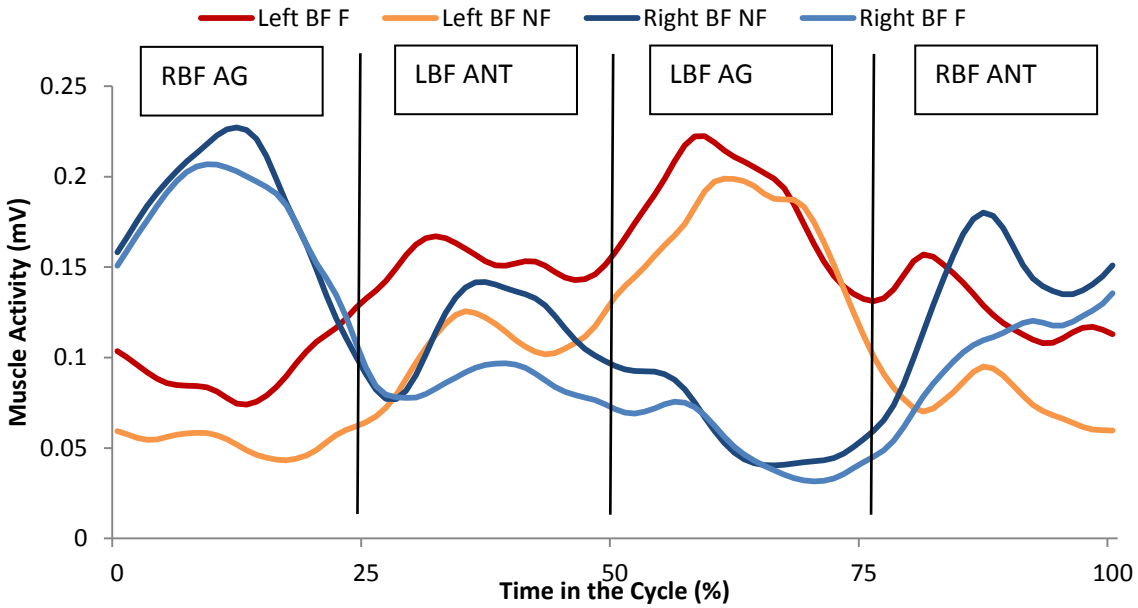


Figure 5.18 Dominant (RBF) and non-dominant (LBF) Biceps Femoris activity for non-fatigued and fatigued conditions across all subjects. Black lines are an estimate indication of when the Biceps Femoris alternated from a main antagonist (ANT) role to a main agonist.

### 5.3.2 Specific Training for the Eggbeater Kick

The previous discussion suggests the necessity of specific training to improve the eggbeater kick. Players and coaches should address the particularities of the eggbeater kick technique in terms of orientation and actions of the lower limbs, but also the role of individual muscles in the movement in relation to the demands on their endurance and power.

Players should train their technique to keep their hips abducted and flexed. Having the thighs in such positions will allow the feet to create more horizontal motions rather than vertical motions. Similar data were reported by Homma and Homma (2005), who

suggested that eggbeater kick performers should keep the knees ‘high and wide’. This was achieved by the players in this study by abduction and flexion of the hip. Endurance of the hip abductors (Gluteus group) and flexors (Iliopsoas and Rectus Femoris) and good flexibility would allow the hip to be abducted and flexed during the eggbeater kick cycle to meet those demands.

Knee extension movements should be fast but not maximum, to allow the feet to attain high speeds and reduce the amount of vertical motion. The agonist/antagonist relationship between the knee extensor (Rectus Femoris) and the knee flexor (Biceps Femoris) should be considered when designing endurance and strength exercises for those muscle groups. The Rectus Femoris and Biceps Femoris muscle activity patterns suggest the addition of plyometric exercises to training programs. This type of exercise reproduces the short and intense agonist/antagonist activity of the knee extensors and flexors (Wang et al., 2001, Schmid et al., 2010) characteristic of the eggbeater kick. Having both muscle groups (Quadriceps and Hamstrings) performing short intense bursts of eccentric/concentric contractions is important. Thus, plyometric extension/flexion of the knee with explosive motions, particularly when the knee is almost fully flexed and almost fully extended, would be beneficial. The use of plyometric training has been proven to increase the development and increase of explosive power (Mehdipour et al., 2008) or agonist-antagonist coactivation (Chimera et al., 2004, Lephart et al., 2005). Additionally, power of the knee extensors (Quadriceps) should be maximized particularly at larger degrees of flexion of the knee (100° - 140°) and with the hip internally rotated. This suggests the use of short but intense eggbeater kick repetitions in the pool but also of specific dry land exercises. This can be

accomplished by the use of elastic bands resisting knee extension while the hip is abducted, flexed and internally rotated, or particularly deep squats with a wide stance.

Players also need to address the difficulty of dosrflexing the ankle when the Tibialis Anterior becomes fatigued. While improvements in endurance can be achieved by executing the eggbeater kick for long periods of time, this training should be complemented with land-based exercises including elastic band or weight exercises that can provide heavier loads resisting the dorsiflexion of the foot. Adaptation to increased loads in dry-land training could allow the Tibialis Anterior to work at lower submaximal intensities during the performance of the eggbeater kick in the water, thereby improving endurance and eggbeater kick performance in competition. Furthermore, additional attention should be given to asymmetries in the movement. Because of limitations in the orientation of the non-dominant foot, players tend to have an inefficient non-dominant knee flexion that creates more negative pitch angles than the dominant side. This is accompanied by a larger rotation range of motion for the non-dominant hip. This can be corrected by directing more attention to the excessive adduction of the non-dominant foot, particularly during the learning stages of the movement when it should be easier to correct.

# Chapter Six: Conclusions

# 6 Conclusions

The purpose of this study was to analyse the kinematics and muscle activity of the water polo eggbeater kick in fatigued and unfatigued states to provide foundational knowledge on which training programs can be based.

The main findings and implications for each of the three purposes of this study, as well as the limitations of this study and recommendations for future work are outlined and described in this section.

## 6.1 Technique and Performance

The instantaneous vertical force produced during the eggbeater kick was used as a performance indicator. Players that produced more average vertical force normalized to body weight were considered the better performers.

Similar to Sanders (1999a) and Homma and Homma (2005), better performance was related to increased abduction and flexion of the hips during the cycle. Performance was also associated with foot paths being mostly horizontal rather than vertical. The small range of motion of hip flexion and abduction indicate that these motions are primarily responsible for orientating and keeping the thighs in favorable positions for the movement of the feet. On the other hand, hip internal and external rotation and knee flexion had a major role in moving the feet in the medio-lateral and anterio-posterior motions respectively.

Eggbeater performance was also associated with knee flexion and knee extension. Knee extension was the main action producing foot speed. The highest foot speeds in the cycle

were achieved when the knee was extending and were accompanied by positive pitch angles created with medial flow on the feet. This was concluded to be the most propulsive part of the eggbeater kick cycle. However, large knee extension would be a disadvantage because of the difficulty of recovering the foot without having substantial magnitude and duration of negative pitch. Large knee flexion was important to increase knee range of motion and time of positive pitch during knee extension.

The period of negative pitch was observed during knee flexion and could be minimized by the ability to quickly dorsiflex, abduct and evert the ankle when the knee is near maximum knee flexion.

## 6.2 Fatigue

Fatigue reduced the vertical force observed throughout the whole cycle, particularly during the time near the positive force peaks for which the difference between fatigue conditions was consistently statistically significant. This corresponded to the part in the cycle during which the knee was being extended.

The reduced vertical force produced across fatigue levels was a consequence of decreased foot speed which also resulted in increasing duration of the cycle, and changes in the amplitude and range of joint motions. Players kept their hip abduction and flexion range of motion by decreasing their maximum and minimum angles, and increased hip internal rotation.

The knee reduced its range of motion with fatigue by decreasing its maximum flexion while maintaining its maximum extension, suggesting that the phase of the cycle where

the knee was flexed might have been more demanding than the phase when the knee was extended. When the knee was flexed the Rectus Femoris was highly involved in agonist/antagonist activity with the Biceps Femoris, when the knee was extended only the Biceps Femoris increased activity.

Range of motion of the ankle was reduced with fatigue by decreasing maximum dorsiflexion. The difficulty in dorsiflexing the foot when fatigued was shown to be detrimental to performance and can be explained by the reduced activity of the Tibialis Anterior with fatigue. Despite the differences between fatigue levels in the eggbeater kick technique, particularly in terms of amplitude of the movement and sweepback angles, the resultant feet pitch angles remained unchanged across fatigued states. Thus, the decrease in performance was not related to a decrease in ability to maintain appropriate pitch angles.

### 6.3 Dominance

The pattern of vertical force produced during the eggbeater kick cycle showed asymmetries between the equivalent phases in the cycle of the dominant and non-dominant limbs. This asymmetry can be explained by differences in the technique of the dominant and non-dominant side, particularly during the phase of knee flexion. Differences in controlling the inversion of the ankle resulted in the non-dominant foot being moved laterally with the ankle more inverted and adducted than the dominant side. This caused the non-dominant foot to have a longer period of negative pitch than the dominant foot during this phase.

The dominant and non-dominant hips had similar average angles, but the non-dominant side had a larger range of internal and external rotational motion. This seemed to be related to the large inversion of the non-dominant ankle. The non-dominant hip compensated the less efficient non-dominant ankle motions by increasing its rotation, thereby giving more time for the ankle to evert and abduct. This contrasted with the smoother, more refined motions of the dominant ankle during the phase of knee flexion that resulted in longer positive pitch angles than the non-dominant side.

## 6.4 Practical Applications

The findings in this study revealed some factors related to maximum eggbeater kick performance when fatigued and not fatigued that have important implications in the training and instruction of the eggbeater kick.

During the eggbeater kick the hips should be kept largely abducted and flexed while going through a large rotation range of motion. The combination and amplitude of these motions is not common in other activities, suggesting the need to address these specific hip actions in the training of the eggbeater kick. Although muscles in the hip region were not tested in this study, this evidence indicates that training these muscles is fundamental to maximize eggbeater kick performance. Because several muscles can be both hip adductors and internal rotators simultaneously (e.g. Adductor Longus, Adductor Magnus…) or hip abductors and internal rotators (e.g. Gluteus Medius, Gluteus Minimus…) it is important to develop both flexibility and strength in these muscles. In order to keep the hips abducted, hip abductors such as the Gluteus Medius, Gluteus

Minimus, or the Tensor Fascia Latae should be trained for endurance and strength. On the other hand, flexibility of hip adductors like the Adductor Longus, Adductor Magnus, Pectineus or Gracilis should be increased to facilitate hip abduction. Another fundamental action of the hip is internal and external rotation. It is responsible for the medial-lateral motion of the feet, thus contributing to foot speed. Therefore, it is important to develop power and strength of the muscles involved in the internal and external rotation of the hip.

The action of the knee is critical to improve performance in the eggbeater kick. The knee's major role in the eggbeater kick cycle is to give amplitude and speed to the feet motion. Knee extension/flexion through the action of the Rectus Femoris and Biceps Femoris proved to be critical for foot speed and minimizing non propulsive periods in the cycle when the knee flexes. The phase of knee extension, because of the high foot speeds and positive pitch angles created by the feet is also the most propulsive phase in the cycle.

Although endurance and some flexibility can be addressed during the usual water training sessions through the execution of the movement for long periods of time, this should be complemented with maximal intensity eggbeater kick sets and with dry land exercises. High intensity eggbeater kick sets with short repetitions can address the specific strength and power required to execute the eggbeater kick under maximum effort. Dry land exercises for the lower limbs are recommended to reinforce the flexibility and strength of muscle groups involved in the movement. In this particular topic, squats with a wide stance seem to be appropriate. A wide stance (with feet wider that shoulder line) will have the hips abducted throughout hip and knee

flexion/extension and, if executed as a plyometric exercise, can resemble the agonist/antagonist activity of the Rectus Femoris and Biceps Femoris observed in this study. Another important action that could benefit from specific strength exercises is the internal and external rotation of the hip. Internally and externally rotating the hip with the knee flexed and with elastic bands providing resistance at the ankle might be a good way to strengthen the hip rotators and improve this motion.

The ankle had smaller ranges of motion than the hip and knee joints. As the muscle activity of the Tibialis Anterior significantly decreased with fatigue, reducing the ability of the ankle to dorsiflex and invert. This evidence supports the water training exercises for endurance and strength previously recommended. Dry land exercises to develop strength in the Tibialis Anterior should consist of dorsiflexion, inversion and abduction of the ankle under the resistance of elastic bands.

Another important finding of this study was the asymmetry between the dominant and non-dominant ankle motions. The larger inversion and adduction of the non-dominant ankle results in a longer period of negative pitch angles during the cycle for the non-dominant foot. This pattern of the non-dominant ankle can result from a wide variety of factors and should be addressed and corrected particularly during the phase of instruction when it is easier to modify motor behaviors.

## 6.5 Limitations and Future Work

This study investigated the eggbeater kick technique between three different fatigue levels and found differences between them. However, it is speculated that looking into

fatigue from a more continuous perspective – by analyzing longer periods of time or periods at closer intervals – could provide useful information about the fatigue process in the eggbeater kick including information about when changes occur and which ones happen first.

In this study the water polo eggbeater kick was investigated using surface electromyography. One of the difficulties of applying surface electromyography in the water is the limited time the sensors can be waterproofed. This limited the duration of the warm up in this study to two minutes. Additionally, the maximum isometric voluntary contraction tests had to be performed after the water trial, this might have resulted in reduced activation of the muscles tested.

In this study the eggbeater kick in the vertical position was examined. However, the eggbeater kick in water polo is executed under many different contexts. It can be performed in different positions or while executing other skills (passing, shooting, blocking, jumping…). Investigating these variations of the eggbeater kick can deepen the information about its training and provide a more complete picture of the skill. It would be possible to examine whether the technique and muscle demands between variants differ.

All the subjects recruited in this study had the right leg as dominant. This can be a limitation when interpreting the dominance data. It is suggested that to further investigate this issue a larger sample with subjects both right and left leg dominant should be used. Additionally, it is suggested that the data and results obtained from this study, may be examined from a motor control perspective in order to shed light on the aforementioned questions. In particular, the application of the dynamical systems theory

which has frequently been used to analyse athletic performance across many sports, due to its emphasis on processes of coordination and control in human movement systems, may prove useful (Bartlett et al., 1996, Glazier et al., 2002).

# Bibliography

# 7 Bibliography


AAGAARD, P., SIMONSEN, E. B., ANDERSEN, J. L., MAGNUSSON, S. P., BOJSEN-MOLLER, F. & DYHRE-POULSEN, P. 2000. Antagonist muscle coactivation during isokinetic knee extension. *Scand J Med Sci Sports,* 10**,** 58-67.

AAGAARD, P., SIMONSEN, E. B., TROLLE, M., BANGSBO, J. & KLAUSEN, K. 1995. Isokinetic hamstring/quadriceps strength ratio: influence from joint angular velocity, gravity correction and contraction mode. *Acta Physiologica Scandinavica,* 154**,** 421-427.

ABDEL-AZIZ, Y. I. & KARARA, H. M. 1971. Direct linear transformation from comparator coordinates into object space coordinates in close-range photogrammetry. *American Society for Photogrammetry Symposium on Close Range Photogrammetry.* Falls Church, VA: American Society for Photogrammetry.

ACKLAND, T. R., HENSON, P. W. & BAILEY, D. A. 1988. The Uniform Density Assumption - Its Effect Upon the Estimation of Body Segment Inertial Parameters. *International Journal of Sport Biomechanics,* 4**,** 146-155.

ALKNER, B. A., TESCH, P. A. & BERG, H. E. 2000. Quadriceps EMG/force relationship in knee extension and leg press. *Med Sci Sports Exerc,* 32**,** 459-63.

ALLARD, P., STOKES, I. & JEAN-PIERRE, B. 1995. *Three-Dimensional Analysis of Human Movement,* Champaign, IL, Human Kinetics.

AN, K. N. & CHAO, E. Y. S. 1991. Kinematic analysis. *In:* AN, K. N., BERGER, R. A. & COONEY, W. P. (eds.) *Biomechanics of the Wrist Joint.* New York, NY: Springer-Verlag.

ANNETT, J., ANNETT, M., HUDSON, P. T. & TURNER, A. 1979. The control of movement in the preferred and non-preferred hands. *Q J Exp Psychol,* 31**,** 641-52.

ANTONSSON, E. K. & MANN, R. W. 1985. The frequency content of human gait. *Journal of Biomechanics,* 18**,** 39-47.

AOKI, F., NAGASAKI, H. & NAKAMURA, R. 1986. The relation of integrated EMG of the triceps brachii to force in rapid elbow extension. *Tohoku J Exp Med,* 149**,** 287-91.

APKARIAN, J., NAUMANN, S. & CAIRNS, B. 1989. A three-dimensional kinematic and dynamic model of the lower limb. *J Biomech,* 22**,** 143-55.

ARAUJO, L., PEREIRA, S., GATTI, R., FREITAS, E., JACOMEL, G., ROESLER, H. & VILLAS-BOAS, J. 2010. Analysis of the lateral push-off in the freestyle flip turn. *J Sports Sci,* 28**,** 1175-81.

ARELLANO, R., BROWN, P., CAPPAERT, J. & NELSON, R. C. 1994. Analysis of 50-M, 100-M, and 200-M Freestyle Swimmers at the 1992 Olympic Games. *Journal of Applied Biomechanics,* 10**,** 189-199.

ARENDT-NIELSEN, L., GANTCHEV, N. & SINKJAER, T. 1992. The influence of muscle length on muscle fiber conduction velocity and development of muscle fatigue. . *Electroencephalography and Clinical Neurophysiology,,* 85**,** 166-172.

ARENDT-NIELSEN, L. & MILLS, K. R. 1985. The relationship between mean power frequency of the EMG spectrum and muscle fibre conduction velocity. *Electroencephalography and Clinical Neurophysiology,* 60**,** 130-134.

ARENDT-NIELSEN, L. & SINKJAER, T. 1991. Quantification of human dynamic muscle fatigue by electromyography and kinematic profiles. *J Electromyogr Kinesiol,* 1**,** 1-8.

ARENDT-NIELSEN, L. & ZWARTS, M. 1989. Measurement of muscle fiber conduction velocity in humans: techniques and applications. *J Clin Neurophysiol,* 6**,** 173-90.

AUERBACK, B. M. & RUFF, C. B. 2006. Limb bone bilateral asymmetry: variability and commonality among modern humans. *Journal of Human Evolution,* 50**,** 203-218.
BAGESTEIRO, L. B. & SAINBURG, R. L. 2002. Handedness: dominant arm advantages in control of limb dynamics. *J Neurophysiol,* 88**,** 2408-21.
BARDEN, J. M., KELL, R. T. & KOBSAR, D. 2011. The effect of critical speed and exercise intensity on stroke phase duration and bilateral asymmetry in 200-m front crawl swimming. *J Sports Sci,* 29**,** 517-26.
BARNES, W. S. 1980. The Relationship of Motor-Unit Activation to Isokinetic Muscular-Contraction at Different Contractile Velocities. *Physical Therapy,* 60**,** 1152-1158.
BARNETT, C. H. & HARDING, D. 1955. The activity of antagonist muscles during voluntary movement. *Ann Phys Med,* 2**,** 290-3.
BARTER, J. T. 1957. Estimation of the Mass of Body Segments. *WADC Technical Report.* Wright-Patterson Air Force Base, Ohio: Wright Air Development Center.
BARTLETT, R. 1997. *Introduction to Sports Biomechanics,* London, E & FN Spon.
BARTLETT, R. 1999. *Sports biomechanics: reducing injury and improving performance,* London, E & FN Spon.
BARTLETT, R. M., STOCKILL, N. P., ELLIOTT, B. C. & BURNETT, A. F. 1996. The biomechanics of fast bowling in men's cricket: a review. *J Sports Sci,* 14**,** 403-24.
BASMAJIAN, J. V. 1978. *Muscles Alive,* Baltimore, MD, The Williams & Wilkins Company.
BELLEMARE, F. & GARZANITI, N. 1988. Failure of neuromuscular propagation during human maximal voluntary contraction. *J Appl Physiol (1985),* 64**,** 1084-93.
BIGLAND-RITCHIE, B. 1979. Factors contributing to quantitative surface electromyographic recording and how they are affected by fatigue. . *American Review of Respiratory Disease,* 119**,** 95-97.
BIGLAND-RITCHIE, B., JOHANSSON, R., LIPPOLD, O. C., SMITH, S. & WOODS, J. J. 1983. Changes in motoneurone firing rates during sustained maximal voluntary contractions. *J Physiol,* 340**,** 335-46.
BIGLAND, B. & LIPPOLD, O. C. J. 1954. The Relation between Force, Velocity and Integrated Electrical Activity in Human Muscles. *Journal of Physiology-London,* 123**,** 214-224.
BOUISSET, S. 1973. EMG and muscle force in normal motor activities. *In:* DESMEDT, J. E. (ed.) *New developments in electromyography and clinical neurophysiology,*. Basel: Karger.
BOUISSET, S. & LESTIENNE, F. 1974. The organization of a simple voluntary movement as analysed from its kinematic properties. *Brain Research,* 71**,** 451-457.
BOUISSET, S. & MATON, B. 1972. Quantitative Relationship between Surface Emg and Intramuscular Electromyographic Activity in Voluntary Movement. *American Journal of Physical Medicine & Rehabilitation,* 51**,** 285-295.
BOUISSOU, P., ESTRADE, P. Y., GOUBEL, F., GUEZENNEC, C. Y. & SERRURIER, B. 1989. Surface EMG power spectrum and intramuscular pH in human vastus lateralis muscle during dynamic exercise. *J Appl Physiol (1985),* 67**,** 1245-9.
BRATUSA, Z., MATKOVIĆ, I. & DOPSAJ, M. 2003. Model characteristics of water polo players' activities in vertical position during game. *IX International Simposium Biomechanics and Medicine in Swimming.* Saint Ettiene, France: University of Sanint-Etienne.
BRONKS, R. & BROWN, J. M. 1987. IEMG/force relationships in rapidily contracting human hand muscles. *Electromyography and Clinical Neurophysiology,* 27**,** 509-515.
BROOKS, G. A., FAHEY, T. D. & WHITE, T. P. 1996. *Exercise Physiology: Human Bioenergetics and its Applications,* Mountain View, CA, Mayfield Publishing.

BROPHY, R. H., BACKUS, S. I., PANSY, B. S., LYMAN, S. & WILLIAMS, R. J. 2007. Lower extremity muscle activation and alignment during the soccer instep and side-foot kicks. *J Orthop Sports Phys Ther,* 37**,** 260-8.

BROWN, S. H. & COOKE, J. D. 1981. Amplitude- and instruction-dependent modulation of movement-related electromyogram activity in humans. *J Physiol,* 316**,** 97-107.

CAMPANINI, I., MERLO, A., DEGOLA, P., MERLETTI, R., VEZZOSI, G. & FARINA, D. 2007. Effect of electrode location on EMG signal envelope in leg muscles during gait. *J Electromyogr Kinesiol,* 17**,** 515-26.

CARPES, F. P., ROSSATO, M., FARIA, I. E. & BOLLI MOTA, C. 2007. Bilateral pedaling asymmetry during a simulated 40-km cycling time-trial. *J Sports Med Phys Fitness,* 47**,** 51-7.

CARVALHO, R. G. D., AMORIM, C. F., PERACIO, L. H. R., COELHO, H. F., VIEIRA, A. C., MENZEL, H. J. K. & SZMUCHROWSKI, L. A. 2010. Analysis of various conditions in order to measure electromyography of isometric contractions in water and on air. *Journal of Electromyography and Kinesiology,* 20**,** 988-993.

CATY, V., AUJOUANNET, Y., HINTZY, F., BONIFAZI, M., CLARYS, J. P. & ROUARD, A. H. 2007. Wrist stabilisation and forearm muscle coactivation during freestyle swimming. *Journal of Electromyography and Kinesiology,* 17**,** 285-291.

CHANDLER, R. F., CLAUSER, C. E., MCCONVILLE, J. T., REYNOLDS, H. M. & YOUNG, J. M. 1975. Investigation of inertial properties of the human body. *AMRL Technical Report* Wright-Patterson Air Force Base, OH.

CHAO, E. Y. 1980. Justification of triaxial goniometer for the measurement of joint rotation. *J Biomech,* 13**,** 989-1006.

CHATARD, J. C., CAUDAL, N., COSSOR, J. & MASON, B. Specific strategy for the medallists versus finalists and semi-finalists in the men's 200m breaststroke at the Sidney Olympic games. *In:* BLACKWELL, J. R. & SANDERS, R. H., eds. XIX International Symposium on Biomechanics in Sports, 2001a San Francisco: University of San Francisco. 10-13.

CHATARD, J. C., CAUDAL, N., COSSOR, J. & MASON, B. Specific strategy for the medallists versus finalists and semi-finalists in the women's 200m breaststroke at the Sidney Olympic games. *In:* BLACKWELL, J. R. & SANDERS, R. H., eds. XIX International Symposium on Biomechanics in Sports, 2001b San Francisco, CA. University of San Francisco, 14-17.

CHATARD, J. C., GIROLD, S., COSSOR, J. & MASON, B. Specific strategy for the medallists versus finalists and semi-finalists in the men's 200m freestyle at the Sidney Olympic games. *In:* BLACKWELL, J. R. & SANDERS, R. H., eds. XIX International Symposium on Biomechanics in Sports, 2001c San Francisco, CA. University of San Francisco, 57-60.

CHATARD, J. C., GIROLD, S., COSSOR, J. & MASON, B. Specific strategy for the medallists versus finalists and semi-finalists in the women's 200m backstroke at the Sidney Olympic games. *In:* H, B. J. R. S. R., ed. XIX International Symposium on Biomechanics in Sports, 2001d San Francisco, CA. University of San Francisco, 6-9.

CHEN, L., ARMSTRONG, C. W. & RAFTOPOULOS, D. D. 1994. An investigation on the accuracy of three-dimensional space reconstruction using the direct linear transformation technique. *Journal of Biomechanics,* 27**,** 493-500.

CHEVUTSCHI, A., LENSEL, G., VAAST, D. & THEVENON, A. 2007. An Electromyographic Study of Human Gait both in Water and on Dry Ground. *Journal Physiology Anthropology,* 26**,** 467-473.

CHIMERA, N. J., SWANIK, K. A., SWANIK, C. B. & STRAUB, S. J. 2004. Effects of Plyometric Training on Muscle-Activation Strategies and Performance in Female Athletes. *J Athl Train,* 39**,** 24-31.

CHRISTINA, K. A., WHITE, S. C. & GILCHRIST, L. A. 2001. Effect of localized muscle fatigue on vertical ground reaction forces and ankle joint motion during running. *Hum Mov Sci,* 20**,** 257-76.

CHUNG, L. H., REMELIUS, J. G., VAN EMMERIK, R. E. & KENT-BRAUN, J. A. 2008. Leg power asymmetry and postural control in women with multiple sclerosis. *Med Sci Sports Exerc,* 40**,** 1717-24.

CLARYS, J. P. 1979. Human morphology and hydrodynamics. *Swimming III.* Baltimore, MD: University Park Press.

CLARYS, J. P., MASSEZ, C., VAN DEN BROECK, M., PIETTE, G. & ROBEAUX, R. 1983. Total telemetric surface EMG of the front crawl. *Biomechanics VIII.* Champaign, IL: Human Kinetics.

CLARYS, J. P., ROBEAUX, R. & DELBEKE, G. 1985. Telemetrical versus conventional EMG in air and water. *In:* WINTER, N. R., HAYES, R. & PATLA, A. E. (eds.) *Biomechanics, vol IX.* . Champaign, IL: Human kinetics.

CLAUSER, C. E., MCCONVILLE, J. T. & YOUNG, J. M. 1969. Weight, volume and centre of mass of segments of the human body. *AMRL Technical Report.* Wright-Patterson Air Force Base, OH.

COE, R. 2002. It's the effect size, stupid: what effect size is and why it is important. *Annual Conference of the British Educational Research Association.* University of Exeter, England.

COHEN, J. 1992. 'A power primer'. *Psychological Bulletin,* 112**,** 155-159.

COLE, G. K., NIGG, B. M., RONSKY, J. L. & YEADON, M. R. 1993. Application of the joint coordinate system to three-dimensional joint attitude and movement representation: a standardization proposal. *J Biomech Eng,* 115**,** 344-9.

CONCEICAO, A., SILVA, A. J., BARBOSA, T., KARSAI, I. & LOURO, H. 2014. Neuromuscular fatigue during 200 m breaststroke. *J Sports Sci Med,* 13**,** 200-10.

CORMIE, P., MCCAULLEY, G. O. & MCBRIDE, J. M. 2007. Power versus strength-power jump squat training: influence on the load-power relationship. *Med Sci Sports Exerc,* 39**,** 996-1003.

CORTES, N., QUAMMEN, D., LUCCI, S., GRESKA, E. & ONATE, J. 2012. A functional agility short-term fatigue protocol changes lower extremity mechanics. *J Sports Sci,* 30**,** 797-805.

COULANGE, M., HUG, F., KIPSON, N., ROBINET, C., DESRUELLE, A. V., MELIN, B., JIMENEZ, C., GALLAND, F. & JAMMES, Y. 2006. Consequences of prolonged total body immersion in cold water on muscle performance and EMG activity. *Pflugers Arch,* 452**,** 91-101.

CURRIER, D. P. 1972. Maximal isometric tension of the elbow extensors at varied positions. Assessment of extensor components by quantitative electromyography. *Physical Therapy,* 52**,** 1265-1276.

CZABANSKI, B. 1975. Asymmetry of lower limbs in breastroke swimming. *In:* LEWILLIE, L. & CLARYS, J. P. (eds.) *Swimming II.* Baltimore, MD: University Park Press.

CZABANSKI, B. & KOSZCYC, T. 1979. Relationship of stroke asymmetry and speed of breastroke swimming. *In:* TERAUDS, J. & BEDINGFIELD, E. W. (eds.) *Swimming III.* Baltimore, MD: University Park Press.

DAVIS, R. B., OUNPUU, S., TYBURSKI, D. & GAGE, J. R. 1991. A Gait Analysis Data-Collection and Reduction Technique. *Human Movement Science,* 10**,** 575-587.

DAVIS, T. & BLANKSBY, B. A. 1977. A cinematographic analysis of the overhand water polo throw. *J Sports Med Phys Fitness,* 17**,** 5-16.

DE JESUS, K., DE JESUS, K., FIGUEIREDO, P., GONÇALVES, P., PEREIRA, S., VILLAS-BOAS, J. P. & FERNANDES, R. 2011. Electromyographic Analysis of two Different Feet Positions in Backstroke Start. . *Portuguese Journal of Sport Sciences,* 11**,** 191-194.

DE LA BARRERA, E. J. & MILNER, T. E. 1994. The effect of skinfold thickness on the selectivity of surface EMG. . *Electroencephalography and Clinical Neurophysiology,* 93**,** 91-99.

DE LEVA, P. 1996. Adjustments to Zatsiorsky-Seluyanov's segment inertia parameters. *J Biomech,* 29**,** 1223-30.

DE LUCA, C. J. 1997. The use of surface electromyography in biomechanics. *Journal of Applied Biomechanics,* 13**,** 135-163.

DE LUCA, C. J., FOLEY, P. I. & ERIM, Z. 1996. Motor unit control properties in voluntary isometric isotonic contractions. *Journal of Neurophysiology, ,* 76**,** 1503-1516.

DE LUCA, C. J. & FORREST, W. I. 1973. Force analysis of individual muscles acting simultaneously on the shoulder joint during isometric abduction. . *Journal of Biomechanics,,* 6**,** 385-393.

DE LUCA, C. J., KUZNETSOV, M., GILMORE, L. D. & ROY, S. H. 2012. Inter-electrode spacing of surface EMG sensors: reduction of crosstalk contamination during voluntary contractions. *J Biomech,* 45**,** 555-61.

DE LUCA, C. J. & MERLETTI, R. 1988. Surface myoelectric signal cross-talk among muscles of the leg. *Electroencephalography and Clinical Neurophysiology,* 69**,** 568-575.

DEFFEYES, J. & SANDERS, R. H. Elliptical zone body segment modelling software: digitising, modelling and body segment parameter calculation. *In:* WANG, Q., ed. XXIII International Symposium on Biomechanics in Sports, 2005 Beijing. The China Institute of Sports Science.

DEMBIA, C. 2011.

DEMPSTER, W. T. 1955. Space requirements of the seated operator. *WADC Technical Report (55-159).* Wright-Patterson Air Force Base, OH.

DIGIOVINE, N. M., JOBE, F. W., PINK, M. & PERRY, J. 1992. An electromyography analysis of the upper extremity in pitching. *Journal of Shoulder and Elbow Surgery,* 1**,** 15-25.

DORGE, H. C., ANDERSEN, T. B., SORENSEN, H., SIMONSEN, E. B., AAGAARD, H., DYHRE-POULSEN, P. & KLAUSEN, K. 1999. EMG activity of the iliopsoas muscle and leg kinetics during the soccer place kick. *Scand J Med Sci Sports,* 9**,** 195-200.

DOS SANTOS, K. B., PEREIRA, G., PAPOTI, M., BENTO, P. C. & RODACKI, A. 2013. Propulsive force asymmetry during tethered-swimming. *Int J Sports Med,* 34**,** 606-11.

DOWNWAR, J. M. & SAUERS, E. L. 2005. Clinical measures of shoulder mobility in the professional baseball player. *Journal of Athletic Training,* 40**,** 23-29.

DUCHER, G., JAFFRE, C., ARLETTAZ, A., BENHAMOU, C. & COURTEIX, D. 2005. Effects of long term tennis playing on the muscle-bone relationship in the dominant and non-dominant forearms. *Canadian Journal of Applied Physiology,* 30**,** 3-17.

EDWARDS, R. G. & LIPPOLD, O. C. J. 1956. The Relation between Force and Integrated Electrical Activity in Fatigued Muscle. *Journal of Physiology-London,* 132**,** 677-681.

ENGSBERG, J., GRIMSTONE, S. K. & WACKWITZ, J. 1988. Predicting talocalcaneal joint attitudes from talocalcaneal/talocrural joint attitudes. *Journal of Orthopedic Research,* 6**,** 749-757.

ESCAMILLA, R. F., FLEISIG, G. S., ZHENG, N., BARRENTINE, S. W., WILK, K. E. & ANDREWS, J. R. 1998. Biomechanics of the knee during closed kinetic chain and open kinetic chain exercises. *Med Sci Sports Exerc,* 30**,** 556-69.

ESCAMILLA, R. F., FLEISIG, G. S., ZHENG, N., LANDER, J. E., BARRENTINE, S. W., ANDREWS, J. R., BERGEMANN, B. W. & MOORMAN, C. T., 3RD 2001. Effects of technique variations on knee biomechanics during the squat and leg press. *Med Sci Sports Exerc,* 33**,** 1552-66.

FARINA, D. & MERLETTI, R. 2000. Comparison of algorithms for estimation of EMG variables during voluntary isometric contractions. *J Electromyogr Kinesiol,* 10**,** 337-49.

FERDJALLAH, M., WERTSCH, J. J. & SHAKER, R. 2000. Spectral analysis of surface electromyography (EMG) of upper esophageal sphincter-opening muscles during head lift exercise. *J Rehabil Res Dev,* 37**,** 335-40.

FIGUEIREDO, P., ROUARD, A., VILAS-BOAS, J. P. & FERNANDES, R. J. 2013a. Upper- and lower-limb muscular fatigue during the 200-m front crawl. *Applied Physiology, Nutrition, and Metabolism,* 38**,** 716-724.

FIGUEIREDO, P., SANDERS, R., GORSKI, T., VILAS-BOAS, J. P. & FERNANDES, R. J. 2013b. Kinematic and Electromyographic Changes During 200 m Front Crawl at Race Pace. *International Journal of Sports Medicine,* 34**,** 49-55.

FITTS, R. H. 1994. *Cellular mechanisms of muscle fatigue*.

FORMOSA, D. P., SAYERSA, M. G. L. & BURKETTA, B. 2014. Stroke-coordination and symmetry of elite backstroke swimmers using a comparison between net drag force and timing protocols. *Journal of Sports Sciences,* 32**,** 220-228.

FRENCH, A. P. 1970. *Newtonian Mechanics (The M.I.T. Introductory Physics Series)* New York, W. W. Norton & Company Inc.

FUGLEVAND, A. J., WINTER, D. A., PATLA, A. E. & STASHUK, D. 1992. Detection of motor unit action potentials with surface electrodes: influence of electrode size and spacing. *Biol Cybern,* 67**,** 143-53.

FUGLEVAND, A. J., ZACKOWSKI, K. M., HUEY, K. A. & ENOKA, R. M. 1993. Impairment of Neuromuscular Propagation during Human Fatiguing Contractions at Submaximal Forces. *Journal of Physiology-London,* 460**,** 549-572.

FUJISAWA, H., SUENAGA, N. & MINAMI, A. 1998. Electromyographic study during isometric exercise of the shoulder in head-out water immersion. *J Shoulder Elbow Surg,* 7**,** 491-4.

FULLER, J., LIU, L. J., MURPHY, M. C. & MANN, R. W. 1997. A comparison of lower-extremity skeletal kinematics measured using skin- and pin-mounted markers. *Human Movement Science,* 16**,** 219-242.

GANTCHEV, N., KOSSEV, A., GYDIKOV, A. & GERASIMENKO, Y. 1992. Relation between the motor units recruitment threshold and their potentials propagation velocity at isometric activity. *Electromyography and Clinical Neurophysiology,* 32**,** 221-228.

GERDLE, B., ELERT, J. & HENRIKSSON-LARSEN, K. 1989. Muscular fatigue during repeated isokinetic shoulder forward flexions in young females. *Eur J Appl Physiol Occup Physiol,* 58**,** 666-73.

GERDLE, B. & FUGL-MEYER, A. R. 1992. Is the mean power frequency shift of the EMG a selective indicator of fatigue of the fast twitch motor units? *Acta Physiologica Scandinavica,* 145**,** 129-138.

GERDLE, B., HEDBERG, R., JONSSON, B. & FUGL-MEYER, A. R. 1987. Mean power frequency and integrated electromyogram of repeated isokinetic plantar flexions. *Acta Physiol Scand,* 130**,** 501-6.

GERDLE, B., WRETLING, M. L. & HENRIKSSON-LARSEN, K. 1988. Do the fiber type proportion and the angular velocity influence the mean power frequency of the electromyogram? *Acta Physiologica Scandinavica Supplementum,* 134**,** 341-346.

GLAZIER, P. S., DAVIDS, K. & BARTLETT, R. M. 2002. Grip force dynamics in cricket batting. *In:* K. DAVIDS, G. S., S.J. BENNETT, J. VAN DER KAMP (ed.) *Interceptive Actions in Sport: Information and Movement.* London: Taylor and Francis.

GRAY, J. 2010. *Gray's anatomy*, Random House LLC.

GROOD, E. S. & SUNTAY, W. J. 1983. A joint coordination system for the clinical description of three-dimensional motions: Application to the knee. *Journal of Biomechanical Engineering,* 105**,** 136-144.

HALL, S. 1995. *Basic Biomechanics* St Louis, MO, Mosby-Year Book.

HALLETT, M. & MARSDEN, C. D. 1979. Ballistic flexion movements of the human thumb. *J Physiol,* 294**,** 33-50.

HALLETT, M., SHAHANI, B. T. & YOUNG, R. R. 1975. EMG analysis of stereotyped voluntary movements in man. *J Neurol Neurosurg Psychiatry,* 38**,** 1154-62.

HAMILL, J. & KNUTZEN, K. M. 2003. *Biomechanical Basis of Human Movement,* Baltimore, MD, Lippincott Williams & Wilkins.

HANAVAN, E. P. 1964. A mathematical model of the human body. *AMRL Technical Report* Wright-Patterson Air Force Base, OH.

HATZE, H. 1980. A mathematical model for the computational determination of parameter values of anthropometric segments. . *Journal of Biomechanics,* 13**,** 833-843.

HATZE, H. 1988. High-precision three dimensional photogrammetric calibration and object space reconstruction using a modified DLT-approach. *Journal of Biomechanics,* 21**,** 533-538.

HAY, J. G. 1985. *The Biomechanics of Sports Techniques,* Englewood Cliffs, NJ, Prentice-Hall.

HERMENS, H. J., FRERIKS, B., DISSELHORST-KLUG, C. & RAU, G. 2000. Development of recommendations for SEMG sensors and sensor placement procedures. *J Electromyogr Kinesiol,* 10**,** 361-74.

HERZOG, W., NIGG, B. M., READ, L. J. & OLSSON, E. 1989. Asymmetries in ground reaction force patterns in normal human gait. *Med Sci Sports Exerc,* 21**,** 110-4.

HILL, A. V. 1938. The heat of shortening and the dynamic constants of muscle. *Proceedings of the Royal Society Series B-Biological Sciences,* 126**,** 136-195.

HOHMANN, A., FEHR, U., KIRSTEN, R. & KRUEGER, T. 2008. Biomechanical Analysis of the Backstroke Start Technique in Swimming. *Bewegung und Training,* 2**,** 28-33.

HOMMA, M. & HOMMA, M. 2005. Coaching points for the technique of the eggbeater kick in synchronized swimming based on three-dimensional motion analysis. *Sports Biomech,* 4**,** 73-87.

HOOPER, D. R., SZIVAK, T. K., DISTEFANO, L. J., COMSTOCK, B. A., DUNN-LEWIS, C., APICELLA, J. M., KELLY, N. A., CREIGHTON, B. C., VOLEK, J. S., MARESH, C. M. & KRAEMER, W. J. 2013. Effects of resistance training fatigue on joint biomechanics. *J Strength Cond Res,* 27**,** 146-53.

HOPF, H. C., HERBORT, R. L., GNASS, M., GUNTHER, H. & LOWITZSC.K 1974. Fast and Slow Contraction Times Associated with Fast and Slow Spike Conduction of Skeletal-Muscle Fibers in Normal Subjects and in Spastic Hemiparesis. *Zeitschrift Fur Neurologie,* 206**,** 193-202.

HOPKINS, W. G. 2000. *Effect statistics. In: A New View of Statistics* [Online]. Available: newstats.org/effect.html.

HOPKINS, W. G. 2002. *A scale of magnitudes for effect statistics In: A New View of Statistics* [Online]. Available: newstats.org/effectmag.html [Accessed November 2013].

HUANG, H. K. & WU, S. C. 1976. The evaluation of mass densities of the human body in vivo. *Computers in Biology and Medicine,* 6**,** 337-343.

HUIGEN, E., PEPER, A. & GRIMBERGEN, C. A. 2002. Investigation into the origin of the noise of surface electrodes. *Medical & Biological Engineering & Computing,* 40**,** 332-338.

HUNT, M. A., SANDERSON, D. J., MOFFET, H. & INGLIS, T. J. 2004. Interlimb asymmetry in persons with and without an ACL deficiency during stationary cycling. *Archives of Physical Medicine and Rehabilitation,* 85**,** 1475-1478.

HUXLEY, H. E. 1965. The mechanism of muscular contraction. *Sci Am,* 213**,** 18-27.

ISEAR, J. A., JR., ERICKSON, J. C. & WORRELL, T. W. 1997. EMG analysis of lower extremity muscle recruitment patterns during an unloaded squat. *Med Sci Sports Exerc,* 29**,** 532-9.

JACOBS, R. & VAN INGEN SCHENAU, G. J. 1992. Control of an external force in leg extensions in humans. *J Physiol,* 457**,** 611-26.

JANSEN, R., AMENT, W., VERKERKE, G. J. & HOF, A. L. 1997. Median power frequency of the surface electromyogram and blood lactate concentration in incremental cycle ergometry. *Eur J Appl Physiol Occup Physiol,* 75**,** 102-8.

JENSEN, R. K. 1976. Model for body segment parameters. *In:* KOMI, P. V. (ed.) *Biomechanics VB.* Baltimore, MD: University Park Press.

JENSEN, R. K. 1978. Estimation of the biomechanical properties of three body types using a photgrammetric method. *Journal of Biomechanics,* 11**,** 349-358.

JENSEN, R. K. 1986. Body segment mass, radius and radius of gyration proportions of children. *J Biomech,* 19**,** 359-68.

JENSEN, R. K. & NASSAS, G. 1988. Growth of segment principal moments of inertia between four and twenty years. *Medicine and Science in Sports and Exercise,* 20**,** 594-604.

JOYCE, G. C., RACK, P. M. H. & WESTBURY, D. R. 1969. The mechnaical properties of cat soleus muscle during controlled lengthening and shortening movements. *J. Physiol. Lond.,* 204**,** 461-467.

JUEL, C. 1988. Muscle action potential propagation velocity changes during activity. *Muscle Nerve,* 11**,** 714-9.

JUNG, T., LEE, D., CHARALAMBOUS, C. & VRONGISTINOS, K. 2010. The influence of applying additional weight to the affected leg on gait patterns during aquatic treadmill walking in people poststroke. *Arch Phys Med Rehabil,* 91**,** 129-36.

KABADA, M. P., RAMAKRISHNAN, H. K. & WOOTTEN, M. E. 1990. Measurement of Lower Extremity Kinematics During Level Walking. *Journal of Orthopaedic Reasearch,* 8**,** 383-392.

KALJUMAE, U., HANNINEN, O. & AIRAKSINEN, O. 1994. Knee extensor fatigability and strength after bicycle ergometer training. *Arch Phys Med Rehabil,* 75**,** 564-7.

KAMEN, G. & CALDWELL, G. E. 1996. Physiology and interpretation of the electromyogram. *J Clin Neurophysiol,* 13**,** 366-84.

KANEDA, K., WAKABAYASHI, H., SATO, D., UEKUSA, T. & NOMURA, T. 2008. Lower extremity muscle activity during deep-water running on self-determined pace. *J Electromyogr Kinesiol,* 18**,** 965-72.

KARAMANIDIS, K., ARAMPATZIS, A. & BRUGGEMANN, G. P. 2003. Symmetry and reproducibility of kinematic parameters during various running techniques. *Medicine and Science in Sports and Exercise,* 35**,** 1009-1016.

KARLSON, S., YU, J. & AKAY, M. 1999. Enhancement of spectral analysis of myoelectric signals during static contractions using wavelet methods. *IEEE Transactions on Biomedical Engineering,* 46**,** 670-684.

KARLSSON, D. & TRANBERG, R. 1999. On skin movement artefact-resonant frequencies of skin markers attached to the leg. *Human Movement Science,* 18**,** 627-635.

KARLSSON, S. & GERDLE, B. 2001. Mean frequency and signal amplitude of the surface EMG of the quadriceps muscles increase with increasing torque - a study using the continuous wavelet transform. *Journal of Electromyography and Kinesiology,* 11**,** 131-140.

KATCH, V. & GOLD, E. 1976. Normative data for body segment weights, volumes, and densities in cadaver and living subjects. *Res Q,* 47**,** 542-7.

KAWAZOE, Y., KOTANI, H., MAETANI, T., HAMADA, T. & YATANI, H. 1981. Integrated electromyography activity and biting force during rapid isometric contraction of fatigued masseter muscle in man. *Archives of Oral Biology,* 26**,** 795-801.

KELLIS, E. & KATIS, A. 2007. The relationship between isokinetic knee extension and flexion strength with soccer kick kinematics: an electromyographic evaluation. *Journal of Sports Medicine and Physical Fitness,* 47**,** 385-394.

KELLY, B. T., ROSKIN, L. A., KIRKENDALL, D. T. & SPEER, K. P. 2000. Shoulder muscle activation during aquatic and dry land exercises in nonimpaired subjects. *J Orthop Sports Phys Ther,* 30**,** 204-10.

KESKINEN, O. P. & KESKINEN, K. L. Velocity profiles of competitive swimmers and triathlonists during an all-out 100-m swim. *In:* ERIKSSON, B. O. & GULLSTRAND, L., eds. XII FINA World Congress on Sports Medicine, 1997 Goteborg, Sweden., 351-356.

KLAUCK, J., DANIEL, K. & BAYAT, M. 2006. Goalkeeper's eggbeater kick in waterpolo: hinematics, dynamics and muscular coordination. *In:* VILAS-BOAS, J. P., ALVES, F. & MARQUES, A. S. (eds.) *Xth International symposium biomechanics and medicine in swimming.* Porto: Port J Sport Sci.

KNOWLTON, G. C., HINES, T. F., KEEVER, K. V. & BENNETT, R. L. 1956. Relation between electromyogram voltage and load. . *Journal of Applied Physiology,* 9**,** 472-476.

KOBAYASHI, Y., KUBO, J., MATSUO, A., MATSUBAYASHI, T., KOBAYASHI, K. & ISHII, N. 2010. Bilateral asymmetry in joint torque during squat exercise performed by long jumpers. *J Strength Cond Res,* 24**,** 2826-30.

KOMI, P. V. 1973. Relationship between muscle tension, EMG and velocity of contraction under concentric and eccentric work. *In:* DESMEDT, J. E. (ed.) *New Developments in Electromyography and Clinical Neurophysiology.* Basel: Karger.

KOMI, P. V. & TESCH, P. 1979. EMG frequency spectrum, muscle structure, and fatigue during dynamic contractions in man. *Eur J Appl Physiol Occup Physiol,* 42**,** 41-50.

KOSSEV, A., GANTCHEV, N., GYDIKOV, A., GERASIMENKO, Y. & CHRISTOVA, P. 1992. The effect of muscle fiber length change on motor units potentials propagation velocity. *Electromyogr Clin Neurophysiol,* 32**,** 287-94.

KRAEMER, W. J., DUNCAN, N. D. & VOLEK, J. S. 1998. Resistance training and elite athletes: adaptations and program considerations. *J Orthop Sports Phys Ther,* 28**,** 110-9.

KROGH-LUND, C. 1993. Myo-electric fatigue and force failure from submaximal static elbow flexion sustained to exhaustion. *Eur J Appl Physiol Occup Physiol,* 67**,** 389-401.

KROGH-LUND, C. & JORGENSEN, K. 1991. Changes in conduction velocity, median frequency, and root mean square-amplitude of the electromyogram during 25% maximal voluntary contraction of the triceps brachii muscle, to limit of endurance. *Eur J Appl Physiol Occup Physiol,* 63**,** 60-9.

KUPA, E. J., ROY, S. H., KANDARIAN, S. C. & DE LUCA, C. J. 1995. Effects of muscle fiber type and size on EMG median frequency and conduction velocity. *J Appl Physiol (1985),* 79**,** 23-32.

KWON, Y. H. 1999. Object plane deformation due to refraction in two-dimensional underwater motion analysis. *Journal of Applied Biomechanics,* 15**,** 396-403.

KWON, Y. H. & CASEBOLT, J. B. 2006. Effects of light refraction on the accuracy of camera calibration and reconstruction in underwater motion analysis. *Sports Biomechanics,* 5**,** 95-120.

LANGLEY, L. L. & TELFORD, I. R. 1980. *Dynamic Anatomy and Physiology* New York, McGraw-Hill.

LARSSON, S. E., LARSSON, R., ZHANG, Q., CAI, H. & OBERG, P. A. 1995. Effects of psychophysiological stress on trapezius muscles blood flow and electromyography during static load. *Eur J Appl Physiol Occup Physiol,* 71**,** 493-8.

LAWRENCE, J. H. & DE LUCA, C. J. 1983. Myoelectric signal versus force relationship in different human muscles. *J Appl Physiol Respir Environ Exerc Physiol,* 54**,** 1653-9.

LEPHART, S. M., ABT, J. P., FERRIS, C. M., SELL, T. C., NAGAI, T., MYERS, J. B. & IRRGANG, J. J. 2005. Neuromuscular and biomechanical characteristic changes in high school athletes: a plyometric versus basic resistance program. *Br J Sports Med,* 39**,** 932-8.

LEROY, D., POLIN, D., TOURNY-CHOLLET, C. & WEBER, J. 2000. Spatial and temporal gait variable differences between basketball, swimming and soccer players. *International Journal of Sports Medicine,* 21**,** 158-162.

LESTICNNE, F. 1979. Effects of inertial load and velocity on the braking process of voluntary limb movcments. *Experimental Brain Research,* 35**,** 407-418.

LI, W. & SAKAMOTO, K. 1996. The influence of location of electrode on muscle fiber conduction velocity and EMG power spectrum during voluntary isomeric contraction measured with surface array electrodes. *Applied Human Science,* 15**,** 25-32.

LINDSTROM, L., MAGNUSSON, R. & PETERSEN, I. 1974. Muscle load influence on myo-electric signal characteristics. *Scand J Rehabil Med,* 0**,** 127-48.

LINDSTROM, L. & PETERSEN, I. 1983. Power spectrum analysis of EMG signals and its applications. *In:* DESMEDT, J. E. (ed.) *Computer-aided electromyography.* Basel: Karger.

LIPPOLD, O. C. J. 1952. The Relation between Integrated Action Potentials in a Human Muscle and Its Isometric Tension. *Journal of Physiology-London,* 117**,** 492-499.

MARSDEN, C. D., OBESO, J. A. & ROTHWELL, J. C. 1983. The function of the antagonist muscle during fast limb movements in man. *J Physiol,* 335**,** 1-13.

MARZAN, T. & KARARA, H. M. 1975. A computer program for direct linear transformation of the colinearity condition and some applications of it. *American Society for Photogrammetry Symposium on Close Range Photogrammetry*. Falls Church, VA: American Society for Photogrammetry.

MASUMOTO, K., TAKASUGI, S., HOTTA, N., FUJISHIMA, K. & IWAMOTO, Y. 2004. Electromyographic analysis of walking in water in healthy humans. *J Physiol Anthropol Appl Human Sci,* 23**,** 119-27.

MASUMOTO, K., TAKASUGI, S., HOTTA, N., FUJISHIMA, K. & IWAMOTO, Y. 2005. Muscle activity and heart rate response during backward walking in water and on dry land. *Eur J Appl Physiol,* 94**,** 54-61.

MATON, B. & BOUISSET, S. 1977. The distribution of activity among the muscles of a single group during isometric contraction. *European Journal of Applied Physiology,* 37**,** 101-109.

MATON, B. & GAMET, D. 1989. The fatigability of two agonistic muscles in human isometric voluntary submaximal contraction: an EMG study. II. Motor unit firing rate and recruitment. *Eur J Appl Physiol Occup Physiol,* 58**,** 369-74.

MCARDLE, W. D., KATCH, F. & KATCH, V. 2001. *Exercise Physiology: Energy, Nutrition and Human Performance,* Baltimore, MD, Lippincott Williams and Wilkins.

MCCABE, C. 2008. Effects of 50m and 400m Race Paces on Three-Dimensional Kinematics and Linear Kinetics of Sprint and Distance Front Crawl Swimmers. Edinburgh: University of Edinburgh.

MCCAW, S. T. & MELROSE, D. R. 1999. Stance width and bar load effects on leg muscle activity during the parallel squat. *Med Sci Sports Exerc,* 31**,** 428-36.

MEHDIPOUR, A. R., FERDOWSI, M. H., ALIJANI, A. & GOHARPEY, S. 2008. A Study of Electromyography of Lower Extremities and Comparison of Efects of Plyometric and Isotonic Weight Training. *Human Movement,* 9**,** 103-106.

MESIN, L., MERLETTI, R. & RAINOLDI, A. 2009. Surface EMG: the issue of electrode location. *J Electromyogr Kinesiol,* 19**,** 719-26.

METRAL, S. & CASSAR, G. 1981. Relationship between force and integrated EMG activity during voluntary isometric anisometric contraction. . *European Journal of Applied Physiology,* 46**,** 185-198.

MILLER, D. I. & NELSON, R. C. 1973. *Biomechanics of sport- a research approach.,* Baltimore, Md, Lea & Febiger.

MILLER, N. R., SHAPIRO, R. & MCLAUGHLIN, T. M. 1980. A Technique for Obtaining Spatial Kinematic Parameters of Segments of Biomechanical Systems from Cinematographic Data. *Journal of Biomechanics,* 13**,** 535-&.

MILNER-BROWN, H. S. & STEIN, R. B. 1975. The relation between the surface electromyogram and muscular force. *Journal of Physiology (London),* 246**,** 549-569.

MILNER-BROWN, H. S., STEIN, R. B. & LEE, R. G. 1975. Synchronization of human motor units: possible roles of exercise and supraspinal reflexes. *Electroencephalogr Clin Neurophysiol,* 38**,** 245-54.

MIYOSHI, T., SHIROTA, T., YAMAMOTO, S., NAKAZAWA, K. & AKAI, M. 2004. Effect of the walking speed to the lower limb joint angular displacements, joint moments and ground reaction forces during walking in water. *Disabil Rehabil,* 26**,** 724-32.

MORIMOTO, S. 1986. Effect of length change in muscle fibers on conduction velocity in human motor units. *Jpn J Physiol,* 36**,** 773-82.

MORITANI, T. & DEVRIES, H. A. 1978. Reexamination of the relationship between the surface integrated electromyogram and force of isometric contraction. *American Journal of Physical Medicine,* 57**,** 263-277.

MORITANI, T., MURO, M. & NAGATA, A. 1986. Intramuscular and surface electromyogram changes during muscle fatigue. *J Appl Physiol (1985),* 60**,** 1179-85.

MUNGIOLE, M. & MARTIN, P. E. 1990. Estimating segment inertial properties: comparison of magnetic resonance imaging with existing methods. *J Biomech,* 23**,** 1039-46.

OLIVEIRA, N., FERNANDES, R. J., SARMENTO, M., LIBERAL, S., FIGUEIREDO, P. A., GONÇALVES, P. & VILLAS-BOAS, J. P. 2010. Muscle Activity During the Typical Water Polo Eggbeater Kick. *International Journal of Aquatic Research & Education,* 4**,** 163-174.

PALMER, A. R. & STROBECK, C. 1986. Fluctuating Asymmetry - Measurement, Analysis, Patterns. *Annual Review of Ecology and Systematics,* 17**,** 391-421.

PARSON, A. R. 1990. Fluctuating asymmetry: An epigenetic measure of stress. *Biological Review,* 65**,** 131-145.

PELAYO, P., SIDNEY, M., KHERIF, T., CHOLLET, D. & TOURNY, C. 1996. Stroking characteristics in freestyle swimming and relationships with anthropometric characteristics. *Journal of Applied Biomechanics,* 12**,** 197-206.

PINTO, S. S., LIEDTKE, G. V., ALBERTON, C. L., DA SILVA, E. M., CADORE, E. L. & KRUEL, L. F. 2010. Electromyographic signal and force comparisons during maximal

voluntary isometric contraction in water and on dry land. *Eur J Appl Physiol,* 110**,** 1075-82.
PLAGENHOEF, S., EVANS, F. G. & ABDELNOUR, T. 1983. Anatomical Data for Analyzing Human Motion. *Research Quarterly for Exercise and Sport,* 54**,** 169-178.
PLATANOU, T. & GELADAS, N. 2006. The influence of game duration and playing position on intensity of exercise during match-play in elite water polo players. *Journal of Sports Sciences,* 24**,** 1173-1181.
PLATANOU, T. & THANOPOULOS, V. 2002. Time analysis of the goalkeeper's movements in water polo. *Kinesiology,* 34**,** 94-102.
POYHONEN, T., KESKINEN, K. L., HAUTALA, A., SAVOLAINEN, J. & MALKIA, E. A. 1999. Human isometric force production and electromyogram activity of knee extensor muscle in water and on dry land. *Eur J Appl Physiol,* 80**,** 52-56.
POYHONEN, T., KESKINEN, K. L., KYROLAINEN, H., HAUTALA, A., SAVOLAINEN, J. & MALKIA, E. 2001. Neuromuscular function during therapeutic knee exercise under water and on dry land. *Arch Phys Med Rehabil,* 82**,** 1446-52.
PSYCHARAKIS, S. 2006. A 3D analysis of intra-cycle kinematics during 200m freestyle swimming. Edinburgh: University of Edinburgh.
PSYCHARAKIS, S. G. & SANDERS, R. H. 2009. Validity of the use of a fixed point for intracycle velocity calculations in swimming. *Journal of Science and Medicine in Sport,* 12**,** 262-265.
PSYCHARAKIS, S. G., SANDERS, R. H. & MILL, F. A calibration frame for 3D analysis of swimming. *In:* WANG, Q., ed. XXIII International Symposium on Biomechanics in Sports, 2005 Beijing. The China Institute of Sports Science, 901-904.
RAINOLDI, A., CESCON, C., BOTTIN, A., CASALE, R. & CARUSO, I. 2004. Surface EMG alterations induced by underwater recording. *J Electromyogr Kinesiol,* 14**,** 325-31.
REINSCHMIDT, C., VAN DEN BOGERT, A. J., NIGG, B. M., LUNDBERG, A. & MURPHY, N. 1997. Effect of skin movement on the analysis of skeletal knee joint motion during running. *J Biomech,* 30**,** 729-32.
ROBERTSON, D., CALDWELL, G., HAMILL, J., KAMEN, G. & WHITTLESEY, S. 2004. *Research Methods in Biomechanics,* Champaign, IL, Human Kinetics.
RODRIGUE, D. & GAGNON, M. 1983. The evaluation of forearm density with axial tomography. *J Biomech,* 16**,** 907-13.
ROUARD, A. H., BILLAT, R. P., DESCHODT, V. & CLARYS, J. P. 1997. Muscular activations during repetitions of sculling movements up to exhaustion in swimming. *Arch Physiol Biochem,* 105**,** 655-62.
ROUARD, A. H. & CLARYS, J. P. 1995. Cocontraction in the elbow and shoulder muscles during rapid cyclic movements in an aquatic environment. *J Electromyogr Kinesiol,* 5**,** 177-83.
SADEGHI, H., ALLARD, P., PRINCE, F. & LABELLE, H. 2000. Symmetry and limb dominance in able-bodied gait: a review. *Gait Posture,* 12**,** 34-45.
SADOYAMA, T., MASUDA, T. & MIYANO, H. 1985. Optimal conditions for the measurement of muscle fibre conduction velocity using surface electrodes arrays. *Medical and Biological Engineering and Computing,* 23**,** 339-342.
SADOYAMA, T., MASUDA, T., MIYATA, H. & KATSUTA, S. 1988. Fibre conduction velocity and fibre composition in human vastus lateralis. *Eur J Appl Physiol Occup Physiol,* 57**,** 767-71.
SAINBURG, R. L. 2002. Evidence for a dynamic-dominance hypothesis of handedness. *Experimental Brain Research,* 142**,** 241-258.

SAINBURG, R. L. & KALAKANIS, D. 2000. Differences in control of limb dynamics during dominant and nondominant arm reaching. *J Neurophysiol,* 83**,** 2661-75.
SANDERS, R. H. Lifting Performance in Aquatic Sports. *In:* H. J. RIEHLE, M. M. V., ed. XVI International Symposium on Biomechanics in Sports, 1998 Konstanz, Spain.
SANDERS, R. H. 1999a. Analysis of the eggbeater kick used to maintain height in water polo. *Journal of Applied Biomechanics,* 15**,** 284-291.
SANDERS, R. H. 1999b. A model of kinematic variables determining height achieved in water polo boosts. *Journal of Applied Biomechanics,* 15**,** 270-283.
SANDERS, R. H. 2002. *RE: Strength, flexibility and timing in the eggbeater kick.*
SANDERS, R. H. 2013. How do asymmetries affect swimming performance? *Journal of Swimming Research,* 21.
SANDERS, R. H., ALCOCK, A., DONALD, N., RIACH, I., WRIGHT, L. & FAIRWEATHER, M. 2012a. The swimming asymmetry puzzle: Putting the pieces together. *Sports Science Conference.* Denizli, Turkey.
SANDERS, R. H., ALCOCK, A. & FAIRWEATHER, M. 2012b. Is correction of asymmetries important in swimming? . *FINA World Medicine Conference.* Istanbul, Turkey.
SANDERS, R. H., THOW, J., ALCOCK, A., FAIRWEATHER, M., RIACH, I. & MATHER, F. 2012c. How can asymmetries in swimming be measured? *Journal of Swimming Science,* 19.
SANDERS, R. H., WILSON, B. D. & JENSEN, R. K. 1991. Accuracy of Derived Ground Reaction Force Curves for a Rigid Link Human-Body Model. *International Journal of Sport Biomechanics,* 7**,** 330-343.
SANTSCHI, J., DUBOIS, J. & OMOTO, C. 1963. Moments of inertia and centres of gravity of the living human body. *WADC Technical Report.* Dayton, OH: Wright-Patterson Air Force Base.
SCHILTZ, M., LEHANCE, C., MAQUET, D., BURY, T., CRIELAARD, J. M. & CROISIER, J. L. 2009. Explosive strength imbalances in professional basketball players. *J Athl Train,* 44**,** 39-47.
SCHLEIHAUF, R. E. 1979. A hydrodynamic analysis of swimming propulsion. *In:* TERAUDS, J. & BEDINGFIELD, E. W. (eds.) *Swimming III.* Baltimore, MD: University Park Press.
SCHMID, S., MOFFAT, M. & GUTIERREZ, G. M. 2010. Effect of knee joint cooling on the electromyographic activity of lower extremity muscles during a plyometric exercise. *J Electromyogr Kinesiol,* 20**,** 1075-81.
SEIFERT, L., CHEHENSSE, A., TOURNY-CHOLLET, C., LEMAITRE, F. & CHOLLET, D. 2008. Effect of breathing pattern on arm coordination symmetry in front crawl. *J Strength Cond Res,* 22**,** 1670-6.
SEIFERT, L., CHOLLET, D. & ALLARD, P. 2005. Arm coordination symmetry and breathing effect in front crawl. *Hum Mov Sci,* 24**,** 234-56.
SENIAM 1999. *European recommendations for surface electromyography, results of the SENIAM project.* , Roessingh Research and Development b.v.
SHAFFER, B., JOBE, F. W., PINK, M. & PERRY, J. 1993. Baseball batting. An electromyographic study. *Clin Orthop Relat Res,* 292**,** 285-93.
SHAPIRO, R. 1978. Direct linear transformation method for three-dimensional cinematography. *Res Q,* 49**,** 197-205.
SILVERS, W. M. & DOLNY, D. G. 2011. Comparison and reproducibility of sEMG during manual muscle testing on land and in water. *J Electromyogr Kinesiol,* 21**,** 95-101.
SMAK, W., NEPTUNE, R. R. & HULL, M. L. 1999. The influence of pedaling rate on bilateral asymmetry in cycling. *J Biomech,* 32**,** 899-906.
SMITH, H. K. 1998. Applied physiology of water polo. *Sports Med,* 26**,** 317-34.

SMITH, J., PADGETT, D. J., DAHM, D. L., KAUFMAN, K. R., HARRINGTON, S. P., MORROW, D. A. & IRBY, S. E. 2004. Electromyographic activity in the immobilized shoulder girdle musculature during contralateral upper limb movements. *J Shoulder Elbow Surg,* 13**,** 583-8.

SO, R., CHAN, K. M. & SIU, O. 2002. EMG power frequency spectrum shifts during repeated isokinetic knee and arm movements. *Res Q Exerc Sport,* 73**,** 98-106.

SOUTAS-LITTLE, R. W., BEAVIS, G. C., VERSTRAETE, M. C. & MARKUS, T. L. 1987. Analysis of foot motion during running using a joint co-ordinate system. *Medicine and Science in Sports and Exercise,* 19**,** 391-393.

SPARTO, P. J., PARNIANPOUR, M., REINSEL, T. E. & SIMON, S. 1997. The effect of fatigue on multijoint kinematics, coordination, and postural stability during a repetitive lifting test. *J Orthop Sports Phys Ther,* 25**,** 3-12.

SPOOR, C. W. & VELDPAUS, F. E. 1980. Rigid body motion calculated from special coordinates of markers. *Journal of Biomechanics,* 13**,** 391-393.

SPRIGINGS, E. J., BURKO, D. B., WATSON, G. & LAVERTY, W. H. 1987. An evaluation of three segmental methods used to predict the location of the total body CG for human airborne movements. *Journal of Human Movement Studies,* 13**,** 57-68.

STALBERG, E. 1966. Propagation velocity in human muscle fibers in situ. *Acta Physiol Scand Suppl,* 287**,** 1-112.

STEENHUIS, R. E. & BRYDEN, M. P. 1989. Different Dimensions of Hand Preference That Relate to Skilled and Unskilled Activities. *Cortex,* 25**,** 289-304.

STEPHENS, J. A. & TAYLOR, A. 1972. Fatigue of maintained voluntary muscle contraction in man. *J Physiol,* 220**,** 1-18.

STOKES, I. A., RUSH, S., MOFFROID, M., JOHNSON, G. B. & HAUGH, L. D. 1987. Trunk extensor EMG-torque relationship. *Spine (Phila Pa 1976),* 12**,** 770-6.

SWAINE, I. L. 1997. Time course of changes in bilateral arm power of swimmers during recovery from injury using a swim bench. *British Journal of Sports Medicine,* 31**,** 213-216.

TARATA, M. T. 2003. Mechanomyography versus electromyography, in monitoring the muscular fatigue. *Biomed Eng Online,* 2**,** 3.

TESCH, P. A., DUDLEY, G. A., DUVOISIN, M. R., HATHER, B. M. & HARRIS, R. T. 1990. Force and EMG signal patterns during repeated bouts of concentric or eccentric muscle actions. *Acta Physiol Scand,* 138**,** 263-71.

TESCH, P. A., KOMI, P. V., JACOBS, I., KARLSSON, J. & VIITASALO, J. T. 1983. Influence of lactate accumulation of EMG frequency spectrum during repeated concentric contractions. *Acta Physiologica Scandinavica,* 119**,** 61-67.

THORSTENSSON, A., KARLSSON, J., VIITASALO, J. H., LUHTANEN, P. & KOMI, P. V. 1976. Effect of strength training on EMG of human skeletal muscle. *Acta Physiol Scand,* 98**,** 232-6.

TORTORA, J. G. & DERRICKSON, B. H. 2008. *Principles of Anatomy and Physiology,* Hoboken, NJ, Wiley.

TOUSSAINT, H. M., DE GROOT, G., SAVELBERG, H. H., VERVOORN, K., HOLLANDER, A. P. & VAN INGEN SCHENAU, G. J. 1988. Active drag related to velocity in male and female swimmers. *J Biomech,* 21**,** 435-8.

TOVIN, B. J., WOLF, S. L., GREENFIELD, B. H., CROUSE, J. & WOODFIN, B. A. 1994. Comparison of the effects of exercise in water and on land on the rehabilitation of patients with intra-articular anterior cruciate ligament reconstructions. *Phys Ther,* 74**,** 710-9.

TRIGGS, W. J., CALVANIO, R., LEVINE, M., HEATON, R. K. & HEILMAN, K. M. 2000. Predicting hand preference with performance on motor tasks. *Cortex,* 36**,** 679-89.

VENEZIANO, W. H., DA ROCHA, A. F., GONCALVES, C. A., PENA, A. G., CARMO, J. C., NASCIMENTO, F. A. & RAINOLDI, A. 2006. Confounding factors in water EMG recordings: an approach to a definitive standard. *Med Biol Eng Comput,* 44**,** 348-51.

WANG, H., LIU, T., CHEN, C. & SHIANG, T. Comparision of the EMG activity between passive repeated plyometric half squat and traditional isotonic half squat. *In:* SANDERS, R. H. & BLACKWELL, J. R., eds. XIX International Symposium on Biomechanics in Sports, 2001 San Francisco, CA.

WEIR, J. P., KEEFE, D. A., EATON, J. F., AUGUSTINE, R. T. & TOBIN, D. M. 1998. Effect of fatigue on hamstring coactivation during isokinetic knee extensions. *Eur J Appl Physiol Occup Physiol,* 78**,** 555-9.

WEIR, J. P., MAHONEY, K. P., HAAN, K. G. & DAVIS, A. 1999. Influence of Electrode Orientation on Electromyographic Fatigue Indices of the Vastus Lateralis. *Journal of Exercise Physiology,* 2**,** 15-20.

WICKE, J. & LOPERS, B. 2003. Validation of the volume function within Jensen's (1978) elliptical cylinder model. *Journal of Applied Biomechanics,* 19**,** 3-12.

WIERZBICKA, M. M., WIEGNER, A. W. & SHAHANI, B. T. 1986. Role of agonist and antagonist muscles in fast arm movements in man. *Exp Brain Res,* 63**,** 331-40.

WILKIE, D. R. 1950. The relation between force and velocity in human muscle. *Journal Physiology London,* 110**,** 249-280.

WOLTRING, H. J. 1991. Representation and calculation of 3D joint movement. *Human Movement Science,* 10**,** 603-616.

WOODS, J. J. & BIGLANDRITCHIE, B. 1983. Linear and Non-Linear Surface Emg Force Relationships in Human Muscles - an Anatomical Functional Argument for the Existence of Both. *American Journal of Physical Medicine & Rehabilitation,* 62**,** 287-299.

WRETENBERG, P., FENG, Y. & LINDBERG, F. 1993. Joint moments of force and quadriceps muscle activity during squatting exercise. *Scandinavian Journal of Medicine & Science in Sports,* 3**,** 244-250.

YAO, W., FUGLEVAND, R. J. & ENOKA, R. M. 2000. Motor-unit synchronization increases EMG amplitude and decreases force steadiness of simulated contractions. *J Neurophysiol,* 83**,** 441-52.

YEADON, M. R. 1990. The simulation of aerial movement--II. A mathematical inertia model of the human body. *J Biomech,* 23**,** 67-74.

YEADON, M. R. & CHALLIS, J. H. 1990. Future directions for performance related research in sports biomechanics. The Sports Council London.

YOKOI, T., SHIBUKAWA, K., AE, M., ISHIJIMA, S. & HASHIHARA, Y. 1985. Body segment parameters of Japanese Children. *In:* PATLA, A. E. (ed.) *Biomechanics IX-B.* Champaign, Il: Human Kinetics.

YOSHIZAWA, M., OKAMOTO, T. & KUMAMOTO, M. 1983. Effects of EMG-biofeedback training on swimming. *Biomechanics VIII-B.* Champaign, IL: Human Kinetics.

YOUNG, W. B., JENNER, A. & GRIFFITHS, K. 1998. Acute enhancement of power performance from heavy load squats. *Journal of Strength and Conditioning Research,* 12**,** 82-84.

ZATSIORSKY, V. & SELUYANOV, V. 1983. The mass and inertia characteristics of the main segments of the human body. . *In:* H. MATSUI, A. K. K. (ed.) *Biomechanics VIII-B.* Illinois: Human Kinetics.

ZATSIORSKY, V. M. 2002. *Kinetics of Human Motion.,* Illinois, Human Kinetics.

ZEDKA, M., KUMAR, S. & NARAYAN, Y. 1997. Comparison of surface EMG signals between electrode types, interelectrode distances and electrode orientations in isometric exercise of the erector spinae muscle. *Electromyography and Clinical Neurophysiology,* 37**,** 439-447.

ZIFCHOCK, R. A., DAVIS, I. & HAMILL, J. 2006. Kinetic asymmetry in female runners with and without retrospective tibial stress fractures. *Journal of Biomechanics,* 39**,** 2792-2797.

ZIPP, P. 1978. Effect of electrode parameters on the bandwidth of the surface e.m.g. power-density spectrum. *Med Biol Eng Comput,* 16**,** 537-41.

ZWARTS, M. J. & ARENDT-NIELSEN, L. 1988. The influence of force and circulation on average muscle fiber conduction velocity during local muscle fatigue. *European Journal of Applied Physiology and Occupational Physiology,* 58**,** 278-283.

# 8 Appendix A

# Appendix A: Players' data and consent sheets

## 1.1 Players' information sheet

Dear water polo player,

I am seeking your involvement in a study designed to examine the technique and muscle activity of the eggbeater kick in water polo. This is the topic of my PhD. The eggbeater kick is an essential technique used in water polo that can directly and indirectly affect the performance of other components of the game (fighting for a position in the water, passing, shooting, blocking…). Performance of the eggbeater kick is the result of a variety of factors and is often limited by fatigue, a factor you will often associate with tiredness, pain and an inability to sustain optimal performance. Despite the knowledge that fatigue can influence the muscles' ability to contract effectively as well as control technical actions, both of which are vital for optimal eggbeater kick performance, little is known about these effects in the movement.

Therefore the general aim of this study is to investigate the movement of the lower limbs and respective muscle activities that are associated with the performance of the eggbeater kick. By investigating the movement of the legs we can calculate velocities, angles and forces produced by the movement. Muscle activity from electromyography will assess the activity of 3 different muscles in each leg and determine variables such as magnitude of the contractions, activation timings or indication of fatigue.

Requirements of each participant

The testing will be conducted over 2-3 weeks and you will be required to be available for one test session over this period. The duration of each session is estimated to be around 4 hour and will be allocated to fit around your training and personal routine and lifestyle.

During each session you will be videotaped for subsequent analysis. To aid this process you will be marked with black marker paint (applied by a sponge) and eight 2cm diameter balls (taped on you) on joint and anatomical markers. You will also be required to have surface electrodes (sensors that record the electrical activity produced by the muscles) placed upon your skin to record activity levels of certain muscles, again for subsequent analysis. This will require the placement of Flexifix waterproof covering and adhesive tape to waterproof each electrode (Fig. 1). For this preparation to be more effective it is recommended that you shave your legs on the day before your session, this will allow the taping and waterproof material to stick better to your legs. In addition, you should wear fitted trunks as opposed to training shorts so that each joint marker can be easily identified.

Figure 1. Legs fully prepared with the sensors and body markers.

Potential benefits for your participation

On completion of the study, an individual report with the results and findings will be made available to each player. This report will consist of the data from your testing session, videos from your trials and possible suggestions for the improvement of your performance.

Additional Information

Each testing session will be carried out in the St Leonards Land swimming pool. If you decide to take part in the study, you will be fully briefed in terms of the nature of the task, the procedure and layout of the pool. You will be required to give informed consent and complete a medical questionnaire and information sheet detailing aspects of your water polo history, injury history and personal details. All information obtained will remain strictly confidential. In any subsequent use of the data, any identifiable information will be removed. You should be made aware that you are under no obligation to complete the testing sessions and are at a liberty to withdraw at any time.

If you have any further questions or concerns at any point throughout the duration of the study, please do not hesitate to contact me.

Researcher: Nuno Oliveira
Telephone: 07736921030
E-mail: nunocancela@gmail.com

Sincerely,

Nuno Oliveira (Experimenter)

Professor Ross Sanders (Thesis Supervisor)

## 1.2 Informed Consent Form

I (print name clearly)…… hereby give my consent to participate in the exercise test(s) explained to me. I fully understand the following aspects of this study:

- The procedures involved and the purpose, details and requirements of the study as well as the possible benefits.
- That I will be required to provide some personal information, water polo history and medical details prior to participation
- That underwater and above water views of my eggbeater kick execution will be recorded using video cameras.
- That electric sensor's will be placed on the surface of my skin, non-invasively, to measure muscular activity.
- That I have been informed of the possible risks or discomfort associated with this study and its design.
- I can withdraw my involvement at any stage of the study without prejudice.
- That the researchers will answer any questions regarding the procedures.
- That I have responsibilities as a participant in informing the researcher of any problems during the investigation and I am aware of these.
- I have been informed that any information or data I provide will be kept strictly confidential and that my identity will be kept anonymous in any presentation of this material.
- My participation in the analysis is not in response to financial or other inducements.

I acknowledge I have received a copy of this form and that I have read and understood the instructions regarding my participation in this study and agree to fulfil these.

I DO/ DO NOT grant permission for physiological measures to be taken, including heart rate and muscular activity.

Date……/……/……

Subjects Full Signature……..

Print Name…….

Experimenters Signature……

## 1.3 Players' data information

1. **Name:**
2. **D.O.B:**
3. **Age:**
4. **Height (cm):**
5. **Weight (kg):**
6. **Dominant limb (Arm):**
7. **Dominant limb (Leg):**
8. **Number of training sessions per week/ hours training per week:**
9. **Have you suffered from any previous injuries/pain which affected your playing**

   (Please indicate for all injuries/pain)

**Where was the injury located/ which side of the body:……**

**Did you have to cease training? For how long:……**

**How long were you in rehabilitation for this injury/pain:……**

**Has the injury or pain re-occurred:……..**

10. **What is your water polo experience/history:……..**

**……**

**…….**

11. **What is your main position/s in the game (center forward, wing…):……..**

……..

Additional information for day of test Session:

12. **What activities/training were you involved in two days prior to this test?**.....

**…**……

……

## 1.4 Medical Questionnaire

Before participating in the experimental protocol that has been outlined to you we would like to establish that the exercise is safe for you. Therefore please complete the following questionnaire. All information given will be treated as strictly confidential.

1. Name:

2. During your water polo career have you participated in a fatiguing 'anaerobic' set at maximum effort as part of your training?

Yes/No

3. If yes, did you have any lasting discomfort or unusual after effects or symptoms other than some muscle soreness following that test?

Yes/No If yes, give details:

4. Have you had to consult your doctor in the last six months?

Yes/No

5. Have you experienced chest pain when performing physical activity?

Yes/No

6. Have you experienced chest pain when you were not doing physical activity?

Yes/No

7. Is there a history of early onset heart disease in your family?

Yes/No

8. Do you lose your balance because of dizziness or do you ever lose consciousness?

Yes/No

9. Do you have any form of muscular/ joint injury that could be made worse by a change in your physical activity?

Yes/No If yes, give details:

10. Do you have or have you suffered from any of the following conditions that could be made worse by a change in your physical activity?

Diabetes Heart condition/complaints

Asthma Hepatitis

Bronchitis Blood pressure problems

Viral/bacterial infection

11. Are you presently taking any medication, particularly for blood pressure problems or a heart condition?

Yes/No If yes, give details:

12. Have you had, for any reason, to suspend your normal training for the past two weeks prior to this test?

Yes/No If yes, give details:

13. Is there anything to prevent you from successfully completing the tests that have been outlined to you?

Yes/No If yes, give details:

I _____declare that the above information is correct at the time of completing this questionnaire.

Date: ……/……/……
Signature of Supervisor:

Researcher: Nuno Oliveira
Telephone: 07736921030
E-mail: nunocancela@gmail.com

Supervisor: Prof. Ross Sanders
Telephone:
E-mail: r.sanders@ed.ac.uk

Thank you

Nuno Oliveira (Experimenter)

Professor Ross Sanders (Thesis Supervisor)

# 9 Appendix B

## Rectus Femoris

| | | |
|---|---|---|
| Function | Extension of the knee joint and flexion of the hip joint. | 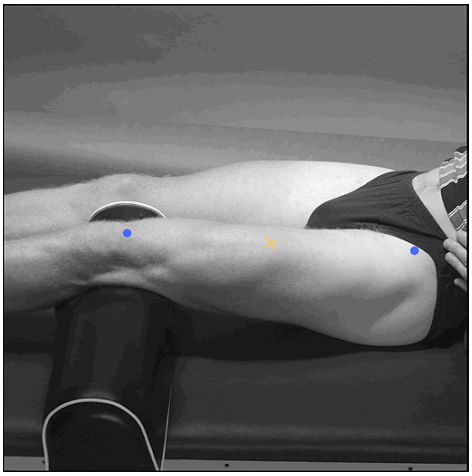 |
| Location | The electrodes need to be placed at 50% on the line from the anterior spina iliaca superior to the superior part of the patella | |
| Orientation of the electrodes | In the direction of the line from the anterior spina iliaca superior to the superior part of the patella. | |
| Test | Sitting on a table with the knees in slight flexion and the upper body slightly bend backward. Extend the knee without rotating the thigh while applying pressure against the leg above the ankle in the direction of flexion. | |

## Biceps Femoris

| | | |
|---|---|---|
| Function | Flexion and lateral rotation of the knee joint. The long head also extends and assists in lateral rotation of the hip joint. | 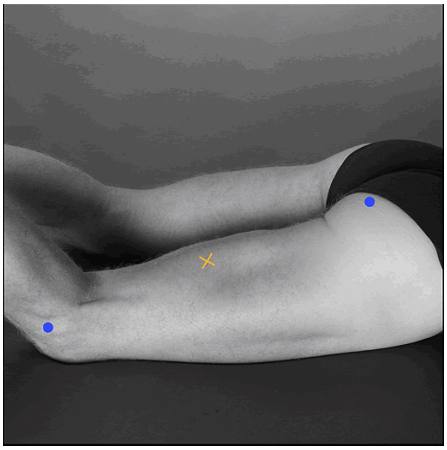 |
| Location | The electrodes need to be placed at 50% on the line between the ischial tuberosity and the lateral epicondyle of the tibia. | |
| Orientation of the electrodes | In the direction of the line between the ischial tuberosity and the lateral epicondyle of the tibia. | |
| Test | Lying on the belly with the face down with the thigh down on the table and the knees flexed (to less than 90 degrees) with the thigh in slight lateral rotation and the leg in slight lateral rotation with respect to the thigh. Press against the leg proximal to the ankle in the direction of knee extension. | |

Tibialis Anterior

| | | |
|---|---|---|
| Function | Dorsiflexion of the ankle joint and assistance in inversion of the foot. | 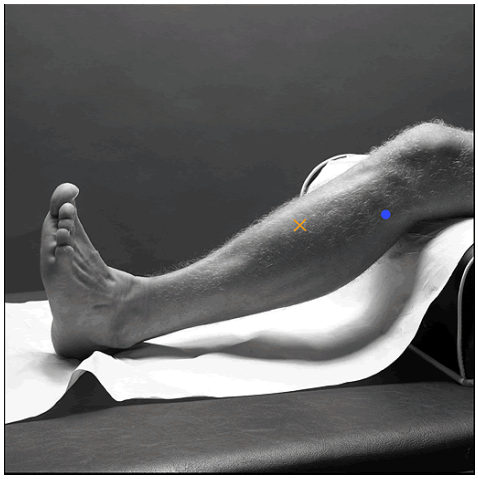 |
| Location | The electrodes need to be placed at 1/3 on the line between the tip of the fibula and the tip of the medial malleolus. | |
| Orientation of the electrodes | In the direction of the line between the tip of the fibula and the tip of the medial malleolus. | |
| Test | Supine or sitting. Support the leg just above the ankle joint with the ankle joint in dorsiflexion and the foot in inversion without extension of the great toe. Apply pressure against the medial side, dorsal surface of the foot in the direction of plantar flexion of the ankle joint and eversion of the foot. | |

# 10 Appendix C

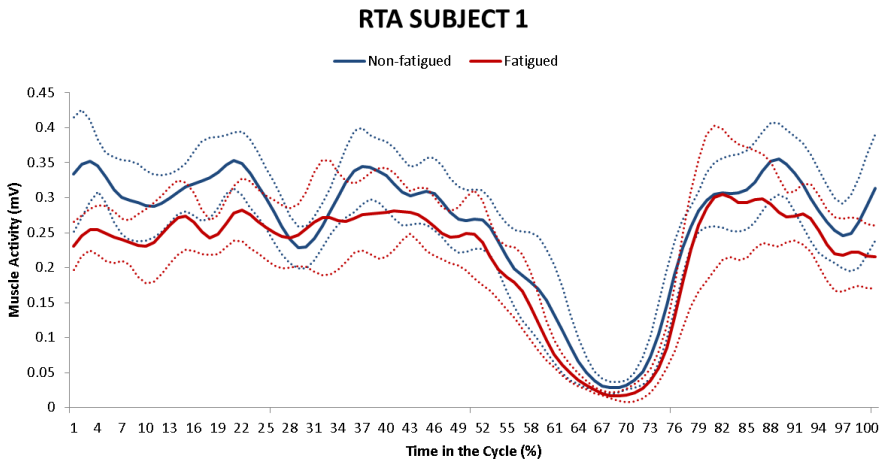
RTA SUBJECT 1
Non-fatigued
Fatigued
Muscle Activity (mV)
0.45
0.4
0.35
0.3
0.25
0.2
0.15
0.1
0.05
0
1 4 7 10 13 16 19 22 25 28 31 34 37 40 43 46 49 52 55 58 61 64 67 70 73 76 79 82 85 88 91 94 97 100
Time in the Cycle (%)

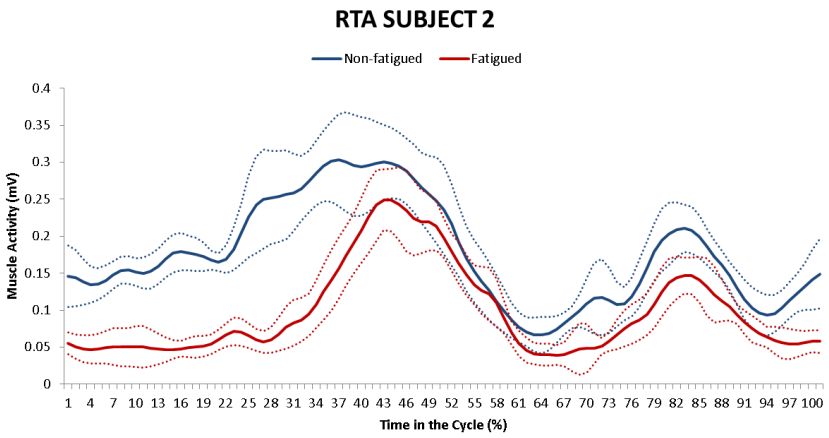
RTA SUBJECT 2
Non-fatigued
Fatigued
Muscle Activity (mV)
0.4
0.35
0.3
0.25
0.2
0.15
0.1
0.05
0
1 4 7 10 13 16 19 22 25 28 31 34 37 40 43 46 49 52 55 58 61 64 67 70 73 76 79 82 85 88 91 94 97 100
Time in the Cycle (%)

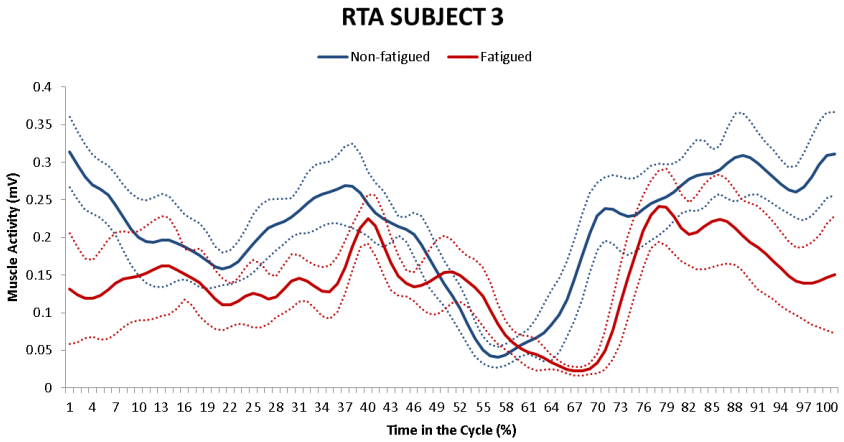
RTA SUBJECT 3
Non-fatigued
Fatigued
Muscle Activity (mV)
0.4
0.35
0.3
0.25
0.2
0.15
0.1
0.05
0
1 4 7 10 13 16 19 22 25 28 31 34 37 40 43 46 49 52 55 58 61 64 67 70 73 76 79 82 85 88 91 94 97 100
Time in the Cycle (%)

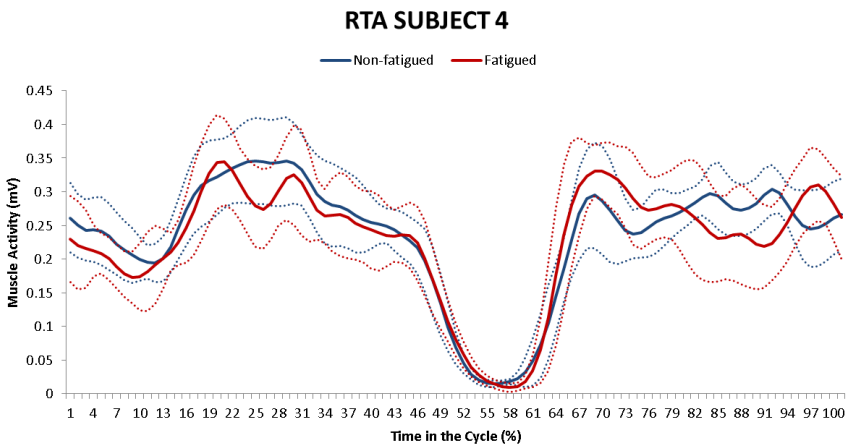
RTA SUBJECT 4
Non-fatigued
Fatigued
Muscle Activity (mV)
0.45
0.4
0.35
0.3
0.25
0.2
0.15
0.1
0.05
0
1 4 7 10 13 16 19 22 25 28 31 34 37 40 43 46 49 52 55 58 61 64 67 70 73 76 79 82 85 88 91 94 97 100
Time in the Cycle (%)

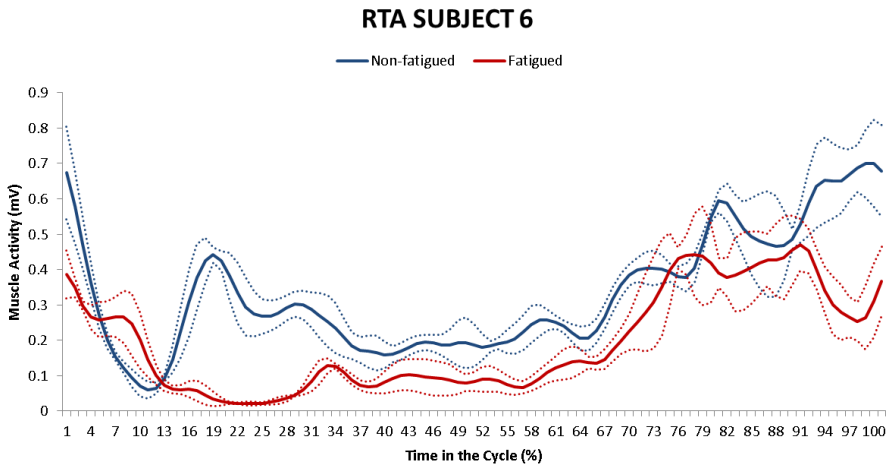
RTA SUBJECT 6
Non-fatigued
Fatigued
Muscle Activity (mV)
0.9
0.8
0.7
0.6
0.5
0.4
0.3
0.2
0.1
0
1 4 7 10 13 16 19 22 25 28 31 34 37 40 43 46 49 52 55 58 61 64 67 70 73 76 79 82 85 88 91 94 97 100
Time in the Cycle (%)

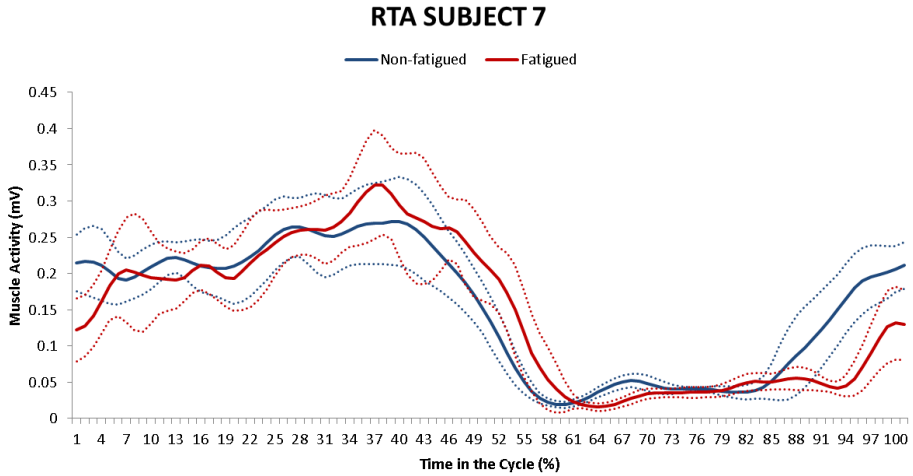
RTA SUBJECT 7
Non-fatigued
Fatigued
Muscle Activity (mV)
0.45
0.4
0.35
0.3
0.25
0.2
0.15
0.1
0.05
0
1 4 7 10 13 16 19 22 25 28 31 34 37 40 43 46 49 52 55 58 61 64 67 70 73 76 79 82 85 88 91 94 97 100
Time in the Cycle (%)

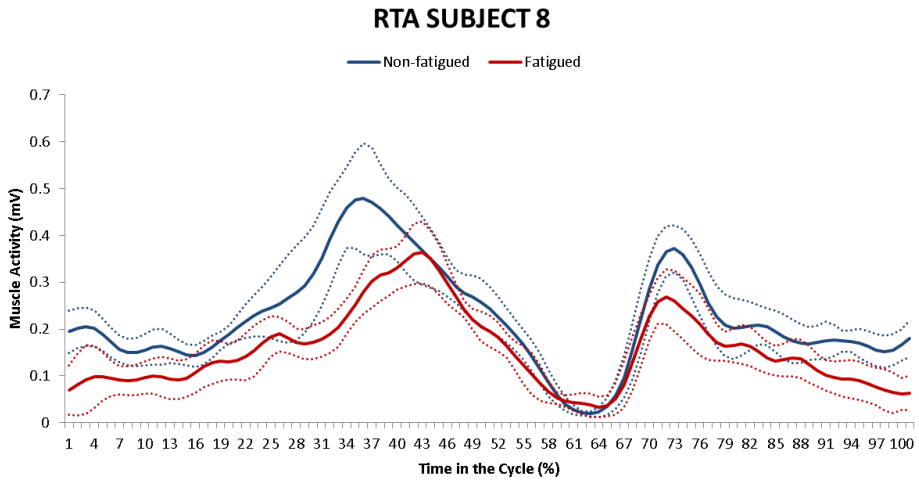
RTA SUBJECT 8
Non-fatigued
Fatigued
Muscle Activity (mV)
0.7
0.6
0.5
0.4
0.3
0.2
0.1
0
1 4 7 10 13 16 19 22 25 28 31 34 37 40 43 46 49 52 55 58 61 64 67 70 73 76 79 82 85 88 91 94 97 100
Time in the Cycle (%)

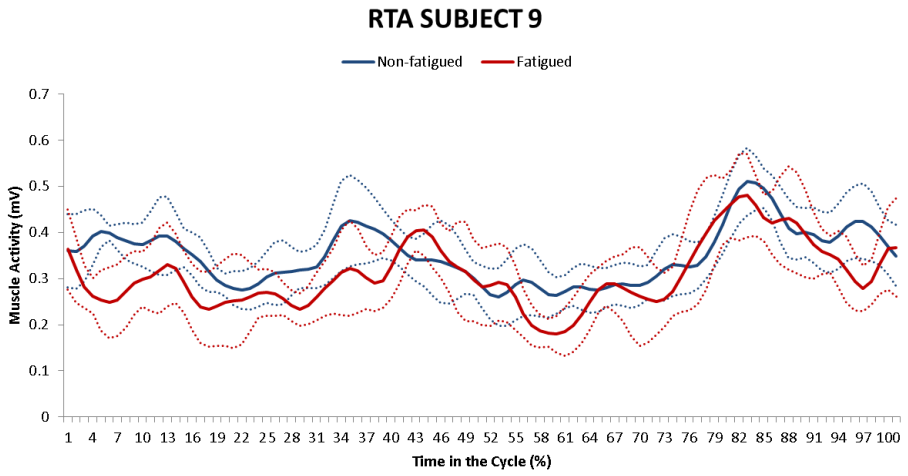
RTA SUBJECT 9
Non-fatigued
Fatigued
Muscle Activity (mV)
0.7
0.6
0.5
0.4
0.3
0.2
0.1
0
1 4 7 10 13 16 19 22 25 28 31 34 37 40 43 46 49 52 55 58 61 64 67 70 73 76 79 82 85 88 91 94 97 100
Time in the Cycle (%)

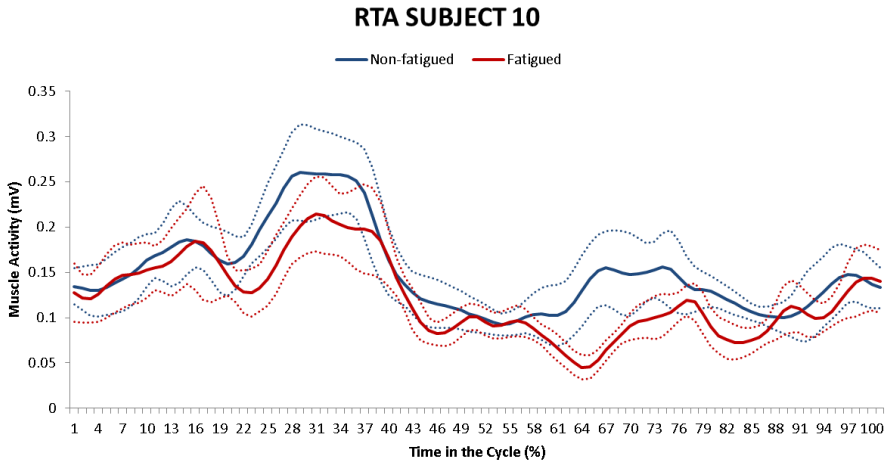
RTA SUBJECT 10
Non-fatigued
Fatigued
Muscle Activity (mV)
0.35
0.3
0.25
0.2
0.15
0.1
0.05
0
1 4 7 10 13 16 19 22 25 28 31 34 37 40 43 46 49 52 55 58 61 64 67 70 73 76 79 82 85 88 91 94 97 100
Time in the Cycle (%)

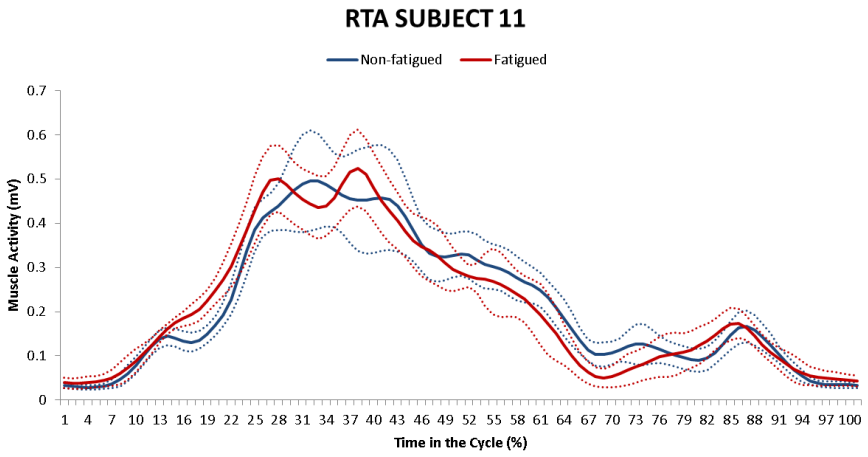
RTA SUBJECT 11
Non-fatigued
Fatigued
Muscle Activity (mV)
0.7
0.6
0.5
0.4
0.3
0.2
0.1
0
1 4 7 10 13 16 19 22 25 28 31 34 37 40 43 46 49 52 55 58 61 64 67 70 73 76 79 82 85 88 91 94 97 100
Time in the Cycle (%)

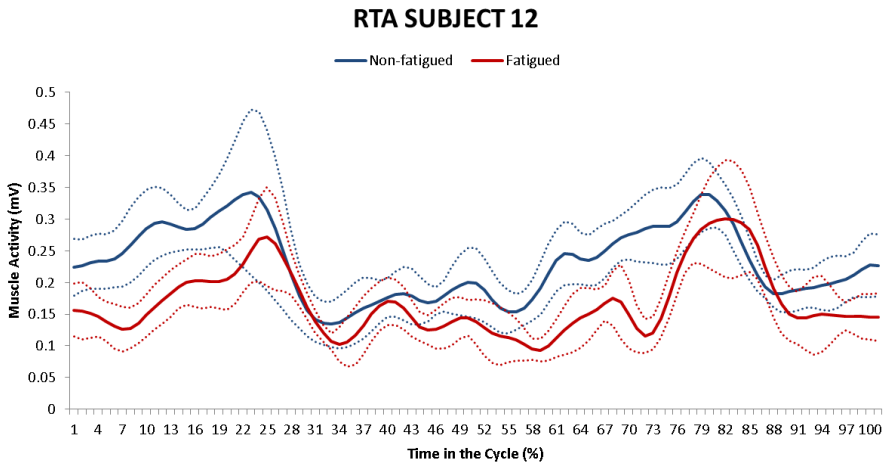
RTA SUBJECT 12
Non-fatigued
Fatigued
Muscle Activity (mV)
0.5
0.45
0.4
0.35
0.3
0.25
0.2
0.15
0.1
0.05
0
1 4 7 10 13 16 19 22 25 28 31 34 37 40 43 46 49 52 55 58 61 64 67 70 73 76 79 82 85 88 91 94 97 100
Time in the Cycle (%)

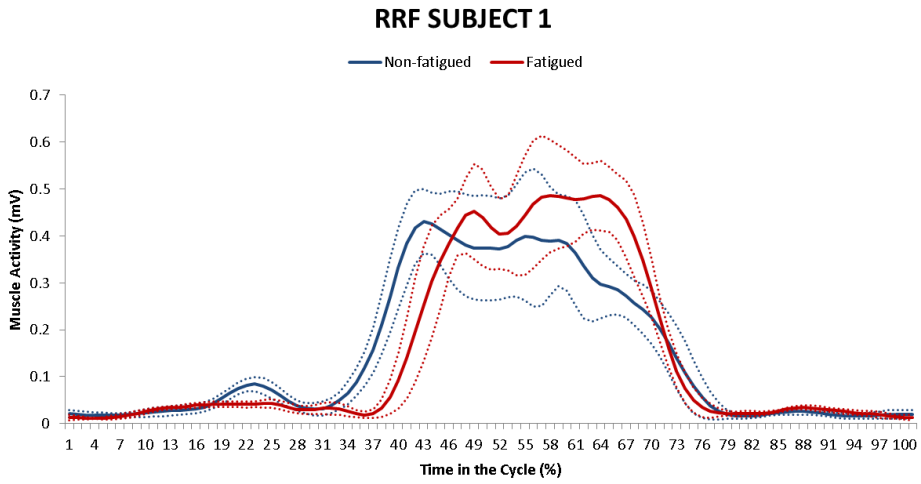
RRF SUBJECT 1
Non-fatigued
Fatigued
Muscle Activity (mV)
0.7
0.6
0.5
0.4
0.3
0.2
0.1
0
1 4 7 10 13 16 19 22 25 28 31 34 37 40 43 46 49 52 55 58 61 64 67 70 73 76 79 82 85 88 91 94 97 100
Time in the Cycle (%)

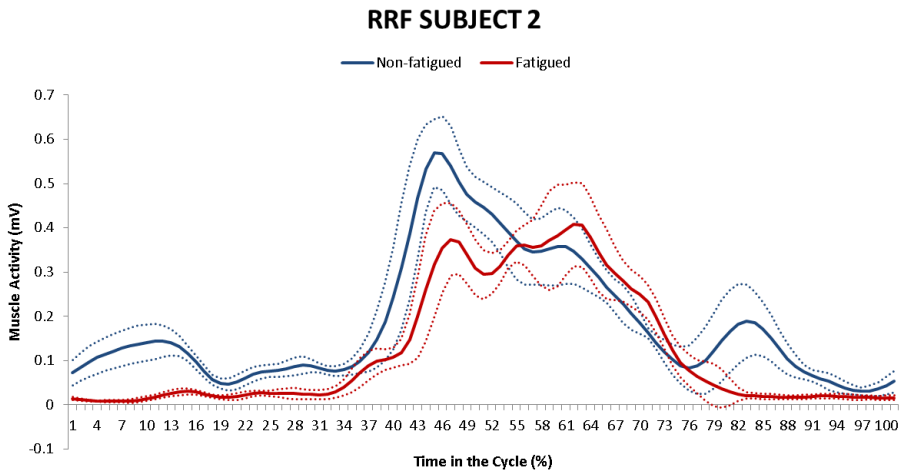
RRF SUBJECT 2
Non-fatigued
Fatigued
Muscle Activity (mV)
0.7
0.6
0.5
0.4
0.3
0.2
0.1
0
-0.1
1 4 7 10 13 16 19 22 25 28 31 34 37 40 43 46 49 52 55 58 61 64 67 70 73 76 79 82 85 88 91 94 97 100
Time in the Cycle (%)

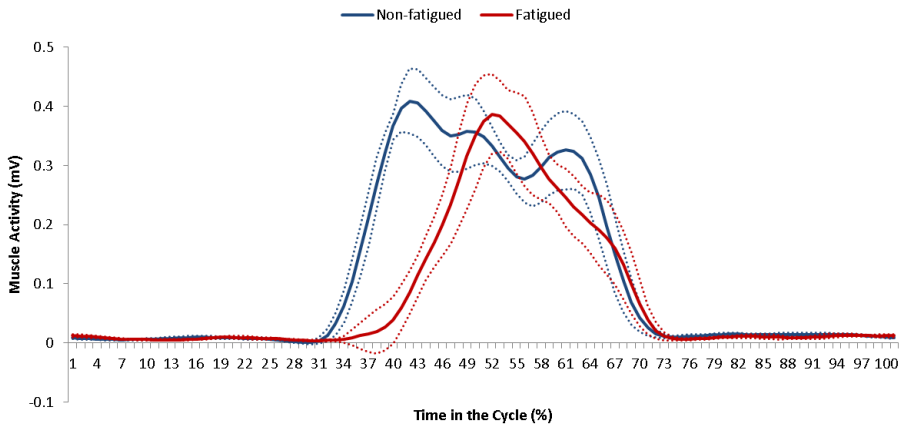
RRF SUBJECT 3
Non-fatigued
Fatigued
Muscle Activity (mV)
0.5
0.4
0.3
0.2
0.1
0
-0.1
1 4 7 10 13 16 19 22 25 28 31 34 37 40 43 46 49 52 55 58 61 64 67 70 73 76 79 82 85 88 91 94 97 100
Time in the Cycle (%)

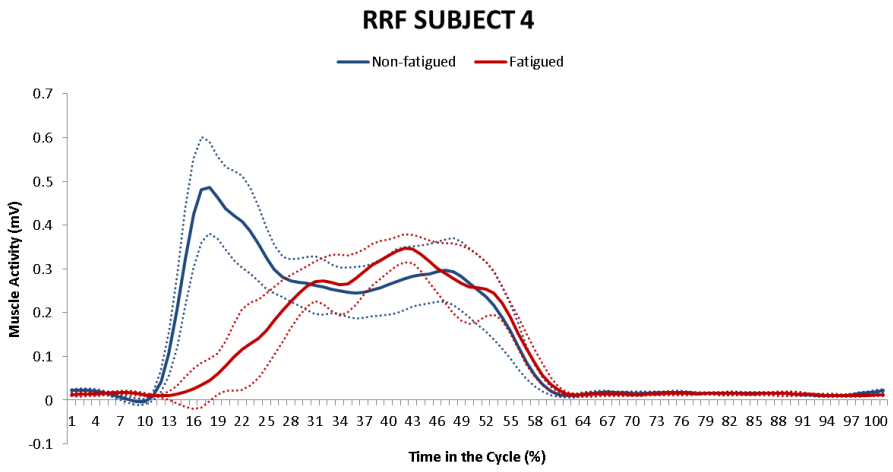
RRF SUBJECT 4
Non-fatigued
Fatigued
Muscle Activity (mV)
0.7
0.6
0.5
0.4
0.3
0.2
0.1
0
-0.1
1 4 7 10 13 16 19 22 25 28 31 34 37 40 43 46 49 52 55 58 61 64 67 70 73 76 79 82 85 88 91 94 97 100
Time in the Cycle (%)

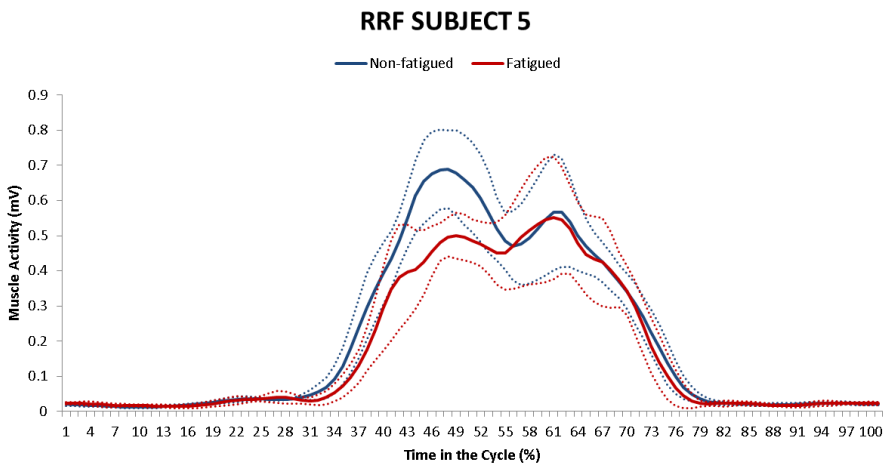
RRF SUBJECT 5
Non-fatigued
Fatigued
Muscle Activity (mV)
0.9
0.8
0.7
0.6
0.5
0.4
0.3
0.2
0.1
0
1 4 7 10 13 16 19 22 25 28 31 34 37 40 43 46 49 52 55 58 61 64 67 70 73 76 79 82 85 88 91 94 97 100
Time in the Cycle (%)

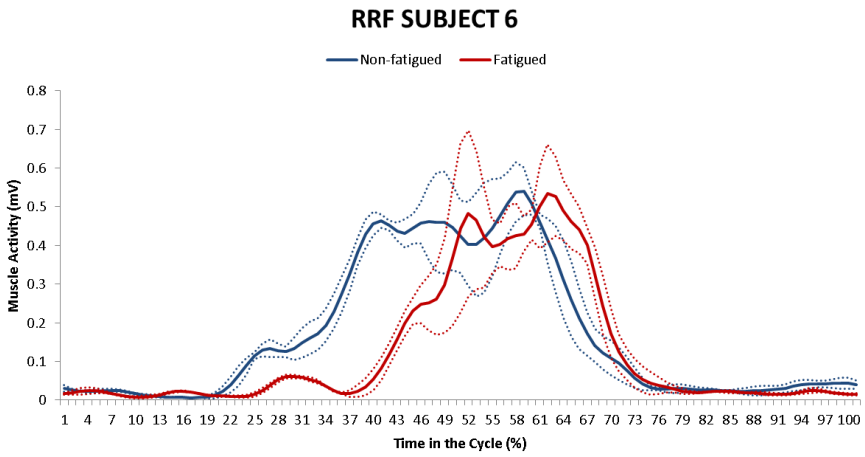
RRF SUBJECT 6
Non-fatigued
Fatigued
Muscle Activity (mV)
0.8
0.7
0.6
0.5
0.4
0.3
0.2
0.1
0
1 4 7 10 13 16 19 22 25 28 31 34 37 40 43 46 49 52 55 58 61 64 67 70 73 76 79 82 85 88 91 94 97 100
Time in the Cycle (%)

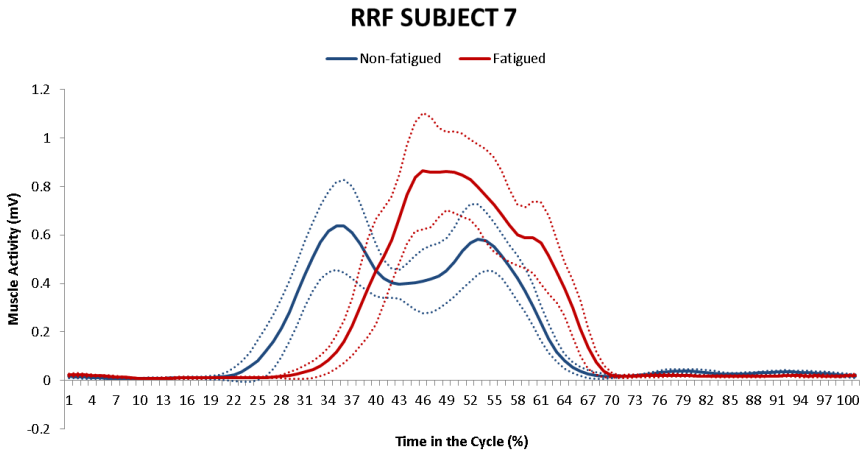
RRF SUBJECT 7
Non-fatigued
Fatigued
Muscle Activity (mV)
1.2
1
0.8
0.6
0.4
0.2
0
-0.2
1 4 7 10 13 16 19 22 25 28 31 34 37 40 43 46 49 52 55 58 61 64 67 70 73 76 79 82 85 88 91 94 97 100
Time in the Cycle (%)

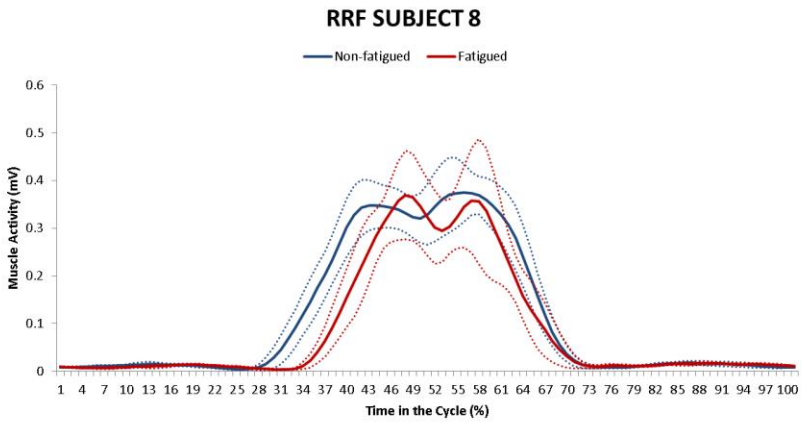
RRF SUBJECT 8
Non-fatigued
Fatigued
Muscle Activity (mV)
0.6
0.5
0.4
0.3
0.2
0.1
0
1 4 7 10 13 16 19 22 25 28 31 34 37 40 43 46 49 52 55 58 61 64 67 70 73 76 79 82 85 88 91 94 97 100
Time in the Cycle (%)

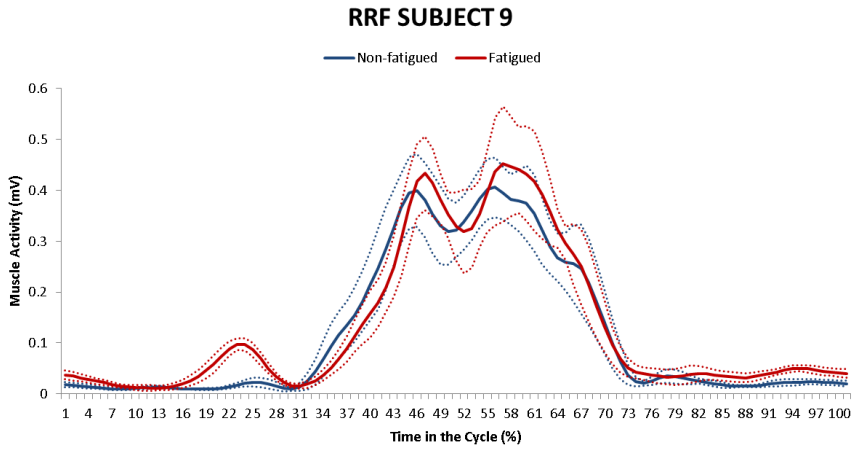
RRF SUBJECT 9
Non-fatigued
Fatigued
Muscle Activity (mV)
0.6
0.5
0.4
0.3
0.2
0.1
0
1 4 7 10 13 16 19 22 25 28 31 34 37 40 43 46 49 52 55 58 61 64 67 70 73 76 79 82 85 88 91 94 97 100
Time in the Cycle (%)

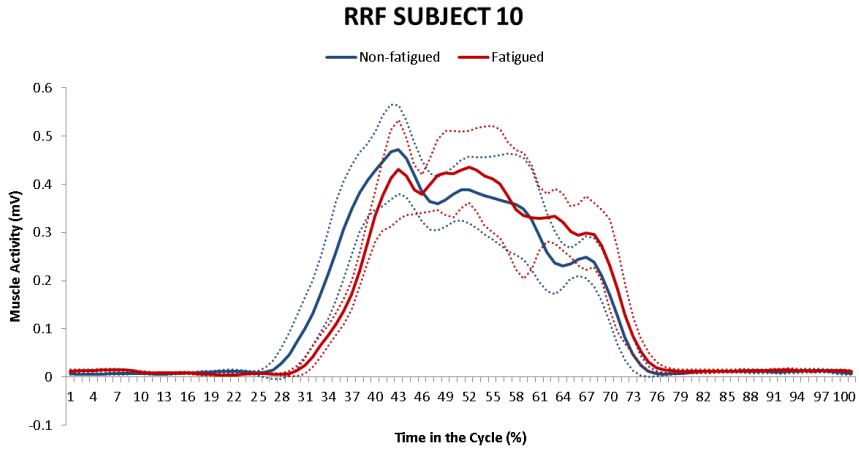
RRF SUBJECT 10
Non-fatigued
Fatigued
Muscle Activity (mV)
0.6
0.5
0.4
0.3
0.2
0.1
0
-0.1
1 4 7 10 13 16 19 22 25 28 31 34 37 40 43 46 49 52 55 58 61 64 67 70 73 76 79 82 85 88 91 94 97 100
Time in the Cycle (%)

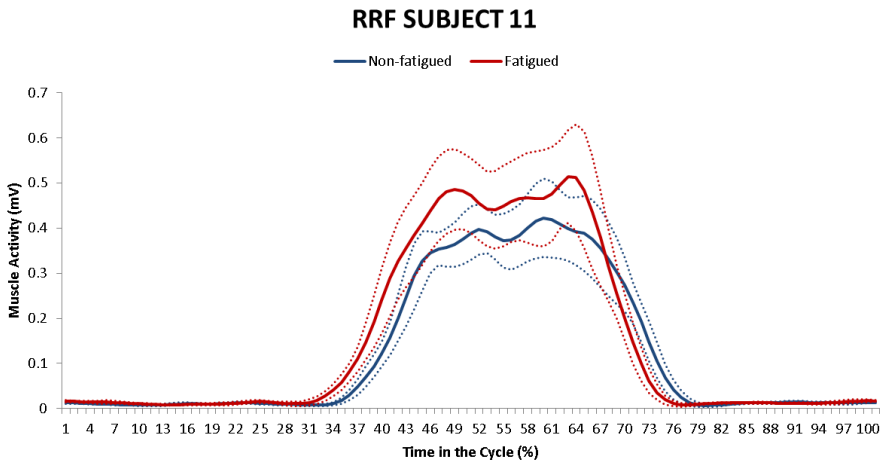
RRF SUBJECT 11
Non-fatigued
Fatigued
Muscle Activity (mV)
0.7
0.6
0.5
0.4
0.3
0.2
0.1
0
1 4 7 10 13 16 19 22 25 28 31 34 37 40 43 46 49 52 55 58 61 64 67 70 73 76 79 82 85 88 91 94 97 100
Time in the Cycle (%)

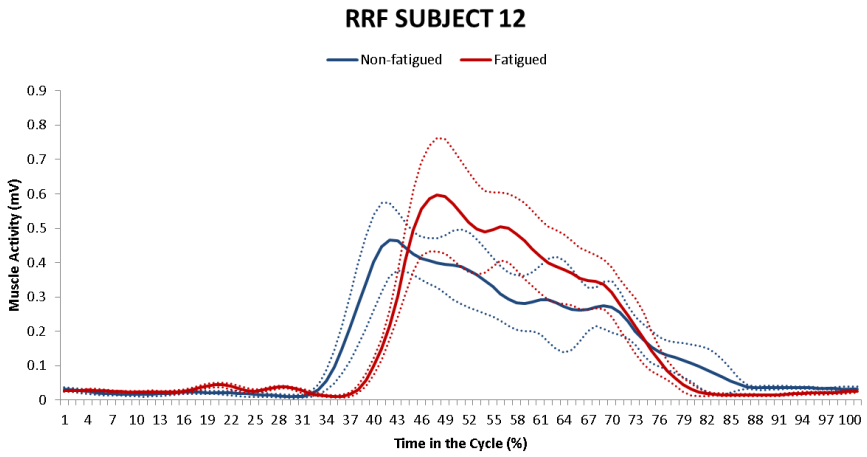
RRF SUBJECT 12
Non-fatigued
Fatigued
Muscle Activity (mV)
0.9
0.8
0.7
0.6
0.5
0.4
0.3
0.2
0.1
0
1 4 7 10 13 16 19 22 25 28 31 34 37 40 43 46 49 52 55 58 61 64 67 70 73 76 79 82 85 88 91 94 97 100
Time in the Cycle (%)

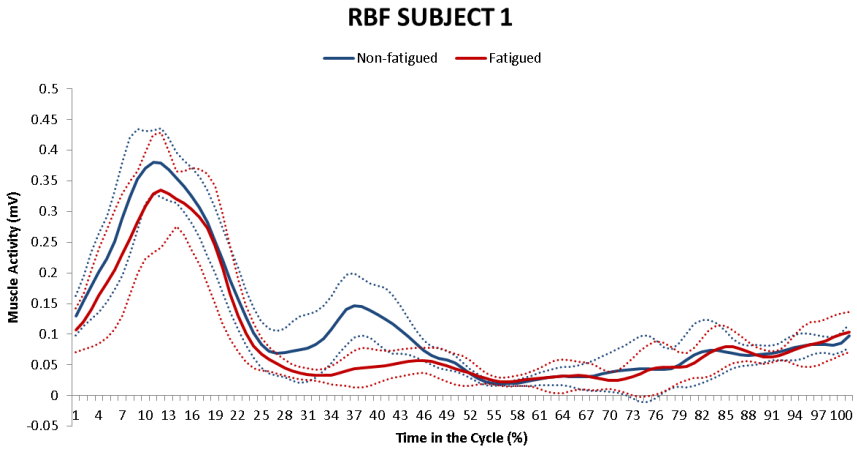
RBF SUBJECT 1
Non-fatigued
Fatigued
Muscle Activity (mV)
0.5
0.45
0.4
0.35
0.3
0.25
0.2
0.15
0.1
0.05
0
-0.05
1 4 7 10 13 16 19 22 25 28 31 34 37 40 43 46 49 52 55 58 61 64 67 70 73 76 79 82 85 88 91 94 97 100
Time in the Cycle (%)

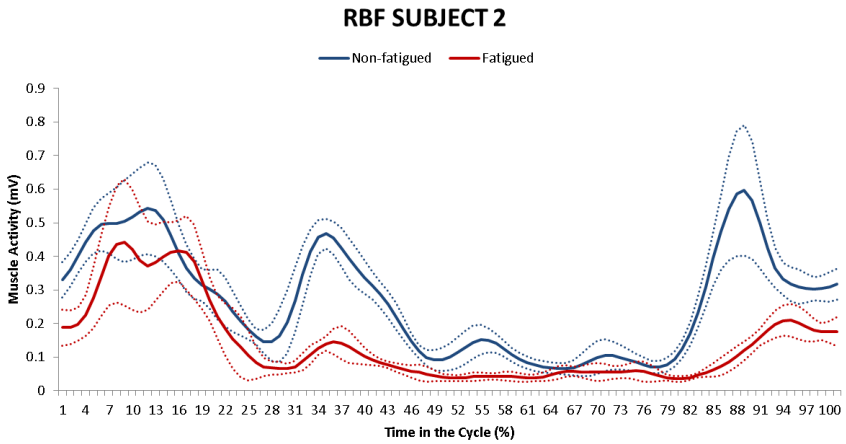
RBF SUBJECT 2
Non-fatigued
Fatigued
Muscle Activity (mV)
0.9
0.8
0.7
0.6
0.5
0.4
0.3
0.2
0.1
0
1 4 7 10 13 16 19 22 25 28 31 34 37 40 43 46 49 52 55 58 61 64 67 70 73 76 79 82 85 88 91 94 97 100
Time in the Cycle (%)

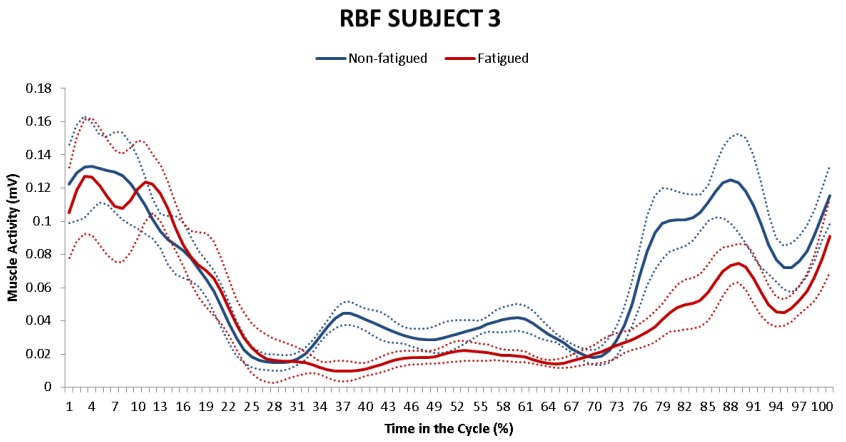
RBF SUBJECT 3
Non-fatigued
Fatigued
Muscle Activity (mV)
0.18
0.16
0.14
0.12
0.1
0.08
0.06
0.04
0.02
0
1 4 7 10 13 16 19 22 25 28 31 34 37 40 43 46 49 52 55 58 61 64 67 70 73 76 79 82 85 88 91 94 97 100
Time in the Cycle (%)

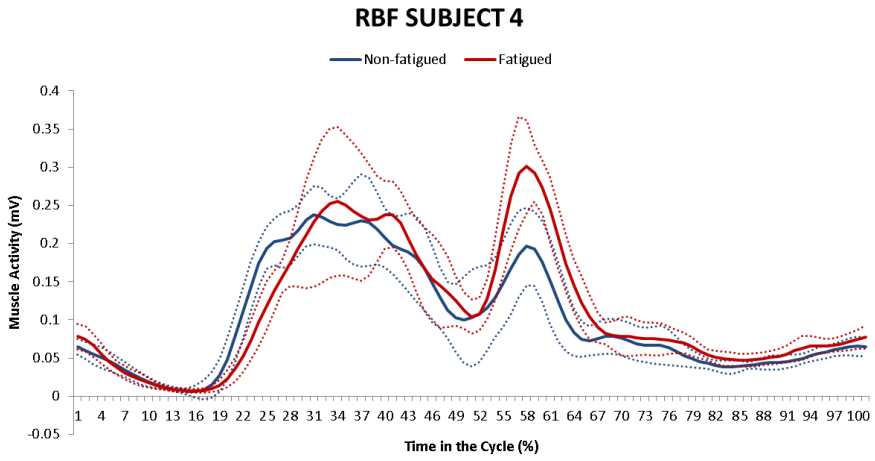
RBF SUBJECT 4
Non-fatigued
Fatigued
Muscle Activity (mV)
0.4
0.35
0.3
0.25
0.2
0.15
0.1
0.05
0
-0.05
1 4 7 10 13 16 19 22 25 28 31 34 37 40 43 46 49 52 55 58 61 64 67 70 73 76 79 82 85 88 91 94 97 100
Time in the Cycle (%)

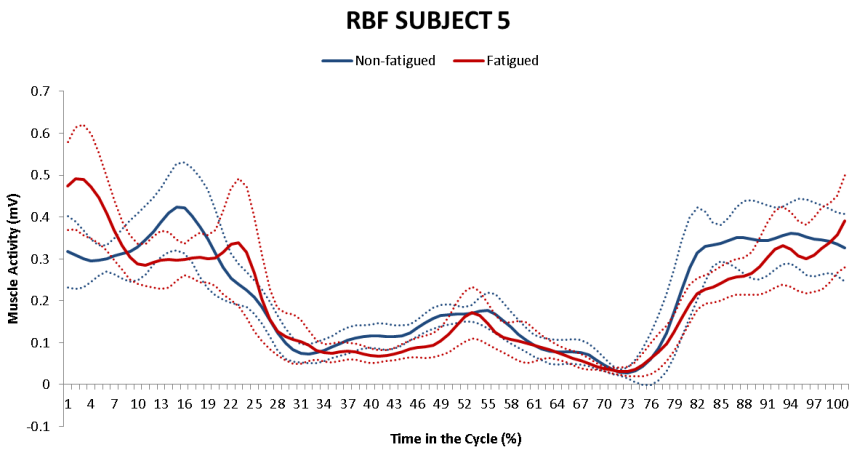
RBF SUBJECT 5
Non-fatigued
Fatigued
Muscle Activity (mV)
0.7
0.6
0.5
0.4
0.3
0.2
0.1
0
-0.1
1 4 7 10 13 16 19 22 25 28 31 34 37 40 43 46 49 52 55 58 61 64 67 70 73 76 79 82 85 88 91 94 97 100
Time in the Cycle (%)

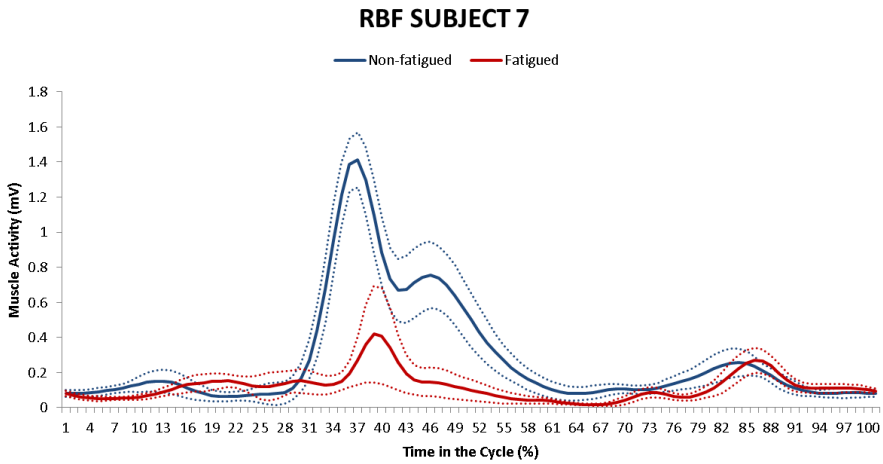
RBF SUBJECT 7
Non-fatigued
Fatigued
Muscle Activity (mV)
1.8
1.6
1.4
1.2
1
0.8
0.6
0.4
0.2
0
1 4 7 10 13 16 19 22 25 28 31 34 37 40 43 46 49 52 55 58 61 64 67 70 73 76 79 82 85 88 91 94 97 100
Time in the Cycle (%)

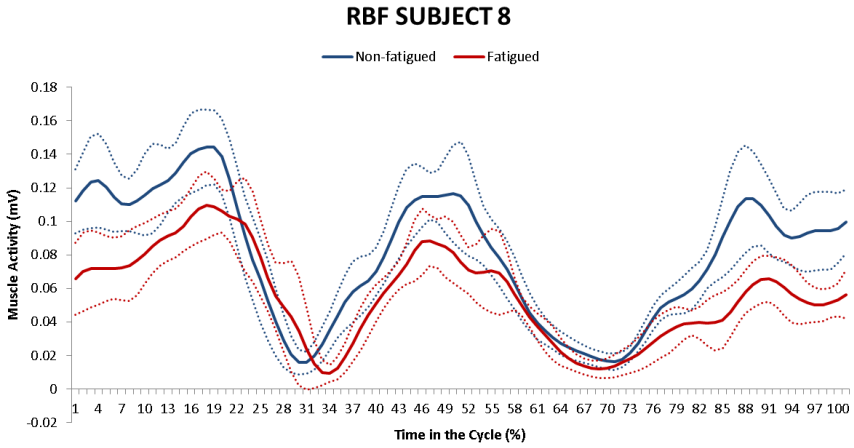
RBF SUBJECT 8
Non-fatigued
Fatigued
Muscle Activity (mV)
0.18
0.16
0.14
0.12
0.1
0.08
0.06
0.04
0.02
0
-0.02
1 4 7 10 13 16 19 22 25 28 31 34 37 40 43 46 49 52 55 58 61 64 67 70 73 76 79 82 85 88 91 94 97 100
Time in the Cycle (%)

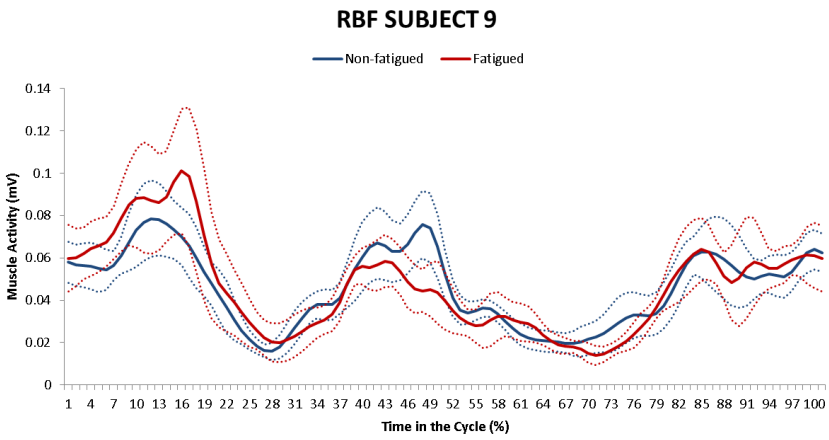
RBF SUBJECT 9
Non-fatigued
Fatigued
Muscle Activity (mV)
0.14
0.12
0.1
0.08
0.06
0.04
0.02
0
1 4 7 10 13 16 19 22 25 28 31 34 37 40 43 46 49 52 55 58 61 64 67 70 73 76 79 82 85 88 91 94 97 100
Time in the Cycle (%)

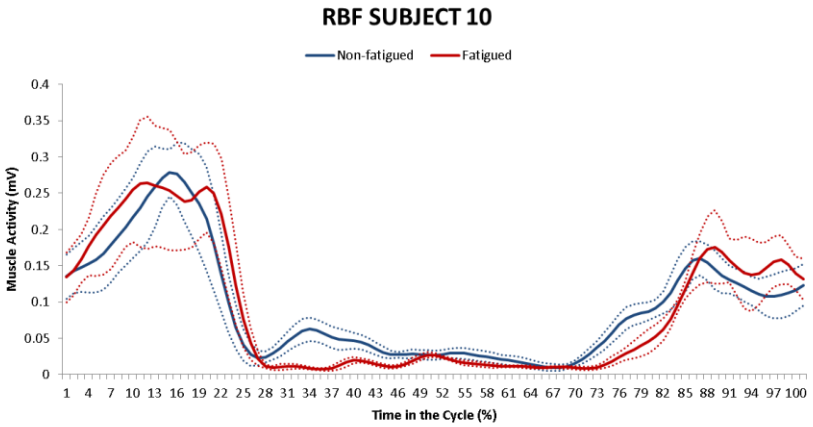
RBF SUBJECT 10
Non-fatigued
Fatigued
Muscle Activity (mV)
0.4
0.35
0.3
0.25
0.2
0.15
0.1
0.05
0
1 4 7 10 13 16 19 22 25 28 31 34 37 40 43 46 49 52 55 58 61 64 67 70 73 76 79 82 85 88 91 94 97 100
Time in the Cycle (%)

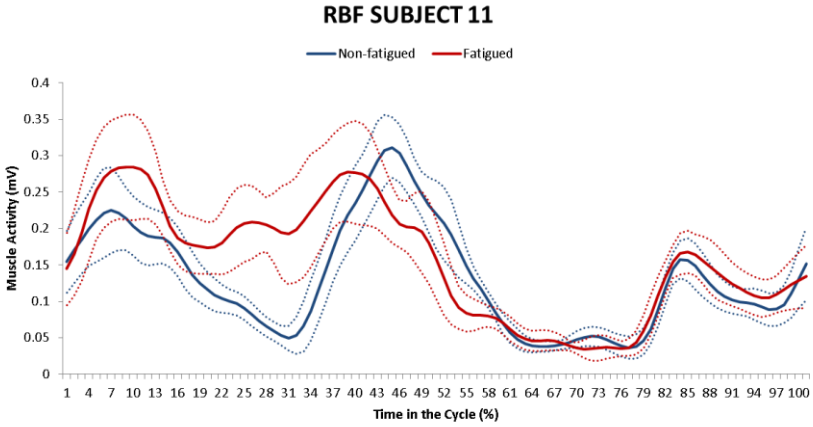
RBF SUBJECT 11
Non-fatigued
Fatigued
Muscle Activity (mV)
0.4
0.35
0.3
0.25
0.2
0.15
0.1
0.05
0
1 4 7 10 13 16 19 22 25 28 31 34 37 40 43 46 49 52 55 58 61 64 67 70 73 76 79 82 85 88 91 94 97 100
Time in the Cycle (%)

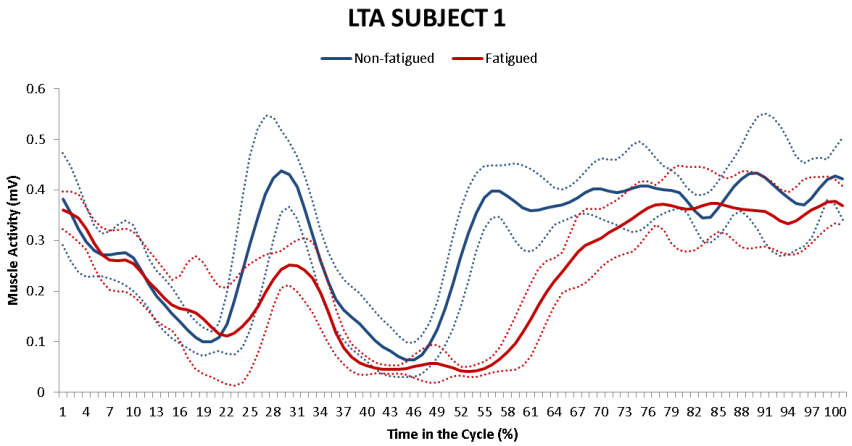
LTA SUBJECT 1
Non-fatigued
Fatigued
Muscle Activity (mV)
0.6
0.5
0.4
0.3
0.2
0.1
0
1 4 7 10 13 16 19 22 25 28 31 34 37 40 43 46 49 52 55 58 61 64 67 70 73 76 79 82 85 88 91 94 97 100
Time in the Cycle (%)

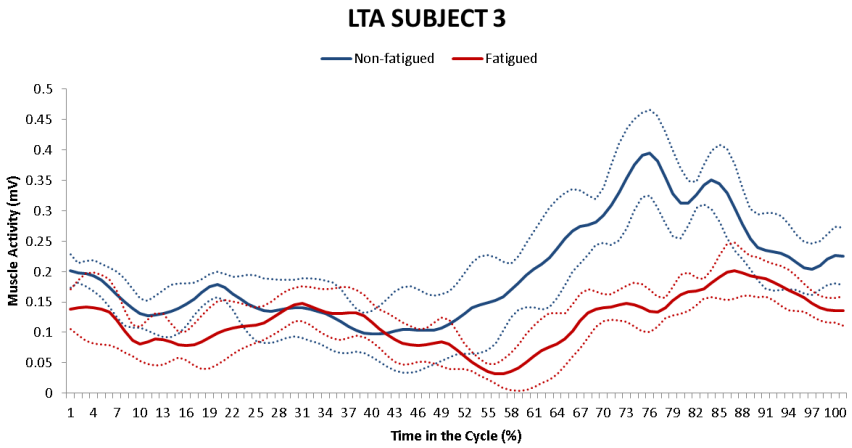
LTA SUBJECT 3
Non-fatigued
Fatigued
Muscle Activity (mV)
0.5
0.45
0.4
0.35
0.3
0.25
0.2
0.15
0.1
0.05
0
1 4 7 10 13 16 19 22 25 28 31 34 37 40 43 46 49 52 55 58 61 64 67 70 73 76 79 82 85 88 91 94 97 100
Time in the Cycle (%)

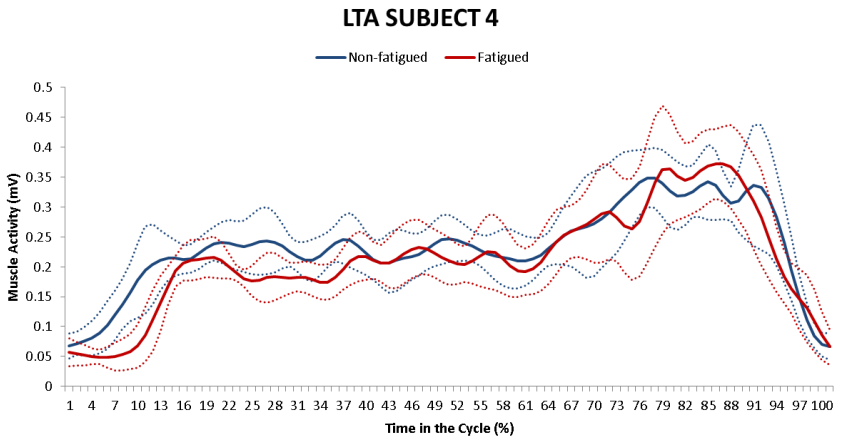
LTA SUBJECT 4
Non-fatigued
Fatigued
Muscle Activity (mV)
0.5
0.45
0.4
0.35
0.3
0.25
0.2
0.15
0.1
0.05
0
1 4 7 10 13 16 19 22 25 28 31 34 37 40 43 46 49 52 55 58 61 64 67 70 73 76 79 82 85 88 91 94 97 100
Time in the Cycle (%)

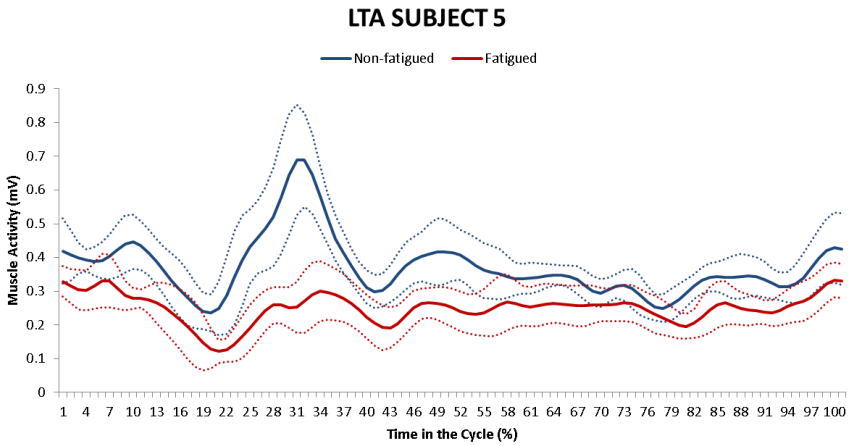
LTA SUBJECT 5
Non-fatigued
Fatigued
Muscle Activity (mV)
0 0.1 0.2 0.3 0.4 0.5 0.6 0.7 0.8 0.9
1 4 7 10 13 16 19 22 25 28 31 34 37 40 43 46 49 52 55 58 61 64 67 70 73 76 79 82 85 88 91 94 97 100
Time in the Cycle (%)

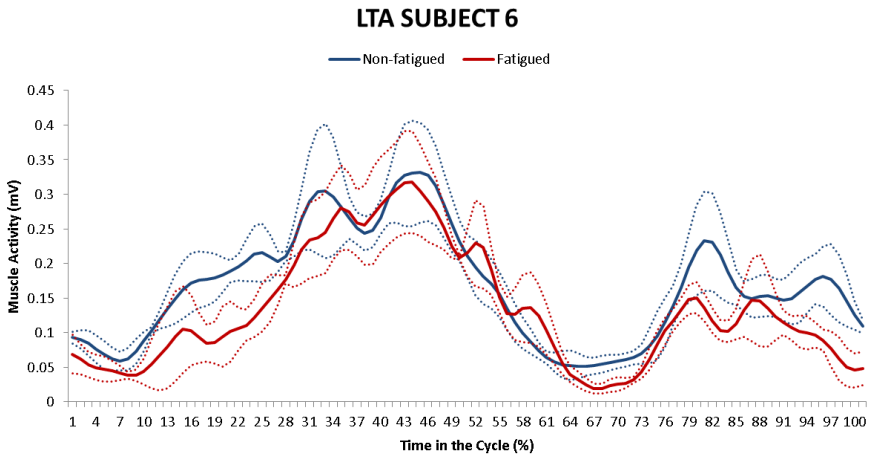
LTA SUBJECT 6
Non-fatigued
Fatigued
Muscle Activity (mV)
0 0.05 0.1 0.15 0.2 0.25 0.3 0.35 0.4 0.45
1 4 7 10 13 16 19 22 25 28 31 34 37 40 43 46 49 52 55 58 61 64 67 70 73 76 79 82 85 88 91 94 97 100
Time in the Cycle (%)

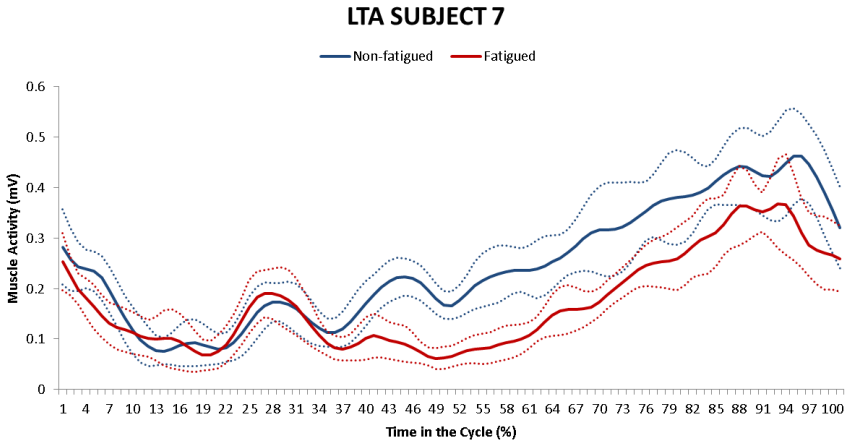
LTA SUBJECT 7
Non-fatigued
Fatigued
Muscle Activity (mV)
0 0.1 0.2 0.3 0.4 0.5 0.6
1 4 7 10 13 16 19 22 25 28 31 34 37 40 43 46 49 52 55 58 61 64 67 70 73 76 79 82 85 88 91 94 97 100
Time in the Cycle (%)

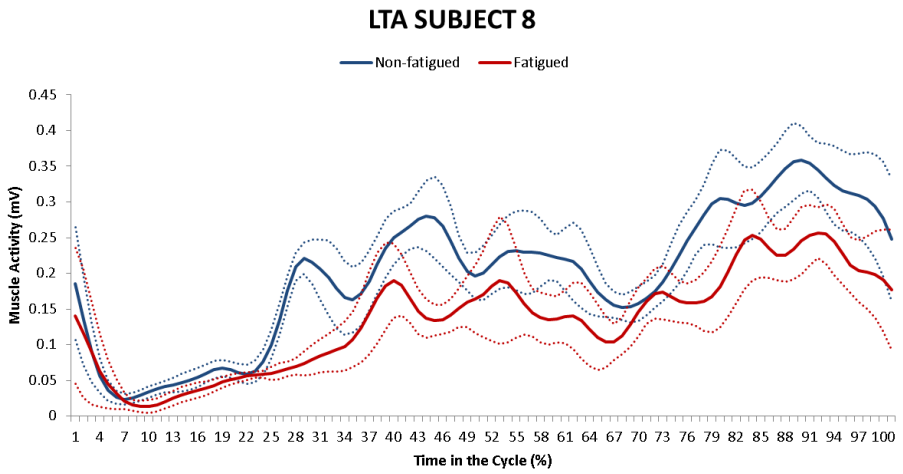
LTA SUBJECT 8
Non-fatigued
Fatigued
Muscle Activity (mV)
0.45
0.4
0.35
0.3
0.25
0.2
0.15
0.1
0.05
0
1 4 7 10 13 16 19 22 25 28 31 34 37 40 43 46 49 52 55 58 61 64 67 70 73 76 79 82 85 88 91 94 97 100
Time in the Cycle (%)

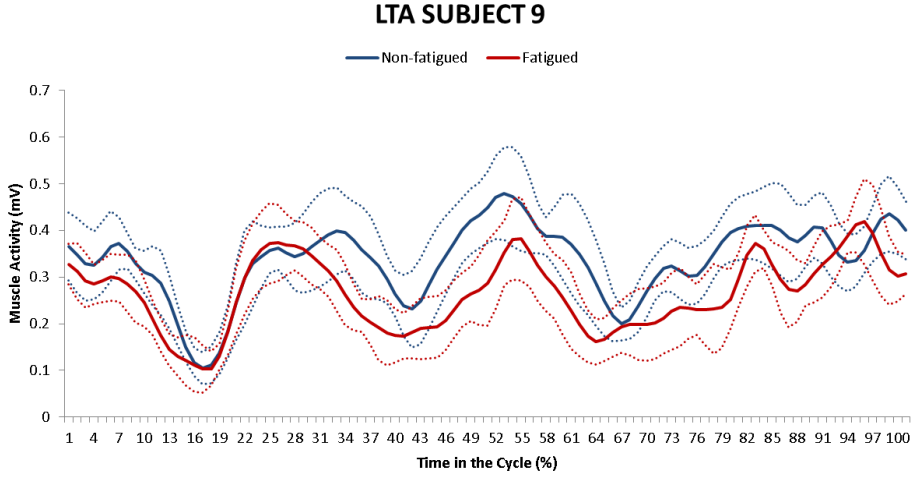
LTA SUBJECT 9
Non-fatigued
Fatigued
Muscle Activity (mV)
0.7
0.6
0.5
0.4
0.3
0.2
0.1
0
1 4 7 10 13 16 19 22 25 28 31 34 37 40 43 46 49 52 55 58 61 64 67 70 73 76 79 82 85 88 91 94 97 100
Time in the Cycle (%)

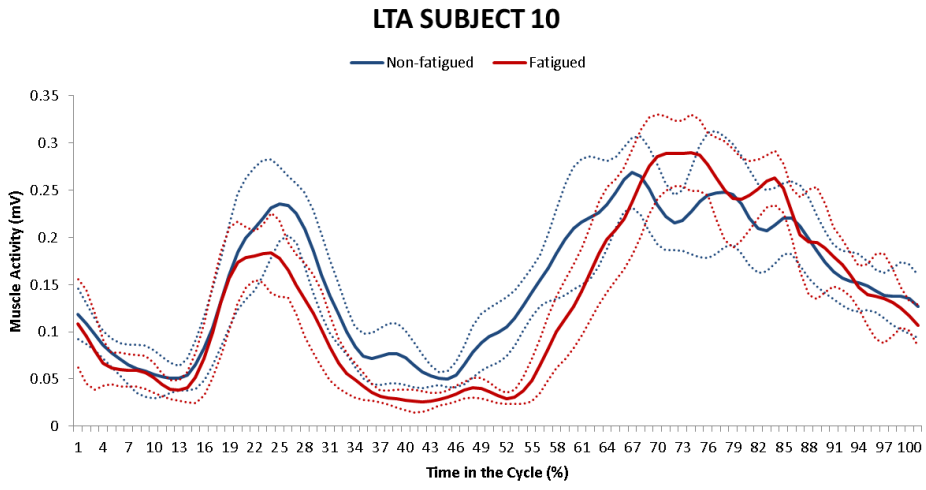
LTA SUBJECT 10
Non-fatigued
Fatigued
Muscle Activity (mV)
0.35
0.3
0.25
0.2
0.15
0.1
0.05
0
1 4 7 10 13 16 19 22 25 28 31 34 37 40 43 46 49 52 55 58 61 64 67 70 73 76 79 82 85 88 91 94 97 100
Time in the Cycle (%)

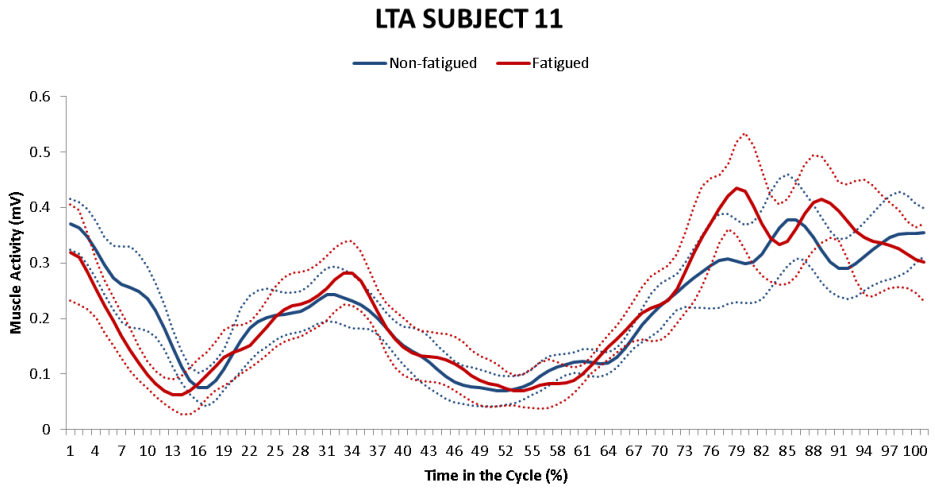
LTA SUBJECT 11
Non-fatigued
Fatigued
Muscle Activity (mV)
0.6
0.5
0.4
0.3
0.2
0.1
0
1 4 7 10 13 16 19 22 25 28 31 34 37 40 43 46 49 52 55 58 61 64 67 70 73 76 79 82 85 88 91 94 97 100
Time in the Cycle (%)

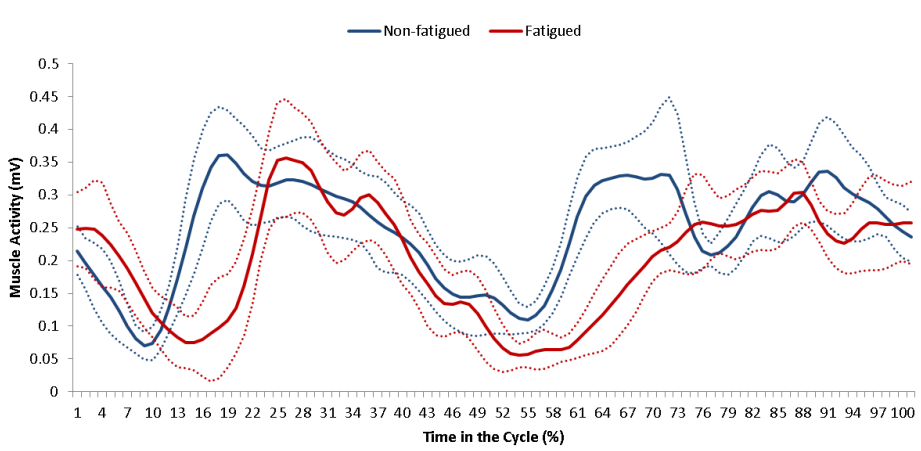
LTA SUBJECT 12
Non-fatigued
Fatigued
Muscle Activity (mV)
0.5
0.45
0.4
0.35
0.3
0.25
0.2
0.15
0.1
0.05
0
1 4 7 10 13 16 19 22 25 28 31 34 37 40 43 46 49 52 55 58 61 64 67 70 73 76 79 82 85 88 91 94 97 100
Time in the Cycle (%)

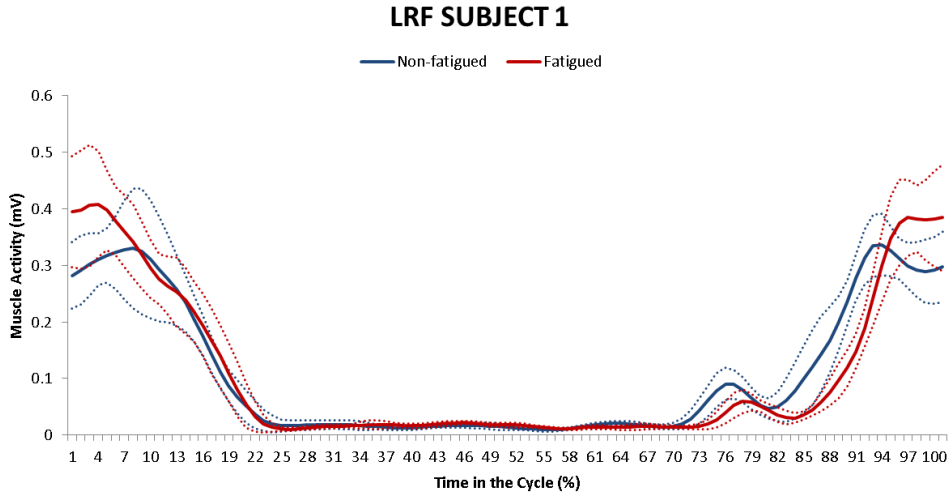
LRF SUBJECT 1
Non-fatigued
Fatigued
Muscle Activity (mV)
0.6
0.5
0.4
0.3
0.2
0.1
0
1 4 7 10 13 16 19 22 25 28 31 34 37 40 43 46 49 52 55 58 61 64 67 70 73 76 79 82 85 88 91 94 97 100
Time in the Cycle (%)

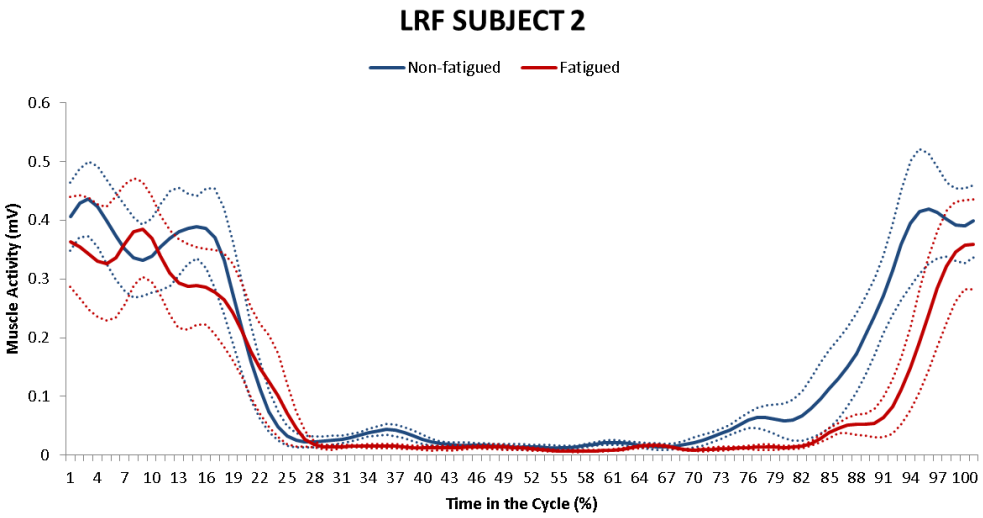
LRF SUBJECT 2
Non-fatigued
Fatigued
Muscle Activity (mV)
0.6
0.5
0.4
0.3
0.2
0.1
0
1 4 7 10 13 16 19 22 25 28 31 34 37 40 43 46 49 52 55 58 61 64 67 70 73 76 79 82 85 88 91 94 97 100
Time in the Cycle (%)

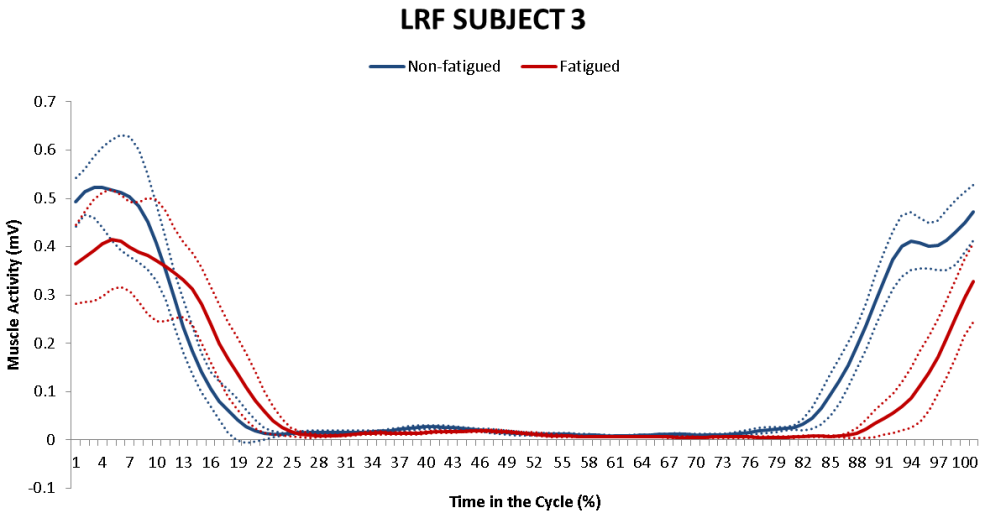
LRF SUBJECT 3
Non-fatigued
Fatigued
Muscle Activity (mV)
0.7
0.6
0.5
0.4
0.3
0.2
0.1
0
-0.1
1 4 7 10 13 16 19 22 25 28 31 34 37 40 43 46 49 52 55 58 61 64 67 70 73 76 79 82 85 88 91 94 97 100
Time in the Cycle (%)

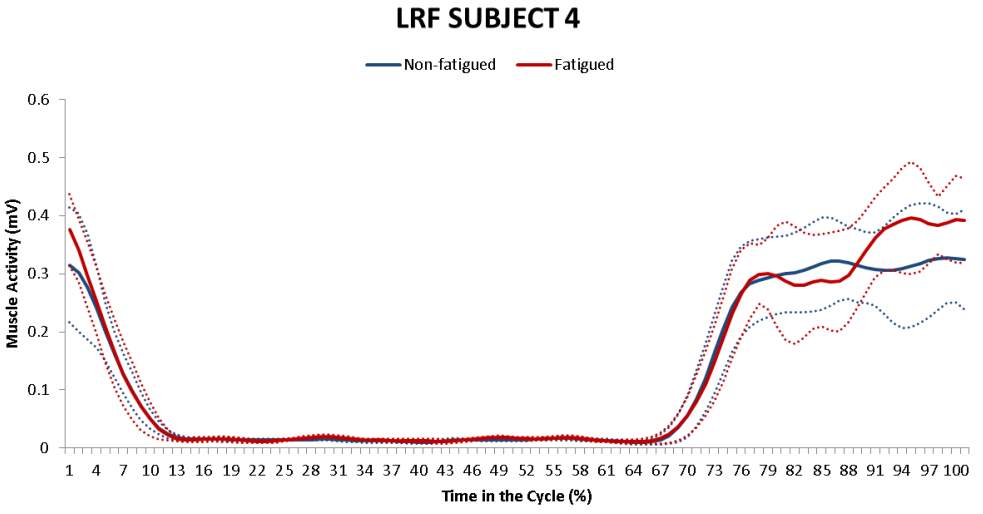
LRF SUBJECT 4
Non-fatigued
Fatigued
Muscle Activity (mV)
0.6
0.5
0.4
0.3
0.2
0.1
0
1 4 7 10 13 16 19 22 25 28 31 34 37 40 43 46 49 52 55 58 61 64 67 70 73 76 79 82 85 88 91 94 97 100
Time in the Cycle (%)

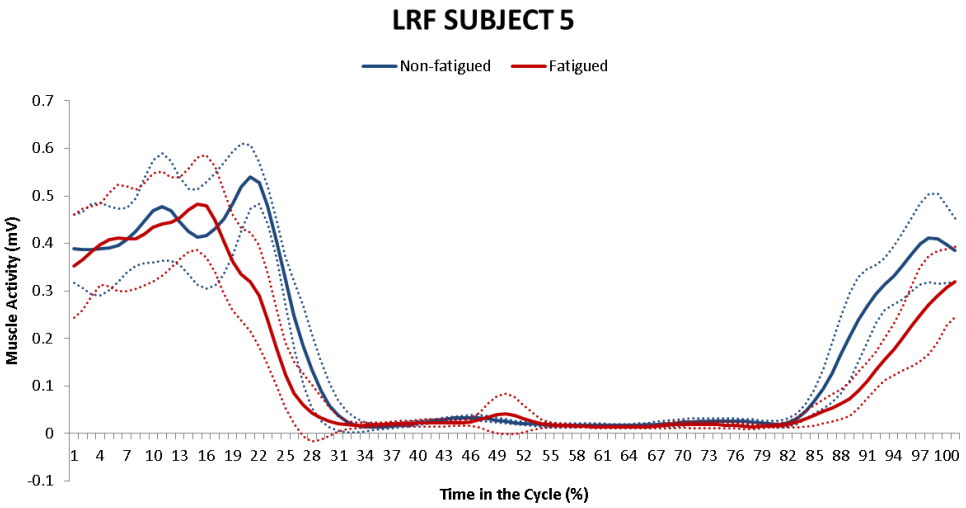
LRF SUBJECT 5
Non-fatigued
Fatigued
Muscle Activity (mV)
0.7
0.6
0.5
0.4
0.3
0.2
0.1
0
-0.1
1 4 7 10 13 16 19 22 25 28 31 34 37 40 43 46 49 52 55 58 61 64 67 70 73 76 79 82 85 88 91 94 97 100
Time in the Cycle (%)

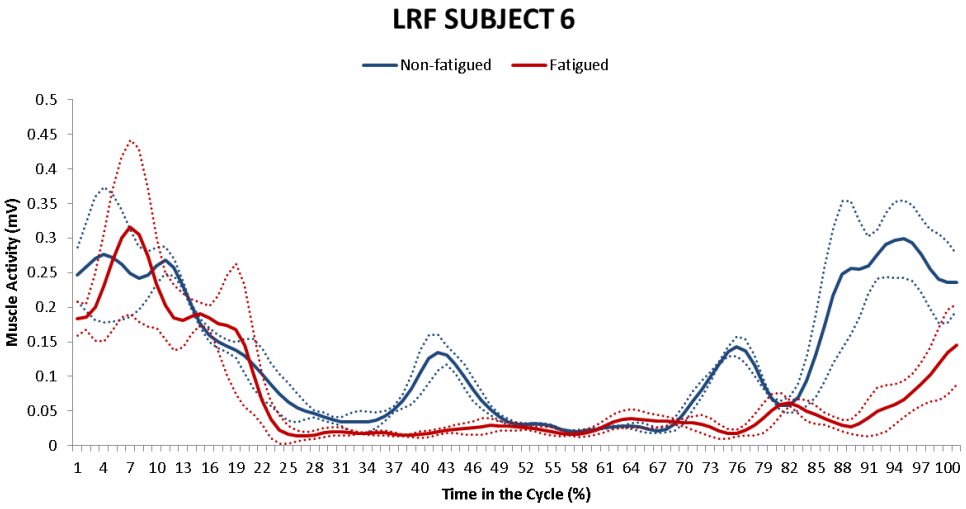
LRF SUBJECT 6
Non-fatigued
Fatigued
Muscle Activity (mV)
0.5
0.45
0.4
0.35
0.3
0.25
0.2
0.15
0.1
0.05
0
1 4 7 10 13 16 19 22 25 28 31 34 37 40 43 46 49 52 55 58 61 64 67 70 73 76 79 82 85 88 91 94 97 100
Time in the Cycle (%)

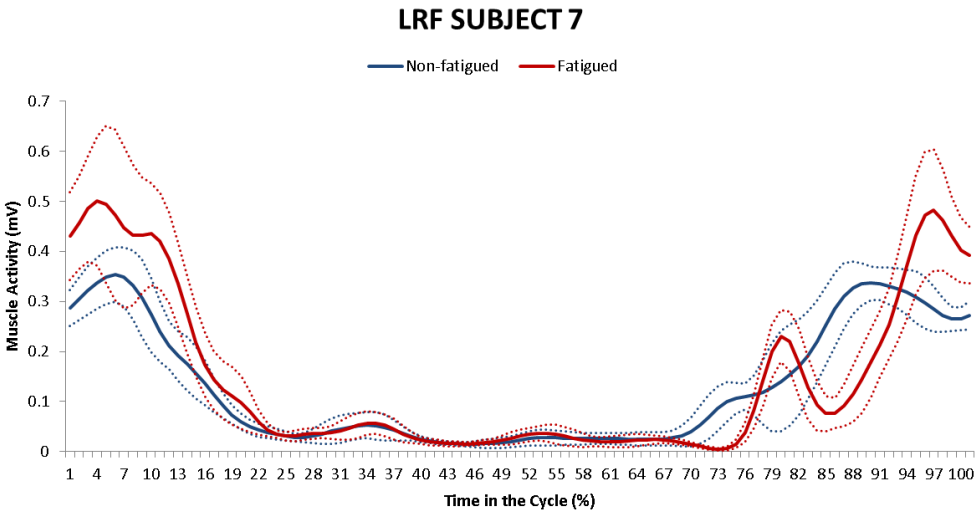
LRF SUBJECT 7
Non-fatigued
Fatigued
Muscle Activity (mV)
0.7
0.6
0.5
0.4
0.3
0.2
0.1
0
1 4 7 10 13 16 19 22 25 28 31 34 37 40 43 46 49 52 55 58 61 64 67 70 73 76 79 82 85 88 91 94 97 100
Time in the Cycle (%)

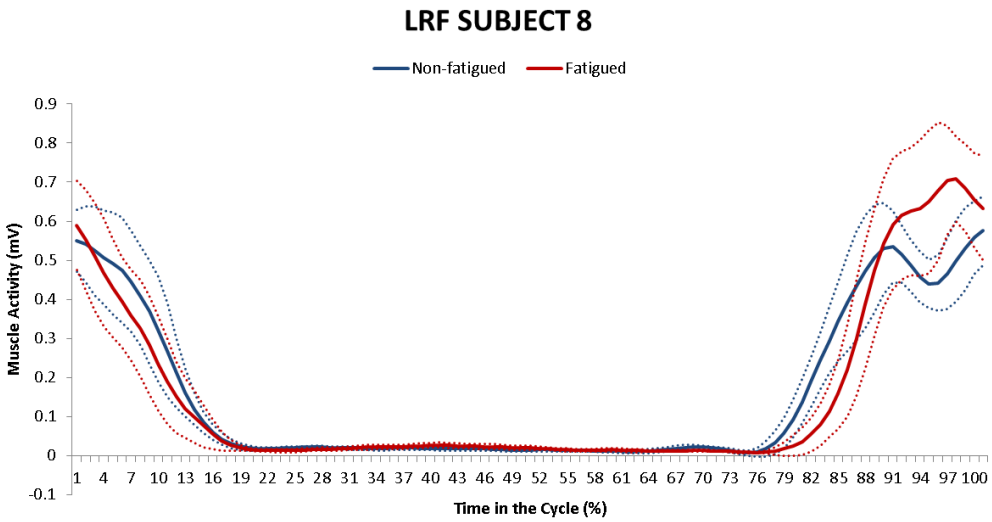
LRF SUBJECT 8
Non-fatigued
Fatigued
Muscle Activity (mV)
0.9
0.8
0.7
0.6
0.5
0.4
0.3
0.2
0.1
0
-0.1
1 4 7 10 13 16 19 22 25 28 31 34 37 40 43 46 49 52 55 58 61 64 67 70 73 76 79 82 85 88 91 94 97 100
Time in the Cycle (%)

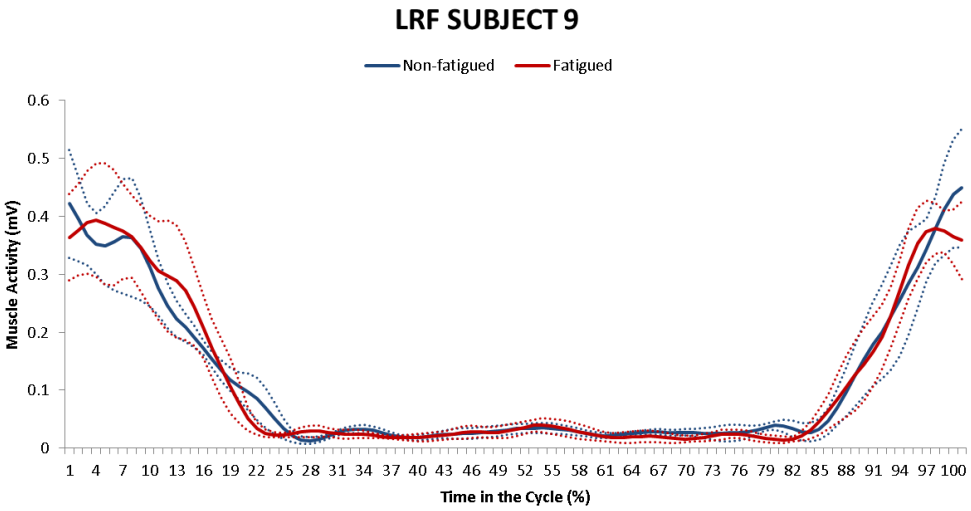
LRF SUBJECT 9
Non-fatigued
Fatigued
Muscle Activity (mV)
0.6
0.5
0.4
0.3
0.2
0.1
0
1 4 7 10 13 16 19 22 25 28 31 34 37 40 43 46 49 52 55 58 61 64 67 70 73 76 79 82 85 88 91 94 97 100
Time in the Cycle (%)

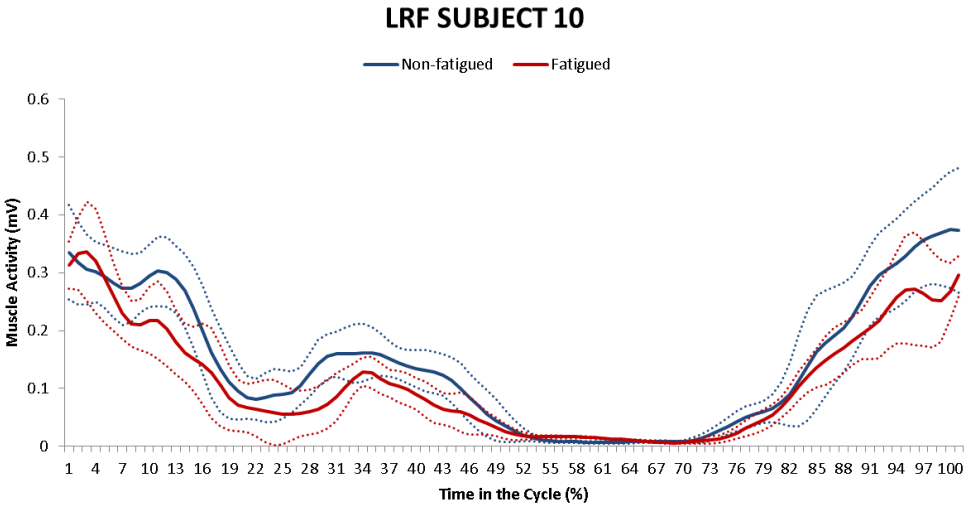
LRF SUBJECT 10
Non-fatigued
Fatigued
Muscle Activity (mV)
0.6
0.5
0.4
0.3
0.2
0.1
0
1 4 7 10 13 16 19 22 25 28 31 34 37 40 43 46 49 52 55 58 61 64 67 70 73 76 79 82 85 88 91 94 97 100
Time in the Cycle (%)

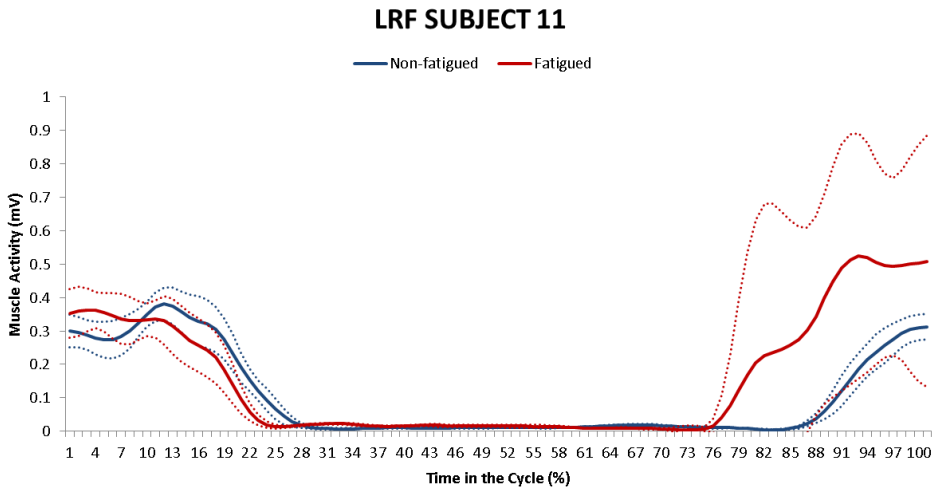
LRF SUBJECT 11
Non-fatigued
Fatigued
Muscle Activity (mV)
Time in the Cycle (%)

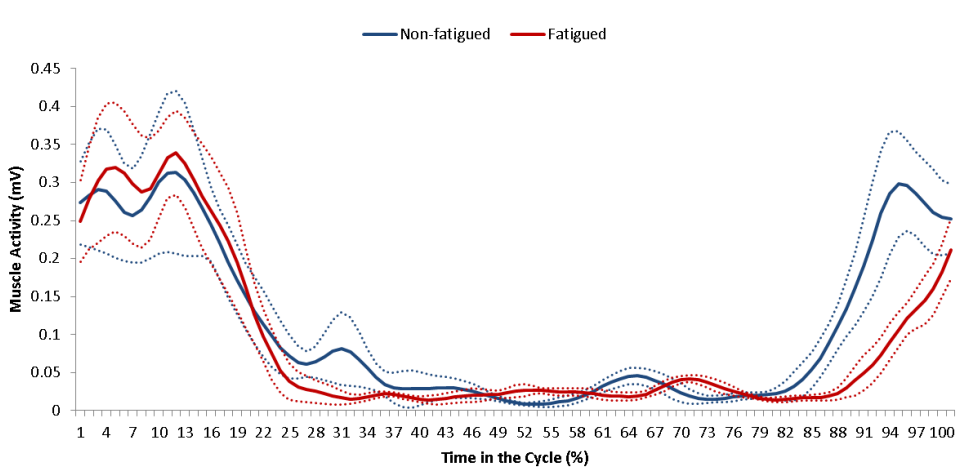
LRF SUBJECT 12
Non-fatigued
Fatigued
Muscle Activity (mV)
Time in the Cycle (%)

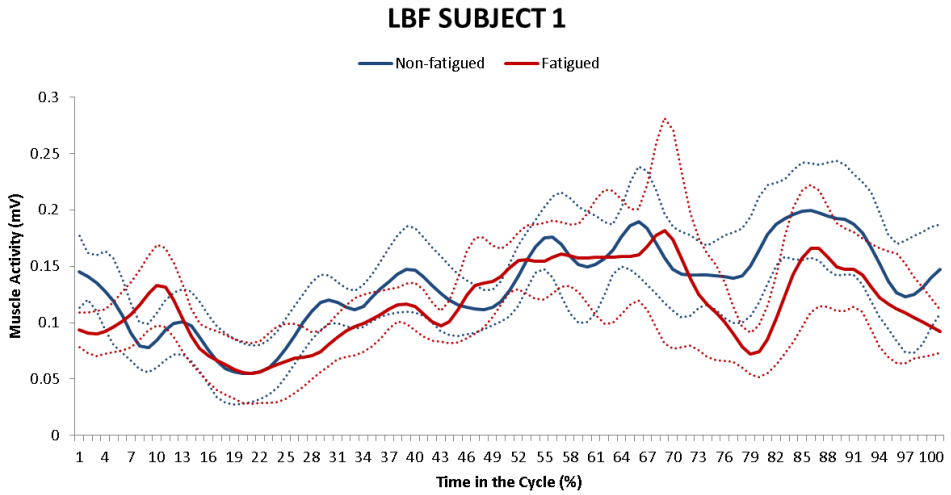
LBF SUBJECT 1
Non-fatigued
Fatigued
Muscle Activity (mV)
Time in the Cycle (%)

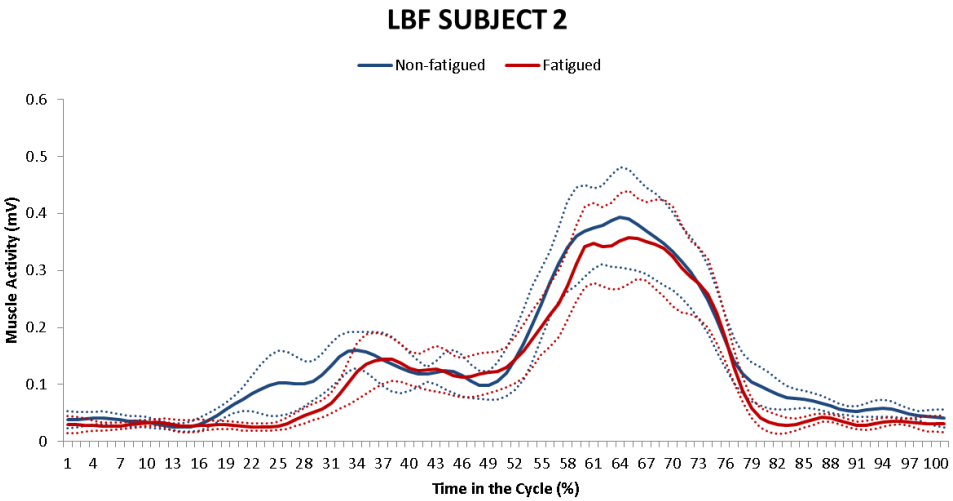
LBF SUBJECT 2
Non-fatigued
Fatigued
Muscle Activity (mV)
0.6
0.5
0.4
0.3
0.2
0.1
0
1 4 7 10 13 16 19 22 25 28 31 34 37 40 43 46 49 52 55 58 61 64 67 70 73 76 79 82 85 88 91 94 97 100
Time in the Cycle (%)

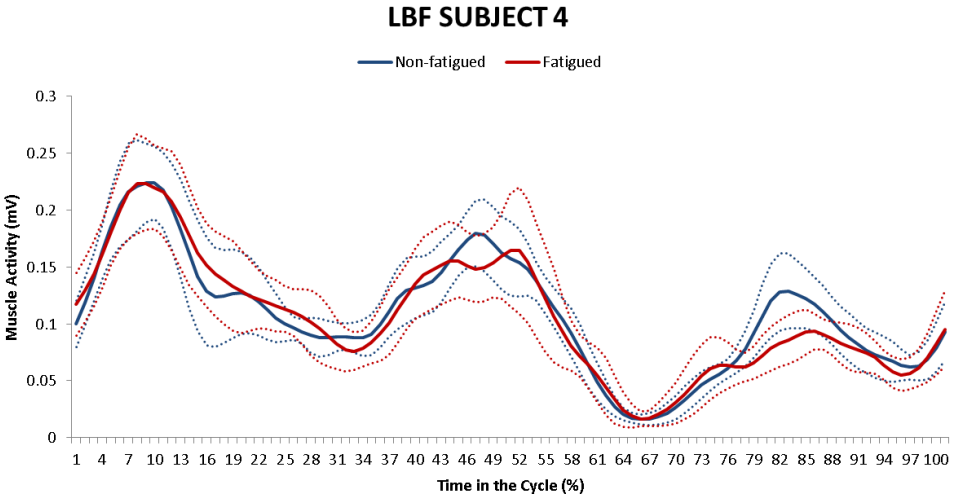
LBF SUBJECT 4
Non-fatigued
Fatigued
Muscle Activity (mV)
0.3
0.25
0.2
0.15
0.1
0.05
0
1 4 7 10 13 16 19 22 25 28 31 34 37 40 43 46 49 52 55 58 61 64 67 70 73 76 79 82 85 88 91 94 97 100
Time in the Cycle (%)

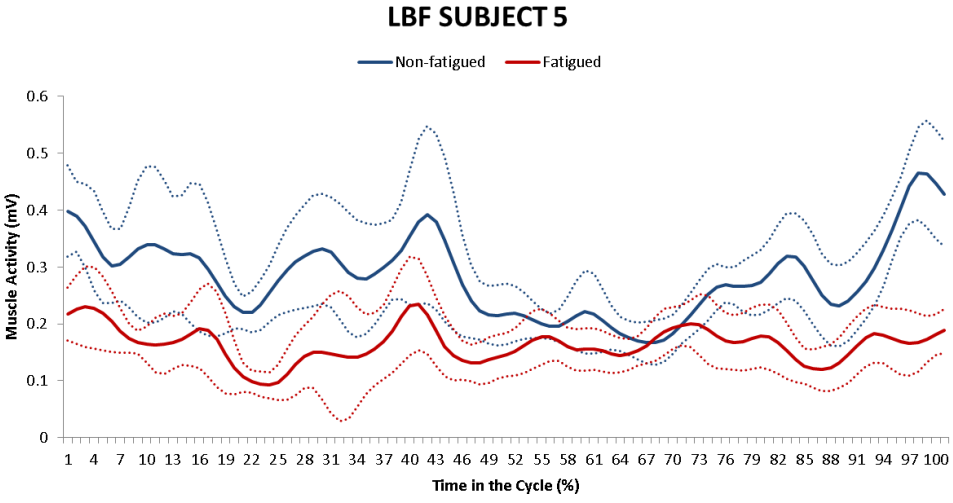
LBF SUBJECT 5
Non-fatigued
Fatigued
Muscle Activity (mV)
0.6
0.5
0.4
0.3
0.2
0.1
0
1 4 7 10 13 16 19 22 25 28 31 34 37 40 43 46 49 52 55 58 61 64 67 70 73 76 79 82 85 88 91 94 97 100
Time in the Cycle (%)

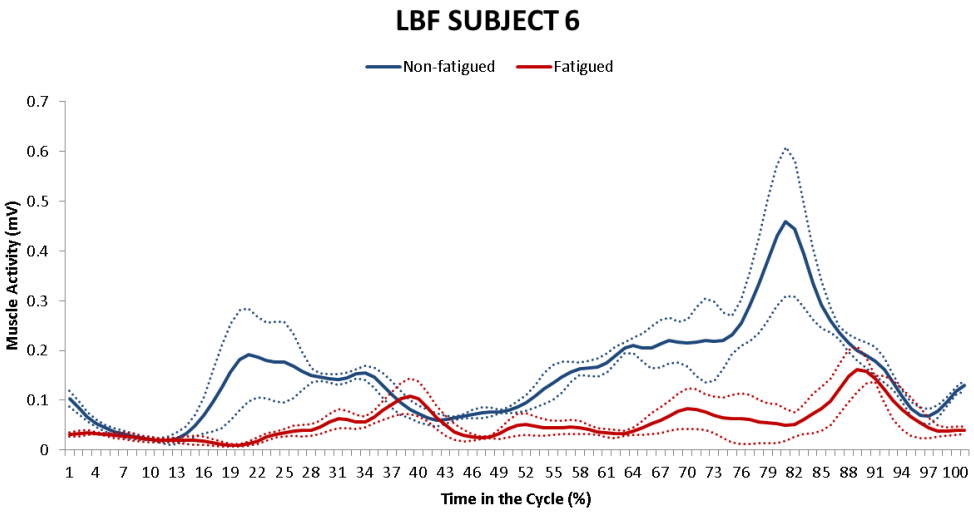
LBF SUBJECT 6
Non-fatigued
Fatigued
Muscle Activity (mV)
0.7
0.6
0.5
0.4
0.3
0.2
0.1
0
1 4 7 10 13 16 19 22 25 28 31 34 37 40 43 46 49 52 55 58 61 64 67 70 73 76 79 82 85 88 91 94 97 100
Time in the Cycle (%)

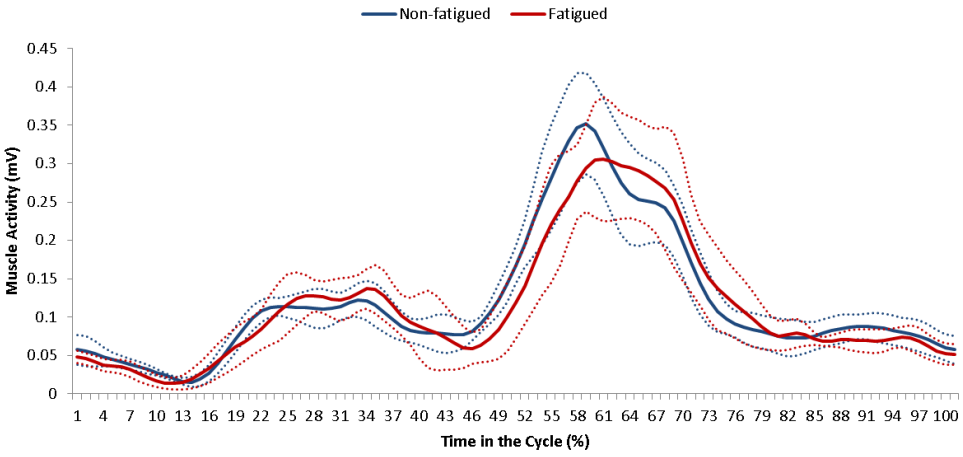
LBF SUBJECT 8
Non-fatigued
Fatigued
Muscle Activity (mV)
0.45
0.4
0.35
0.3
0.25
0.2
0.15
0.1
0.05
0
1 4 7 10 13 16 19 22 25 28 31 34 37 40 43 46 49 52 55 58 61 64 67 70 73 76 79 82 85 88 91 94 97 100
Time in the Cycle (%)

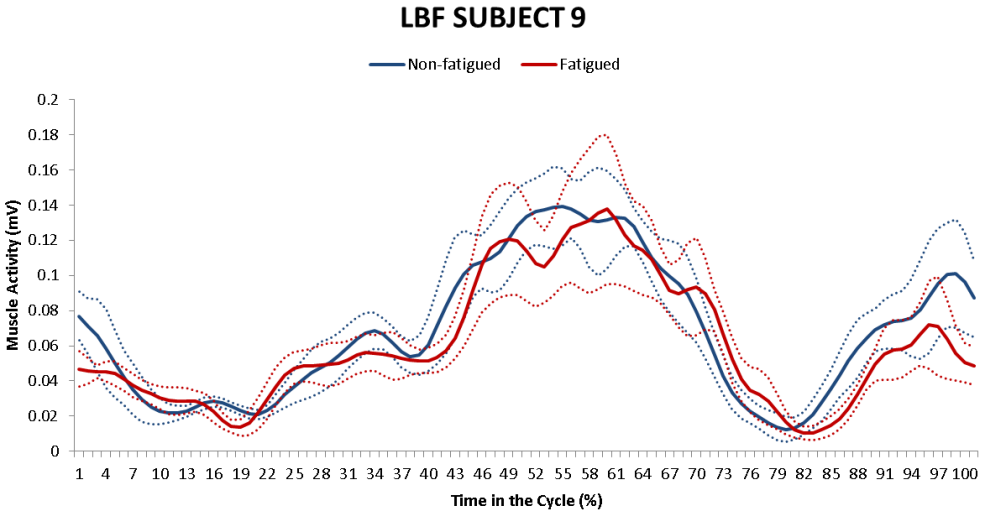
LBF SUBJECT 9
Non-fatigued
Fatigued
Muscle Activity (mV)
0.2
0.18
0.16
0.14
0.12
0.1
0.08
0.06
0.04
0.02
0
1 4 7 10 13 16 19 22 25 28 31 34 37 40 43 46 49 52 55 58 61 64 67 70 73 76 79 82 85 88 91 94 97 100
Time in the Cycle (%)

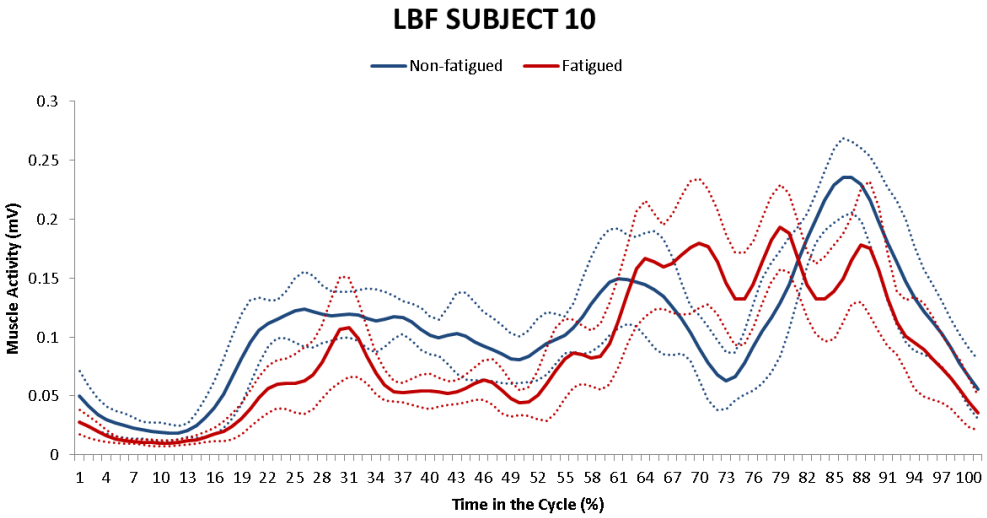
LBF SUBJECT 10
Non-fatigued
Fatigued
Muscle Activity (mV)
0.3
0.25
0.2
0.15
0.1
0.05
0
1 4 7 10 13 16 19 22 25 28 31 34 37 40 43 46 49 52 55 58 61 64 67 70 73 76 79 82 85 88 91 94 97 100
Time in the Cycle (%)

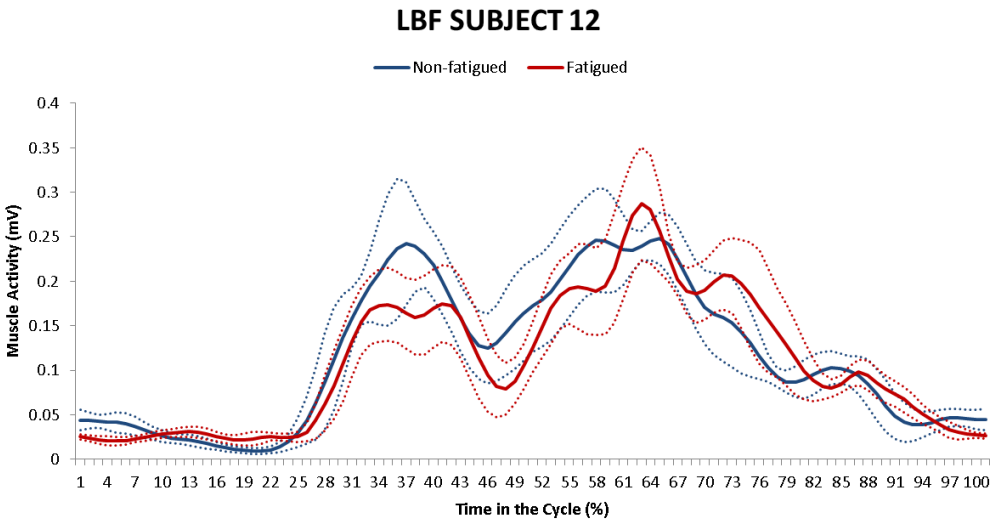
LBF SUBJECT 12
Non-fatigued
Fatigued
Muscle Activity (mV)
0.4
0.35
0.3
0.25
0.2
0.15
0.1
0.05
0
1 4 7 10 13 16 19 22 25 28 31 34 37 40 43 46 49 52 55 58 61 64 67 70 73 76 79 82 85 88 91 94 97 100
Time in the Cycle (%)